

# Networks of Self-Adaptive Dynamical Systems

THÈSE N° 5221 (2011)

PRÉSENTÉE LE 25 NOVEMBRE 2011

À LA FACULTÉ DES SCIENCES ET TECHNIQUES DE L'INGÉNIEUR  
LABORATOIRE DE PRODUCTION MICROTECHNIQUE 1  
PROGRAMME DOCTORAL EN SYSTÈMES DE PRODUCTION ET ROBOTIQUE

ÉCOLE POLYTECHNIQUE FÉDÉRALE DE LAUSANNE

POUR L'OBTENTION DU GRADE DE DOCTEUR ÈS SCIENCES

PAR

**Julio RODRIGUEZ**

acceptée sur proposition du jury:

Prof. R. Glardon, président du jury  
Prof. M.-O. Hongler, Prof. Ph. Blanchard, directeurs de thèse  
Prof. B. Cessac, rapporteur  
Prof. R. Filliger, rapporteur  
Prof. C. Pfister, rapporteur



ÉCOLE POLYTECHNIQUE  
FÉDÉRALE DE LAUSANNE

Suisse  
2011





... aux autres ... à tous ...

... au temps ... qui s'échoue ... qui s'écoule ... qui s'éclôt ...



---

## Summary

The present work belongs to the vast body of research devoted to behaviors that emerge when homogeneous or heterogeneous agents interact. We adopt a stylized point of view in which the individual agents' activities can be assimilated into nonlinear dynamical systems, each with their own set of specific parameters. Since the pioneering work of C. HUYGHENS in the seventeenth century it has been established that interactions between agents modify their individual evolutions - and that for ad-hoc interactions and agents that are not too dissimilar, synchronized behaviors emerge. In this classical approach, however, each agent recovers its individual evolution when interactions between them are removed or as summarized by a French aphorism: "*Chasser le naturel et il revient au galop*".

The position we adopt in this work differs qualitatively from this classical approach. Here, we construct a mathematical framework that depicts the idea of systems interacting not only via their state variables, but also via a self-adaptive capability of the agents' local parameters. Specifically, we consider a network where each vertex is endowed with a dynamical system having initially different parameters. We explicitly construct adaptive mechanisms which, according to the system's state, tune the value of the local parameters. In our construction, the agents are modeled by dissipative ortho-gradient vector fields possessing local attractors (e.g. limit cycles). The forces describing the agents' interactions derive either from a generalized potential or from a linear combinations of coupling functions.

Contrary to classical synchronization behavior which disappears when interactions are removed, here the system self-adapts and acquires consensual values for the set of local parameters. The consensual values are definitely "learned" (i.e. they stay in consensus even when interactions are removed). We analytically show for a wide class of dynamical systems how such a "plastic" and self-adaptive training of parameters can be achieved. We calculate the resulting consensual state and their relevant stability issues. The connectivity of the network (i.e. FIEDLER number) affects the convergence rate but not the asymptotic consensual values.

We then extend this idea to enable adaptation of parameters characterizing the coupling functions themselves. Self-learning mechanisms simultaneously operate at the agents' level and at the level of their connections. Finally, we analytically explore a set of dynamical systems involving the simultaneous action of two time-dependent networks (i.e. where edges evolve with time). The first network describes the interactions between the state variables, and the second affects the adaptive mechanisms themselves. In this last case, we show that for ad hoc time-dependent networks, parametric resonance phenomena occur in the dynamics.

While our work puts a strong effort into explicit derivations and analytic results, we do not refrain from reporting a set of numerical investigations that show how our explicit construction can be implemented in various classes of dynamical systems.

Keywords: Ortho-gradient dynamics, mixed canonical-dissipative systems, limit cycle oscillators, self-adaptive mechanisms, adaptive coupling, time-dependent Laplacian matrices, FIEDLER number, parametric resonance, HILL and MATHIEU equation, Ляпунов method, FLOQUET analysis



---

## Résumé

Le présent travail appartient au vaste domaine de recherche consacré aux comportements qui se manifestent lorsque des agents homogènes ou hétérogènes interagissent. Nous adoptons un point de vue stylisé sous lequel les activités individuelles des agents peuvent être assimilées à des systèmes dynamiques non linéaires, chacun avec son propre ensemble spécifique de paramètres. Depuis les pionniers travaux de C. HUYGHENS au 17<sup>ème</sup>, il a été établi que les interactions entre agents modifient leurs évolutions individuelles - et que pour des interactions ad-hoc et des agents qui ne sont pas trop dissemblables, des comportements synchronisés émergent. Cependant, dans cette approche classique, lorsque les interactions entre les agents sont supprimées, chaque agent récupère sa propre évolution - ou comme le résume l'aphorisme: "*Chasser le naturel et il revient au galop*".

La position que nous adoptons dans ce travail se distingue qualitativement de l'approche classique. Ici, nous construisons un cadre mathématique qui décrit l'idée de systèmes en interaction non seulement via leur variables d'état, mais aussi via une capacité d'auto-adaptative des paramètres locaux des agents. Plus précisément, nous considérons un réseau où chaque sommet est doté d'un système dynamique ayant des paramètres initialement différents. Nous construisons explicitement des mécanismes adaptatifs qui, selon l'état du système, règlent la valeur des paramètres locaux. Dans notre construction, les agents sont modélisés par des champs de vecteurs dissipatif ortho-gradient possédant des attracteurs locaux (par exemple, cycles limites). Les forces décrivant les interactions des agents dérivent soit d'un potentiel généralisé, soit d'une combinaison linéaire de fonctions de couplage.

Contrairement au comportement de synchronisation classique qui disparaît lorsque les interactions sont retirées, ici le système d'auto-adaptation acquiert des valeurs consensuelles pour l'ensemble des paramètres locaux. Les valeurs consensuelles sont "appprises" définitivement (c'est à dire, qu'elles restent dans le consensus, même si les interactions sont supprimées). Pour une large classe de systèmes dynamiques, nous démontrons analytiquement comment une telle déformation "plastique" et "auto-adaptative" des paramètres peut être atteinte. Nous calculons l'état consensuel résultant et les problèmes de stabilité revlevant. La connectivité du réseau (c'est à dire, le nombre de FIEDLER) affecte le taux de convergence, mais pas les valeurs consensuelles asymptotiques.

Nous étendons cette idée d'adaptation aux paramètres qui caractérisent les fonctionnelles de couplage. Des mécanismes d'auto-apprentissage opèrent simultanément au niveau des agents et au niveau de leurs connexions. Enfin, nous explorons analytiquement un ensemble de systèmes dynamiques impliquant l'action simultanée de deux réseaux dépendant du temps (c'est à dire, où les arêtes évoluent avec le temps). Le premier réseau décrit les interactions entre les variables d'état, et le second concerne les mécanismes adaptatifs eux-mêmes. Dans ce dernier cas, nous montrons que pour des réseaux dépendant du temps ad hoc, le phénomène de résonance paramétrique se produit dans la dynamique.

Bien que notre travail met l'accent sur les dérivations explicites et les résultats analytiques, nous exposons un ensemble de d'investigations numériques qui montrent comment nos constructions explicites peuvent être mis en œuvre dans diverses classes de systèmes dynamiques.

Mots-clés: Dynamique Ortho-gradient, Systèmes mixte canonique-dissipatif systèmes, oscillateurs à cycle limites, mécanismes auto-adaptatifs, couplage adaptatif, matrices Laplacienne dépendant du temps, nombre FIEDLER, résonance paramétrique, équation d'HILL et de MATHIEU, méthode de Ляпунов, analyse de FLOQUET



---

## Remerciements

Je remercie ...

... mes professeurs de thèse pour leur disponibilité, pour tout ce qu'ils m'ont enseigné et apporté. Max, merci pour le temps, le temps que tu m'as accordé, le temps que tu m'as donné ... le temps que tu m'as laissé avoir, seul et libre pour essayer ... essayer de trouver ou de perdre ... perdre du temps pour essayer de trouver. Philippe, merci pour votre positivité, pour être toujours constructif, toujours partant, toujours en avant ... et tout ceci, dans le calme et dans l'agréable. Max et Philippe, merci pour nos conversions de maths, de physique ... et toutes autres et d'avoir partagé avec moi quelques unes de vos anecdotes du Portugal, de Berlin-Ost. Merci.

... mon jury de thèse pour avoir consacré du temps à lire ce présent manuscrit. Merci pour vos questions et commentaires très enrichissants lors de ma soutenance privée, soutenance qui s'est déroulée dans une atmosphère conviviale - et je vous en remercie. Merci Roger pour tes remarques et d'avoir si consciencieusement noté les coquilles de la première version de ma thèse.

... Martin pour avoir trouvé de très bonnes idées concernant la généralisation d'une partie spécifique de ma thèse. Merci pour ce lemme, technique mais magnifique! Merci pour nos maths dans le train, pour ces maths après Genf!

... Ludovic et Auke pour nos séances de travail au tout début de ma thèse. Merci pour ces échanges.

... Jacques et Peter pour m'avoir accueilli dans le Laboratoire de Production Microtechnique. Un chouette labo avec une bonne atmosphère de travail. Merci pour les soupés de Noël et surtout pour les sorties de labo très intéressantes!

... mes collègues de labo pour l'ambiance sympathique, pour les barbecues et les raclettes sauvages et, surtout, les пиво @ SaT! Merci Olivier pour "le flambeau" et notre "cohabitation". Nous nous sommes bien amusés!

... Karine et Claire pour leur assistances dans toutes les tâches administratives, mais surtout pour leur bonne humeur.

... ma mère pour tout ce qu'elle m'a donné ... donné en abondance ... tout ses conseils, la valeur du travail et, surtout, mon éducation. Mère, merci d'avoir toujours été là. Merci pour ton écoute.

... mon frère avec qui j'ai pu partager un bout de chemin des mathématiques. Léon, merci pour ton soutien et ton aide. De la construction avec les Legos aux démonstrations de théorèmes, merci.

... mes amis et collègues de la section de maths pour ces superbes années universitaires - 10 ans déjà les amis! Anne, Benoit, Ghislain, Luc, Manuela, Martin, Nicola, Philippe et Yves, merci pour ces années rythmées par les cours, les séries d'exercices, les examens et les soirées дача.

... tous les autres, ceux du passé comme ceux du présent, les grands de l'Histoire comme les oubliés, qui ont contribué et construit l'édifice sur lequel nous, aujourd'hui, on pose les dalles sur lesquelles ceux de demain continueront à marcher, à denser. Tout simplement, merci ... à tous ...

Lausanne, 11.11.11

Julio RODRIGUEZ



---

# Contents

<b>Introduction</b> .....	1
0.1 Framework .....	1
0.2 Motivation .....	2
0.3 Objective .....	4
0.4 Contributions .....	4
0.5 Organization .....	5
<b>1 General Setting</b> .....	7
1.1 Network's Dynamical System - No Adaptive Mechanisms .....	7
1.1.1 Local Dynamics: $L_k$ .....	7
1.1.2 Coupling Dynamics: $C_k$ .....	13
1.2 Network's Dynamical System - With Adaptive Mechanisms .....	15
1.2.1 Parametric Dynamics: $P_k$ .....	15
1.2.2 Binding Dynamics: $B_k$ .....	16
1.2.3 Dynamical States .....	16
1.2.4 Aim of the Parametric Dynamics .....	17
1.2.5 Aim of the Binding Dynamics .....	18
1.3 Basic Example .....	18
1.3.1 Miscellaneous Remark: Adaptation as an Optimal Control Problem .....	19
<b>2 Networks of Ortho-Gradient Systems with Adapting Flow Parameters</b> .....	21
2.1 Network's Dynamical System .....	21
2.1.1 Local Dynamics: $L_k$ .....	21
2.1.2 Coupling Dynamics: $C_k$ .....	22
2.1.3 Parametric Dynamics: $P_k$ .....	22
2.1.3.1 Dynamics of Flow Parametric Variables .....	22
2.2 Dynamics of the Network .....	26
2.2.1 Network of Homogeneous Local Dynamics with constant identical Parameters .....	28
2.2.2 Network of Homogeneous Local Dynamics with Single Adapting Flow Parameters .....	30
2.2.3 Network of Homogeneous Local Dynamics with Multi Adapting Flow Parameters .....	33
2.2.4 Network of Heterogeneous Local Dynamics with Single and Multi Adapting Flow Parameters .....	36
2.2.5 Miscellaneous Remark: Adaptation on Geometric Parameters .....	39
2.3 Numerical Simulations .....	41
2.3.1 Homogeneous Local Dynamics .....	41
2.3.2 Heterogeneous Local Dynamics .....	42
<b>3 Networks of Mixed Canonical-Dissipative Systems with Adapting Flow and Geometric Parameters</b> .....	49
3.1 Network's Dynamical System .....	49
3.1.1 Local Dynamics: $L_k$ .....	49
3.1.2 Coupling Dynamics: $C_k$ .....	50
3.1.3 Parametric Dynamics: $P_k$ .....	50
3.1.3.1 Dynamics of Flow Parametric Variables .....	51
3.1.3.2 Dynamics of Geometric Parametric Variables .....	51

3.2	Dynamics of the Network	55
3.2.1	Network of Ellipsoidal HOPF Oscillators	61
3.2.2	Miscellaneous Remark: Variation in the Adaptive mechanism	62
3.3	Numerical Simulations	65
3.3.1	Ellipsoidal HOPF Oscillators	65
3.3.2	CASSINI Oscillators	65
3.3.3	MATHEWS-LAKSHMANAN Oscillators	75
<b>4</b>	<b>Networks of Mixed Canonical-Dissipative Systems with Adapting Coupling Weights</b>	<b>79</b>
4.1	Network's Dynamical System	79
4.1.1	Local Dynamics: $L_k$	80
4.1.2	Coupling Dynamics: $C_k$	80
4.1.3	Parametric Dynamics: $P_k$	80
4.1.4	Binding Dynamics: $B_k$	82
4.2	Dynamics of the Network	84
4.2.1	Homogeneous Case with c-PV independent Binding Dynamics	84
4.2.2	Heterogenous Case with c-PV dependent Binding Dynamics	86
4.2.2.1	Two types of c-PV	89
4.2.3	Miscellaneous Remark: Three types of adapting parameters: f-PV, g-PV and c-PV	91
4.3	Numerical Simulations	93
4.3.1	MATHEWS-LAKSHMANAN Oscillators	93
4.3.2	OHR Oscillators	93
4.3.3	Ellipsoidal HOPF Oscillators with two c-PV	96
4.3.4	Ellipsoidal HOPF Oscillators with f-PV, g-PV and c-PV	96
4.3.5	Heterogeneous network of HOPF and MATHEWS-LAKSHMANAN Oscillators	96
<b>5</b>	<b>Time-dependent Networks of Hopf Oscillators with Adapting Frequencies and Radii</b>	<b>101</b>
5.1	Network's Dynamical System	101
5.1.1	Local Dynamics: $L_k$	101
5.1.2	Coupling Dynamics: $L_k$	102
5.1.3	Parametric Dynamics: $P_k$	102
5.2	Dynamics of the Network	103
5.2.0.1	Time-independent Case	108
5.2.1	Parametric Resonance	109
5.2.2	Miscellaneous Remark: Variation in the Interactions	109
5.3	Numerical Simulations	111
5.3.1	Time-dependent	111
5.3.2	Time-independent	114
5.3.3	Parametric Resonance	114
<b>6</b>	<b>Numerical Investigations and Perspectives</b>	<b>119</b>
6.1	Numerical Investigations for Networks of none O-G systems with Adapting Parameters	119
6.1.1	Adaptive "Frequency" in Nonharmonic Oscillators	119
6.1.2	The BOUASSE SARDA Regulator	121
6.2	Perspectives	130
<b>7</b>	<b>Towards Potential Applications</b>	<b>133</b>
	<b>Conclusions</b>	<b>137</b>

<b>Appendices</b> .....	141
A Asymptotic Stability of a Compact Set .....	141
A.1 Principal of Linearized Stability .....	141
A.1.1 Periodic Solutions - FLOQUET Theory .....	141
B Analytic Solutions for some MCD Oscillators .....	143
C Networks and Laplacian Matrices .....	145
D Symmetric and Anti-Symmetric Matrices .....	149
E Equality between kernels .....	150
F Linearization and Diagonalization of Eqs. (3.9) .....	151
G HOPF Oscillators in Polar Coordinates .....	152
<b>References</b> .....	155
<b>Curriculum Vitae</b> .....	157



---

# Introduction

## 0.1 Framework

The class of dynamics to be studied consists of a  $N$ -vertex network where each vertex is equipped with an individual dynamical system. The  $N$  local systems are additively coupled via time- and state variable-dependent edges. The global dynamical system reads

$$\begin{aligned}\dot{X}_k &= \underbrace{\mathbf{L}_k(X_k; \Lambda_k)}_{\text{local dynamics}} + \underbrace{\mathbf{C}_k(X, \Delta)}_{\text{coupling dynamics}} \\ \dot{\Delta} &= \underbrace{\mathbf{B}(X, \Delta)}_{\text{binding dynamics}}\end{aligned} \quad k = 1, \dots, N \quad (0.1)$$

where  $X_k \in \mathbb{R}^{p_k}$  are the **state variables** of the  $k^{\text{th}}$  vertex,  $\mathbf{L}_k$  is the local vector field governing the **local dynamics**, and  $\Lambda_k \in \mathbb{R}^{q_k}$  are local constant parameters of the dynamics<sup>1</sup>. The **coupling dynamics**  $\mathbf{C}_k(X, \Delta) \in \mathbb{R}^{p_k}$  describe how the **local dynamics** interact. The notation is  $X := (X_1, \dots, X_N)$  and  $\Delta$  stands for the variables influencing the environment (e.g. coupling weights, edges between vertices of the network, etc) and are governed by the **binding dynamics**  $\mathbf{B}$ .

Eqs. (0.1) is a general mathematical formulation for problems composed of isolated systems, whose dynamics are modeled with ordinary differential equations, and where the individual units interact together with an additive term. These equations cover models ranging from mechanical devices (e.g. C. HUYGHENS' clocks) to highly complex dynamical systems coupled via networks (e.g. social communities, spreading processes, biological interactions, chemical reactions, swarm behavior, etc). Eqs. (0.1) is encompassed into the conceptual framework presented in [5].

In the sequel we focus on situations for which the local system's behavior is known (e.g. fixed point, oscillatory, chaotic, limit cycle or dynamical system on attracting submanifolds). When the constituent units are coupled together, the following question arises

What type of “ordered” dynamical patterns exist in Eqs. (0.1)?

Synchronized<sup>2</sup> evolution is one of numerous possibilities of “ordered” dynamical patterns. It is among the most studied and fascinating behaviors in complex dynamical systems. Broadly put, synchronization consists of a large number of individual systems forming a common dynamical pattern, regardless of the built-in differences in their **local dynamics**.

From C. HUYGHENS' “sympathie des horloges”, to satellite distributing time and frequency, passing by fireflies' flashing and neuronal firing, synchronization ‘*has commanded attention as a spectacle and in relation to its function. However, the greatest interest [] has centered on mechanisms by which synchrony might be attained and maintained*’<sup>3</sup>. Let us now briefly discuss these two issues separately.

### Attaining a synchronized pattern

---

<sup>1</sup> We use the following notation: we use ; to separate the variables from the parameters in the arguments of a function.

<sup>2</sup> The word is related to “synchronous”, coming from the Greek  $\sigma\acute{\upsilon}\nu$  - “same” and  $\chi\rho\acute{o}\nu\omicron\varsigma$  - “time”, meaning “sharing the common time” or “occurring in the same time” (c.f. [38])

<sup>3</sup> Refer to [8]

When studying the emergence of dynamical patterns, one can qualitatively distinguish between two categories: either the system’s constituents are initially very disperse (far from one another) or they are all in the vicinity of a chosen dynamical pattern when they start to interact. Analytic tractability of the first category is generally out of reach. It implies the understanding of complicated transient states before the ultimate pattern is reached. Analytic discussions of the second category are more available and hence readily fruitful.

For functionally homogeneous dynamics  $L_k \equiv L$  with  $\Lambda_k = \Lambda_j$  and with linear time-independent coupling (i.e. here  $B \equiv 0$ ), the master stability equation proposed by L. M. PECORA and T. L. CARROLL in [37] allows to investigate the propensity of a network to reach a synchronized state (i.e.  $X_k(t) = X_c(t)$  for all  $k$ ). For heterogeneous parameters  $\Lambda_k \neq \Lambda_j$  (and with constant **binding dynamics**), it is generally unknown when collective dynamical patterns may emerge from Eq.(0.1). For slight heterogeneity and even if this is not fully rigorous (c.f. [26]), small  $\Lambda_k$  mismatches still allow for the use of the master stability equation to characterize the resulting synchronized motion - as corroborated by numerical probing (c.f. [9, 26]). However, in general, ‘*As soon as nonidentity in the networking elements is considered, [], there is no choice but to restrict oneself to numerical simulations on synchronization and control processes of complex networks.*’<sup>4</sup> Indeed, the advent of computational power allows numerous numerical investigations among which the study of synchronization of phase oscillators with different *eigen* frequencies in scale-free networks (c.f. [33]) with different clustering coefficient (c.f. [31]).

### Maintaining a synchronized pattern

Once attained, the collective behavior of a complex system is preserved thanks to the mutual interactions between the individual units and the **coupling dynamics**. If local entities are no longer present, it is assumed that the collective dynamical pattern vanishes. Indeed, if all flies desert the swarm, the swarm ceases to exist. Likewise, and in the general case, removing the **coupling dynamics**, implies the end of the collective phenomenon.

## 0.2 Motivation

The following two questions form the basis of the main motivation for this thesis

- What can be implemented to a complex system of homogeneous dynamics with heterogeneous parameters to analytically tackle the issue of “attaining” a synchronized pattern?
- How can a collective dynamical state be “maintained” even if connections are removed?

A common feature of previous papers describing synchronization of systems with  $L_k \equiv L$  but different  $\Lambda_k$  is that the synchronized states are maintained as long as the action of the network operates. Hence, if network interactions are removed, synchronization is destroyed and each local system is restored to its individual and distinct evolution.

This limitation has the following consequences

- The collective behavior can only be preserved at the price of maintaining the network connections. This might be viewed as a drawback since it incurs a cost. Furthermore, any perturbation in the **coupling dynamics** (e.g. random on and off switching of edges) will affect the local systems’ dynamics since these are inter-dependent.
- The dynamics of the local systems under the influence of the network will not persist once the local systems are isolated: individual evolutions will fall back under the regimen of their local characteristics if the interactions are removed. In other words, local systems are not able to *adapt* their local features so that they can still perpetuate their dynamics without being under the influence of the interactions. This is another drawback since the interactions are unable to leave any long-lasting effect on the local units.

<sup>4</sup> Refer to [2]

To tackle these drawbacks, local systems should *self-adapt* their individual characteristics (i.e. parameters  $\Lambda_k$ ) so as to be less dependent on the interactions.

## Adaptation

The modeling of adaptation phenomena is an established research axis with wide interdisciplinary relevance. This research axis has been triggered by the seminal work of B. ERMENTROUT in [15]. In close relation to our contribution, frequency adaptation in coupled phase oscillators has been considered in [49, 1, 50]. Recently, adaptive coupling strengths in connecting networks are discussed in [13, 29, 12].

Here, in this thesis, *adaptation* is to be interpreted as allowing the parameters  $\Lambda_k$  to have their own dynamics (i.e. letting the parameters be time-dependent), such that the global system converges towards a *consensual state* - a state of dynamical pattern that persist even if the network is removed. It has to be emphasized that such type of *adaptation*<sup>5</sup> motivates the investigation of interactions that structurally modify the local characteristics and thus affect the local systems at the level of their specific features (i.e. the parameters  $\Lambda_k$ ).

As an example, consider a musical performance. Each musician with his instrument is a local entity. Before the concert, the musicians must tune their instruments to a reference note. The global tuning of the orchestra is achieved by adjusting the strings (i.e. parameters) of each musical instrument. This process is performed by each musician by listening (i.e. interactions turned on) to his neighbours. Once this stage is completed, playing the reference note is no longer needed - imagine if through-out the whole concert a reference note was necessary for the musicians to perform (it would be extremely annoying!). Furthermore, once the reference note has ceased to be played (i.e. interactions turned off), all instruments are adequately tuned - and this for the whole concert (i.e. fixed parameters).

At the level of the environment, adaptation is implemented with the **binding dynamics**. Adaptations in the **local dynamics** is achieved by effectively enlarging the dimensionality of the global system by introducing additional **parametric dynamics**  $P_k$  in Eq.(0.1). This leads us to consider dynamical systems of the form

$$\begin{aligned} \dot{X}_k &= \underbrace{L_k(X_k, \Lambda_k)}_{\text{local dynamics}} + \underbrace{C_k(X, \Lambda, \Delta)}_{\text{coupling dynamics}} \\ \dot{\Lambda}_k &= \underbrace{P_k(X, \Lambda, \Delta)}_{\text{parametric dynamics}} & k = 1, \dots, N, \\ \dot{\Delta} &= \underbrace{B(X, \Lambda, \Delta)}_{\text{binding dynamics}} \end{aligned} \quad (0.2)$$

with  $\Lambda = (\Lambda_1, \dots, \Lambda_N)$ . We thus confer to the  $\Lambda_k$  the status of variables of the global dynamics. Once acquiring this status, they are referred to as **parametric variables**. In the general case, the **parametric dynamics**  $P_k$  dependent on an additional network as the one for  $C_k$ . Note that by suitably renaming the variables, Eq.(0.2) is encompassed by Eq.(0.1). Nevertheless, it is worthwhile to present the network dynamics in the form of Eqs. (0.2) which explicitly isolates the self-adaptive mechanism that, via the network environment, *plastically* deforms the local parameters.

## Types of Adapting Parameters

In this contribution, three types of parameters are considered for adaptation. Two of them belong to the **local dynamics** (i.e.  $\Lambda_k$ ), and one to the **coupling dynamics** (i.e.  $\Delta$ ). Those parameters

<sup>5</sup> Note that the notion of “adaptive systems” may have other meanings. For example, as stated in [21], *Adaptive Systems [are] neither fully conserving nor fully dissipative. Adaptive systems will have periods where they take up energy and periods where they give energy back to the environment.*

belonging to the local systems are known as *flow parameters* and *geometric parameters*. The latter are concerned with the shape of the local attractor. The former are those that control the dynamics on the attractor only (they can be thought of as time-scales). As an example, consider a 2-dimensional system oscillating on a circle. The parameter determining the radius of the circle is a geometric parameter whereas a parameter that exclusively controls the angular velocity is a flow parameter.

### 0.3 Objective

The central objective of this thesis is to explicitly construct adaptive mechanisms that are governed by  $P_k$  and  $B$  in Eqs. (0.2). The aim of  $P_k$  and  $B$  is to modify the values of  $\Lambda_k$  and  $\Delta$  so that

$$\lim_{t \rightarrow \infty} (\Lambda_1(t), \dots, \Lambda_N(t), \Delta(t)) = (\bar{\Lambda}, \bar{\Delta}), \quad (0.3)$$

where  $\bar{\Lambda} = (\bar{\Lambda}_1, \dots, \bar{\Lambda}_N)$  and  $\bar{\Delta}$  are constants with values enabling Eqs. (0.2) to admit the existence of a *consensual state*. Simultaneously, the **coupling dynamics** drives the **state variables** towards this *consensual state* (i.e. attaining a synchronized pattern). In the particular case of homogeneous local systems with no **binding dynamics**,  $\Lambda_k$  converge towards a single common consensual  $\Lambda_c$ . In this case, by allowing local systems to ultimately acquire identical parameters, one is able to analytically discuss both the existence and the convergence issues. Summarizing, the questions addressed in this thesis are

- 1) What are the necessary conditions for convergence towards a *consensual state*?
- 2) How can  $(\bar{\Lambda}, \bar{\Delta})$  be calculated?
- 3) How does  $(\bar{\Lambda}, \bar{\Delta})$  depend on the topology of the network?
- 4) How does the connectivity of the network influence the convergence rate towards the *consensual state*?

### 0.4 Contributions

We summarize the main original contributions of the thesis as follows.

#### “Plasticity” and Adaptation Aspects

- I Construction of a new class of dynamical system for which the network interactions confer persistent features in the **local dynamics**. The dynamics induce “plastic” deformations which are persistent even if one removes the mutual interactions. In other words, the **local dynamics** do not return to their original evolution but exhibit a permanent alteration. This contribution was published in [42, 41].
- II Elaboration of a general framework covering the concept of “plastically” modifying parameters in order to *self-adapt* to a given environment. The adaptation process results from a convergence towards a specific dynamical state. This is achieved by using well established tools from nonlinear dynamical theory. Two types of local parameters are distinguished: flow parameters that influence the dynamics on the attractor and geometric parameters that shape the attractor itself. For both type of parameters, explicit adaptive mechanisms are constructed and the relevant convergence issues are analytically discussed. For flow parameters exhibiting a higher propensity to adapt, ad hoc Ляпунов functions are constructed. For geometric parameters, FLOQUET exponents analysis are computed. For both type of parameter, their asymptotic values are analytically determined (i.e. the values of  $\bar{\Lambda}_k$  in (0.3) are analytically expressed for all  $k$ ). This contribution was published in [42, 41, 45] and is under revision in [44].



III Introduction of a class of adaptive mechanisms influencing the **coupling dynamics**. Here, one allows general adjustments involving coupling weights together with the adapting parameters of the local dynamics. One is able to analytically determine the resulting asymptotic parameter values (i.e. the values of  $\bar{\Delta}$  in (0.3)).

IV Adaptation in a complex system of HOPF oscillators with two time-dependent networks. One network governs the interactions between the **state variables** while the other determines the adaptive mechanisms. Analytical results can be derived in this complex situation. In particular, the conditions for convergence towards a consensual state are explicitly given. Destabilization due to parametric resonance are explicitly studied. This contribution was published in [43].

### Dynamical Systems

V Generalization of simple limit cycle oscillators to arbitrary dimension **ortho-gradient** vector fields. These are constructed by adding non-Liouvillian dissipative terms to a “driving” part which, when solenoidal, generates a canonical evolution. The non-Liouville contributions derive from the gradient of a generalized local potential. The dissipative part is orthogonal to the “driving” part. The local potential, controlling the dissipation, asymptotically drives the orbits towards limit cycles or more general attracting manifolds. For orbits evolving on the attractor, the dissipative character of the dynamics vanishes. This contribution is under revision in [44].

VI Presentation of an extended collection of explicitly soluble illustrations of mixed canonical-dissipative systems.

### Differences with “Classical Synchronization”

Let us here emphasize once more that our present approach fundamentally differs from synchronization problems where local parameters are kept constant. Here, one explicitly studies self-organized “plastic” deformations of the local parameters. Once a consensual state is reached, it remains permanent even if interactions are removed. This has to be definitely contrasted with classical synchronization problems where the presence of interactions are mandatory to dynamically sustain a synchronized state.

## 0.5 Organization

The thesis is composed of seven chapters with, additionally, a conclusion and an appendix.

The first chapter, **General Setting**, presents the most general form of dynamical system that will be studied all along this thesis. The different constituents are detailed and basic definitions are set out.

In Chapter two, **Networks of Ortho-Gradient Systems with Adapting Flow Parameters**, O-G systems are coupled via the gradient of a general potential and the adaptive mechanisms tune the respective local flow parameters.

Chapter three, **Networks of Mixed Canonical-Dissipative Systems with Adapting Flow and Geometric Parameters**, considers coupled limit cycle oscillators that mutually tune their angular velocities and shape their attractor.

The same coupled limit cycle oscillators as in the previous chapter are considered but here, in the fourth Chapter, **Networks of Mixed Canonical-Dissipative Systems with Adapting Coupling Weights**, the effect of different types of coupling weights adjustment in the **coupling**

dynamics is investigated.

Relaxing the hypothesis of one constant network in the system, Chapter five, **Time-dependent Networks of Hopf Oscillators with Adapting Frequencies and Radii**, deals with two time-dependent networks (one for the **state variables** and one for the frequency tuning and attractor shaping) of frequency and radii adapting HOPF oscillators.

Other types of **local dynamics** that allow for parametric adaptability, are numerically investigated in Chapter six, **Numerical Investigations and Perspectives**. A list of perspective is presented.

Finally, Chapter 7, **Towards Potential Applications**, is devoted to potential applications.

Chapters two to five begin with a short description of what type of **local** and **coupling dynamics** and what kind of adaptation are studied. They are then followed by a brief recap of the necessary notions for the chapter in question. They are thus self-contained. Each of these chapters finishes with a selection of numerical simulations that confirm the theoretical assertions. Figure 0.1 represents the structure of these four chapters with respect to the type of adaptation and underlying network.

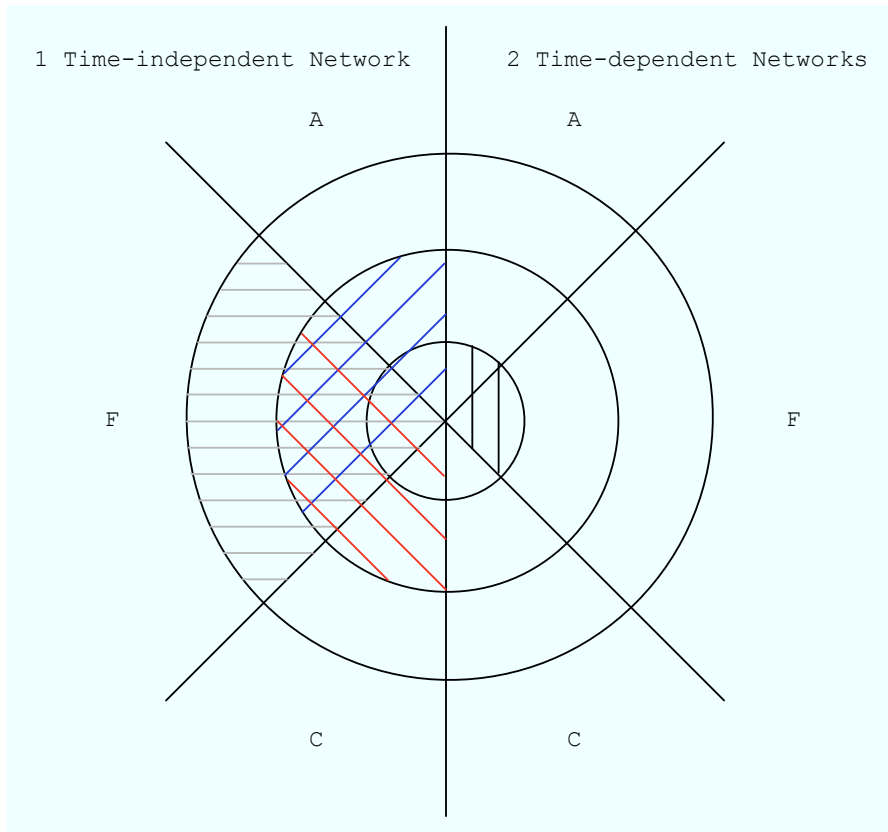


Fig. 0.1: The smallest circle represent the HOPF oscillators. The second circle represent the set of mixed canonical-dissipative systems that is considered in this thesis. The largest circle is the set of ortho-gradient systems. The letter A, F and C stand for, respectively, attractor shaping (i.e. adapting the geometric parameters), flow tuning (i.e. adapting the flow parameters) and coupling weight adjustment (i.e. adapting the coupling weights). The coloring scheme is: gray for Chapter 2, blue for Chapter 3, red for Chapter 4 and black for Chapter 5.

## General Setting

La poésie doit être faite par tous. Non par un.

LAUTREAMONT

### 1.1 Network's Dynamical System - No Adaptive Mechanisms

In this section, we present the general form of the dynamical system that is considered in this thesis when no adaptive mechanism is implemented. The dynamical system reads

$$\dot{X}_k = \underbrace{D_k(X_k; \Phi_k, \Gamma_k) - \nabla A_k(X_k; \Gamma_k)}_{\text{local dynamics}} - \underbrace{C_k(t, X; \Gamma, \Delta)}_{\text{coupling dynamics}} \quad k = 1, \dots, N. \quad (1.1)$$

**Local Dynamics** Local systems are of dimension  $p$  and belong to the class of ortho-gradient (O-G) systems (refer to Section 1.1.1).

**Coupling Dynamics** Interactions will either derive from the gradient of a given positive function or through a linear combination of coupling functions (refer to Section 1.1.2).

#### 1.1.1 Local Dynamics: $\mathcal{L}_k$

All **local dynamics** belong to the class of ortho-gradient (O-G) systems. This class of dynamical system is split into two  $p$ -dimensional vector fields  $D_k$  and  $\nabla A_k$  and are defined as

$$\mathcal{L}_k(X_k; \Lambda_k) := \underbrace{D_k(X_k; \Phi_k, \Gamma_k)}_{\text{orthogonal evolution}} - \underbrace{\nabla A_k(X_k; \Gamma_k)}_{\text{gradient evolution}} \quad k = 1, \dots, N$$

where  $X_k \in \mathbb{R}^p$  are the **state variables** and  $\Lambda_k = \{\Phi_k, \Gamma_k\}$  is a set of  $q_k$  fixed and constant parameters composed of two disjoint sets  $\Phi_k$  and  $\Gamma_k$  (i.e.  $\Lambda_k = \Phi_k \uplus \Gamma_k$ ) that we will distinguish below.

Dissipation is due to the *gradient evolution*, which arises from  $\nabla A_k$ , the gradient of a potential  $A_k(X_k; \Gamma_k) := \frac{1}{2} \sum_{j \in I_k} G_j(X_k; \Gamma_k)^2$  and  $I_k \subseteq \{0, \dots, p-1\}$ . The real-valued functions  $G_j$  are sufficiently continuously differentiable and are defined such that the set

$$\mathcal{L}_k := \{X \in \mathbb{R}^p \mid G_j(X; \Gamma_k) = 0 \quad j \in I_k\}$$

is a  $m_k$ -dimensional compact submanifold with  $m_k := p - |I_k|$  ( $p$  minus the cardinality of the set of indices  $I_k$ ). This implies, by definition, that  $\mathcal{L}_k$  is not empty, and for all  $X^* \in \mathcal{L}_k$  there exists a neighborhood  $\mathcal{U}_{X^*} \subset \mathbb{R}^p$  of  $X^*$  such that for all  $X \in \mathcal{U}_{X^*}$  the  $(p - m_k) \times p$  Jacobian  $\mathfrak{D}\vec{G}_k(X; \Lambda)$  has rank  $p - m$  ( $\mathfrak{D}$  stands for the derivative operator and  $\vec{G}_k \equiv (G_{j_1}, \dots, G_{j_{p-m_k}})$  with  $j_s \in I_k$ ,  $s = 1, \dots, p - m_k$  and  $p - m_k = |I_k|$ ). Since  $\mathcal{L}_k$  is the preimage of the closed set  $\mathbf{0} \in \mathbb{R}^{p-m_k}$  by a continuous function  $\vec{G}_k$ , it is closed. We assume it is bounded (there exists  $b > 0$  such that  $\|X\| \leq b$  for all  $X \in \mathcal{L}_k$ ) and thus  $\mathcal{L}_k$  is compact.

The *orthogonal evolution*  $D_k$  is, as its name suggests, orthogonal to  $\nabla A_k$ . That is, for fixed values of the parameters  $\Phi_k$  and  $\Gamma_k$ , one has

$$\langle D_k(X; \Phi_k, \Gamma_k) | \nabla A_k(X; \Gamma_k) \rangle = 0 \quad \forall X. \quad (1.2)$$

This orthogonality condition leads us to distinguish the two disjoint set of parameters  $\Phi_k$  and  $\Gamma_k$ .

- $\Phi_k$  are called **flow parameters**. They parametrize the time evolution on  $\mathcal{L}_k$  without affecting its geometry. They are characterized by the fact that they do not affect the orthogonality between the vector fields  $D_k$  and  $\nabla A_k$ . In other words,  $\Phi_k$  are the parameters of  $D_k$  with the following property

$$\langle D_k(X; \Phi_k, \Gamma_k) | \nabla A_k(X; \Gamma_k) \rangle = 0 \quad \forall X, \Phi_k.$$

This implies that one can arbitrarily fix the values for  $\Phi_k$  and, once fixed, one has the orthogonality of condition in 1.2. When the local attracting submanifold  $\mathcal{L}_k$  has a dimension of 1, there is only one flow parameter. It effectively defines the time scale of the orbits on  $\mathcal{L}_k$  but not its geometry. For  $\mathcal{L}_k$  with higher dimensions, several flow parameters may exist. Note that any O-G system has always at least one flow parameter (i.e.  $\Phi_k$  is not empty) since  $D_k$  can always be multiplied by a scalar which fixes a time scale of the dynamics.

- $\Gamma_k$  are called **geometric parameters**. They determine the geometry of  $\mathcal{L}_k$ . They also affect  $D_k$ , since the orthogonality of  $D_k$  with  $\nabla A_k$  must be maintained.

Note that the generalized Hamiltonian dynamical systems discussed in [35] offer an alternatively way to classify our dynamics by following the lines recently exposed in [19]. We distinguish between a *collection of homogeneous* and a *collection of heterogeneous* O-G systems that we now define.

**Definition 1.1.** *A collection of homogeneous O-G systems have the same  $D_k$  functional, that is*

$$\text{for all } \Lambda_*, D_k(\cdot; \Lambda_*) \equiv D_j(\cdot; \Lambda_*) \text{ for all } k, j.$$

*A collection of heterogeneous O-G systems have different functional  $D_k$ , that is*

$$\text{there exists } k, j, \Lambda_k \text{ and } \Lambda_j \text{ such that } D_k(\cdot; \Lambda_k) \not\equiv D_j(\cdot; \Lambda_j).$$

Note that the definition for a collection of homogeneous O-G systems implies that all **local dynamics** have the same number of parameters (i.e.  $|\Lambda_k| = |\Lambda_j|$  for all  $j, k$ ) but the values of these parameters are not necessarily the same. The following lemma characterizes the stability of the **local dynamics**. For simplicity's sake, we omit the index  $k$  for the rest of this section.

**Lemma 1.1.** *There exists a set  $\mathcal{U} \supset \mathcal{L}$  such that all orbits solving*

$$\dot{X} = D(X; \Phi, \Gamma) - \nabla A(X; \Gamma)$$

*with initial conditions in  $\mathcal{U}$  converge towards  $\mathcal{L}$ .*

*Proof.* In this proof, we will not explicitly write the parameters  $\Lambda$ . Since  $\mathcal{L}$  is a submanifold, for all  $X^* \in \mathcal{L}$ , there exists a neighborhood  $\mathcal{U}_{X^*}$  of  $X^*$ . Let  $\mathcal{U}$  be the union of all these neighborhoods (i.e.  $\mathcal{U} \subseteq \bigcup_{X^* \in \mathcal{L}} \mathcal{U}_{X^*}$ ). The convergence towards  $\mathcal{L}$  follows from Ляпунов's second method with Ляпунов function:

$$A(X) = \frac{1}{2} \sum_{j \in I} G_j(X)^2$$

By construction, we have  $\mathcal{L} = \{X \in \mathbb{R}^p | A(X) = 0\}$ . Computing the time derivative

$$\begin{aligned} \langle \nabla A(X) | \dot{X} \rangle &= \langle \nabla A(X) | D(X) - \nabla A(X) \rangle \\ &= \underbrace{\langle \nabla A(X) | D(X) \rangle}_{=0} - \|\nabla A(X)\|^2 \leq 0 \end{aligned}$$

and we have

$$\|\nabla A(X)\|^2 = 0 \iff \sum_{s=1}^p \left( \sum_{j \in I} G_j(X) \frac{\partial G_j}{\partial x_s}(X) \right)^2 = 0 \iff \sum_{j \in I} G_j(X) \nabla G_j(X) = \mathbf{0},$$

where  $\mathbf{0}$  is a  $p$ -dimensional zero vector. We note  $G \equiv (G_{j_1}, \dots, G_{j_{p-m}})$  with  $j_s \in I$ ,  $s = 1, \dots, p-m$  and  $p-m = |I|$ . Since  $\mathfrak{D}G(X)$  has full rank  $p-m$  for  $X \in \mathcal{U}$ , its row vectors are linearly independent ( $\mathfrak{D}$  stands for the derivative operator). Therefore  $\sum_{j \in I} G_j(X) \nabla G_j(X) = \mathbf{0}$  if and only if the scalars  $G_j(X) = 0$  for all  $j \in I$ . This is equivalent to saying that  $X \in \mathcal{L}$ . Therefore, the strict inequality  $\langle \nabla A(X) | \dot{X} \rangle < 0$  holds for  $X \in \mathcal{U} \setminus \mathcal{L}$ , and the compact set  $\mathcal{L}$  is asymptotically stable (refer to Appendix A). □

Here are examples of O-G systems, among which, the well known mixed canonical-dissipative systems, initially introduced in [24, 47, 46].

**Example 1.1. Mixed Canonical-Dissipative (MCD) Dynamics** Here,  $p = 2$ ,  $m = 1$  and  $G_1(x, y; \Gamma) := H(x, y; \Gamma) - r$ , where  $H(x, y; \Gamma)$  is a Hamiltonian (i.e. energy) function on  $\mathbb{R}^2$  into  $\mathbb{R}_{\geq 0}$  and  $\Gamma$  a set of geometric parameters. For a given  $0 < r \in \Gamma$ , the set  $\mathcal{L} := \{(x, y) \in \mathbb{R}^2 \mid H(x, y; \Gamma) - r = 0\}$  is a finite number of closed, none-intersecting curves in  $\mathbb{R}^2$ . Their shapes are determined by  $\Gamma$  and by the functional  $H$ . We define (without explicitly writing  $\Gamma$ )

$$D(x, y) := \mathbf{w} \begin{pmatrix} \frac{\partial H}{\partial y}(x, y) \\ -\frac{\partial H}{\partial x}(x, y) \end{pmatrix}$$

where  $\mathbf{w}$  is fixed and constant flow parameter. A MCD is given as

$$\begin{aligned} \dot{x} &= \mathbf{w} \frac{\partial H}{\partial y}(x, y) - (H(x, y) - r) \frac{\partial H}{\partial x}(x, y), \\ \dot{y} &= \underbrace{-\mathbf{w} \frac{\partial H}{\partial x}(x, y)}_{\text{canonical evolution}} - \underbrace{(H(x, y) - r) \frac{\partial H}{\partial y}(x, y)}_{\text{dissipative evolution}}. \end{aligned} \tag{1.3}$$

The *dissipative evolution* is the gradient of the potential  $A(x, y) := \frac{1}{2}(H(x, y) - r)^2$ . According to the value of  $H$ , this non-conservative controller feeds or dissipates energy until equilibrium state is reached, i.e. when  $H(x, y) - r = 0$ . Therefore, the energy-type control  $(H - r)$  drives all orbits towards the attractor  $\mathcal{L}$ . On  $\mathcal{L}$  the dynamics is purely Hamiltonian and it is governed by the *canonical evolution*. The system defined by Eqs. (1.3) belongs to the general class of mixed canonical-dissipative (MCD) systems initially introduced in [24, 47, 46].

The general form of MCD systems are given by Eqs. (1.3) when the scalar  $(H(x, y) - r)$  in front of the gradient in the *dissipative evolution* is replaced by  $U(H(x, y))$  where  $U$  is a function on  $\mathbb{R}_{\geq 0}$  into  $\mathbb{R}$  that only vanishes at  $r$  (i.e.  $U(r) = 0$ ). If, furthermore, its derivative is strictly positive (i.e.  $U'(x) > 0$ ), then  $(x, y) \mapsto \frac{1}{2}U(H(x, y))^2$  is a Ляпунов function and hence  $\mathcal{L}$  is an attractor.

In Eqs. (1.3),  $\Lambda = \{\mathbf{w}, \Gamma\}$  are, for the time being, fixed parameters: the flow parameter  $\mathbf{w}$  controls the angular velocity of the *canonical evolution* while the geometric parameters  $\Gamma$  determine the shape of the attractor.

**HOPF** The Hamiltonian is  $H(x, y) = x^2 + y^2$  and its' dynamics reads as (after a time rescaling:  $x(t) \mapsto x(2t)$ )

$$\begin{aligned} \dot{x} &= \mathbf{w} y - (x^2 + y^2 - r)x, \\ \dot{y} &= -\mathbf{w} x - (x^2 + y^2 - r)y. \end{aligned}$$

The solution is explicitly given by

$$\begin{aligned}x(t) &= \sqrt{r} \left(1 + \exp(-2rt) \left(\frac{r}{x_0^2 + y_0^2} - 1\right)\right)^{-\frac{1}{2}} \sin(\omega t + \theta_0), \\y(t) &= \sqrt{r} \left(1 + \exp(-2rt) \left(\frac{r}{x_0^2 + y_0^2} - 1\right)\right)^{-\frac{1}{2}} \cos(\omega t + \theta_0),\end{aligned}$$

with initial condition  $(x_0, y_0) \in \mathbb{R}^2$  and its argument  $\theta_0$  (counted positively from the y-axis in clockwise direction). For a given  $r$ , the attractor is a limit cycle whose geometry is a circle with radius  $\sqrt{r}$ .

**MATHEWS-LAKSHMANAN** As an example of a none linear *canonical evolution*, consider the MATHEWS-LAKSHMANAN oscillator presented in [30]. The Hamiltonian is  $H(x, y; \mathbf{a}) = \log(\cosh(y)) + \frac{1}{2} \log(\mathbf{a} + x^2)$  with  $\mathbf{a} > 0$ , and its' dynamics reads as

$$\begin{aligned}\dot{x} &= \omega \tanh(y) - (H(x, y; \mathbf{a}) - r) \frac{x}{\mathbf{a} + x^2}, \\ \dot{y} &= -\omega \frac{x}{\mathbf{a} + x^2} - (H(x, y; \mathbf{a}) - r) \tanh(y).\end{aligned}$$

The solution of the canonical dynamics (i.e. initial condition on  $\mathcal{L}$ ) is explicitly given by (refer to Appendix B)

$$\begin{aligned}x(t) &= \sqrt{\exp(2r) - \mathbf{a}} \sin\left(\frac{\omega}{\exp(r)} t + \theta_0\right), \\ y(t) &= \tanh^{-1}\left(\frac{\sqrt{\exp(2r) - \mathbf{a}}}{\exp(r)} \cos\left(\frac{\omega}{\exp(r)} t + \theta_0\right)\right).\end{aligned}$$

Note that the solution exhibits an amplitude-dependent frequency which is a typical signature of nonlinear oscillators.

**Глаз** The Hamiltonian is  $H(x, y; \mathbf{a}, \mathbf{b}) = \frac{x^2}{\mathbf{a}(x^2 + y^2) + 1 - \mathbf{a}} + \frac{y^2}{\mathbf{b}(x^2 + y^2) + 1 - \mathbf{b}}$  with  $\mathbf{a}, \mathbf{b} \in ]0, 1[$  and  $\mathbf{a} \neq \mathbf{b}$ , and its' dynamics reads as

$$\begin{aligned}\dot{x} &= \omega \left(\frac{2y(\mathbf{b}x^2 + 1 - \mathbf{b})}{g_b^2} - \frac{2axyx^2}{g_a^2}\right) - (H(x, y; \mathbf{a}, \mathbf{b}) - r) \left(\frac{2x(\mathbf{a}y^2 + 1 - \mathbf{a})}{g_a^2} - \frac{2byy^2}{g_b^2}\right), \\ \dot{y} &= -\omega \left(\frac{2x(\mathbf{a}y^2 + 1 - \mathbf{a})}{g_a^2} - \frac{2bxy^2}{g_b^2}\right) - (H(x, y; \mathbf{a}, \mathbf{b}) - r) \left(\frac{2y(\mathbf{b}x^2 + 1 - \mathbf{b})}{g_b^2} - \frac{2axyx^2}{g_a^2}\right).\end{aligned}$$

with  $g_a = \mathbf{a}(x^2 + y^2) + 1 - \mathbf{a}$  and  $g_b = \mathbf{b}(x^2 + y^2) + 1 - \mathbf{b}$ . The solution of the canonical dynamics on the specific limit cycle  $\mathcal{L} = \mathbb{S}^1$  is explicitly given by (refer to Appendix B)

$$\begin{aligned}x(t) &= \cos\left(\tan^{-1}\left(\frac{\sqrt{1-\mathbf{a}}}{\sqrt{1-\mathbf{b}}}\right) \tan(-2\sqrt{1-\mathbf{a}}\sqrt{1-\mathbf{b}}\omega t) + \theta_0\right), \\ y(t) &= \sin\left(\tan^{-1}\left(\frac{\sqrt{1-\mathbf{a}}}{\sqrt{1-\mathbf{b}}}\right) \tan(-2\sqrt{1-\mathbf{a}}\sqrt{1-\mathbf{b}}\omega t) + \theta_0\right).\end{aligned}$$

**CASSINI** The Hamiltonian is  $H(x, y; \mathbf{a}) = ((x - \sqrt{\mathbf{a}})^2 + y^2)((x + \sqrt{\mathbf{a}})^2 + y^2)$  and its' dynamics reads as

$$\begin{aligned}\dot{x} &= \omega 4y(x^2 + y^2 + \mathbf{a}) - (H(x, y; \mathbf{a}) - r) 4x(x^2 + y^2 - \mathbf{a}), \\ \dot{y} &= -\omega 4x(x^2 + y^2 - \mathbf{a}) - (H(x, y; \mathbf{a}) - r) 4y(x^2 + y^2 + \mathbf{a}).\end{aligned}$$

Here, for a  $\mathcal{L}$  to be a unique closed curve, the parameters must satisfy  $0 \leq \sqrt{\mathbf{a}} < r$ . When  $\mathbf{a} = 0$ , the limit cycle  $\mathcal{L}$  is a circle of radius  $r^{\frac{1}{4}}$ .

**ENTROPY** The Hamiltonian is  $H(x, y; \mathbf{a}, \mathbf{b}, \mathbf{d}) = -\mathbf{a}x \ln(x) - \mathbf{b}y \ln(y) - \mathbf{d}(1 - x - y) \ln(1 - x - y)$  and it is defined in the interior of a 1-simplex  $\{(x, y) \in \mathbb{R}_{\geq 0}^2 \mid x + y < 1\}$ . Its' MCD dynamics reads as

$$\begin{aligned}\dot{x} &= \omega (-\mathbf{b} \ln(x) + \mathbf{d} \ln(1 - y - x) + \mathbf{d} - \mathbf{b}) \\ &\quad - (H(x, y; \mathbf{a}, \mathbf{b}, \mathbf{d}) - r) (-\mathbf{a} \ln(x) + \mathbf{d} \ln(1 - y - x) + \mathbf{d} - \mathbf{a}), \\ \dot{y} &= -\omega (-\mathbf{a} \ln(x) + \mathbf{d} \ln(1 - y - x) + \mathbf{d} - \mathbf{a}) \\ &\quad - (H(x, y; \mathbf{a}, \mathbf{b}, \mathbf{d}) - r) (-\mathbf{b} \ln(y) + \mathbf{d} \ln(1 - y - x) + \mathbf{d} - \mathbf{b}).\end{aligned}$$

OHR The Hamiltonian is  $H(x, y) = (\sqrt{\sin(x^2 + y^2 - 1)^2 + 1})x^2 + y^2$ . Its' MCD dynamics reads as

$$\begin{aligned}\dot{x} &= w \left( 2y + \frac{2x^2 y c_r s_r}{\sqrt{s_r^2 + 1}} \right) - (H(x, y) - r) \left( 2x \sqrt{s_r^2 + 1} + \frac{2x^3 c_r s_r}{\sqrt{s_r^2 + 1}} \right) \\ \dot{y} &= -w \left( 2x \sqrt{s_r^2 + 1} + \frac{2x^3 c_r s_r}{\sqrt{s_r^2 + 1}} \right) - (H(x, y) - r) \left( 2y + \frac{2x^2 y c_r s_r}{\sqrt{s_r^2 + 1}} \right)\end{aligned}$$

with  $c_r = \cos(x^2 + y^2 - 1)$  and  $s_r = \sin(x^2 + y^2 - 1)$ . At  $r = 1$  and  $\pi + 1$ , the respective limit cycles are circles ( $\mathbb{S}^1$  and a circle with radius  $\sqrt{\pi + 1}$ ). On these two limit cycles, the dynamics is the same as a HOPF oscillator.

*Example 1.2. Mixed Canonical Modulated-Dissipative (MCMD) Dynamics* For a given strictly positive (or negative) function  $W(x, y; \Lambda)$ , we define (without explicitly writing the parameters  $\Lambda$ )

$$D(x, y) := W(x, y) \begin{pmatrix} \frac{\partial H}{\partial y}(x, y) \\ -\frac{\partial H}{\partial x}(x, y) \end{pmatrix}.$$

A MCMD is given as

$$\begin{aligned}\dot{x} &= W(x, y) \frac{\partial H}{\partial y}(x, y) - (H(x, y) - r) \frac{\partial H}{\partial x}(x, y), \\ \dot{y} &= -W(x, y) \frac{\partial H}{\partial x}(x, y) - (H(x, y) - r) \frac{\partial H}{\partial y}(x, y).\end{aligned}$$

This is a limit cycle oscillator with function  $W$  playing the role of a clock controlling the local time scale of the orbits on  $\mathcal{L}$ . As an illustration, consider  $H(x, y; \mathbf{a}, \mathbf{b}, \mathbf{d}, \mathbf{e}) = -\mathbf{a} \log(y) + \mathbf{b}y - \mathbf{d} \log(x) + \mathbf{e}x$  and  $W(x, y; \Lambda) = wxy$  ( $w$  a flow parameter), both defined on the strictly positive quadrant  $\mathbb{R}_{>0}^2$  and with strictly positive geometric parameters  $\Gamma = \{r, \mathbf{a}, \mathbf{b}, \mathbf{d}, \mathbf{e}\}$ . The resulting dynamics on the limit cycle  $\mathcal{L}$  is described by the LOTKA-VOLTERRA equations

$$\begin{aligned}\dot{x} &= w(\mathbf{a}x - \mathbf{b}xy), \\ \dot{y} &= -w(\mathbf{d}y - \mathbf{e}xy).\end{aligned}$$

*Example 1.3. Dynamics on  $\mathbb{S}^2$*  Here,  $p = 3$ ,  $m = 2$  and  $G_1(x, y, z) := x^2 + y^2 + z^2 - 1$ . Hence, the attracting submanifold is  $\mathbb{S}^2$ . Due to the dimensionality of the attracting submanifold, several possibilities exist for  $D$ . For instance, with three flow parameters  $\Phi := \{w_1, w_2, w_3\}$

EULER equations	Linear solenoidal vector field
$D(X; \Lambda) = \begin{pmatrix} (w_2 - w_3)yz \\ (w_3 - w_1)xz \\ (w_1 - w_2)xy \end{pmatrix}$	$D(X; \Lambda) = \begin{pmatrix} 0 & w_1 & w_2 \\ -w_1 & 0 & w_3 \\ -w_2 & -w_3 & 0 \end{pmatrix} \begin{pmatrix} x \\ y \\ z \end{pmatrix}.$

*Example 1.4. Dynamics on 1-dimensional submanifold* Here,  $p = 3$  and  $m = 1$  and to create an attractor of dimension 1, we need two functions:  $G_1$  and  $G_2$ . Let us explicit three illustrations. For all cases, the vector  $D$  is uniquely determined, up to a constant and orientation.

*i) Sphere - Sphere*

$G_1(x, y, z) := x^2 + y^2 + z^2 - 1$  and  $G_2(x, y, z) := (x - \frac{2}{3})^2 + (y - \frac{2}{3})^2 + (z - \frac{2}{3})^2 - 1$

$$\begin{pmatrix} \dot{x} \\ \dot{y} \\ \dot{z} \end{pmatrix} = w \begin{pmatrix} y - z \\ z - x \\ x - y \end{pmatrix} - 2G_1(x, y, z) \begin{pmatrix} x \\ y \\ z \end{pmatrix} - 2G_2(x, y, z) \begin{pmatrix} x - \frac{2}{3} \\ y - \frac{2}{3} \\ z - \frac{2}{3} \end{pmatrix}$$

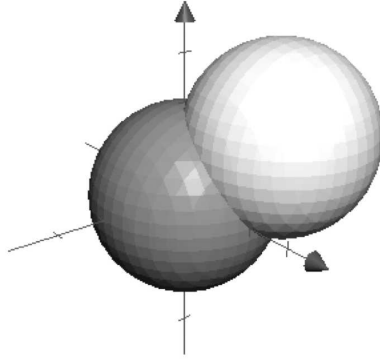


Fig. 1.1: Two spheres given by  $G_1(x, y, z) := x^2 + y^2 + z^2 - 1$  (dark gray) and  $G_2(x, y, z) := (x - \frac{2}{3})^2 + (y - \frac{2}{3})^2 + (z - \frac{2}{3})^2 - 1$  (light gray).

*ii) Sphere - Plane*

$G_1(x, y, z) := x^2 + y^2 + z^2 - 1$  and  $G_2(x, y, z) := x + y + z - 1$

$$\begin{pmatrix} \dot{x} \\ \dot{y} \\ \dot{z} \end{pmatrix} = w \begin{pmatrix} y - z \\ z - x \\ x - y \end{pmatrix} - 2G_1(x, y, z) \begin{pmatrix} x \\ y \\ z \end{pmatrix} - G_2(x, y, z) \begin{pmatrix} 1 \\ 1 \\ 1 \end{pmatrix}$$

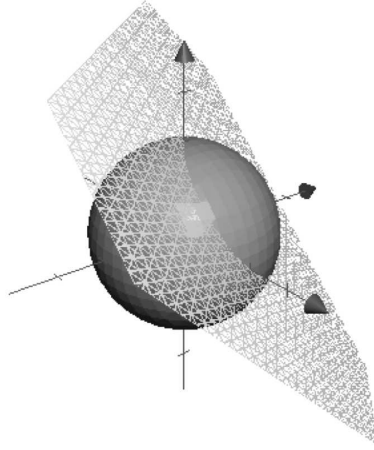


Fig. 1.2: One sphere given by  $G_1(x, y, z) := x^2 + y^2 + z^2 - 1$  (dark gray) and one plane given by  $G_2(x, y, z) := x + y + z - 1$  (light striped gray).

For both cases *i)* and *ii)*, all orbits converge towards a circle lying on the plane  $G_2(x, y, z) := x + y + z - 1$  with radius  $\sqrt{\frac{2}{3}}$  and center  $(\frac{1}{3}, \frac{1}{3}, \frac{1}{3})$ . The orbit circulation on this attracting sub-manifold is identical for both examples. However, the transient dynamics (i.e. the convergence rate towards the attractor) explicitly depends on the choice of the  $G_j$  functions.

*iii) Torus - Sphere*

$G_1(x, y, z; r_1, r_2) := (x^2 + y^2 + z^2 + r_1^2 - r_2^2)^2 - 4r_1^2(x^2 + y^2)$  (a torus centered at the origin) and  $G_2(x, y, z; a) := (x - a)^2 + y^2 + z^2 - 1$ . The geometric parameters  $r_1, r_2$  and  $a$  are chosen such that the intersection between the torus and the sphere forms a closed curve.

$$\begin{pmatrix} \dot{x} \\ \dot{y} \\ \dot{z} \end{pmatrix} = w \begin{pmatrix} -2yz r_1^2 \\ z(g_m(x - a) - g_p x) \\ a y g_p \end{pmatrix} - 4G_1(x, y, z; r_1, r_2) \begin{pmatrix} g_p x \\ g_p y \\ g_m z \end{pmatrix} - 2G_2(x, y, z; a) \begin{pmatrix} x - a \\ y \\ z \end{pmatrix}$$



with  $g_p = x^2 + y^2 + z^2 - (r_2^2 + r_1^2)$  and with  $g_m = x^2 + y^2 + z^2 - (r_2^2 - r_1^2)$ .

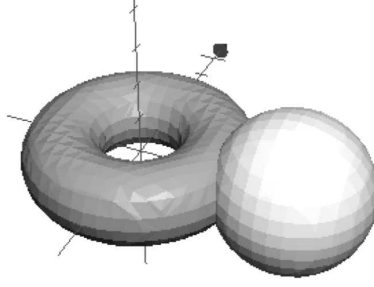


Fig. 1.3: One torus given by  $G_1(x, y, z; 1, \frac{1}{2}) := (x^2 + y^2 + z^2 + \frac{3}{4})^2 - 4(x^2 + y^2)$  (dark gray) and one sphere given by  $G_2(x, y, z; 2) := (x-2)^2 + y^2 + z^2 - 1$  (light gray).

### 1.1.2 Coupling Dynamics: $C_k$

**Local dynamics** are coupled together through two different types of interactions: via a potential or through a linear combination of coupling functions. The latter type will be applied only for local system of dimension 2 (i.e.  $p = 2$ ). We therefore present it here for this case, although it can be straightforwardly generalized to any arbitrary dimension.

Concerning the explicit dependence of  $C_k$  on time, we use the following convention. If  $C_k$  explicitly depends on  $t$ , it implies that the connections between the vertices of the underlying network are time-dependent. If not, it means that the connections are fixed once and for all.

#### Potential Coupling

Consider the gradient of a twice continuously differentiable positive semi-definite potential  $V(t, X) \geq 0$  for all  $t$ . Here, **coupling dynamics** is defined as

$$C_k(t, X) := -c_k \frac{\partial V}{\partial X_k}(t, X),$$

with  $X = (X_1, \dots, X_N) \in \mathbb{R}^{pN}$  and strictly positive, fixed and constant, *coupling strengths*  $c_k > 0$ . The function  $V$  depends on different parameters, in particular, the entries of a  $N \times N$  weighted adjacency matrix  $A(t)$  associated to a given connected, undirected and time-dependent network (refer to Appendix C). To ensure consistency of function  $V$  with respect to the entries  $a_{k,j}$  of  $A$ , we impose that if  $a_{k,j}(t) = 0$  for all  $t$  (and hence  $a_{j,k}(t) = 0$ , since the network is undirected), then the  $p \times p$  dimensional matrix  $\frac{\partial^2 V}{\partial X_j \partial X_k}(t, X) = \mathbf{0}$  for all  $t$ . This ensures that only adjacent vertices interact<sup>1</sup>. We further suppose that

$$X_k = X_j \quad \forall k, j \quad \iff \quad V(t, X) = 0 \quad \forall t, \quad (1.4)$$

where  $X_k = (x_{k,1}, \dots, x_{k,p}) \in \mathbb{R}^p$  are the **state variables**. Any  $X \in \mathbb{R}^{pN}$  satisfying Eqs. (1.4) is a minimum of  $V$ , and therefore  $\nabla V(t, X) = \mathbf{0}$  for all  $t$  (i.e. local systems with equal dynamical states do not interact).

**Example 1.5. Laplacian Potential** Let  $L$  be a  $N \times N$  Laplacian matrix associated to an adjacency matrix  $A$  of a connected and undirected network (refer to Appendix C) with  $N$  vertices and positive entries (i.e.  $a_{k,j} = a_{j,k} \geq 0$  for all  $j, k$ ). The Laplacian Potential is defined as

<sup>1</sup> Since  $V$  is twice continuously differentiable, then interchanging the order of differentiation gives the same second partial derivatives and so  $\frac{\partial^2 V}{\partial X_k \partial X_j}(t, X) = \mathbf{0}$ .

$$V(X) = \frac{1}{2} \sum_{j=1}^p \mathbf{a}_j \langle x_j | Lx_j \rangle$$

with  $0 < \mathbf{a}_j$  and  $x_j := (x_{1,j}, \dots, x_{N,j})$ ,  $j = 1, \dots, p$ , and where  $x_{k,j}$  is the  $j^{\text{th}}$  state variable of the  $k^{\text{th}}$  local dynamics. Defined as such,  $V$  is positive semi-definite and the equivalence in Eqs. (1.4) holds (refer to Appendix C). The Laplacian potential type of coupling is straightforwardly generalized to the time-dependent case: it suffice to introduce time dependent edges via the underlying connected, undirected and time-dependent network.

### Linear combination of Coupling Functions

Let  $L(t)$  be a Laplacian matrix associated to a connected, undirected and time-dependent network with positive adjacency entries. Here  $X_k = (x_k, y_k)$  and the coupling dynamics is defined as

$$\begin{aligned} \mathbf{C}_{k,1}(t, X; \Gamma, \Delta) &:= c_k \sum_{j=1}^N l_{k,j}(t) \mathbf{u}_j \mathbf{Q}_{x_j}(X_j; \Gamma_j), \\ \mathbf{C}_{k,2}(t, X; \Gamma, \Delta) &:= c_k \sum_{j=1}^N l_{k,j}(t) \mathbf{v}_j \mathbf{Q}_{y_j}(X_j; \Gamma_j), \end{aligned}$$

with  $\Gamma = \{\Gamma_1, \dots, \Gamma_N\}$ ,  $\Delta = \{\mathbf{u}_1, \dots, \mathbf{u}_N, \mathbf{v}_1, \dots, \mathbf{v}_N\}$  a set of fixed and constant coupling weights and where  $0 < c_k$  are strictly positive, fixed and constant, coupling strengths,  $l_{k,j}$  are the entries of  $L$  and finally

$$\mathbf{Q}_x, \mathbf{Q}_y : \mathbb{R}^{2N} \longrightarrow \mathbb{R}^N.$$

are two coupling functions. We distinguish between homogenous and heterogenous coupling functions that we define below.

**Definition 1.2.** Homogenous coupling functions  $\mathbf{Q}_x$  and  $\mathbf{Q}_y$  are such that, respectively, their coordinates have the same functional, that is

$$\text{for all } \Gamma_*, \mathbf{Q}_{x_k}(\cdot; \Gamma_*) \equiv \mathbf{Q}_{x_j}(\cdot; \Gamma_*) \text{ and } \mathbf{Q}_{y_k}(\cdot; \Gamma_*) \equiv \mathbf{Q}_{y_j}(\cdot; \Gamma_*) \text{ for all } k, j.$$

Heterogenous coupling functions  $\mathbf{Q}_x$  and  $\mathbf{Q}_y$  are such that, either  $\mathbf{Q}_x$  or  $\mathbf{Q}_y$  has at least two coordinates with different functionals, that is

$$\text{there exists } k, j, \Gamma_k \text{ and } \Gamma_j \text{ or, there exists, } m, n, \Gamma_m \text{ and } \Gamma_n \text{ such that} \\ \mathbf{Q}_{x_k}(\cdot; \Gamma_k) \not\equiv \mathbf{Q}_{x_j}(\cdot; \Gamma_j) \text{ or } \mathbf{Q}_{y_m}(\cdot; \Gamma_m) \not\equiv \mathbf{Q}_{y_n}(\cdot; \Gamma_n).$$

Here are examples of coupling functions.

#### Example 1.6. Coupling Functions

**Identity**  $\mathbf{Q}_{x_k}(x, y) = x$  and  $\mathbf{Q}_{y_k}(x, y) = y$ . In this case, local dynamics interact as if they were coupled via the gradient of a Laplacian potential (refer to Example (1.5))  $V(X) = \frac{1}{2}(\langle x | Lx \rangle + \langle y | Ly \rangle)$  with  $x = (x_1, \dots, x_N)$  (idem for  $y$ ).

**Gradient**  $\mathbf{Q}_{x_k}(x, y; \Gamma_k) = \frac{\partial H_k}{\partial x}(x, y; \Gamma_k)$  and  $\mathbf{Q}_{y_k}(x, y; \Gamma_k) = \frac{\partial H_k}{\partial y}(x, y; \Gamma_k)$ .

**Normalized Gradient**  $\mathbf{Q}_{x_k}(x, y; \Gamma_k) = \frac{\frac{\partial H_k}{\partial x}}{\sqrt{\frac{\partial H_k}{\partial x}^2 + \frac{\partial H_k}{\partial y}^2}}$  and  $\mathbf{Q}_{y_k}(x, y; \Gamma_k) = \frac{\frac{\partial H_k}{\partial y}}{\sqrt{\frac{\partial H_k}{\partial x}^2 + \frac{\partial H_k}{\partial y}^2}}$  with evaluation at  $(x, y; \Gamma_k)$ .

The nature of the coupling dynamics is characterized by the following Lemma.

**Lemma 1.2.** Let  $L(t)$  be a Laplacian matrix associated to a connected, undirected and time-dependent network with positive adjacency entries. We have, for any  $X \in \mathbb{R}^{2N}$

$$\left. \begin{aligned} \mathbf{C}_{k,1}(t, X; \Gamma, \Delta) = 0 \\ \mathbf{C}_{k,2}(t, X; \Gamma, \Delta) = 0 \end{aligned} \right\} \forall k, t \iff \left\{ \begin{aligned} \mathbf{u}_j \mathbf{Q}_{x_j}(X_j; \Gamma_j) = \mathbf{u}_k \mathbf{Q}_{x_k}(X_k; \Gamma_k) =: \bar{x} \\ \mathbf{v}_j \mathbf{Q}_{y_j}(X_j; \Gamma_j) = \mathbf{v}_k \mathbf{Q}_{y_k}(X_k; \Gamma_k) =: \bar{y} \end{aligned} \right\} \forall j, k, t.$$

*Proof.* [ $\Rightarrow$ ] Since the network is connected, the dimension of the kernel of  $L(t)$  is one for all  $t$ . As  $C_{k,1}(t, X; \Gamma, \Delta)$  (respectively  $C_{k,2}(t, X; \Gamma, \Delta)$ ) is the product between  $c_k > 0$ , the  $k^{th}$  line of  $L(t)$  and  $(u_1 Q_{x_1}(X_1; \Gamma_1), \dots, u_N Q_{x_N}(X_N; \Gamma_N))$  (respectively  $(v_1 Q_{y_1}(X_1; \Gamma_1), \dots, v_N Q_{y_N}(X_N; \Gamma_N))$ ), there exist  $\bar{x}$  and  $\bar{y}$  such that

$$\bar{x} = u_j Q_{x_j}(X_j; \Gamma_j) \quad \text{and} \quad \bar{y} = v_j Q_{y_j}(X_j; \Gamma_j) \quad \forall j$$

and therefore

$$u_j Q_{x_j}(X_j; \Gamma_j) = u_k Q_{x_k}(X_k; \Gamma_k) \quad \text{and} \quad v_j Q_{y_j}(X_j; \Gamma_j) = v_k Q_{y_k}(X_k; \Gamma_k) \quad \forall j, k.$$

[ $\Leftarrow$ ] By definition of the matrix  $L(t)$ , we have:

$$\sum_{j=1}^N l_{k,j}(t) u_j Q_{x_j}(X_j; \Gamma_j) = \bar{x} \sum_{j=1}^N l_{k,j}(t) = 0.$$

Along the same lines for  $v_j Q_{y_j}$ , the proof follows. □

## 1.2 Network's Dynamical System - With Adaptive Mechanisms

We here present the general form of the dynamical system that is considered in this work with adaptive mechanism. It is encompassed by Eqs. (0.1) and reads

$$\begin{aligned} \dot{X}_k &= \underbrace{D_k(X_k, \Phi_k, \Gamma_k) - \nabla A_k(X_k, \Gamma_k)}_{\text{local dynamics}} - \underbrace{C_k(t, X, \Gamma, \Delta)}_{\text{coupling dynamics}} \\ \dot{\Phi}_k &= P_k^\Phi(X, \Gamma, \Delta) \\ \dot{\Gamma}_k &= \underbrace{P_k^\Gamma(X, \Gamma, \Delta)}_{\text{parametric dynamics}} \\ \dot{\Delta} &= \underbrace{B(X, \Gamma, \Delta)}_{\text{binding dynamics}} \end{aligned} \quad k = 1, \dots, N. \quad (1.5)$$

**Local Dynamics** Local system are of dimension  $p$  and belong to the class of ortho-gradient (O-G) systems (refer to Section 1.1.1).

**Coupling Dynamics** Interactions will either derive from the gradient of a given positive function or through a linear combination of coupling functions (refer to Section 1.1.2).

**Parametric Dynamics** Adaptive mechanisms are introduced to tune the flow parameters and shape the local attractors (refer to Section 1.2.1).

**Binding Dynamics** The coupling weights are dynamically self-adjusted (refer to Section 1.1.2).

### 1.2.1 Parametric Dynamics: $P_k$

The **parametric dynamics** are functions  $P_k$  that govern the adaptation in the local systems' parameters  $\Lambda_k$ . Adaptivity in the local systems is realized by letting the fixed and constant local parameters  $\Lambda_k$  become time-dependent. When this is done, we use the following notation

$$\begin{aligned} \Lambda_k &= \Phi_k \uplus \Gamma_k \\ &= \{w_{k,1}, \dots, w_{k,n_k}\} \uplus \{g_{k,1}, \dots, g_{k,n_k-q_k}\} \rightsquigarrow \{\omega_{k,1}(t), \dots, \omega_{k,n_k}(t)\} \uplus \{\gamma_{k,1}(t), \dots, \gamma_{k,n_k-q_k}(t)\} \\ &= \Phi_k(t) \uplus \Gamma_k(t) = \Lambda_k(t). \end{aligned}$$

Fixed and constant local parameters are denoted with thick Latin letters. When they become time-dependent, they are written with Greek letters. Their rate of change  $\dot{A} = (\dot{A}_1, \dots, \dot{A}_N)$  is determined by the **parametric dynamics**  $\mathbf{P} \equiv (\mathbf{P}_1, \dots, \mathbf{P}_N)$  and  $\mathbf{P}_k \equiv (\mathbf{P}_k^\Phi, \mathbf{P}_k^\Gamma)$ . The functions  $\mathbf{P}_k^\Phi$  and  $\mathbf{P}_k^\Gamma$  act on  $\Phi_{k(t)}$  and  $\Gamma_{k(t)}$  respectively.

When  $\mathbf{P} \neq \mathbf{0}$ , the elements in the set  $A_k$  acquire the status of variables of the global dynamical system and are known as **parametric variables**. Along the same line of denomination,  $\Phi_{k(t)}$  are known as **flow parametric variables** (f-PV) and  $\Gamma_{k(t)}$  as **geometric parametric variables** (g-PV). If, after a certain time,  $\mathbf{P} \equiv \mathbf{0}$ , then the **parametric variables**  $A_{k(t)}$  are constants for all  $k$  and they recover their original status of fixed and constant parameters.

In general,  $\mathbf{P}$  depends on an underlying network and on  $X = (X_1, \dots, X_N)$  and  $\Lambda = (\Lambda_1, \dots, \Lambda_N)$ .

- The  $A_k$  interact through a connected and undirected network with positive adjacency entries. If not explicitly stated, this network is supposed to be the same as the one considered in Section 1.1.2.
- There are three different ways in which  $\mathbf{P}$  can depend on the variables  $X$  and  $\Lambda$ : either only on  $X$ , either only on  $\Lambda$  or on both,  $X$  and  $\Lambda$ . The function  $\mathbf{P}$  will never depend on  $\Lambda$  alone - this would correspond to a collection of local systems with given time-dependent parameters. This is the case when the network is influenced by an external signal. To justify the wording “self-adaptive”, we always suppose that  $\mathbf{P}$  depends either only on  $X$  or on  $X$  and  $\Lambda$ . The basic intuitive case, in this context of self-adaptivity, is when  $\mathbf{P}$  depends only on  $X$ . Here, only **state variables** interactions are responsible for modifying the values of  $A_k$  - no extra information from the **parametric variables** is needed. From now on, we use “self-adaptive” and “adaptive” as synonyms.

### 1.2.2 Binding Dynamics: $\mathbf{B}_k$

The **binding dynamics** are functions  $\mathbf{B}_k$  that govern the adaptation of the coupling weights  $\Delta$  entering into the **coupling functions** (refer to Section 1.1.2). The set  $\Delta$  has been presented for local system of dimension 2 (i.e  $p = 2$ ) and we will stick to that dimension in what follows - although everything can be generalized to any arbitrary dimension.

Adaptation in the **coupling dynamics** is realized, as in Section 1.2.1, by letting the fixed and constant coupling weights  $\mu_k$  and  $\nu_k$  become time-dependent. With the same convention for the notation as in Section 1.2.1, we have

$$\{\mathbf{u}_k, \mathbf{v}_k\} \rightsquigarrow (\mu_k(t), \nu_k(t)) .$$

Their rate of change  $\dot{\mu}_k$  and  $\dot{\nu}_k$  are determined by the **binding dynamics**  $\mathbf{B} \equiv (\mathbf{B}_1^\mu, \dots, \mathbf{B}_N^\mu, \mathbf{B}_1^\nu, \dots, \mathbf{B}_N^\nu)$ . The functions  $\mathbf{B}_k^\mu$  and  $\mathbf{B}_k^\nu$  act on  $\mu_k(t)$  and  $\nu_k(t)$  respectively.

When  $\mathbf{B} \neq \mathbf{0}$ ,  $\mu_k$  and  $\nu_k$  acquire the status of variables of the global dynamical system. They now play the role of **coupling parametric variables** (c-PV). If, after a certain time,  $\mathbf{B} \equiv \mathbf{0}$ , then  $\mu_k(t)$  and  $\nu_k(t)$  are constants, and they recover their original status of fixed and constant parameters.

In general,  $\mathbf{B}$  is a function of  $X = (X_1, \dots, X_N)$ ,  $\mu = (\mu_1, \dots, \mu_N)$  and  $\nu = (\nu_1, \dots, \nu_N)$ . It makes  $\mu_k$  and  $\nu_k$  interact via a connected and undirected network with positive adjacency entries that is considered in Section 4.1.2.

### 1.2.3 Dynamical States

We now give the definition of a consensual state for Eqs. (1.5).

**Definition 1.3.** *Suppose there exists constants  $\bar{A} = (\bar{A}_1, \dots, \bar{A}_N)$  and  $\bar{\Delta}$ , invertible functions  $\mathbf{F}_k$  and a time-dependent function  $\bar{\varphi}(t)$  such that*

- $\mathbf{C}_k(\cdot, \cdot, \bar{\Gamma}, \bar{\Delta}) \neq \mathbf{0}$ ,  $\mathbf{P}_k(\cdot, \bar{\Gamma}, \bar{\Delta}) \neq \mathbf{0}$  and  $\mathbf{B}(\cdot, \bar{\Gamma}, \bar{\Delta}) \neq \mathbf{0}$ ,
- for all  $k$ ,  $\varphi_k(t)$  solves

$$\dot{X}_k = \mathbf{L}_k(X_k, \bar{\Lambda}_k)$$

with  $\varphi_k(t) = \mathbf{F}_k(\bar{\varphi}(t))$ ,

- and

$$\mathbf{C}_k(t, \varphi(t), \bar{\Gamma}, \bar{\Delta}) = \mathbf{0}, \quad \mathbf{P}_k(\varphi(t), \bar{\Gamma}, \bar{\Delta}) = \mathbf{0} \quad \text{and} \quad \mathbf{B}(\varphi(t), \bar{\Gamma}, \bar{\Delta}) = \mathbf{0} \quad \forall t,$$

with  $\bar{\Gamma} = (\bar{\Gamma}_1, \dots, \bar{\Gamma}_N)$  and  $\varphi(t) = (\varphi_1(t), \dots, \varphi_N(t))$ .

The function  $\varphi(t)$  together with  $\bar{\Lambda}$  and  $\bar{\Delta}$  are a **consensual state** of Eqs. (1.5).

In other words, a consensual state is such that local systems share a common dynamical pattern given by  $\bar{\varphi}(t)$ . Since the **coupling**, **parametric** and **binding dynamics** are zero for all  $t$ , this means that any change in the underlying network or even if the network is removed, the consensual state persists. This is to be contrasted with a synchronized state, that we define below. Since in this thesis we will make use of this definition only in the case of time-independent networks, we define a synchronized state when  $\mathbf{C}_k$  does not depend on  $t$ .

**Definition 1.4.** Suppose there exists constants  $\bar{\Lambda} = (\bar{\Lambda}_1, \dots, \bar{\Lambda}_N)$  and  $\bar{\Delta}$ , invertible functions  $\mathbf{F}_k$  and a time-dependent function  $\bar{\varphi}(t)$  such that

- $\mathbf{C}_k(\cdot, \bar{\Gamma}, \bar{\Delta}) \neq \mathbf{0}$ ,  $\mathbf{P}_k(\cdot, \bar{\Gamma}, \bar{\Delta}) \neq \mathbf{0}$  and  $\mathbf{B}(\cdot, \bar{\Gamma}, \bar{\Delta}) \neq \mathbf{0}$ ,
- for all  $k$ ,  $\varphi_k(t)$  solves

$$\dot{X}_k = \mathbf{L}_k(X_k, \bar{\Lambda}_k) + \mathbf{C}_k(X, \bar{\Gamma}, \bar{\Delta})$$

with  $\varphi_k(t) = \mathbf{F}_k(\bar{\varphi}(t))$ ,

- and

$$\mathbf{P}_k(\varphi(t), \bar{\Gamma}, \bar{\Delta}) = \mathbf{0} \quad \text{and} \quad \mathbf{B}(\varphi(t), \bar{\Gamma}, \bar{\Delta}) = \mathbf{0} \quad \forall t,$$

with  $\bar{\Gamma} = (\bar{\Gamma}_1, \dots, \bar{\Gamma}_N)$  and  $\varphi(t) = (\varphi_1(t), \dots, \varphi_N(t))$

The function  $\varphi(t)$  together with  $\bar{\Lambda}$  and  $\bar{\Delta}$  are a **synchronized state** of Eqs. (1.5) (with  $\mathbf{C}_k$  not depending on  $t$ ).

Similar to a consensual state, a synchronized state is composed of local common dynamical patterns. However, this state depends on the topology of the network. Hence, this state will not necessarily persist if a connection is changed or if the **coupling dynamics** is entirely removed.

#### 1.2.4 Aim of the Parametric Dynamics

For the sake of explanation, let us suppose that Eqs. (1.5) has no **binding dynamics**. Among the different possible P, we select those for which

$$\lim_{t \rightarrow \infty} \Lambda_k(t) = \bar{\Lambda}_k \quad \forall k \quad (\bar{\Lambda}_k \text{ constant})$$

and that the new values  $\bar{\Lambda}_k$  are such that the complex system has the possibility to converge towards a consensual state. We now discuss the convergence issue and the resulting limit values.

#### Convergence

The convergence towards a consensual state  $(\varphi(t), \bar{\Lambda})$  is interpreted as a stability problem. Introducing perturbations  $(\epsilon_{\varphi}(t), \epsilon_{\bar{\Lambda}}(t))$  on a consensual state gives  $(\varphi(t) + \epsilon_{\varphi}(t), \bar{\Lambda} + \epsilon_{\bar{\Lambda}}(t))$ . The aim is to find function P for which

$$\lim_{t \rightarrow \infty} (\epsilon_{\varphi}(t), \epsilon_{\bar{\Lambda}}(t)) = \mathbf{0}. \quad (1.6)$$

The initial perturbations  $\epsilon_{\bar{\Lambda}}(0)$  play the role of mismatches.

## Limit Values

The aim is to determine the set  $\bar{\Lambda}$  - in general, this is not ensured a priori. Let us exhibit a class of dynamics for which this can be done explicitly. Consider orbits  $\Lambda_k(t)$  ( $k = 1, \dots, N$ ) solving Eqs. (0.2) (with  $\mathbf{B} \equiv \mathbf{0}$ ), and let us construct functions  $P_k$  for which i) Eqs. (1.6) hold and ii) there exists a  $\mathbb{R}^q$  valued function  $J(\Lambda_1, \dots, \Lambda_N)$  such that

$$\frac{d[J(\Lambda_1(t), \dots, \Lambda_N(t))]}{dt} = \mathbf{0} \quad \forall t \geq 0 \quad \iff \quad J(\Lambda_1(t), \dots, \Lambda_N(t)) = \mathbf{C} \quad \forall t \geq 0,$$

where  $\mathbf{C}$  is a  $q$ -dimensional constant vector determined by the initial values  $(\Lambda_1(0), \dots, \Lambda_N(0))$ . In other words, the coordinates  $J_k$  ( $k = 1, \dots, q$ ) of  $J$  are constant of motions of the dynamics. In the case of homogeneous O-G systems (i.e.  $|\Lambda_k| = q$  for all  $k$ ) and when the consensual state admits common local parameters (i.e.  $\bar{\Lambda}_k = \Lambda_c$  for all  $k$ ), then, since Eqs. (1.6) hold, we have

$$\lim_{t \rightarrow \infty} J(\Lambda_1(t), \dots, \Lambda_N(t)) = J(\Lambda_c, \dots, \Lambda_c) = \mathbf{C}. \quad (1.7)$$

Eq. (1.7) is a system of  $q$  unknowns with  $q$  equations, which can now be solved. When the consensual state does not admit common local parameters (i.e.  $\bar{\Lambda}_k \neq \bar{\Lambda}_j$ ), more information on the system itself is needed to determine the values of  $\bar{\Lambda}$ . For the heterogeneous case that we focus on, refer to Section 2.2.4.

### 1.2.5 Aim of the Binding Dynamics

Similar to what has been presented in Section 1.2.4, we need to suitably construct the **binding dynamics**  $\mathbf{B}$  such that the coupling weights  $(\mu_k, \nu_k)$  will ultimately converge towards specific values. This makes it possible for the system to converge to a synchronized or consensual state. Also, as discussed in Section 1.2.4, we want to determine these consensual values. These two issues (convergence and limit values) are treated along the same lines as for the **parametric variables** in Section 1.2.4. That is, perturbing a consensual state with analysis of the asymptotic behavior of the perturbations and the constructing constants of motion in order to determine the limiting values.

## 1.3 Basic Example

Building on the example presented in [39], where a single externally excited oscillator is subject to an adaptive frequency mechanism, the paradigmatic illustration of the class of dynamics to be discussed is

$$\begin{aligned} \dot{x}_k &= \omega_k y_k - (x_k^2 + y_k^2 - \rho_k)x_k - \sum_{j=1}^N l_{k,j} x_j \\ \dot{y}_k &= \underbrace{-\omega_k x_k - (x_k^2 + y_k^2 - \rho_k)y_k}_{\text{local dynamics}} - \underbrace{\sum_{j=1}^N l_{k,j} y_j}_{\text{coupling dynamics}} \\ \dot{\omega}_k &= - \sum_{j=1}^N l_{k,j} (x_j y_k - y_j x_k) \\ \dot{\rho}_k &= - \underbrace{\sum_{j=1}^N l_{k,j} (x_j^2 + y_j^2)}_{\text{parametric dynamics}} \end{aligned} \quad k = 1, \dots, N, \quad (1.8)$$

where  $l_{k,j}$  are the entries of the Laplacian matrix associated to the underlying network.

Local system are HOPF oscillators with **parametric variables**  $\Lambda_k = (\omega_k, \rho_k)$ . If kept constant,  $\omega_k$  and  $\rho_k$  are flow and geometric parameters respectively. Here, **parametric dynamics** tune the

values of the frequencies  $\omega_k$  and shape the attractors by modifying the radii  $\rho_k$ . The resulting “plasticity” induces convergence towards common and constant values  $\omega_c$  and  $\rho_c$  with the result to ultimately drive the system towards a consensual oscillatory state.

### Convergence

For flow parameter adaptation only, the  $\omega_c$ -convergence is established by explicitly constructing ad-hoc Ляпунов functions. When the two types of parameters adapt, linear analysis around a consensual state will reveal the conditions for convergence.

### Limit Values

The consensual  $\omega_c$  and  $\rho_c$  can be analytically calculated thanks to the constant of motions (refer to Lemma D.1 and D.2, Appendix D)

$$J_\omega(\omega_1, \dots, \omega_N) = \sum_{k=1}^N \omega_k \quad \text{and} \quad J_\rho(\rho_1, \dots, \rho_N) := \sum_{k=1}^N \rho_k . \quad (1.9)$$

The values  $\omega_c$  and  $\rho_c$  only depend on the initial values  $\omega_k(0) := w_k$  and  $\rho_k(0) := r_k$  but not on  $L$  (i.e. topology of the network). For adapting parameters in the local systems, this will always be the case. However, asymptotic values of adapting coupling weights may explicitly depend on  $L$ . It will be observed that the network topology does however strongly influence the convergence rate (i.e. the adaptation rate). In this example, linear analysis shows clearly the explicit interplay between network connectivity and convergence rate.

#### 1.3.1 Miscellaneous Remark: Adaptation as an Optimal Control Problem

Alternatively, one may also interpret adaptation as an optimal control problem. Focusing on Eqs. (1.8) with flow parameter adaptation only, the problem is to determine a **parametric dynamics**  $P_k$  such that the constant of motion for  $J_\omega$  in 1.9 holds and such that the system converges towards a consensual state.

For the set of all admissible control functions we propose to take all continuously differentiable functions on  $\mathbb{R}^{2N}$  onto  $\mathbb{R}^N$  defined as  $P_R \equiv (P_{1,R}, \dots, P_{N,R})$  with

$$P_{k,R}(X) := \sum_{j=1}^N l_{k,j} (R_{x_j}(x_j, y_j) R_{y_k}(x_k, y_k) - R_{y_j}(x_j, y_j) R_{x_k}(x_k, y_k))$$

and where  $R_x \equiv (R_{x_1}, \dots, R_{x_N})$  and  $R_y \equiv (R_{y_1}, \dots, R_{y_N})$  are coupling functions on  $\mathbb{R}^{2N}$  onto  $\mathbb{R}^N$ . Such functions preserve the constant of motion  $J_\omega$  (refer to Lemma D.1, Appendix D).

One may associate a payoff functional defined as

$$E(P_R) = \int_0^\infty U_{P_R}(X(t), \Omega(t)) dt ,$$

with  $U_{P_R}(X, \Omega) = \left| \sum_{k=1}^N \omega_k \left( \sum_{j=1}^N l_{k,j} (x_j y_k - y_j x_k) - P_{k,R}(X) \right) \right|$ . The optimal control problem is therefore to find  $P_R$  such that  $E(P_R)$  is minimal. By choosing  $R_{x_k}(x, y) = x$  and  $R_{y_k}(x, y) = y$  for all  $k$  (i.e.  $R$  is the identity function  $\text{Id}$ ), the minimal is found since  $U_{P_R}(X, \Omega) \geq 0$  and with this choice,  $U_{P_{\text{Id}}}(X, \Omega) = 0$ . This corresponds to an optimal solution. Accordingly, our **parametric dynamics** in Eqs. (1.8) can be viewed as an optimal controller to the consensual state.





# Networks of Ortho-Gradient Systems with Adapting Flow Parameters

Tu dépasses sans te perdre

Les frontières de ton corps

Paul ELUARD

In this chapter, the complex dynamical system is composed of one  $N$ -vertex network with constant edges. The **local dynamics** are  $p$ -dimensional belonging to the class of ortho-gradient (O-G) systems. The **coupling dynamics** derives from the gradient of a potential. Adaptation occurs in the **local dynamics**. Here, flow parameters only are allowed to adapt.

## 2.1 Network's Dynamical System

In this section, we detail the constituent parts that compose the global dynamics

$$\dot{X}_k = \underbrace{D_k(X_k, \Phi_k; \Gamma_k) - \nabla A_k(X_k; \Gamma_k)}_{\text{local dynamics}} - \underbrace{c_k \frac{\partial V}{\partial X_k}(X)}_{\text{coupling dynamics}} \quad k = 1, \dots, N. \quad (2.1a)$$

$$\dot{\Phi}_k = \underbrace{P_k^{\Phi}(X)}_{\text{parametric dynamics}} \quad (2.1b)$$

**Local Dynamics** Local systems belong to the class of ortho-gradient (O-G) systems (refer to Section 2.1.1).

**Coupling Dynamics** The gradient of a given positive function characterizes the interactions of the **state variables** (refer to Section 2.1.2).

**Parametric Dynamics** Through adaptive mechanisms, parameters are influenced by **state variable** interactions (refer to Section 2.1.3).

### 2.1.1 Local Dynamics: $L_k$

The **local dynamics** belong to the class of ortho-gradient (O-G) systems as presented in Section 1.1.1 and for which we recall their dynamics

$$L_k(X_k; \Lambda_k) := \underbrace{D_k(X_k; \Phi_k, \Gamma_k)}_{\text{orthogonal evolution}} - \underbrace{\nabla A_k(X_k; \Gamma_k)}_{\text{gradient evolution}} \quad k = 1, \dots, N$$

where  $X_k = (x_{k,1}, \dots, x_{k,p})$  are the **state variables** and  $\Phi_k$  and  $\Gamma_k$  are, respectively, fixed and constant flow and geometric parameters. The gradient evolution  $\nabla A_k$  has a zero scalar product with the orthogonal evolution  $D_k$  (i.e.  $\langle D_k(X; \Lambda_k) | \nabla A_k(X; \Gamma_k) \rangle = 0$  for all  $X$ ). It derives from the potential  $A_k(X_k; \Gamma_k) := \frac{1}{2} \sum_{j \in I_k} G_j(X_k; \Gamma_k)^2$  (and  $I_k \subseteq \{0, \dots, p-1\}$ ) and accounts for the dissipative aspect of the dynamics. The real-valued functions  $G_j$  define the local attractor  $\mathcal{L}_k := \{X \in \mathbb{R}^p \mid G_j(X; \Gamma_k) = 0 \ j \in I_k\}$ , which is a  $m_k$ -dimensional compact submanifold (with  $m_k := p - |I_k|$ ).

### 2.1.2 Coupling Dynamics: $C_k$

As discussed in Section 1.1.2, **local dynamics** are coupled together via the gradient of a positive semi-definite potential  $V(X) \geq 0$ , that is

$$C_k(X) := -c_k \frac{\partial V}{\partial X_k}(X),$$

with  $X = (X_1, \dots, X_N) \in \mathbb{R}^{pN}$ , strictly positive, fixed and constant, *coupling strengths*  $c_k > 0$  and  $V$  depends on the entries of a  $N \times N$  weighted adjacency matrix  $A$  associated to a given connected and undirected network (refer to Appendix C). We suppose that

$$X_k = X_j \quad \forall k, j \quad \iff \quad V(X) = 0. \quad (2.2)$$

### 2.1.3 Parametric Dynamics: $P_k$

Apart from Section 2.2.5, in this chapter, adaptation in the local systems' parameter concerns only the flow parameters  $\Phi_k$ . As discussed in Section 1.2.1, we let the fixed and constant  $\Phi_k$  become time-dependent. That is,

$$\Phi_k = \{\mathbf{w}_{k,1}, \dots, \mathbf{w}_{k,n_k}\} \rightsquigarrow (\omega_{k,1}(t), \dots, \omega_{k,n_k}(t)) = \Phi_k(t).$$

Their rate of change  $\dot{\Phi}_k$  is determined by the **parametric dynamics**  $P_k^\Phi$ . Here, for each  $k$ ,  $P_k^\Phi$  is a function of  $X = (X_1, \dots, X_N)$  only. Interactions are through the same connected and undirected network with positive adjacency entries that is considered in Section 2.1.2. By introducing the **parametric dynamics**,  $\Phi_k$  have acquired the status of variables of the global dynamical system and are known as **flow parametric variables** (f-PV).

The functions  $P_k^\Phi$  must fulfill the objectives presented in Section 1.2.4. In this chapter, for homogenous O-G systems (i.e.  $|\Phi_k| = n \forall k$ ) we require that the  $\Phi_k(t)$  ultimately converge towards a common and constant set  $\Phi_c$  for all  $k$  (i.e.  $\lim_{t \rightarrow \infty} \Phi_k(t) = \Phi_c \forall k$ ). For heterogeneous O-G systems (i.e.  $|\Phi_k| = n_k \neq n_j = |\Phi_j| \forall k, j$ ) we require that all the elements in  $\Phi_k(t)$  ultimately converge towards a common constant  $\omega_c$  for all  $k$  (i.e.  $\lim_{t \rightarrow \infty} \Phi_k(t) = \omega_c \mathbf{1}_k \forall k$  with  $\mathbf{1}_k$  is a  $n_k$  dimensional vector of 1). Let us now explicitly construct a **parametric dynamics**  $P_k^\Phi$ .

#### 2.1.3.1 Dynamics of Flow Parametric Variables

To get insights on the role played by the **flow parametric variables**, we first focus on systems of dimension 2 (i.e. MCD oscillators) all having the same potential (i.e.  $A_k \equiv \frac{1}{2}G^2$  for all  $k$ ). In this case, for a given  $G$ ,  $D_k \equiv \mathbf{w}_k K$  is uniquely determined up to a multiplicative factor - here, a constant  $\mathbf{w}_k$  - (we exclude here the explicit dependence of the g-PV  $I$ )

$$D(X_k; \mathbf{w}_k) = \mathbf{w}_k K(X_k) := \mathbf{w}_k \begin{pmatrix} \frac{\partial G}{\partial y}(X_k) \\ -\frac{\partial G}{\partial x}(X_k) \end{pmatrix} = \begin{pmatrix} 0 & \mathbf{w}_k \\ -\mathbf{w}_k & 0 \end{pmatrix} \begin{pmatrix} \frac{\partial G}{\partial x}(X_k) \\ \frac{\partial G}{\partial y}(X_k) \end{pmatrix} \quad (2.3)$$

with  $X_k = (x_k, y_k)$ . Here,  $\mathbf{w}_k$  controls the angular velocity of the  $k^{th}$  local dynamics on its attractor (i.e. closed curve in  $\mathbb{R}^2$ ). We now assign to  $\mathbf{w}_k$  the role of a **parametric variable** (i.e.  $\mathbf{w}_k \rightsquigarrow \omega_k(t)$ ) with dynamics defined as

$$\dot{\omega}_k = -s_k \left\langle \begin{pmatrix} \frac{\partial V}{\partial x_k}(X) \\ \frac{\partial V}{\partial y_k}(X) \end{pmatrix} \middle| \begin{pmatrix} \frac{\partial G}{\partial y}(X_k) \\ -\frac{\partial G}{\partial x}(X_k) \end{pmatrix} \right\rangle, \quad (2.4)$$

where  $0 < s_k$  are strictly positive, fixed, *susceptibility constants*. For  $s_k \gg 1$ , the  $k^{th}$  oscillator is strongly influenced by its neighbor, whereas a  $s_k \ll 1$  reflects its “stubbornness”. If, in the extreme case,  $s_k = 0$ , the **parametric dynamics**  $P_k$  for  $\omega_k$  is trivial (i.e.  $\dot{\omega}_k(t) = 0$ ) and so the **parametric variable**  $\omega_k(t)$  is a constant and thus it regains its original status of a fixed and constant parameter (i.e.  $\omega_k(t) := w_k$  for a certain value  $w_k$ ).

The aim of the adaptive mechanism in Eqs. (2.4) is to allow each  $\omega_k$  to evolve in time so that they will, via mutual influences of the **state variables**, asymptotically converge towards a single common  $\omega_c$ . For this, each oscillator has to adapt its  $\omega_k$  to those of its connected neighbors. To unveil the adaptive process, let us first consider a simple illustration involving three weakly coupled stable limit cycle oscillators connected as shown in Figure 2.1. Each oscillator has the same limit cycle  $\mathcal{L}$  which is here, for simplicity, a circle.

We consider a discrete time reasoning for the adaptive mechanism. Let  $\{t_n\}_{n=0}^{\infty}$  be a discretization of the time with  $t_0 = 0$  and  $t_{n+1} := t_n + h$  for a given small positive  $h$ . Without loss of generality, assume that  $\omega_1(0) < \omega_2(0) < \omega_3(0)$ . Initiate all three oscillators at the same time  $t_0 = 0$  and on the same point belonging to their respective limit cycle (i.e.  $(0, 1) \in \mathcal{L}$  for each oscillator). Qualitatively, after a small time-lapse  $h$ , the scenario is sketched in Figure 2.2 where all three oscillators are represented on only one of the limit cycle  $\mathcal{L}$ . Since they are weakly coupled, we can neglect the effect of the **coupling dynamics** and hence, for simplicity, we show oscillators on the attractor. For our explanation, we deliberately elongated the oscillators’ trajectories in Figure 2.2. We now examine each oscillator’s behavior individually at time  $t = t_0 + h$ .

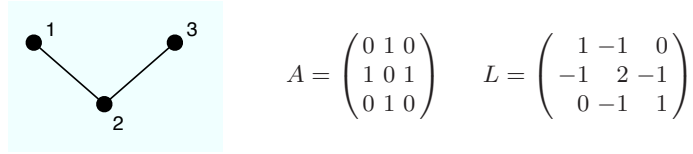


Fig. 2.1: Network of three oscillators with adjacency and Laplacian matrices  $A$  and  $L$  respectively.

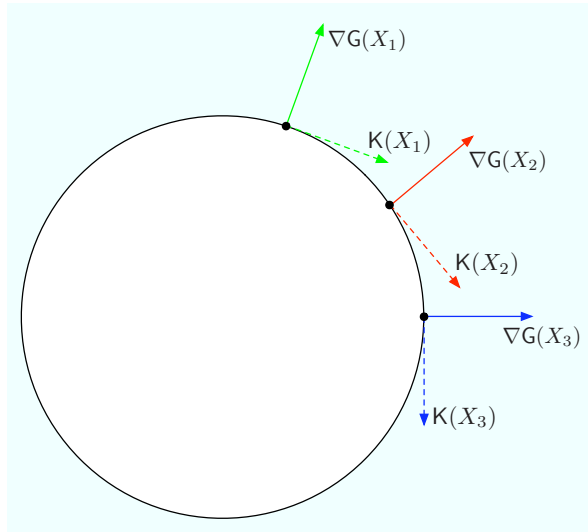


Fig. 2.2: Position on a  $\mathcal{L}$  at time  $t_0 + h$  of three oscillators all initiated on  $(0, 1)$  at  $t_0 = 0$ .

### Oscillator 1

The first oscillator has a lower angular velocity than the second one, hence for adaptation, our rule implies

at time  $t = t_0 + h$  oscillator 1 must go “faster” to adjust with oscillator 2

Since  $\langle \nabla G(X_2) | \mathbf{K}(X_1) \rangle = \|\nabla G(X_2)\| \|\mathbf{K}(X_1)\| \cos(\theta_{1,2}) > 0$ , we propose

$$\omega_{1(t_0+h)} := \omega_{1(t_0)} + h \langle \nabla G(X_2) | \mathbf{K}(X_1) \rangle .$$

### Oscillator 2

For the second oscillator, adaptation implies

at time  $t = t_0 + h$  oscillator 2 must go “slower” to adjust with oscillator 1  
oscillator 2 must go “faster” to adjust with oscillator 3

Since  $\langle \nabla G(X_1) | \mathbf{K}(X_2) \rangle = \|\nabla G(X_1)\| \|\mathbf{K}(X_2)\| \cos(\theta_{2,1}) < 0$  and  $\langle \nabla G(X_3) | \mathbf{K}(X_2) \rangle = \|\nabla G(X_3)\| \|\mathbf{K}(X_2)\| \cos(\theta_{2,3}) > 0$ , we propose

$$\omega_{2(t_0+h)} := \omega_{2(t_0)} + h \langle \nabla G(X_1) | \mathbf{K}(X_2) \rangle + h \langle \nabla G(X_3) | \mathbf{K}(X_2) \rangle .$$

### Oscillator 3

Finally, the same reasoning implies for the third oscillator

$$\omega_{3(t_0+h)} := \omega_{3(t_0)} + h \langle \nabla G(X_2) | \mathbf{K}(X_3) \rangle .$$

since  $\langle \nabla G(X_2) | \mathbf{K}(X_3) \rangle = \|\nabla G(X_2)\| \|\mathbf{K}(X_3)\| \cos(\theta_{3,2}) < 0$ .

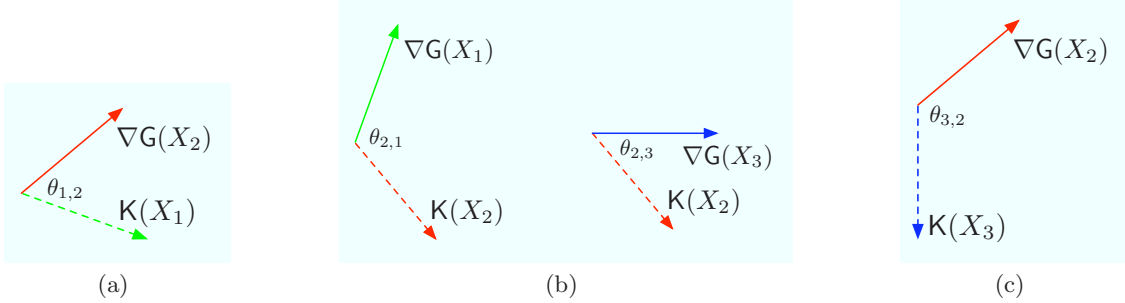


Fig. 2.3: Angle  $\theta_{1,2}$  between vector  $\mathbf{K}(X_1)$  and  $\nabla G(X_2)$  (Figure 2.3(a)). Angle  $\theta_{2,1}$  between vector  $\mathbf{K}(X_2)$  and  $\nabla G(X_1)$  and angle  $\theta_{2,3}$  between vector  $\mathbf{K}(X_2)$  and  $\nabla G(X_3)$  (Figure 2.3(b)). Angle  $\theta_{3,2}$  between vector  $\mathbf{K}(X_3)$  and  $\nabla G(X_2)$  (Figure 2.3(c)).

This can be done at any time step  $t_n$  and it is straightforwardly generalized to  $N$  oscillators by including the connection weights  $a_{k,j}$  and. We propose

$$\begin{aligned} \omega_k(t_{n+h}) &= \omega_k(t_n) + h \sum_{j \neq k}^N a_{k,j} \langle \nabla G(X_j) | \mathbf{K}(X_k) \rangle + l_{k,k} \langle \nabla G(X_k) | \mathbf{K}(X_k) \rangle \\ &= \omega_k(t_n) - h \sum_{j=1}^N l_{k,j} \langle \nabla G(X_j) | \mathbf{K}(X_k) \rangle , \end{aligned}$$

since  $l_{k,j} = -a_{k,j}$  for  $k \neq j$  and  $\langle \nabla G(X_k) | \mathbf{K}(X_k) \rangle = 0$  for all  $k$ . The continuous time version of this procedure follows as

$$\frac{\omega_k(t_n+h) - \omega_k(t_n)}{h} = -\sum_{j=1}^N l_{k,j} \langle \nabla G(X_j) | \mathbf{K}(X_k) \rangle$$

and therefore if we let  $h$  tend to zero ( $h \rightarrow 0$ ), we have  $\dot{\omega}_k(t) = -\langle \sum_{j=1}^N l_{k,j} \nabla G(X_j) | \mathbf{K}(X_k) \rangle$ .

When  $G(X) = x^2 + y^2$ , then

$$\sum_{j=1}^N l_{k,j} \frac{\partial G}{\partial x}(X_j) = \frac{\partial V}{\partial x_k}(X) \quad \text{and} \quad \sum_{j=1}^N l_{k,j} \frac{\partial G}{\partial y}(X_j) = \frac{\partial V}{\partial y_k}(X)$$

since a Laplacian Potential is defined as  $V(X) = \langle x | Lx \rangle + \langle y | Ly \rangle$  with  $x = (x_1, \dots, x_N)$  (idem for  $y$ ). We therefore have, after introducing the susceptibility constants  $s_k$ , Eqs. (2.4).

Note that for this type of **coupling dynamics**, we have the following constant of motion

$$J(\omega_1, \dots, \omega_N) := \sum_{k=1}^N \frac{\omega_k}{s_k}. \quad (2.5)$$

Indeed, for  $\omega_k(t)$  ( $k = 1, \dots, N$ ) orbits of Eqs. (2.4), we have

$$\begin{aligned} \frac{d[J(\omega_1(t), \dots, \omega_N(t))]}{dt} &= \sum_{k=1}^N \frac{\dot{\omega}_k(t)}{s_k} = -\sum_{k=1}^N \langle \frac{\partial V}{\partial X_k}(X) | \mathbf{K}(X_k) \rangle \\ &= -\sum_{k=1}^N \sum_{j=1}^N l_{k,j} \left( \frac{\partial G}{\partial x}(X_j) \frac{\partial G}{\partial y}(X_k) - \frac{\partial G}{\partial y}(X_j) \frac{\partial G}{\partial x}(X_k) \right) = 0 \end{aligned}$$

since, by Lemma D.1 in Appendix D, the last equality is zero. It is important to remark that the constant of motion  $J$  only depends on the f-PV  $\omega_k$  and on the susceptibility constants  $s_k$  and not on the entries of the adjacency matrix  $A$ . Therefore, if a consensual and common  $\omega_c$  is reached, its value will not depend on the topology of the network.

## Generalization

In Eqs. (2.3), the first equality (vector representation) naturally extends to higher dimensions in the case involving single adapting parameters. The matrix representation (second equality) in Eqs. (2.3) enables generalizations to the **multi parametric variable** cases. Let us detail these two situations for homogeneous O-G systems (i.e.  $D_k \equiv D$  for all  $k$ ).

### Single Adapting Flow Parameter

By construction of the **local dynamics**,  $D$  can always be written as  $D(X_k, \omega_k) := \omega_k \mathbf{K}(X_k)$  and so, for this case, the set of f-PV is  $\omega_k$ . For arbitrary dimension  $p$ , a natural generalization for the **parametric dynamics** will be

$$\dot{\omega}_k = -s_k \langle \frac{\partial V}{\partial X_k}(X) | \mathbf{K}(X_k) \rangle.$$

If we suppose that  $\sum_{k=1}^N \langle \frac{\partial V}{\partial X_k}(X) | \mathbf{K}(X_k) \rangle = 0$  for all  $X$ , then we have the constant of motion as in Eq.(2.5). Hence, a single constant of motion  $J$  depending on the  $\omega_k$  and on the susceptibility constants  $s_k$  determines the asymptotic value  $\omega_c$  (i.e. the consensual value is independent of the network topology).

### Multi Adapting Flow Parameters

Here we focus on cases where  $D$  can be written as  $D(X_k, \Phi_k) := T_k \mathbf{K}(X_k)$  with  $T_k$  being a  $p \times p$

anti-symmetric matrix. The upper diagonal elements of  $T_k$  are given<sup>1</sup> by the f-PV  $\Phi_k \in \mathbb{R}^{\frac{p(p-1)}{2}}$ . This is compatible with O-G dynamics, provided orthogonality between  $\mathbf{D}$  and  $\nabla \mathbf{A}_k$  is ensured, namely

$$\langle \mathbf{D}(X, \Phi_k) | \nabla \mathbf{A}_k(X) \rangle = \langle T_k \mathbf{K}(X_k) | \sum_{j \in I_k} \mathbf{G}_j(X_k) \nabla \mathbf{G}_j(X_k) \rangle = 0.$$

In particular, when  $I_k := \{1\}$  for all  $k$ , this holds for  $\mathbf{K}(X_k) := \nabla \mathbf{G}_1(X_k)$  and  $T_k$  any anti-symmetric matrix (refer to Appendix D). Inspired by the matrix representation in Eqs. (2.3), a generalized multi parametric dynamics can be constructed and reads as

$$\dot{\omega}_{k,l,s} = -\mathfrak{s}_{k,l,s} \left\langle \begin{pmatrix} \frac{\partial \mathcal{V}}{\partial x_{k,l}}(X) \\ \frac{\partial \mathcal{V}}{\partial x_{k,s}}(X) \end{pmatrix} \middle| \begin{pmatrix} \frac{\partial \mathbf{G}}{\partial x_s}(X_k) \\ -\frac{\partial \mathbf{G}}{\partial x_l}(X_k) \end{pmatrix} \right\rangle \quad k = 1, \dots, N, \quad l, s = 1, \dots, p, \quad s > l,$$

where  $\omega_{k,l,s}$  are the  $l^{\text{th}}$  row,  $s^{\text{th}}$  column entries of the  $k^{\text{th}}$  matrix  $T_k$ .

Concerning the constants of motion: if we suppose that for all  $s$  and  $l$  ( $l, s = 1 \dots, p$ , and  $s > l$ ),  $\sum_{k=1}^N \left\langle \begin{pmatrix} \frac{\partial \mathcal{V}}{\partial x_{k,l}}(X) \\ \frac{\partial \mathcal{V}}{\partial x_{k,s}}(X) \end{pmatrix} \middle| \begin{pmatrix} \frac{\partial \mathbf{G}_1}{\partial x_s}(X_k) \\ -\frac{\partial \mathbf{G}_1}{\partial x_l}(X_k) \end{pmatrix} \right\rangle = 0$  for all  $X$ , then we have  $\frac{p(p-1)}{2}$  constants of motion:

$J_{l,s}(\omega_{1,l,s}, \dots, \omega_{N,l,s}) := \sum_{k=1}^N \frac{\omega_{k,l,s}}{\mathfrak{s}_{k,l,s}}$ . Again, if a consensual and common  $\omega_{c,l,s}$  is reached, its value will not dependent on the topology of the network since the function  $J_{l,s}$  only depends on  $\omega_{k,l,s}$  and  $\mathfrak{s}_{k,l,s}$ .

## 2.2 Dynamics of the Network

In this section we first discuss the dynamics of interacting homogeneous local dynamics (i.e.  $\mathbf{D}_k \equiv \mathbf{D}$  for all  $k$ )<sup>2</sup> with constant (i.e trivial parametric dynamics  $\mathbf{P}_k \equiv 0$  in Eqs. (2.1b)) and identical parameters (i.e.  $\Lambda_k = \Lambda_c$  for all  $k$ ) (refer to Section 2.2.1). We then consider a network of homogeneous local dynamics with single (refer to Section 2.2.2) and multi (refer to Section 2.2.3) adapting parameters. Finally, we focus on heterogeneous dynamical systems with parametric dynamics (refer to Section 2.2.4).

### Consensual submanifold $\mathcal{M}$

In this chapter, the geometric parameter  $\Gamma$  (i.e. those that control the shape of the local attractor) are fixed, constant and common to each local dynamics. Therefore local attractors  $\mathcal{L}_k$  only differ according to the choice of the functions  $\mathbf{G}_j$ . We will suppose that

$$\mathcal{L} := \bigcap_{k=1}^N \mathcal{L}_k = \{X \in \mathbb{R}^p \mid \mathbf{G}(X; \Gamma) := (\mathbf{G}_{j_1}(X; \Gamma), \dots, \mathbf{G}_{j_m}(X; \Gamma)) = \mathbf{0} \in \mathbb{R}^{p-m}\} \quad (2.6)$$

with  $j_s \in \bigcup_{k=1}^N I_k$ ,  $s = 1, \dots, m$  and  $m := \left| \bigcup_{k=1}^N I_k \right|$  is a  $m$ -dimensional compact submanifold. The set  $\mathcal{L}$  is a local attractor shared by all local dynamics. This, together with Eqs. (2.2), enables us to define

<sup>1</sup> From  $\Phi_k = (\omega_{k,1,2}, \dots, \omega_{k,1,p}, \omega_{k,2,3}, \dots, \omega_{k,2,p}, \dots, \omega_{k,p-1,p}) \in \mathbb{R}^{\frac{p(p-1)}{2}}$ , we define  $T_k$  as

$$\begin{pmatrix} 0 & \omega_{k,1,2} & \dots & \dots & \omega_{k,1,p} \\ -\omega_{k,1,2} & 0 & \omega_{k,2,3} & \dots & \omega_{k,2,p} \\ \vdots & -\omega_{k,2,3} & \ddots & & \vdots \\ \vdots & \vdots & & \ddots & \omega_{k,p-1,p} \\ -\omega_{k,1,p} & -\omega_{k,2,p} & \dots & \dots & 0 \end{pmatrix}.$$

<sup>2</sup> For compatibility with O-G systems, it is implicitly supposed that  $\langle \mathbf{D} | \nabla \mathbf{A}_k \rangle = 0$  for all  $k$ .

$$\mathcal{M} := \{X \in \mathbb{R}^{pN} \mid X_1 \in \mathcal{L} \text{ and } X_k = X_j \ \forall k, j\}. \quad (2.7)$$

For  $X \in \mathcal{M}$ ,  $X_k = X_j$  for all  $k, j$ . In particular,  $X_k = X_1$  and hence, by the condition  $X_1 \in \mathcal{L}$ , all **local dynamics** are to be found on  $\mathcal{L}$  and so,  $\mathcal{M}$  is to be seen as a  $m$ -dimensional compact *consensual* submanifold of  $\mathbb{R}^{pN}$ .

For ease of notation, we will, from now on in this chapter, refrain from explicitly writing the geometric parameter set  $\Gamma$ . Let us now show that  $\mathcal{M}$  is, indeed, a submanifold of  $\mathbb{R}^{pN}$  of dimension  $m$ .

**$\mathcal{M}$  is an  $m$ -dimensional compact submanifold of  $\mathbb{R}^{pN}$**

Let  $\mathbf{G}$  be defined as in (2.6) and denote  $X \in \mathbb{R}^{pN}$  as  $X = (X_1, \dots, X_N)$  with  $X_k = (x_{k,1}, \dots, x_{k,p})$  and we define  $x_k := (x_{1,k}, \dots, x_{N,k})$ . Let  $L$  be an  $N \times N$  Laplacian matrix associated to a connected and undirected network with positive adjacency entries (refer to Appendix C). Finally,  $\hat{L}$  is  $L$  without its last line (i.e. an  $(N-1) \times N$  matrix). We have to show that

$$\mathcal{M} := \{X \in \mathbb{R}^{pN} \mid \mathbf{M}(X) := (\mathbf{G}(X_1), \hat{L}x_1, \dots, \hat{L}x_p) = \mathbf{0} \in \mathbb{R}^{pN-m}\}$$

is not empty, compact and that for all  $X^* \in \mathcal{M}$  there exists a neighborhood  $\mathcal{U}_{X^*} \subset \mathbb{R}^{pN}$  of  $X^*$  such that  $\mathfrak{D}\mathbf{M}(X)$  has rank  $pN - m$  for all  $X \in \mathcal{U}_{X^*}$ .

[ $\mathcal{M} \neq \emptyset$ ] The equations

$$\hat{L}x_1 = \dots = \hat{L}x_p = \mathbf{0} \in \mathbb{R}^{N-1} \quad (2.8)$$

are equivalent to

$$x_{1,1} = \dots = x_{N,1}, x_{1,2} = \dots = x_{N,2}, \dots, x_{1,p} = \dots = x_{N,p} \iff Lx_1 = \dots = Lx_p = \mathbf{0} \in \mathbb{R}^N. \quad (2.9)$$

Obviously, Eqs. (2.9) imply Eqs. (2.8). It is also true the other way round since, for any  $z \in \mathbb{R}^p$  such that  $\hat{L}z = \mathbf{0}$ , we have

$$0 = \sum_{k=1}^{N-1} \left( \sum_{j=1}^N l_{k,j} z_j \right) = \sum_{j=1}^N z_j \left( \sum_{k=1}^{N-1} l_{k,j} \right) = z_N \underbrace{\sum_{k=1}^{N-1} l_{k,N}}_{-l_{N,N}} + \sum_{j=1}^{N-1} z_j \left( \sum_{k=1}^{N-1} l_{k,j} \right)$$

because  $l_{s,s} = -\sum_{j \neq s}^N l_{s,j}$  and  $l_{k,j} = l_{j,k}$  ( $l_{k,j}$  entries of  $L$ ). Since, for  $j = 1, \dots, N-1$ ,  $\sum_{k=1}^{N-1} l_{k,j} = l_{j,j} + \sum_{k \neq j}^{N-1} l_{k,j} = -\sum_{j \neq s}^N l_{j,s} + \sum_{k \neq j}^{N-1} \underbrace{l_{k,j}}_{j,k} = -l_{j,N}$ , then

$$0 = -l_{N,N} z_N + \sum_{j=1}^{N-1} z_j (-l_{j,N}) = -\sum_{j=1}^N l_{N,j} z_j,$$

and therefore  $\hat{L}z = \mathbf{0}$  implies  $Lz = \mathbf{0}$ . Hence, an element  $X$  in  $\mathcal{M}$  must satisfy  $X_k = X_c$  for  $k = 1, \dots, N$  and  $\mathbf{G}(X_c) = \mathbf{0}$ . Since by hypothesis  $\mathcal{L} := \{X \in \mathbb{R}^p \mid \mathbf{G}(X) = \mathbf{0} \in \mathbb{R}^{p-m}\}$  is a submanifold, it is not empty and therefore  $\mathcal{M}$  is not empty as well.

[ $\mathcal{M}$  is compact] Since  $\mathcal{M}$  is the preimage of the closed set  $\mathbf{0} \in \mathbb{R}^{pN-m}$  by a continuous function  $\mathbf{M}$ , it is closed. For any  $X \in \mathcal{M}$ , then  $X_1 \in \mathcal{L}$ . By definition,  $\mathcal{L}$  is compact. Therefore, there exists  $B > 0$  such that  $\|X_1\| \leq B$  for all  $X_1 \in \mathcal{L}$ . Since  $X \in \mathcal{M}$ , then  $X_k = X_1$  for all  $k$  and so  $\|X\|^2 = N\|X_1\|^2 \leq NB^2$ . Hence,  $\mathcal{M}$  is closed and bounded, thus compact.

[ $\mathfrak{D}\mathbf{M}(X)$  has rank  $pN - m$ ] For  $X^* = (X_1^*, \dots, X_1^*) \in \mathcal{M}$ , consider a neighborhood  $\mathcal{U}_{X_1^*} \subset \mathbb{R}^p$  of  $X_1^* \in \mathbb{R}^p$  such that  $\mathfrak{D}\mathbf{G}(X_1)$  has rank  $p - m$  for all  $X_1 \in \mathcal{U}_{X_1^*}$  (such a neighborhood exists since  $\mathcal{L}$  is a submanifold of  $\mathbb{R}^p$ ). Define  $\mathcal{U}_{X^*} := \mathcal{U}_{X_1^*} \times \dots \times \mathcal{U}_{X_1^*}$  ( $p$  times the Cartesian product of  $\mathcal{U}_{X_1^*}$ ). Computing the derivative of  $\mathbf{M}(X)$  and evaluating it on  $X \in \mathcal{U}_{X^*}$  gives

$$\mathfrak{D}\mathcal{M}(X) = \begin{pmatrix} \mathfrak{D}\mathbf{G}(X_1) & \mathbf{0} \\ & Q \end{pmatrix}$$

where  $\mathfrak{D}\mathbf{G}(X_1)$  is the  $(p-m) \times p$  Jacobien of  $\mathbf{G}$ ,  $\mathbf{0}$  is a  $(p-m) \times (N-1)p$  matrix with all entries 0 and  $Q$  is a matrix with  $p \times N$  blocs, each of size  $N-1 \times p$  (i.e.  $Q$  has  $p(N-1)$  rows and  $Np$  columns). Bloc  $l, s$  has the  $s^{th}$  column of matrix  $\hat{L}$  in its  $l^{th}$  column and the rest of the entries are zero. We have to verify that the  $Np-m$  lines of this Jacobien are linearly independent. Let  $\eta_j$  ( $j = 1, \dots, p-m$ ) and  $\lambda_{j,k}$  ( $j = 1, \dots, p, k = 1, \dots, N-1$ ) be real numbers and we verify that they are all zeros if, and only if,

$$\sum_{j=1}^{N-1} l_{j,1} \lambda_{s,j} + \sum_{j=1}^{p-m} \eta_j \frac{\partial \mathbf{G}_j}{\partial x_s}(X_1) = 0 \quad s = 1, \dots, p \quad (2.10a)$$

$$\sum_{j=1}^{N-1} l_{j,r} \lambda_{k,j} = 0 \quad k = 1, \dots, p, r = 2, \dots, N. \quad (2.10b)$$

Since  $L$  is symmetric ( $l_{k,j} = l_{j,k}$ ), Eqs. (2.10b) are equivalent to  $\bar{L}\lambda_k = \mathbf{0} \in \mathbb{R}^{N-1}$  for  $k = 1, \dots, p$ , where  $\bar{L}$  is  $L$  without its first line and without its last column and  $\lambda_k := (\lambda_{k,1}, \dots, \lambda_{k,N-1})$ . Since the rank of  $L$  is  $N-1$  (Laplacian matrix associated to a connected network), the minor of  $\bar{L}$  is none-zero, and therefore  $\bar{L}\lambda_k = \mathbf{0}$  if and only if  $\lambda_k = \mathbf{0}$  for  $k = 1, \dots, p$ . By hypothesis  $X_1 \in \mathcal{U}_{X_1^*}$  and  $\mathfrak{D}\mathbf{G}(X_1)$  has rank  $p-m$ , therefore  $\eta_j = 0$   $j = 1, \dots, p-m$ . Hence, for  $X \in \mathcal{U}_{X_1}$ ,  $\mathfrak{D}\mathcal{M}(X)$  has rank  $pN-m$  and thus,  $\mathcal{M}$  has dimension  $m$ .

## 2.2.1 Network of Homogeneous Local Dynamics with constant identical Parameters

Consider the dynamical System (2.1a) where all vertices are endowed with homogeneous **local dynamics** (i.e.  $\mathbf{D}_k \equiv \mathbf{D}$  for all  $k$ ). We here suppose that  $\mathbf{P}_k \equiv 0$  in Eqs. (2.1b) and so there are no **parametric variables**. Therefore, **local dynamics** have a constant set of parameters which we suppose to be common to all local systems (i.e.  $A_k = A_c$  for all  $k$ ). Let us discuss the existence of a consensual state and the convergence towards it.

### Existence of a consensual state

The existence of a consensual state for System (2.1a) ( $\mathbf{P}_k \equiv 0$  in Eqs. (2.1b)) is guaranteed if initial conditions are in  $\mathcal{M}$  (c.f. (2.7)).

### Convergence towards a consensual state

The convergence towards a consensual state is established by the following lemma. For ease of notation, we remove the explicit dependence of  $A_c$ .

**Proposition 2.1.** *Suppose that*

- for all  $X^* \in \mathcal{M}$ ,  $\langle X | \mathfrak{D}^2\mathbf{V}(X^*)X \rangle = 0 \iff X_k = X_j \quad \forall k, j$
- $\sum_{k=1}^N \langle \frac{\partial \mathbf{V}}{\partial X_k}(X) | \mathbf{D}(X_k) \rangle \leq 0 \quad \forall X$ ,

where  $\mathfrak{D}^2\mathbf{V}(X^*)$  is the second total derivative (i.e. the Hessian) of  $\mathbf{V}$  evaluated at  $X^*$ . Then there exists a set  $\mathcal{U} \supset \mathcal{M}$  such that all orbits solving System (2.1a) (here,  $\mathbf{P}_k \equiv 0$  in Eqs. (2.1b) and  $A_k := A_c$  for all  $k$ ) with initial conditions in  $\mathcal{U}$  converge towards  $\mathcal{M}$ .

*Proof.* The convergence towards  $\mathcal{M}$  follows from Ляпунов's second method with Ляпунов function:

$$\mathcal{J}(X) = \sum_{k=1}^N \frac{1}{c_k} A_k(X_k) + \mathbf{V}(X) \geq 0.$$

By construction, we have that  $\mathcal{M} = \{X \in \mathbb{R}^{pN} | \mathcal{J}(X) = 0\}$ . Computing the time derivative



$$\begin{aligned}
\langle \nabla \mathcal{J}(X) | \dot{X} \rangle &= \sum_{k=1}^N \left\langle \frac{1}{c_k} \nabla A_k(X_k) + \frac{\partial \mathcal{V}}{\partial X_k}(X) \mid D(X_k) - \nabla A_k(X_k) - c_k \frac{\partial \mathcal{V}}{\partial X_k}(X) \right\rangle \\
&= \sum_{k=1}^N \frac{1}{c_k} \underbrace{\langle \nabla A_k(X_k) \mid D(X_k) \rangle}_{=0 \forall k} + \sum_{k=1}^N \underbrace{\left\langle \frac{\partial \mathcal{V}}{\partial X_k}(X) \mid D(X_k) \right\rangle}_{\leq 0} \\
&\quad - \underbrace{\sum_{k=1}^N c_k \left\| \frac{1}{c_k} \nabla A_k(X_k) + \frac{\partial \mathcal{V}}{\partial X_k}(X) \right\|^2}_{\leq 0}.
\end{aligned}$$

The last inequality is zero if and only if  $\nabla \mathcal{J}(X) = \mathbf{0}$ . Therefore, to guarantee strict negativity, we need to show that for all  $X^* \in \mathcal{M}$ , the kernel  $\ker(\mathfrak{D}^2 \mathcal{J}(X^*))$  of the  $pN \times pN$  Hessian  $\mathfrak{D}^2 \mathcal{J}(X^*)$  is equal to the kernel  $\ker(\mathfrak{D}\mathcal{M}(X^*))$  of the submanifold  $\mathcal{M}$ . This is done in Appendix E. Then, invoking Corollary 2.1 below, insures the existence of  $\mathcal{U} \supset \mathcal{M}$  such that  $\nabla \mathcal{J}(X) \neq \mathbf{0}$  for all  $X \in \mathcal{U} \setminus \mathcal{M}$ . Therefore, there exists  $\mathcal{U} \supset \mathcal{M}$  such that the strict negativity  $\langle \nabla \mathcal{J}(X) | \dot{X} \rangle < 0$  holds for all  $X \in \mathcal{U} \setminus \mathcal{M}$ . Hence, the compact set  $\mathcal{M}$  is asymptotically stable (refer to Appendix A).  $\square$

To prove Corollary 2.1 below we first need to consider the following Lemma. In words, it states that for the gradient, of a real valued function  $F$ , not to vanish in a neighborhood of a manifold  $\mathcal{M}$ , the kernel of  $F$ 's Hessian must be the same as the kernel of  $\mathcal{M}$ .

**Lemma 2.1.** *Let  $\mathcal{M}$  be a submanifold given by  $\mathbf{M} : \mathbb{R}^m \rightarrow \mathbb{R}^{m-k}$  (i.e.  $\mathcal{M}$  has a dimension of  $k$ ).  $F$  is a real-valued function on  $\mathbb{R}^m$  such that  $F(x) \geq 0$  for all  $x$  and  $F(x) = 0$  if and only if  $x \in \mathcal{M}$ . Suppose there exists  $x^* \in \mathcal{M}$  such that  $\ker(\mathfrak{D}^2 F(x^*)) = \ker(\mathfrak{D}\mathcal{M}(x^*))$ . Then, there exists an open set  $\mathcal{U}_{x^*} \ni x^*$  such that  $\nabla F(x) \neq 0$  for all  $x \in \mathcal{U}_{x^*} \setminus \mathcal{M}$ .*

*Proof.* By hypothesis there exists  $x^* \in \mathcal{M}$  such that  $\ker(\mathfrak{D}^2 F(x^*)) = \ker(\mathfrak{D}\mathcal{M}(x^*))$ . Without loss of generality, we can chose a basis of  $\mathbb{R}^m$  such that the first  $k$  basis vectors span the kernel of  $\mathfrak{D}\mathcal{M}(x^*)$ , and we use the following notation:  $x = (\bar{x}, \hat{x})$ . In this basis,  $\frac{\partial \mathcal{M}}{\partial \bar{x}}(x^*)^{-1}$  exists and since  $\mathbf{M}(x^*) = 0$ , the implicit function theorem guarantees the existence of  $r_{\mathbf{M}}, R_{\mathbf{M}} > 0$  and a unique continuous map  $\mathbf{l}_{\mathbf{M}} : \mathcal{B}(\bar{x}^*, r_{\mathbf{M}}) \rightarrow \mathcal{B}(\hat{x}^*, R_{\mathbf{M}})$  such that

$$\mathbf{M}(\bar{x}, \hat{x}) = 0 \iff \mathbf{l}_{\mathbf{M}}(\bar{x}) = \hat{x} \quad \forall (\bar{x}, \hat{x}) \in \mathcal{B}(\bar{x}^*, r_{\mathbf{M}}) \times \mathcal{B}(\hat{x}^*, R_{\mathbf{M}}),$$

where  $\mathcal{B}(x^*, r)$  is the open ball centered at a point  $x^*$  and of radius  $r > 0$ . Define

$$\begin{aligned}
\mathbf{S} : \mathbb{R}^k \times \mathbb{R}^{m-k} &\longrightarrow \mathbb{R}^{m-k} \\
(\bar{x}, \hat{x}) &\longmapsto \pi(\nabla F(x)),
\end{aligned}$$

with projection  $\pi(x_1, \dots, x_m) = (x_{k+1}, \dots, x_m)$ . By hypothesis  $\ker(\mathfrak{D}^2 F(x^*)) = \ker(\mathfrak{D}\mathcal{M}(x^*))$  and so  $\frac{\partial \mathbf{S}}{\partial \bar{x}}(x^*)^{-1}$  exists. Since  $\mathcal{M}$  is the minimum of  $F$ , we have  $\mathcal{M} \subseteq \nabla F^{-1}(0) \subseteq \mathbf{S}^{-1}(0)$  and so  $\mathbf{S}(x^*) = 0$ . Therefore, applying the implicit function theorem, there exists  $r_{\mathbf{S}}, R_{\mathbf{S}} > 0$  and a unique continuous map  $\mathbf{l}_{\mathbf{S}} : \mathcal{B}(\bar{x}^*, r_{\mathbf{S}}) \rightarrow \mathcal{B}(\hat{x}^*, R_{\mathbf{S}})$  such that

$$\mathbf{S}(\bar{x}, \hat{x}) = 0 \iff \mathbf{l}_{\mathbf{S}}(\bar{x}) = \hat{x} \quad \forall (\bar{x}, \hat{x}) \in \mathcal{B}(\bar{x}^*, r_{\mathbf{S}}) \times \mathcal{B}(\hat{x}^*, R_{\mathbf{S}}).$$

Define  $\mathcal{B} := \mathcal{B}(\bar{x}^*, r) \times \mathcal{B}(\hat{x}^*, R)$  with  $r := \min\{r_{\mathbf{M}}, r_{\mathbf{S}}\}$  and  $R := \min\{R_{\mathbf{M}}, R_{\mathbf{S}}\}$  and let

$$\begin{aligned}
\text{Graph}(\mathbf{l}_{\mathbf{M}}) &:= \left\{ (\bar{x}, \mathbf{l}_{\mathbf{M}}(\bar{x})) \in \mathbb{R}^m \mid \bar{x} \in \mathcal{B}(\bar{x}^*, r) \right\} \quad \text{and} \\
\text{Graph}(\mathbf{l}_{\mathbf{S}}) &:= \left\{ (\bar{x}, \mathbf{l}_{\mathbf{S}}(\bar{x})) \in \mathbb{R}^m \mid \bar{x} \in \mathcal{B}(\bar{x}^*, r) \right\}.
\end{aligned}$$

By the implicit function theorem,  $\text{Graph}(\mathbf{l}_{\mathbf{M}}) := \mathcal{M} \cap \mathcal{B}$  and  $\text{Graph}(\mathbf{l}_{\mathbf{S}}) := \mathbf{S}^{-1}(0) \cap \mathcal{B}$ . Since  $\mathcal{M} \subseteq \nabla F^{-1}(0) \subseteq \mathbf{S}^{-1}(0)$ , then  $\mathcal{M} \cap \mathcal{B} \subseteq \nabla F^{-1}(0) \cap \mathcal{B} \subseteq \mathbf{S}^{-1}(0) \cap \mathcal{B}$  and so

$$\text{Graph}(\mathbf{l}_M) \subseteq \text{Graph}(\mathbf{l}_S) . \quad (2.11)$$

In fact, these two sets are equal. To see this, suppose there exists  $z = (\bar{z}, \hat{z}) \in \mathcal{B}$  such that  $z \in \text{Graph}(\mathbf{l}_S)$  but  $z \notin \text{Graph}(\mathbf{l}_M)$ . Since  $z \in \text{Graph}(\mathbf{l}_S)$ , then  $\mathbf{l}_S(\bar{z}) = \hat{z}$  and since  $z \notin \text{Graph}(\mathbf{l}_M)$ , then  $\mathbf{l}_M(\bar{z}) \neq \hat{z}$ . However, since (2.11), then  $(\bar{z}, \mathbf{l}_M(\bar{z})) \in \text{Graph}(\mathbf{l}_h)$  which implies (because  $\mathbf{l}_S$  is a map) that

$$\mathbf{l}_S(\bar{z}) = \mathbf{l}_M(\bar{z}) \neq \hat{z} ,$$

which is a contradiction. Therefore  $\text{Graph}(\mathbf{l}_M) = \text{Graph}(\mathbf{l}_S)$  and so  $\mathcal{M} \cap \mathcal{B} = \mathcal{S}^{-1}(0) \cap \mathcal{B}$  and hence  $\mathcal{M} \cap \mathcal{B} = \nabla F^{-1}(0) \cap \mathcal{B}$ . Thus, there exists an open set  $\mathcal{U}_{x^*} \ni x^*$  which is  $\mathcal{B}$  such that for all  $x \in \mathcal{U}_{x^*} \setminus \mathcal{M}$ ,  $\nabla F(x) \neq 0$ .

□

**Corollary 2.1.** *With the same hypothesis as in Lemma 2.1 and supposing additionally that for all  $x^* \in \mathcal{M}$ , we have  $\ker(\mathfrak{D}\nabla F(x^*)) = \ker(\mathfrak{D}\mathcal{M}(x^*))$ . Then, there exists an open set  $\mathcal{U} \supset \mathcal{M}$  such that  $\nabla F(x) \neq 0$  for all  $x \in \mathcal{U} \setminus \mathcal{M}$ .*

*Proof.* By Lemma 2.1, there exists an open set  $\mathcal{U}_{x^*} \ni x^*$  such that  $\nabla F(x) \neq 0$  for all  $x \in \mathcal{U}_{x^*} \setminus \mathcal{M}$ . Then  $\mathcal{U}$  is given by

$$\mathcal{U} := \bigcup_{x^* \in \mathcal{M}} \mathcal{U}_{x^*} .$$

□

## 2.2.2 Network of Homogeneous Local Dynamics with Single Adapting Flow Parameters

Let the set of f-PV be reduced to a single element:  $\omega_k$ . Define the local dynamics of the network as

$$D(X_k, \omega_k) := \omega_k \mathbf{K}(X_k) \quad \text{and} \quad A_k(X_k) := \frac{1}{2} \sum_{j \in I_k} G_j(X_k)^2 .$$

The dynamical system is

$$\begin{aligned} \dot{X}_k &= \underbrace{\omega_k \mathbf{K}(X_k) - \sum_{j \in I_k} G_j(X_k) \nabla G_j(X_k)}_{\text{local dynamics}} - \underbrace{c_k \frac{\partial \mathcal{V}}{\partial X_k}(X)}_{\text{coupling dynamics}} \\ \dot{\omega}_k &= \underbrace{-s_k \left\langle \frac{\partial \mathcal{V}}{\partial X_k}(X) \mid \mathbf{K}(X_k) \right\rangle}_{\text{parametric dynamics}} \end{aligned} \quad k = 1, \dots, N . \quad (2.12)$$

Let us discuss the existence of a consensual state and the convergence towards it.

### Existence of a consensual state

The existence of a consensual state for System (2.12) is guaranteed if initial conditions are in  $\mathcal{M}$  (c.f. (2.7)) and  $\omega_k := \omega_c$  for all  $k$  with  $\omega_c$  a given constant.

### Convergence towards a consensual state

The convergence towards a consensual state as well as the explicit value of  $\omega_c$  are established by the following Proposition. For this, we define

$$\mathcal{C}_{\omega_c} := \{(X, \Omega) \in \mathbb{R}^{Np} \times \mathbb{R}^N \mid X \in \mathcal{M} \text{ and } \Omega = \omega_c \mathbf{1}\}$$

where  $\mathbf{1}$  is a  $N$  dimensional vector of 1.

**Proposition 2.2.** *Suppose that*

- for all  $X^* \in \mathcal{M}$ ,  $\langle X | \mathfrak{D}^2 \mathcal{V}(X^*) X \rangle = 0 \iff X_k = X_j \quad \forall k, j$
- $\sum_{k=1}^N \langle \frac{\partial \mathcal{V}}{\partial X_k}(X) | \mathbf{K}(X_k) \rangle = 0 \quad \forall X$ .

Then there exists a set  $\mathcal{U} \supset \mathcal{C}_{\omega_c}$  such that all orbits solving System (2.12) with initial conditions in  $\mathcal{U}$  converge towards  $\mathcal{C}_{\omega_c}$ , and  $\omega_c$  reads

$$\omega_c := \frac{\sum_{k=1}^N \frac{\omega_k(0)}{s_k}}{\sum_{k=1}^N \frac{1}{s_k}}.$$

*Proof.* The convergence towards  $\mathcal{C}_{\omega_c}$  follows from Ляпунов's second method with Ляпунов function:

$$\mathbb{J}_{\omega_c}(X, \Omega) := \mathbb{J}(X) + \frac{1}{2} \sum_{k=1}^N \frac{(\omega_k - \omega_c)^2}{s_k} \geq 0,$$

where  $\mathbb{J}(X)$  is defined in Proposition 2.1. By construction, we have that  $\mathcal{C}_{\omega_c} = \{(X, \Omega) \in \mathbb{R}^{Np} \times \mathbb{R}^N \mid \mathbb{J}(X, \Omega) = 0\}$ . Computing the time derivative

$$\begin{aligned} \langle \nabla \mathbb{J}_{\omega_c}(X, \Omega) | (\dot{X}, \dot{\Omega}) \rangle &= \sum_{k=1}^N \langle \frac{1}{c_k} \nabla A_k(X_k) + \frac{\partial \mathcal{V}}{\partial X_k}(X) | \dot{X}_k \rangle + \sum_{k=1}^N \frac{(\omega_k - \omega_c)}{s_k} \dot{\omega}_k \\ &= \sum_{k=1}^N \langle \frac{1}{c_k} \nabla A_k(X_k) + \frac{\partial \mathcal{V}}{\partial X_k}(X) | \omega_k \mathbf{K}(X_k) - \nabla A_k(X_k) - c_k \frac{\partial \mathcal{V}}{\partial X_k}(X) \rangle \\ &\quad - \sum_{k=1}^N \omega_k \langle \frac{\partial \mathcal{V}}{\partial X_k}(X) | \mathbf{K}(X_k) \rangle + \omega_c \underbrace{\sum_{k=1}^N \langle \frac{\partial \mathcal{V}}{\partial X_k}(X) | \mathbf{K}(X_k) \rangle}_{=0} \\ &= \sum_{k=1}^N \frac{1}{c_k} \underbrace{\langle \nabla A_k(X_k) | \omega_k \mathbf{K}(X_k) \rangle}_{=0} + \sum_{k=1}^N \langle \frac{\partial \mathcal{V}}{\partial X_k}(X) | \omega_k \mathbf{K}(X_k) \rangle \\ &\quad - \underbrace{\sum_{k=1}^N c_k \left\| \frac{1}{c_k} \nabla A_k(X_k) + \frac{\partial \mathcal{V}}{\partial X_k}(X) \right\|^2}_{\leq 0} - \sum_{k=1}^N \langle \frac{\partial \mathcal{V}}{\partial X_k}(X) | \omega_k \mathbf{K}(X_k) \rangle. \end{aligned}$$

Let  $\mathcal{U}_{\omega_c}$  be a neighborhood of  $\omega_c \mathbf{1}$  included in the hyperplane

$$\{\Omega \in \mathbb{R}^N \mid \sum_{k=1}^N \frac{\omega_k}{s_k} = \omega_c \sum_{k=1}^N \frac{1}{s_k}\}.$$

Therefore, by taking the open set  $\mathcal{U} \supset \mathcal{M}$  whose existence we have proven in Proposition 2.1, strict negativity of  $\langle \nabla \mathbb{J}_{\omega_c}(X, \Omega) | (\dot{X}, \dot{\Omega}) \rangle < 0$  holds for all  $(X, \Omega) \in \mathcal{U} \times \mathcal{U}_{\omega_c} \setminus \mathcal{C}_{\omega_c}$ . Hence, the compact set  $\mathcal{C}_{\omega_c}$  is asymptotically stable (refer to Appendix A).

The hypothesis that  $\sum_{k=1}^N \langle \frac{\partial \mathcal{V}}{\partial X_k}(X) | \mathbf{K}(X_k) \rangle = 0$  leads to the existence of a constant of motion:

$\mathbb{J}(\omega_1, \dots, \omega_N) := \sum_{k=1}^N \frac{\omega_k}{s_k}$ . Indeed, for  $\omega_k(t)$  ( $k = 1, \dots, N$ ) orbits of Eqs. (2.12), we have

$$\frac{d[\mathbb{J}(\omega_1(t), \dots, \omega_N(t))]}{dt} = \sum_{k=1}^N \frac{\dot{\omega}_k(t)}{s_k} = - \sum_{k=1}^N \langle \frac{\partial \mathcal{V}}{\partial X_k}(X) | \mathbf{K}(X_k) \rangle = 0.$$

Thus  $\mathbf{C} = \sum_{k=1}^N \frac{\omega_k(t)}{s_k}$  for all  $t$ , and  $\mathbf{C} = \sum_{k=1}^N \frac{\omega_k(0)}{s_k}$ . Due to the convergence,  $\mathbf{C} = \omega_c \sum_{k=1}^N \frac{1}{s_k}$  and therefore

$$\omega_c := \frac{\sum_{k=1}^N \frac{\omega_k(0)}{s_k}}{\sum_{k=1}^N \frac{1}{s_k}}.$$

□

*Example 2.1.* Take  $p = 3$  and the attracting submanifold to be a closed curve in  $\mathbb{R}^3$  (i.e.  $m = 1$ ). Select  $G_1$  and  $G_2$  functions as

$$G_1(X_k) := \mathbf{a} x_k^2 + \mathbf{b} y_k^2 + \mathbf{d} z_k^2 - 1 \quad G_2(X_k) := \mathbf{a} x_k + \mathbf{b} y_k + \mathbf{d} z_k - 1$$

with  $X_k = (x_k, y_k, z_k)$  and  $\mathbf{a}, \mathbf{b}$  and  $\mathbf{d}$  belong to the geometric parameter set  $\Gamma$  which is not explicitly written. The potentials are all identical:  $A_k \equiv \frac{1}{2}(G_1^2 + G_2^2)$ . The vector product between  $\nabla G_1$  and  $\nabla G_2$  determines  $D$  and it is explicitly written as

$$D(X_k, \omega_k) = \omega_k K(X_k) := \omega_k \begin{pmatrix} \mathbf{b}\mathbf{d}(y_k - z_k) \\ \mathbf{a}\mathbf{d}(z_k - x_k) \\ \mathbf{a}\mathbf{b}(x_k - y_k) \end{pmatrix}$$

where the f-PV is  $\omega_k$ . We consider a connected and undirected network with positive adjacency entries (refer to Appendix C), and denote by  $L$  the corresponding Laplacian matrix. The coupling dynamics is given by the gradient of the following Laplacian potential

$$V(X) := \frac{1}{2}(\mathbf{a}\langle x | Lx \rangle + \mathbf{b}\langle y | Ly \rangle + \mathbf{d}\langle z | Lz \rangle)$$

with  $x = (x_1, \dots, x_N)$  (idem for  $y$  and  $z$ ). The orthogonality condition of Proposition 2.2 is satisfied as

$$\begin{aligned} \sum_{k=1}^N \left\langle \frac{\partial V}{\partial X_k}(X) \mid K(X_k) \right\rangle &= \sum_{k=1}^N \left\langle \begin{pmatrix} \sum_{j=1}^N l_{k,j} \mathbf{a} x_j \\ \sum_{j=1}^N l_{k,j} \mathbf{b} y_j \\ \sum_{j=1}^N l_{k,j} \mathbf{d} z_j \end{pmatrix} \mid \begin{pmatrix} \mathbf{b}\mathbf{d}(y_k - z_k) \\ \mathbf{a}\mathbf{d}(z_k - x_k) \\ \mathbf{a}\mathbf{b}(x_k - y_k) \end{pmatrix} \right\rangle \\ &= \sum_{k=1}^N \left( \left( \sum_{j=1}^N l_{k,j} \mathbf{a} x_j \right) \mathbf{b}\mathbf{d}(y_k - z_k) + \left( \sum_{j=1}^N l_{k,j} \mathbf{b} y_j \right) \mathbf{a}\mathbf{d}(z_k - x_k) + \left( \sum_{j=1}^N l_{k,j} \mathbf{d} z_j \right) \mathbf{a}\mathbf{b}(x_k - y_k) \right) \\ &= \mathbf{a}\mathbf{b}\mathbf{d} \left( \sum_{k=1}^N \sum_{j=1}^N (x_j y_k - y_j x_k) + \sum_{k=1}^N \sum_{j=1}^N (y_j z_k - z_j y_k) + \sum_{k=1}^N \sum_{j=1}^N (z_j x_k - x_j z_k) \right) = 0 \end{aligned}$$

since, by Lemma D.1 in Appendix D, each term is zero. For  $k = 1, \dots, N$ , the resulting dynamical system explicitly reads as

$$\begin{pmatrix} \dot{x}_k \\ \dot{y}_k \\ \dot{z}_k \end{pmatrix} = \underbrace{\omega_k \begin{pmatrix} \mathbf{b}\mathbf{d}(y_k - z_k) \\ \mathbf{a}\mathbf{d}(z_k - x_k) \\ \mathbf{a}\mathbf{b}(x_k - y_k) \end{pmatrix} - 2G_1(X_k) \begin{pmatrix} \mathbf{a} x_k \\ \mathbf{b} y_k \\ \mathbf{d} z_k \end{pmatrix} - G_2(X_k) \begin{pmatrix} \mathbf{a} \\ \mathbf{b} \\ \mathbf{d} \end{pmatrix}}_{\text{local dynamics}} - \underbrace{c_k \begin{pmatrix} \sum_{j=1}^N l_{k,j} \mathbf{a} x_j \\ \sum_{j=1}^N l_{k,j} \mathbf{b} y_j \\ \sum_{j=1}^N l_{k,j} \mathbf{d} z_j \end{pmatrix}}_{\text{coupling dynamics}}$$

$$\dot{\omega}_k = -\mathbf{s}_k \left\langle \underbrace{\begin{pmatrix} \sum_{j=1}^N l_{k,j} \mathbf{a} x_j \\ \sum_{j=1}^N l_{k,j} \mathbf{b} y_j \\ \sum_{j=1}^N l_{k,j} \mathbf{d} z_j \end{pmatrix}}_{\text{parametric dynamics}} \mid \begin{pmatrix} \mathbf{b} \mathbf{d} (y_k - z_k) \\ \mathbf{a} \mathbf{d} (z_k - x_k) \\ \mathbf{a} \mathbf{b} (x_k - y_k) \end{pmatrix} \right\rangle .$$

Although  $A$  is symmetric, the heterogeneous *coupling strengths*  $c_k$  confer a weighted character to the (undirected) network (see [34] and [9] for similar situations). As this also holds for the susceptibility constants  $\mathbf{s}_k$ , the resulting dynamics effectively involves two networks: one directly responsible for the state variable interactions and the other governing the connections of the adaptive mechanism.

### 2.2.3 Network of Homogeneous Local Dynamics with Multi Adapting Flow Parameters

We present a class of network dynamics for the second type of generalization discussed in Subsection 2.1.3.1. Let the set  $\Phi_k \in \mathbb{R}^{\frac{p(p-1)}{2}}$  of f-PV define a  $p \times p$  anti-symmetric matrix  $T_k$ . Define the **local dynamics** of the network as

$$D(X_k, \Phi_k) := T_k \nabla G_1(X_k) \quad \text{and} \quad A(X_k) := \frac{1}{2} G_1(X_k)^2 .$$

where we drop the index  $k$  from the potentials  $A$  since they are all identical. Note that  $D$  is always orthogonal to  $\nabla A$  (refer to Appendix D). The dynamical system is

$$\begin{aligned} \dot{X}_k &= \underbrace{T_k \nabla G_1(X_k) - G_1(X_k) \nabla G_1(X_k)}_{\text{local dynamics}} - \underbrace{c_k \frac{\partial V}{\partial X_k}(X)}_{\text{coupling dynamics}} \quad k = 1, \dots, N \\ \dot{\omega}_{k,l,s} &= -\mathbf{s}_{k,l,s} \left\langle \underbrace{\begin{pmatrix} \frac{\partial V}{\partial x_{k,l}}(X) \\ \frac{\partial V}{\partial x_{k,s}}(X) \end{pmatrix}}_{\text{parametric dynamics}} \mid \begin{pmatrix} \frac{\partial G}{\partial x_s}(X_k) \\ -\frac{\partial G}{\partial x_l}(X_k) \end{pmatrix} \right\rangle \quad \begin{matrix} l, s = 1, \dots, p \\ s > l \end{matrix} \end{aligned} \quad (2.13)$$

Let us discuss the existence of a consensual state and the convergence towards it.

#### Existence of a consensual state

The existence of a consensual state for System (2.13) is guaranteed if initial conditions are in  $\mathcal{M}$  (c.f. (2.7)) and  $\Phi_k := \Omega_c$  for all  $k$  with  $\Omega_c$  a given constant vector.

#### Convergence towards a consensual state

The convergence towards a consensual state as well as the explicit value of the coefficients of  $\Omega_c$  are established by the following Proposition. For this, we define

$$\mathcal{C}_{\Omega_c} := \{(X, \Omega) \in \mathbb{R}^{Np} \times \mathbb{R}^{N \frac{p(p-1)}{2}} \mid X \in \mathcal{M} \text{ and } \Omega = \mathbf{1} \otimes \Omega_c\}$$

where  $\mathbf{1}$  is a  $\frac{p(p-1)}{2}$  dimensional vector of 1 and  $\otimes$  is the KRONECKER product.

**Proposition 2.3.** *Suppose that*

- for all  $X^* \in \mathcal{M}$ ,  $\langle X \mid \mathfrak{D}^2 V(X^*) X \rangle = 0 \iff X_k = X_j \quad \forall k, j$
- for all  $s$  and  $l$  ( $l, s = 1, \dots, p$ , and  $s > l$ ),  $\sum_{k=1}^N \left\langle \begin{pmatrix} \frac{\partial V}{\partial x_{k,l}}(X) \\ \frac{\partial V}{\partial x_{k,s}}(X) \end{pmatrix} \mid \begin{pmatrix} \frac{\partial G_1}{\partial x_s}(X_k) \\ -\frac{\partial G_1}{\partial x_l}(X_k) \end{pmatrix} \right\rangle = 0 \quad \forall X .$

Then there exists a set  $\mathcal{U} \supset \mathcal{C}_{\Omega_c}$  such that all orbits solving System (2.12) with initial conditions in  $\mathcal{U}$  converge towards  $\mathcal{C}_{\Omega_c}$ , and the coefficients of  $\Omega_c$  read as

$$\omega_{c,l,s} := \frac{\sum_{k=1}^N \frac{\omega_{k,l,s}(0)}{\mathfrak{s}_{k,l,s}}}{\sum_{k=1}^N \frac{1}{\mathfrak{s}_{k,l,s}}} \quad l, s = 1 \dots, p, \quad s > l.$$

*Proof.* The convergence towards  $\mathcal{C}_{\Omega_c}$  follows from Ляпунов's second method with Ляпунов function:

$$\mathbb{I}_{\Omega_c}(X, \Omega) := \mathbb{I}(X) + \frac{1}{2} \sum_{\substack{s,l=1 \\ s < l}}^p \left( \sum_{k=1}^N \frac{(\omega_{k,l,s} - \omega_{c,l,s})^2}{\mathfrak{s}_{k,l,s}} \right) \geq 0,$$

where  $\mathbb{I}(X)$  is defined in Proposition 2.1 with here  $A_k(X_k) = \frac{1}{2}G(X_k)^2$ . By construction, we have that  $\mathcal{C}_{\Omega_c} = \{(X, \Omega) \in \mathbb{R}^{Np} \times \mathbb{R}^{N\frac{p(p-1)}{2}} \mid \mathbb{I}_{\Omega_c}(X, \Omega) = \mathbf{0}\}$ . Computing the time derivative

$$\begin{aligned} \langle \nabla \mathbb{I}_{\Omega_c}(X, \Omega) \mid (\dot{X}, \dot{\Omega}) \rangle &= \sum_{k=1}^N \left\langle \frac{G(X_k)}{c_k} \nabla G(X_k) + \frac{\partial \mathbb{V}}{\partial X_k}(X) \mid T_k \nabla G(X_k) - G(X_k) \nabla G(X_k) - c_k \frac{\partial \mathbb{V}}{\partial X_k}(X) \right\rangle \\ &\quad - \sum_{\substack{s,l=1 \\ s < l}}^p \left( \sum_{k=1}^N (\omega_{k,l,s} - \omega_{c,l,s}) \left( \frac{\partial \mathbb{V}}{\partial x_{k,l}}(X) \frac{\partial G}{\partial x_s}(X_k) - \frac{\partial \mathbb{V}}{\partial x_{k,s}}(X) \frac{\partial G}{\partial x_l}(X_k) \right) \right) \\ &= \sum_{k=1}^N \frac{1}{c_k} \underbrace{\langle G(X_k) \nabla G(X_k) \mid T_k \nabla G(X_k) \rangle}_{=0} + \left\langle \frac{\partial \mathbb{V}}{\partial X_k}(X) \mid T_k \nabla G(X_k) \right\rangle \\ &\quad - \sum_{k=1}^N c_k \left\| \frac{G(X_k)}{c_k} \nabla G(X_k) + \frac{\partial \mathbb{V}}{\partial X_k}(X) \right\|^2 \\ &\quad - \sum_{\substack{s,l=1 \\ s < l}}^p \left( \sum_{k=1}^N \omega_{k,l,s} \left( \frac{\partial \mathbb{V}}{\partial x_{k,l}}(X) \frac{\partial G}{\partial x_s}(X_k) - \frac{\partial \mathbb{V}}{\partial x_{k,s}}(X) \frac{\partial G}{\partial x_l}(X_k) \right) \right) \\ &\quad + \sum_{\substack{s,l=1 \\ s < l}}^p \omega_{c,l,s} \underbrace{\left( \sum_{k=1}^N \frac{\partial \mathbb{V}}{\partial x_{k,l}}(X) \frac{\partial G}{\partial x_s}(X_k) - \frac{\partial \mathbb{V}}{\partial x_{k,s}}(X) \frac{\partial G}{\partial x_l}(X_k) \right)}_{=0} \\ &= - \underbrace{\sum_{k=1}^N c_k \left\| \frac{G(X_k)}{c_k} \nabla G(X_k) + \frac{\partial \mathbb{V}}{\partial X_k}(X) \right\|^2}_{\leq 0} + \underbrace{\left\langle \frac{\partial \mathbb{V}}{\partial X_k}(X) \mid T_k \nabla G(X_k) \right\rangle}_{\text{I}} \\ &\quad - \underbrace{\sum_{k=1}^N \left( \sum_{\substack{s,l=1 \\ s < l}}^p \omega_{k,l,s} \left( \frac{\partial \mathbb{V}}{\partial x_{k,l}}(X) \frac{\partial G}{\partial x_s}(X_k) - \frac{\partial \mathbb{V}}{\partial x_{k,s}}(X) \frac{\partial G}{\partial x_l}(X_k) \right) \right)}_{\text{II}}. \end{aligned}$$

With Lemma D.4 in Appendix D, the terms I and II cancel each other for each  $k$ . Let  $\mathcal{U}_{\Omega_c}$  be a neighborhood of  $\mathbf{1} \otimes \Omega_c$  included in the hyperplanes

$$\left\{ \Omega \in \mathbb{R}^{N\frac{p(p-1)}{2}} \mid \sum_{k=1}^N \frac{\omega_{k,l,s}}{\mathfrak{s}_{k,l,s}} = \omega_{c,l,s} \sum_{k=1}^N \frac{1}{\mathfrak{s}_{k,l,s}} \quad l, s = 1 \dots, p, \quad s > l \right\}.$$

Therefore, by taking the open set  $\mathcal{U} \supset \mathcal{M}$  whose existence we have proven in Proposition 2.1, strict negativity of  $\langle \nabla \mathbb{I}_{\Omega_c}(X, \Omega) \mid (\dot{X}, \dot{\Omega}) \rangle < 0$  holds for all  $(X, \Omega) \in \mathcal{U} \times \mathcal{U}_{\Omega_c} \setminus \mathcal{C}_{\Omega_c}$ . Hence, the compact set  $\mathcal{C}_{\Omega_c}$  is asymptotically stable (refer to Appendix A).

The hypothesis that  $\sum_{k=1}^N \frac{\partial \mathcal{V}}{\partial x_{k,l}}(X) \frac{\partial \mathcal{G}}{\partial x_s}(X_k) - \frac{\partial \mathcal{V}}{\partial x_{k,s}}(X) \frac{\partial \mathcal{G}}{\partial x_l}(X_k) = 0$ , for all  $l, s = 1 \dots, p$ , and  $s > l$ , leads to the existence of  $\frac{p(p-1)}{2}$  constant of motions:  $J_{l,s}(\omega_{1,l,s}, \dots, \omega_{N,l,s}) := \sum_{k=1}^N \frac{\omega_{k,l,s}}{s_{k,l,s}}$ . Indeed, for  $\omega_{k,l,s}(t)$  ( $k = 1, \dots, N$ ,  $l, s = 1 \dots, p$ , and  $s > l$ ) orbits of Eqs. (2.12), we have

$$\frac{d[J_{l,s}(\omega_{1,l,s}(t), \dots, \omega_{N,l,s}(t))]}{dt} = \sum_{k=1}^N \frac{\dot{\omega}_{k,l,s}(t)}{s_{k,l,s}} = \sum_{k=1}^N \frac{\partial \mathcal{V}}{\partial x_{k,l}}(X) \frac{\partial \mathcal{G}}{\partial x_s}(X_k) - \frac{\partial \mathcal{V}}{\partial x_{k,s}}(X) \frac{\partial \mathcal{G}}{\partial x_l}(X_k) = 0.$$

Thus  $\mathbf{C} = \sum_{k=1}^N \frac{\omega_{k,l,s}(t)}{s_{k,l,s}}$  for all  $t$ , and  $\mathbf{C} = \sum_{k=1}^N \frac{\omega_{k,l,s}(0)}{s_{k,l,s}}$ . Due to the convergence,  $\mathbf{C} = \omega_{c,l,s} \sum_{k=1}^N \frac{1}{s_{k,l,s}}$  and therefore

$$\omega_{c,l,s} := \frac{\sum_{k=1}^N \frac{\omega_{k,l,s}(0)}{s_{k,l,s}}}{\sum_{k=1}^N \frac{1}{s_{k,l,s}}} \quad l, s = 1 \dots, p, \quad s > l.$$

□

*Example 2.2.* Let  $p \geq 2$  be an arbitrary positive integer and the attracting submanifold be a *hyper-ellipsoid* in  $\mathbb{R}^p$  of dimension  $m = p - 1$  defined by

$$\mathbf{G}_1(X_k) := \sum_{j=1}^p \mathbf{a}_j x_{k,j}^2 - 1$$

with  $X_k = (x_{k,1}, \dots, x_{k,p})$  and the  $\mathbf{a}_j$  belong to the geometric parameter set  $\Gamma$  which is not explicitly written. The orthogonal part of the **local dynamics** is given by

$$\mathbf{D}(X_k, \Phi_k) := T_k \nabla \mathbf{G}_1(X_k)$$

where the elements of  $\Phi_k \in \mathbb{R}^{\frac{p(p-1)}{2}}$  define the  $p \times p$  anti-symmetric matrix  $T_k$ . We consider a connected and undirected network with positive adjacency entries (refer to Appendix C), and denote by  $L$  the corresponding Laplacian matrix. The **coupling dynamics** is by the gradient of the following Laplacian potential

$$\mathbf{V}(X) := \frac{1}{2} \sum_{j=1}^p \mathbf{a}_j \langle x_j | L x_j \rangle$$

with  $x_j := (x_{1,j}, \dots, x_{N,j}) \in \mathbb{R}^N$ . The condition of Proposition 2.3 is satisfied because, for all  $s$  and  $l$  ( $l, s = 1 \dots, p$ , and  $s > l$ ),

$$\begin{aligned} \sum_{k=1}^N \left\langle \left( \frac{\partial \mathcal{V}}{\partial x_{k,l}}(X) \right) \middle| \left( \begin{array}{c} \frac{\partial \mathbf{G}}{\partial x_s}(X_k) \\ -\frac{\partial \mathbf{G}}{\partial x_l}(X_k) \end{array} \right) \right\rangle &= \sum_{k=1}^N \left[ \left( \sum_{j=1}^N \mathbf{a}_l l_{k,j} x_{j,l} \right) (\mathbf{a}_s x_{k,s}) - \left( \sum_{j=1}^N \mathbf{a}_s l_{k,j} x_{j,s} \right) (\mathbf{a}_l x_{k,l}) \right] \\ &= \mathbf{a}_l \mathbf{a}_s \left( \sum_{k=1}^N \sum_{j=1}^N l_{k,j} (x_{j,l} x_{k,s} - x_{j,s} x_{k,l}) \right) = 0 \end{aligned}$$

since, by Lemma D.1 in Appendix D, this last sum is zero. Note that for  $p \geq 3$ , the orbit's geometry of the consensual state is not fully characterized: we only know that the orthogonal part of the **local dynamics** (i.e.  $\mathbf{D}$ ) has its orbits lying on the hyper-ellipsoid.

## 2.2.4 Network of Heterogeneous Local Dynamics with Single and Multi Adapting Flow Parameters

We consider a network composed of both single and multi adapting parameters, as presented in Sections 2.2.2 and 2.2.3 respectively. For a fixed integer  $0 < v < N$ , define the local dynamics as

$$\begin{aligned} \text{for } k = 1, \dots, v & : \mathbf{L}_k(X_k, \Omega_k) := \omega_k \mathbf{K}(X_k) - \sum_{j \in I_k} \mathbf{G}_j(X_k) \nabla \mathbf{G}_j(X_k), \\ \text{for } k = v + 1, \dots, N & : \mathbf{L}_k(X_k, \Omega_k) := T_k \nabla \mathbf{G}_1(X_k) - \mathbf{G}_1(X_k) \nabla \mathbf{G}_1(X_k), \end{aligned}$$

where the f-PV are  $\Omega_k = \omega_k$  for  $k = 1, \dots, v$  and, for  $k = v + 1, \dots, N$ ,  $\Omega_k = \Phi_k \in \mathbb{R}^{\frac{p(p-1)}{2}}$  which defines a  $p \times p$  anti-symmetric matrix  $T_k$ . If all the elements in  $\Phi_k$  are equal to  $\omega_c$ , then  $T_k = \omega_c T_{(\mathbf{1})}$  for all  $k$ , where  $T_{(\mathbf{1})}$  is an anti-symmetric matrix with 1 on its upper diagonal. The dynamical system is

$$\begin{aligned} \dot{X}_k &= \underbrace{\mathbf{L}_k(X_k, \Omega_k)}_{\text{local dynamics}} - \underbrace{c_k \frac{\partial \mathcal{V}}{\partial X_k}(X)}_{\text{coupling dynamics}} \quad k = 1, \dots, N \\ \dot{\omega}_k &= -s_k \left\langle \frac{\partial \mathcal{V}}{\partial X_k}(X) \mid \mathbf{K}(X_k) \right\rangle \quad k = 1, \dots, v \\ \dot{\omega}_{k,l,s} &= \underbrace{-s_{k,l,s} \left\langle \left( \begin{array}{c} \frac{\partial \mathcal{V}}{\partial x_{k,l}}(X) \\ \frac{\partial \mathcal{V}}{\partial x_{k,s}}(X) \end{array} \right) \mid \left( \begin{array}{c} \frac{\partial \mathbf{G}_1}{\partial x_s}(X_k) \\ -\frac{\partial \mathbf{G}_1}{\partial x_l}(X_k) \end{array} \right) \right\rangle}_{\text{parametric dynamics}} \quad \begin{array}{l} k = v + 1, \dots, N \\ l, s = 1, \dots, p \\ s > l \end{array} \end{aligned} \quad (2.14)$$

Let us discuss the existence of a consensual state and the convergence towards it.

### Existence of a consensual state

The existence of a consensual state for System (2.14) is guaranteed if initial conditions are in  $\mathcal{M}$  (c.f. (2.7)) and we suppose that  $\omega_c T_{(\mathbf{1})} \nabla \mathbf{G}_1 \equiv \omega_c \mathbf{K}$  with  $\omega_c$  a given constant.

### Convergence towards a consensual state

The convergence towards a consensual state as well as the explicit value of  $\omega_c$  and all coefficients of  $\Omega_c$  are established by the following Proposition. For this, we define

$$\mathcal{C}_{\omega_c \times \Omega_c} := \{(X, \Omega) \in \mathbb{R}^{Np} \times \mathbb{R}^{v+(N-v)\frac{p(p-1)}{2}} \mid X \in \mathcal{M} \text{ and } \Omega = \omega_c \mathbf{1}\}$$

where  $\mathbf{1}$  is a  $v + (N - v)\frac{p(p-1)}{2}$  dimensional vector of 1.

**Proposition 2.4.** *Suppose that*

- for all  $X^* \in \mathcal{M}$ ,  $\langle X \mid \mathfrak{D}^2 \mathcal{V}(X^*) X \rangle = 0 \iff X_k = X_j \quad \forall k, j$
- $\sum_{k=1}^v \left\langle \frac{\partial \mathcal{V}}{\partial X_k}(X) \mid \mathbf{K}(X_k) \right\rangle + \sum_{\substack{s,l=1 \\ s < l}}^p \sum_{k=v+1}^N \left( \left\langle \left( \begin{array}{c} \frac{\partial \mathcal{V}}{\partial x_{k,l}}(X) \\ \frac{\partial \mathcal{V}}{\partial x_{k,s}}(X) \end{array} \right) \mid \left( \begin{array}{c} \frac{\partial \mathbf{G}_1}{\partial x_s}(X_k) \\ -\frac{\partial \mathbf{G}_1}{\partial x_l}(X_k) \end{array} \right) \right\rangle \right) = 0 \quad \forall X.$

Then there exists a set  $\mathcal{U} \supset \mathcal{C}_{\omega_c \times \Omega_c}$  such that all orbits solving System (2.12) with initial conditions in  $\mathcal{U}$  converge towards  $\mathcal{C}_{\omega_c \times \Omega_c}$ , and  $\omega_c$  and all coefficients of  $\Omega_c$  read as

$$\omega_c := \frac{\sum_{k=1}^v \frac{\omega_k(0)}{s_k} + \sum_{\substack{s,l=1 \\ s < l}}^p \sum_{k=v+1}^N \frac{\omega_{k,l,s}(0)}{s_{k,l,s}}}{\sum_{k=1}^v \frac{1}{s_k} + \sum_{\substack{s,l=1 \\ s < l}}^p \sum_{k=v+1}^N \frac{1}{s_{k,l,s}}}.$$



*Proof.* The convergence towards  $\mathcal{C}_{\omega_c \times \Omega_c}$  follows from Ляпунов's second method with Ляпунов function:

$$\mathbb{J}_{\omega_c \times \Omega_c}(X, \Omega) := \mathbb{J}(X) + \frac{1}{2} \sum_{k=1}^v \frac{(\omega_k - \omega_c)^2}{s_k} + \frac{1}{2} \sum_{\substack{s,l=1 \\ s < l}}^p \left( \sum_{k=v+1}^N \frac{(\omega_{k,l,s} - \omega_c)^2}{s_{k,l,s}} \right),$$

where  $\mathbb{J}(X)$  is defined as in Appendix E with  $A_k(X_k) := \frac{1}{2} \sum_{j \in I_k} G_j(X_k)^2$  for  $k = 1, \dots, v$  and  $A_k(X_k) := \frac{1}{2} G_1(X_k)^2$  for  $k = v+1, \dots, N$ . By construction, we have that  $\mathcal{C}_{\omega_c \times \Omega_c} = \{(X, \Omega) \in \mathbb{R}^{pN} \times \mathbb{R}^{v+(N-v)\frac{p(p-1)}{2}} \mid \mathbb{J}_{\omega_c \times \Omega_c}(X, \Omega) = 0\}$ . Computing the time derivative

$$\begin{aligned} \langle \nabla \mathbb{J}_{\omega_c \times \Omega_c}(X, \Omega) \mid (\dot{X}, \dot{\Omega}) \rangle &= \sum_{k=1}^v \left\langle \frac{1}{c_k} \nabla A_k(X_k) + \frac{\partial \mathbb{V}}{\partial X_k}(X) \mid \omega_k \mathbb{K}(X_k) - \nabla A_k(X_k) - c_k \frac{\partial \mathbb{V}}{\partial X_k}(X) \right\rangle \\ &\quad + \sum_{k=v+1}^N \left\langle \frac{G_1(X_k)}{c_k} \nabla G_1(X_k) + \frac{\partial \mathbb{V}}{\partial X_k}(X) \mid T_k \nabla G_1(X_k) - G_1(X_k) \nabla G_1(X_k) - c_k \frac{\partial \mathbb{V}}{\partial X_k}(X) \right\rangle \\ &\quad - \sum_{k=1}^v (\omega_k - \omega_c) \left\langle \frac{\partial \mathbb{V}}{\partial X_k}(X) \mid \mathbb{K}(X_k) \right\rangle \\ &\quad - \sum_{\substack{s,l=1 \\ s < l}}^p \left( \sum_{k=v+1}^N (\omega_{k,l,s} - \omega_c) \left( \frac{\partial \mathbb{V}}{\partial x_{k,l}}(X) \frac{\partial G_1}{\partial x_s}(X_k) - \frac{\partial \mathbb{V}}{\partial x_{k,s}}(X) \frac{\partial G_1}{\partial x_l}(X_k) \right) \right) \\ &= \sum_{k=1}^v \frac{1}{c_k} \underbrace{\left\langle \nabla A_k(X_k) \mid \omega_k \mathbb{K}(X_k) \right\rangle}_{=0} + \sum_{k=1}^v \left\langle \frac{\partial \mathbb{V}}{\partial X_k}(X) \mid \omega_k \mathbb{K}(X_k) \right\rangle - \sum_{k=1}^v \omega_k \left\langle \frac{\partial \mathbb{V}}{\partial X_k}(X) \mid \mathbb{K}(X_k) \right\rangle \\ &\quad - \sum_{k=1}^v c_k \left\| \frac{1}{c_k} \nabla A_k(X_k) + \frac{\partial \mathbb{V}}{\partial X_k}(X) \right\|^2 \\ &\quad + \sum_{k=v+1}^N \left( \underbrace{\frac{1}{c_k} \left\langle G_1(X_k) \nabla G_1(X_k) \mid T_k \nabla G_1(X_k) \right\rangle}_{=0} + \underbrace{\left\langle \frac{\partial \mathbb{V}}{\partial X_k}(X) \mid T_k \nabla G_1(X_k) \right\rangle}_I \right) \\ &\quad - \sum_{k=v+1}^N c_k \left\| \frac{G_1(X_k)}{c_k} \nabla G_1(X_k) + \frac{\partial \mathbb{V}}{\partial X_k}(X) \right\|^2 \\ &\quad - \underbrace{\sum_{k=v+1}^N \sum_{\substack{s,l=1 \\ s < l}}^p \omega_{k,l,s} \left( \frac{\partial \mathbb{V}}{\partial x_{k,l}}(X) \frac{\partial G_1}{\partial x_s}(X_k) - \frac{\partial \mathbb{V}}{\partial x_{k,s}}(X) \frac{\partial G_1}{\partial x_l}(X_k) \right)}_{II} \\ &\quad - \omega_c \underbrace{\left( \sum_{k=1}^v \left\langle \frac{\partial \mathbb{V}}{\partial X_k}(X) \mid \mathbb{K}(X_k) \right\rangle + \sum_{\substack{s,l=1 \\ s < l}}^p \left( \sum_{k=v+1}^N \frac{\partial \mathbb{V}}{\partial x_{k,l}}(X) \frac{\partial G_1}{\partial x_s}(X_k) - \frac{\partial \mathbb{V}}{\partial x_{k,s}}(X) \frac{\partial G_1}{\partial x_l}(X_k) \right) \right)}_{=0} \\ &= \underbrace{- \sum_{k=1}^v c_k \left\| \frac{1}{c_k} \nabla A_k(x_k) + \frac{\partial \mathbb{V}}{\partial X_k}(X) \right\|^2 - \sum_{k=v+1}^N c_k \left\| \frac{G(X_k)}{c_k} \nabla G(X_k) + \frac{\partial \mathbb{V}}{\partial X_k}(X) \right\|^2}_{\leq 0}. \end{aligned}$$

With Lemma D.4 in Appendix D, the terms I and II cancel each other for each  $k$ . Let  $\mathcal{U}_{\omega_c \times \Omega_c}$  be a neighborhood of  $\omega_c \mathbf{1}$  included in the hyperplane

$$\left\{ \Omega \in \mathbb{R}^{v+(N-v)\frac{p(p-1)}{2}} \mid \sum_{k=1}^v \frac{\omega_k}{s_k} + \sum_{\substack{s,l=1 \\ s < l}}^p \sum_{k=v+1}^N \frac{\omega_{k,l,s}}{s_{k,l,s}} = \omega_c \left( \sum_{k=1}^v \frac{1}{s_k} + \sum_{\substack{s,l=1 \\ s < l}}^p \sum_{k=v+1}^N \frac{1}{s_{k,l,s}} \right) \right\}.$$

Therefore, by taking the open set  $\mathcal{U} \supset \mathcal{M}$  whose existence we have proven in Proposition 2.1 (we use here the more generalized form of the function  $\mathbb{J}$  that is found in Appendix E to guarantee the equality of the kernels), strict negativity of  $\langle \nabla \mathbb{J}_{\omega_c \times \Omega_c}(X, \Omega) \mid (\dot{X}, \dot{\Omega}) \rangle < 0$  holds for all

$(X, \Omega) \in \mathcal{U} \times \mathcal{U}_{\omega_c \times \Omega_c} \setminus \mathcal{C}_{\omega_c \times \Omega_c}$ . Hence, the compact set  $\mathcal{C}_{\omega_c \times \Omega_c}$  is asymptotically stable (refer to Appendix A).

The hypothesis that  $\sum_{k=1}^v \langle \frac{\partial V}{\partial X_k}(X) | \mathbf{K}(X_k) \rangle + \sum_{\substack{s,l=1 \\ s < l}}^p \sum_{k=v+1}^N \left( \frac{\partial V}{\partial x_{k,l}}(X) \frac{\partial G}{\partial x_s}(X_k) - \frac{\partial V}{\partial x_{k,s}}(X) \frac{\partial G}{\partial x_l}(X_k) \right) = 0$ ,

leads to the existence of a constant of motion:  $\mathbf{J}(\Omega) := \sum_{k=1}^v \frac{\omega_k}{s_k} + \sum_{\substack{s,l=1 \\ s < l}}^p \sum_{k=v+1}^N \frac{\omega_{k,l,s}}{s_{k,l,s}}$ . Indeed, for  $\omega_k(t)$

( $k = 1, \dots, v$ ) and  $\omega_{k,l,s}(t)$  ( $k = v+1, \dots, N$ ,  $l, s = 1, \dots, p$ , and  $s > l$ ) orbits of Eqs. (2.14), we have

$$\begin{aligned} \frac{d[\mathbf{J}(\Omega(t))]}{dt} &= \sum_{k=1}^v \frac{\dot{\omega}_k(t)}{s_k} + \sum_{\substack{s,l=1 \\ s < l}}^p \sum_{k=v+1}^N \frac{\dot{\omega}_{k,l,s}(t)}{s_{k,l,s}} \\ &= \sum_{k=1}^v \langle \frac{\partial V}{\partial X_k}(X) | \mathbf{K}(X_k) \rangle + \sum_{\substack{s,l=1 \\ s < l}}^p \sum_{k=v+1}^N \left( \frac{\partial V}{\partial x_{k,l}}(X) \frac{\partial G_1}{\partial x_s}(X_k) - \frac{\partial V}{\partial x_{k,s}}(X) \frac{\partial G_1}{\partial x_l}(X_k) \right) = 0. \end{aligned}$$

Thus  $\mathbf{C} = \sum_{k=1}^v \frac{\omega_k(t)}{s_k} + \sum_{\substack{s,l=1 \\ s < l}}^p \sum_{k=v+1}^N \frac{\omega_{k,l,s}(t)}{s_{k,l,s}}$  for all  $t$ , and  $\mathbf{C} = \sum_{k=1}^v \frac{\omega_k(0)}{s_k} + \sum_{\substack{s,l=1 \\ s < l}}^p \sum_{k=v+1}^N \frac{\omega_{k,l,s}(0)}{s_{k,l,s}}$ . Due to

the convergence,  $\mathbf{C} = \omega_c \left( \sum_{k=1}^v \frac{1}{s_k} + \sum_{\substack{s,l=1 \\ s < l}}^p \sum_{k=v+1}^N \frac{1}{s_{k,l,s}} \right)$  and therefore

$$\omega_c := \frac{\sum_{k=1}^v \frac{\omega_k(0)}{s_k} + \sum_{\substack{s,l=1 \\ s < l}}^p \sum_{k=v+1}^N \frac{\omega_{k,l,s}(0)}{s_{k,l,s}}}{\sum_{k=1}^v \frac{1}{s_k} + \sum_{\substack{s,l=1 \\ s < l}}^p \sum_{k=v+1}^N \frac{1}{s_{k,l,s}}}.$$

□

*Example 2.3.* Take  $p = 3$ . For  $k = 1, \dots, v$ , define the local dynamics as the local dynamics in Example (2.1) with here  $\mathbf{a} = \mathbf{b} = \mathbf{d} = 1$  and with  $G_2(x, y, z) := (x - \frac{2}{3})^2 + (y - \frac{2}{3})^2 + (z - \frac{2}{3})^2 - 1$  and gradient  $\nabla G_2(x, y, z) = 2(x - \frac{2}{3}, y - \frac{2}{3}, z - \frac{2}{3})$ . For  $k = v+1, \dots, N$ , define the local dynamics as the local dynamics in Example (2.2) with here  $a_j = 1$ ,  $j = 1, 2, 3$ . The coupling dynamics is as in Example (2.1) (with here  $\mathbf{a} = \mathbf{b} = \mathbf{d} = 1$ ).

For  $k = 1, \dots, v$ , the resulting dynamical system is

$$\begin{aligned} \begin{pmatrix} \dot{x}_k \\ \dot{y}_k \\ \dot{z}_k \end{pmatrix} &= \underbrace{\omega_k \begin{pmatrix} y_k - z_k \\ z_k - x_k \\ x_k - y_k \end{pmatrix} - 2G_1(x_k, y_k, z_k) \begin{pmatrix} x_k \\ y_k \\ z_k \end{pmatrix} - 2G_2(x_k, y_k, z_k) \begin{pmatrix} x_k - \frac{2}{3} \\ y_k - \frac{2}{3} \\ z_k - \frac{2}{3} \end{pmatrix}}_{\text{local dynamics}} - \underbrace{c_k \begin{pmatrix} \sum_{j=1}^N l_{k,j} x_j \\ \sum_{j=1}^N l_{k,j} y_j \\ \sum_{j=1}^N l_{k,j} z_j \end{pmatrix}}_{\text{coupling dynamics}}, \\ \dot{\omega}_k &= \underbrace{-s_k \left( \sum_{j=1}^N l_{k,j} x_j (y_k - z_k) + \sum_{j=1}^N l_{k,j} y_j (z_k - x_k) + \sum_{j=1}^N l_{k,j} z_j (x_k - y_k) \right)}_{\text{parametric dynamics}}. \end{aligned}$$

For  $k = v + 1, \dots, N$ , the resulting dynamical system is

$$\begin{pmatrix} \dot{x}_k \\ \dot{y}_k \\ \dot{z}_k \end{pmatrix} = \underbrace{\begin{pmatrix} 0 & \omega_{k,1,2} & -\omega_{k,1,3} \\ -\omega_{k,1,2} & 0 & \omega_{k,2,3} \\ \omega_{k,1,3} & -\omega_{k,2,3} & 0 \end{pmatrix} \begin{pmatrix} x_k \\ y_k \\ z_k \end{pmatrix} - 2G_1(X_k) \begin{pmatrix} x_k \\ y_k \\ z_k \end{pmatrix}}_{\text{local dynamics}} - \underbrace{c_k \begin{pmatrix} \sum_{j=1}^N l_{k,j} x_j \\ \sum_{j=1}^N l_{k,j} y_j \\ \sum_{j=1}^N l_{k,j} z_j \end{pmatrix}}_{\text{coupling dynamics}},$$

$$\begin{aligned} \dot{\omega}_{k,1,2} &= -s_{k,1,2} \left( \sum_{j=1}^N l_{k,j} x_j y_k - \sum_{j=1}^N l_{k,j} y_j x_k \right), \\ \dot{\omega}_{k,1,3} &= -s_{k,1,3} \left( \sum_{j=1}^N l_{k,j} z_j x_k - \sum_{j=1}^N l_{k,j} x_j z_k \right), \\ \dot{\omega}_{k,2,3} &= -s_{k,2,3} \left( \sum_{j=1}^N l_{k,j} y_j z_k - \sum_{j=1}^N l_{k,j} z_j y_k \right). \end{aligned}$$

parametric dynamics

### 2.2.5 Miscellaneous Remark: Adaptation on Geometric Parameters

As a preliminary to Chapter 3, consider the following homogeneous collections of MCD with adaptation on their flow parameter and an additional adaptive mechanism acting on their Hamiltonian heights. The dynamical system reads

$$\begin{aligned} \dot{x}_k &= \omega_k \frac{\partial H}{\partial y}(X_k) - (H(X_k) - \rho_k) \frac{\partial H}{\partial x}(X_k) - c_k \frac{\partial V}{\partial x_k}(X) \\ \dot{y}_k &= -\omega_k \frac{\partial H}{\partial x}(X_k) - (H(X_k) - \rho_k) \frac{\partial H}{\partial y}(X_k) - c_k \frac{\partial V}{\partial y_k}(X) \\ \dot{\omega}_k &= -s_{\omega_k} \left( \frac{\partial V}{\partial x_k}(X) \frac{\partial H}{\partial y}(X_k) - \frac{\partial V}{\partial y_k}(X) \frac{\partial H}{\partial x}(X_k) \right) \\ \dot{\rho}_k &= s_{\rho_k} \sum_{j=1}^N l_{k,j} (H(X_j) - \rho_j) \end{aligned} \quad k = 1, \dots, N, \quad (2.15)$$

local dynamics                      coupling dynamics

parametric dynamics

with  $X_k = (x_k, y_k)$ , susceptibility constants  $s_{\omega_k} > 0$  and  $s_{\rho_k} > 0$ , and where  $l_{k,j}$  are the entries of the Laplacian matrix associated to the network<sup>3</sup>. We suppose that

$$\sum_{j=1}^N \left( \frac{\partial V}{\partial x_j}(X) \frac{\partial H}{\partial y}(X_j) - \frac{\partial V}{\partial y_j}(X) \frac{\partial H}{\partial x}(X_j) \right) = 0$$

and so Eqs. (2.15) admits the following two constant of motions

$$J_{\omega}(\omega_1, \dots, \omega_N) = \sum_{j=1}^N \frac{\omega_j}{s_j}, \quad \text{and} \quad J_{\rho}(\rho_1, \dots, \rho_N) = \sum_{j=1}^N \frac{\rho_j}{s_{\rho_j}}. \quad (2.16)$$

To see this, refer to the end of the Proof of Proposition 2.2 for the first function and for the second one, see Lemma D.2 in Appendix D. We now discuss the existence of a consensual oscillatory state

<sup>3</sup> Note that one can have an additional network that couples the  $\rho_k$  and which must not necessarily be same as the one for the potential  $V$ . In Chapter 5 we develop this idea by introducing two networks: one for the **state variables** and one for the **parametric variables**

and the convergence towards it.

### Existence of a consensual oscillatory state

We will not proceed as we have done up to now since in this case, the local attractor  $\mathcal{L}_\rho := \{(X, \rho) \in \mathbb{R}^3 \mid \mathbf{H}(X) - \rho = 0\}$  is no longer a compact submanifold. However, we can always define the set

$$\mathcal{M}_\rho := \{(X, \rho) \in \mathbb{R}^{3N} \mid (X_1, \rho_1) \in \mathcal{L}_\rho, X_k = X_j \text{ and } \rho_k = \rho_j \ \forall k, j\}$$

with  $\rho = (\rho_1, \dots, \rho_N)$ . We then have the existence of a consensual state by taking all initial conditions for the state variables in  $\mathcal{M}_\rho$ ,  $\omega_k := \omega_c$  and  $\rho_k := \rho_c$  for all  $k$ .

### Convergence towards a consensual state

**Convergence** - We define set towards which we want to converge

$$\mathcal{C}_{\omega_c, \rho_c} := \{(X, \Omega, \rho) \in \mathbb{R}^{3N} \mid X \in \mathcal{M}, \Omega = \omega_c \mathbf{1} \text{ and } \rho = \rho_c \mathbf{1}\}$$

where  $\mathbf{1}$  is a  $N$  dimensional vector of 1. We propose the following Ляпунов function:

$$\mathbb{J}_{\omega_c, \rho_c}(X, \Omega, \rho) = \frac{1}{2} \sum_{k=1}^N \frac{1}{c_k} (\mathbf{H}(X_k) - \rho_k)^2 + \mathbf{V}(X) + \frac{1}{2} \sum_{k=1}^N \frac{(\omega_k - \omega_c)^2}{s_{\omega_k}} \geq 0.$$

By construction, we have that  $\mathcal{M} = \{X \in \mathbb{R}^{pN} \mid \mathbb{J}(X) = 0\}$ . We here use the following notation:  $\mathbf{H}_k := \mathbf{H}(X_k)$  and  $\mathbf{H} - \rho := (\mathbf{H}(X_1) - \rho_1, \dots, \mathbf{H}(X_N) - \rho_N)$ . Computing the time derivative

$$\begin{aligned} \langle \nabla \mathbb{J}(X) \mid \dot{X} \rangle &= \sum_{k=1}^N \left( \frac{1}{c_k} (\mathbf{H}_k - \rho_k) \frac{\partial \mathbf{H}_k}{\partial x} + \frac{\partial \mathbf{V}}{\partial x_k} \right) \left( \omega_k \frac{\partial \mathbf{H}_k}{\partial y} - (\mathbf{H}_k - \rho_k) \frac{\partial \mathbf{H}_k}{\partial x} - c_k \frac{\partial \mathbf{V}}{\partial x_k} \right) \\ &\quad + \sum_{k=1}^N \left( \frac{1}{c_k} (\mathbf{H}_k - \rho_k) \frac{\partial \mathbf{H}_k}{\partial y} + \frac{\partial \mathbf{V}}{\partial y_k} \right) \left( -\omega_k \frac{\partial \mathbf{H}_k}{\partial x} - (\mathbf{H}_k - \rho_k) \frac{\partial \mathbf{H}_k}{\partial y} - c_k \frac{\partial \mathbf{V}}{\partial y_k} \right) \\ &\quad + \sum_{k=1}^N \frac{(\omega_k - \omega_c)}{s_{\omega_k}} (-s_{\omega_k}) \left( \frac{\partial \mathbf{V}}{\partial x_k} \frac{\partial \mathbf{H}_k}{\partial y} - \frac{\partial \mathbf{H}_k}{\partial x} \frac{\partial \mathbf{V}}{\partial y_k} \right) \\ &\quad + \sum_{k=1}^N \left( \frac{-1}{c_k} (\mathbf{H}(X_k) - \rho_k) (s_{\rho_k} \sum_{j=1}^N l_{k,j} (\mathbf{H}(X_j) - \rho_j)) \right) \\ &= - \underbrace{\sum_{k=1}^N c_k \left\| \frac{1}{c_k} (\mathbf{H}_k - \rho_k) \nabla \mathbf{H}_k + \frac{\partial \mathbf{V}}{\partial X_k}(X) \right\|^2}_{\leq 0} \\ &\quad + \sum_{k=1}^N \left( \frac{\omega_k}{c_k} (\mathbf{H}(X_k) - \rho_k) \right) \underbrace{\left( \frac{\partial \mathbf{H}_k}{\partial x} \frac{\partial \mathbf{H}_k}{\partial y} - \frac{\partial \mathbf{H}_k}{\partial y} \frac{\partial \mathbf{H}_k}{\partial x} \right)}_{=0} \\ &\quad + \sum_{k=1}^N \omega_k \left( \frac{\partial \mathbf{V}}{\partial x_k} \frac{\partial \mathbf{H}_k}{\partial y} - \frac{\partial \mathbf{V}}{\partial y_k} \frac{\partial \mathbf{H}_k}{\partial x} \right) - \sum_{k=1}^N \omega_k \left( \frac{\partial \mathbf{V}}{\partial x_k} \frac{\partial \mathbf{H}_k}{\partial y} - \frac{\partial \mathbf{V}}{\partial y_k} \frac{\partial \mathbf{H}_k}{\partial x} \right) \\ &\quad + \omega_c \underbrace{\sum_{k=1}^N \left( \frac{\partial \mathbf{V}}{\partial x_k} \frac{\partial \mathbf{H}_k}{\partial y} - \frac{\partial \mathbf{H}_k}{\partial x} \frac{\partial \mathbf{V}}{\partial y_k} \right)}_{=0} + \underbrace{-\langle \mathbf{H} - \rho \mid DL(\mathbf{H} - \rho) \rangle}_{\leq 0}, \end{aligned}$$

with  $D$  a diagonal matrix with  $\frac{s_{\rho_k}}{c_k} > 0$  on its diagonal. For asymptotic stability (refer to Appendix A), we muss prove strict negativity of either the sum of the norms term or the bilinear product

term or both. This we will not do.

**Limit Values** - With the constant of motions in 2.16, we have

$$J_\omega(\omega(t)) = \mathbf{C}_1 \quad \forall t, \quad \text{and} \quad J_\rho(\rho(t)) = \mathbf{C}_2 \quad \forall t,$$

Therefore, if convergence towards a consensual state holds, then  $\lim_{t \rightarrow \infty} \omega(t) = \omega_c$  and  $\lim_{t \rightarrow \infty} \rho(t) = \rho_c$  and so

$$\omega_c = \frac{\sum_{j=1}^N \frac{\omega_j(0)}{s_{\omega_j}}}{\sum_{j=1}^N \frac{1}{s_{\omega_j}}}, \quad \text{and} \quad \rho_c = \frac{\sum_{j=1}^N \frac{\rho_j(0)}{s_{\rho_j}}}{\sum_{j=1}^N \frac{1}{s_{\rho_j}}}.$$

## 2.3 Numerical Simulations

We perform numerical simulations with 30 homogeneous **local dynamics** (refer to Section 2.3.1) and with 10 heterogeneous **local dynamics** (refer to Section 2.3.2). For each case, three different types of network topology are considered: i) randomly distributed networks, ii) “All-to-All” networks and iii) “All-to-One” networks (i.e. interactions are only through the  $N^{\text{th}}$  **local dynamics**). For the case i), the edges  $a_{l,s}$  (i.e the entries of the symmetric adjacency  $A$ ) of the randomly distributed network are determined as follows

- the  $N^{\text{th}}$  node is connected to all other nodes (in order to guarantee that the network is connected) with intensity one:  $a_{N,s} = 1$  for  $s = 1, \dots, N - 1$ ,
- all other edges are the product of two random variables:  $a_{l,s} = \mathbb{B} \mathbb{I}$  for  $l, s = 1, \dots, N - 1$  and  $l < s$ .  $\mathbb{B}$  is a Bernoulli random variable taking 0 or 1 as a value with probability  $\frac{1}{2}$ , and  $\mathbb{I}$  is uniformly distributed on the interval  $[0, 1]$ ,
- no loop is allowed:  $a_{l,l} = 0$  for  $l = 1, \dots, N$ .

We choose the coupling strengths  $c_k$  and susceptibility constants  $s_k$  as  $(c_1, \dots, c_N) := \mathbf{1s}(0.25, 1, N)$  and  $(s_1, \dots, s_N) := \mathbf{1s}(3.5, 1, N)$  where  $\mathbf{1s}(a, b, N) \in \mathbb{R}^N$  and its coordinates are defined as  $\mathbf{1s}(a, b, N)_j := a + (j - 1) \frac{b - a}{N - 1}$ ,  $j = 1, \dots, N$ . In other words,  $\mathbf{1s}(a, b, N)$  are  $N$  points, equally spaced between  $a$  and  $b$ . Here, then,  $c_1 := 0.25$  and  $s_1 := 3.5$  and  $c_N = s_N = 1$ . For the network of heterogeneous **local dynamics**, we choose  $s_j := \mathbf{1s}(3.5, 1, N)_j$   $j = 1, \dots, v$  and  $s_{k,l,s} = \mathbf{1s}(3.5, 1, N)_k$  for  $k = v + 1, \dots, N$  and for all  $l, s = 1, \dots, p$  and  $s > l$ .

### 2.3.1 Homogeneous Local Dynamics

For the 30 homogeneous **local dynamics**,  $D$  is defined as in Example (2.1) and we choose  $G_1(X_k) := a x_k^2 + b y_k^2 + c z_k^2 - 1$  and  $G_2(X_k) := a (x_k - \frac{1}{2})^2 + b (y_k - \frac{1}{2})^2 + c (z_k - \frac{1}{2})^2 - 1$  with  $X_k = (x_k, y_k, z_k)$  and  $a = 2$ ,  $b = 3$  and  $c = 5$ . These are two identical ellipsoids, with  $G_1$  centered at the origin and  $G_2$  centered at  $(\frac{1}{2}, \frac{1}{2}, \frac{1}{2})$ , as shown in Figure 2.4.

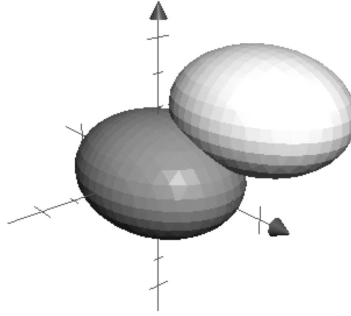


Fig. 2.4: Two ellipsoids given by  $G_1(X) := 2x^2 + 3y^2 + 5z^2 - 1$  (dark gray) and  $G_2(X) := 2(x - \frac{1}{2})^2 + 3(y - \frac{1}{2})^2 + 5(z - \frac{1}{2})^2 - 1$  (light gray).

The potentials are defined as:  $A_k \equiv \frac{1}{2}G_1^2$  if  $k$  is odd and  $A_k \equiv \frac{1}{2}G_2^2$  if  $k$  is even. For each network topology, initial conditions  $x_k(0)$  are randomly uniformly distributed on the following intervals:  $[-\frac{1}{\sqrt{a}} - 0.2, -\frac{1}{\sqrt{a}} + 0.2]$  if  $k$  is odd and on  $[\frac{1}{2} + \frac{1}{\sqrt{a}} - 0.2, \frac{1}{2} + \frac{1}{\sqrt{a}} + 0.2]$  if  $k$  is even. The same applies for  $y_k(0)$  and  $z_k(0)$  with, respectively,  $b$  and  $c$  instead of  $a$ . The initial conditions  $\omega_k(0)$  of the **f-PV** are randomly (uniform distribution) drawn from the interval  $[0.8, 1.2]$  and are rescaled to ensure that the constant of motion is one.

Figures 2.5, 2.6 and 2.7 show, respectively, the resulting dynamics for the **state variables**  $x_k$  and  $z_k$ , and the adaptive mechanism (i.e. **parametric variables**  $\omega_k$ ) with the three types of network: randomly distributed, “All-to-All” and “All-to-One”. To ease comparison, the same time scale is chosen in all examples. The FIEDLER number (refer to Appendix C) for each network is reported.

For  $t \in [0, 2]$ , the **coupling dynamics** and the **parametric dynamics** are switched off (i.e.  $C_k \equiv P_k \equiv 0$  for all  $k$ ) - **local dynamics** are governed by their local parameters and attractors. At  $t = 2$ , interactions are switched on (see black solid line). Switching on (and, if necessary, switching off) can be done with smooth functions that change from 0 to 1 (from 1 to 0) on a unit time interval. For example, with the help of Fresnel Integrals defined as

$$\mathfrak{c}(s) := \int_0^s \cos(\frac{1}{2}\pi z^2) dz \quad \text{and} \quad \mathfrak{s}(s) := \int_0^s \sin(\frac{1}{2}\pi z^2) dz,$$

one can construct continuously differentiable functions that take on the value 0 (respectively 1) until  $t^*$  and 1 (respectively 0) after  $t^* + 1$ , namely

$$\begin{aligned} O_{\uparrow}(t; t^*) &= \begin{cases} \mathfrak{q} \mathfrak{s}(t-t^*) & t \in [t^*, t^* + \frac{1}{\sqrt{2}}] \\ \mathfrak{q} (\mathfrak{c}(t-t^*) - (\mathfrak{c}(\frac{1}{\sqrt{2}}) - \mathfrak{s}(\frac{1}{\sqrt{2}}))) & t \in [t^* + \frac{1}{\sqrt{2}}, t^* + 1] \end{cases} \\ O_{\downarrow}(t; t^*) &= \begin{cases} -\mathfrak{q} \mathfrak{s}(t-t^*) + 1 & t \in [t^*, t^* + \frac{1}{\sqrt{2}}] \\ -\mathfrak{q} (\mathfrak{c}(t-t^*) - (\mathfrak{c}(\frac{1}{\sqrt{2}}) - \mathfrak{s}(\frac{1}{\sqrt{2}}))) + 1 & t \in [t^* + \frac{1}{\sqrt{2}}, t^* + 1] \end{cases} \end{aligned}$$

with  $\mathfrak{q} := (\mathfrak{c}(1) - (\mathfrak{c}(\frac{1}{\sqrt{2}}) - \mathfrak{s}(\frac{1}{\sqrt{2}})))^{-1}$ .

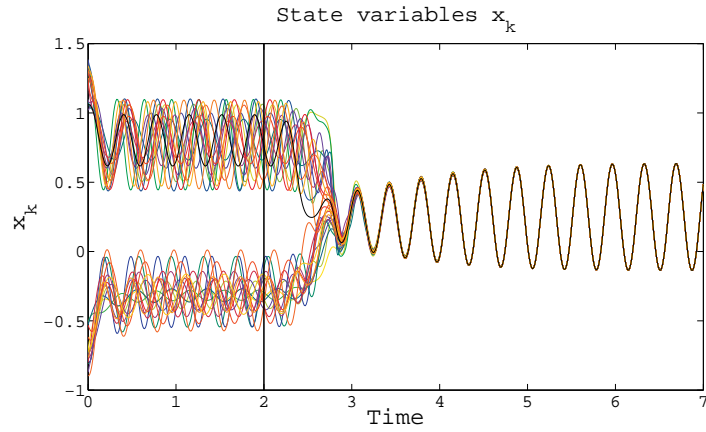
In all simulations, one can observe that during the decoupled phase (i.e. for  $t \in [0, 2]$ ) local systems converge towards their attractor (either one of the ellipsoids in Figure 2.4). Once **coupling dynamics** and **parametric dynamics** are switched on, all local systems converge towards the common attractor being here the intersection of the two ellipsoids.

One can observe that the convergence rate manifestly depends on the FIEDLER number (refer to Appendix C): the larger the FIEDLER number is, the faster is the convergence. As discussed in Section 5.2.0.1 with HOPF oscillators as **local dynamics**, linearization around the consensual state explicitly shows the interplay between FIEDLER number and convergence rate.

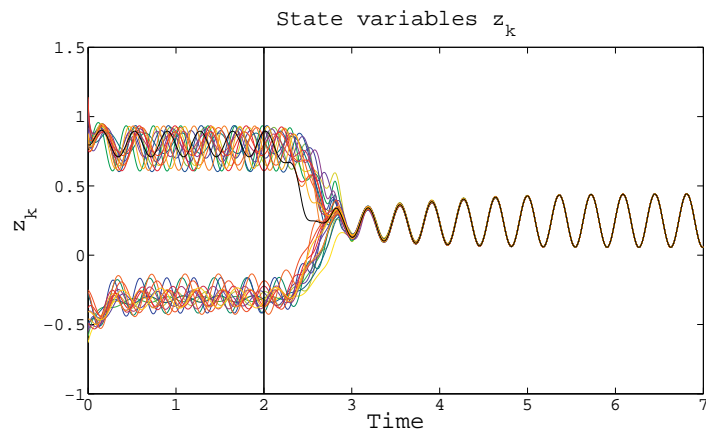
### 2.3.2 Heterogeneous Local Dynamics

For the 10 **local dynamics** defined in Example (2.3) we choose  $v = 3$ . For each network topology, initial conditions  $(x_k(0), y_k(0), z_k(0))$  are randomly uniformly distributed on  $[-0.25, 0.25]$  for  $k = 1, \dots, N$ . The initial conditions of the **f-PV** are randomly (uniform distribution) drawn from the interval  $[-1, 1]$  for  $\omega_k(0)$  (for  $k = 1, 2, 3$ ) and from the intervals  $[0.8, 1.3]$  for  $\omega_{k,1,2}(0)$ ,  $[-1, 1]$  for  $\omega_{k,1,3}(0)$  and  $[1.8, 2.5]$  for  $\omega_{k,2,3}(0)$  (for  $k = 4, \dots, 10$ ). They are rescaled to ensure that the constant of motion is one.

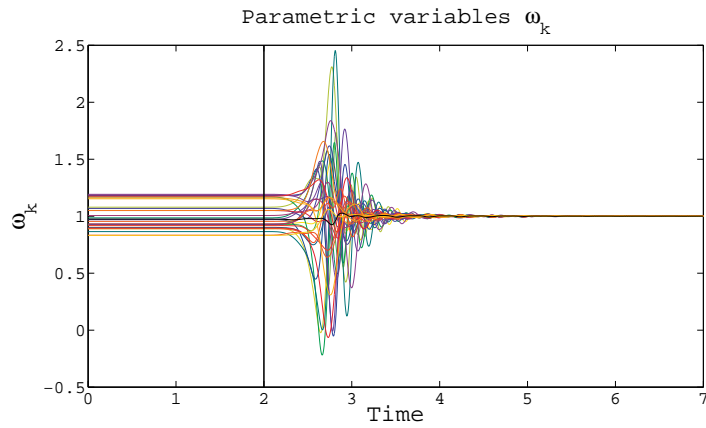
Figures 2.8, 2.9 and 2.10 show, respectively, the resulting dynamics for the **state variables**  $x_k$  and  $z_k$ , and the adaptive mechanism (i.e. **parametric variables**  $\omega_k, \omega_{k,1,2}, \omega_{k,1,3}$  and  $\omega_{k,2,3}$ ) with the three types of network: randomly distributed, “All-to-All” and “All-to-One”. For comparison,



(a)

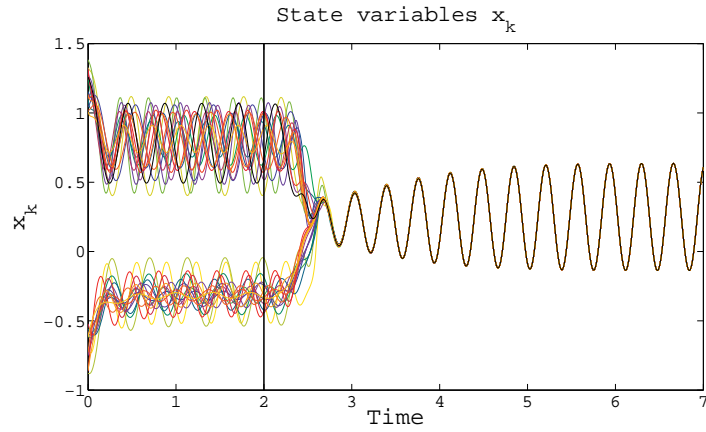


(b)

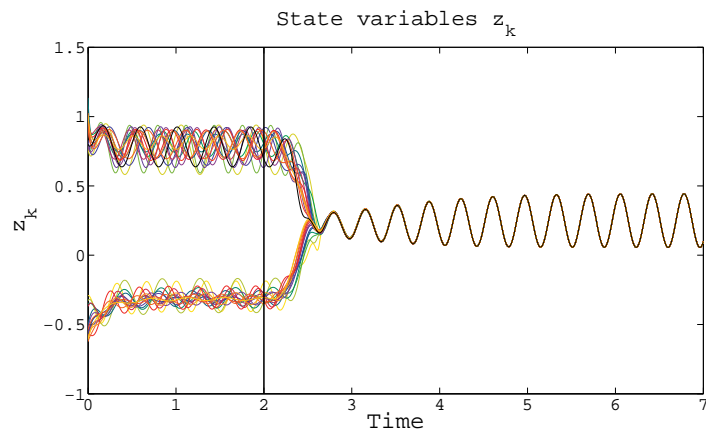


(c)

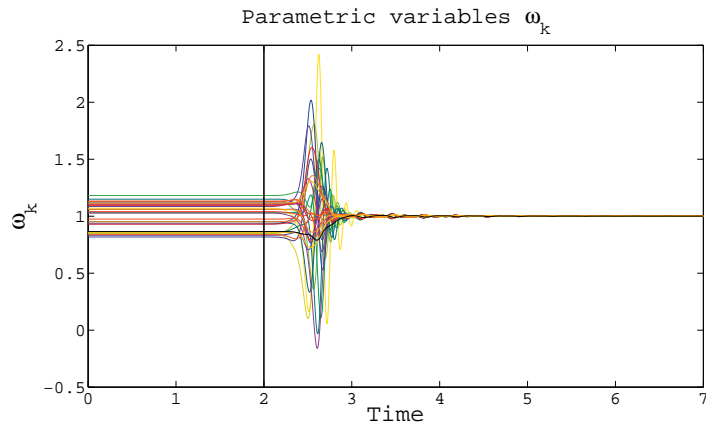
Fig. 2.5: Time evolution of the **state variables**  $x_k$  and  $z_k$  (Figures 2.5(a) & 2.5(b)) and **parametric variables**  $\omega_k$  (Figure 2.5(c)) for 30 homogeneous local dynamics with ellipsoidal attractor as in Figure 2.4, interacting through a randomly distributed network. The FIEDLER number is 4.6049. Coupling dynamics and parametric dynamics are switched on at  $t = 2$  (black solid line).



(a)



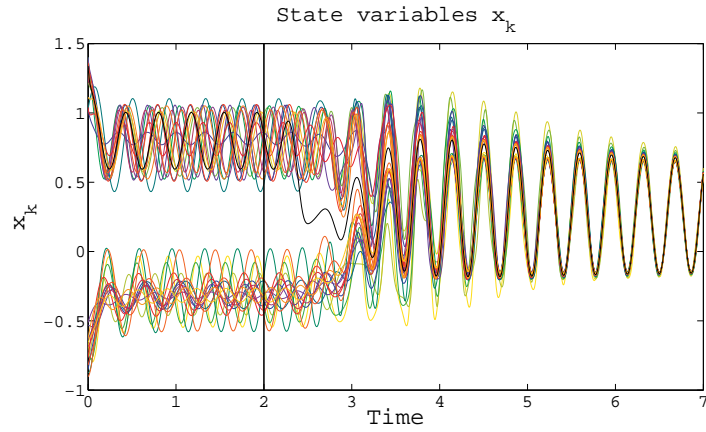
(b)



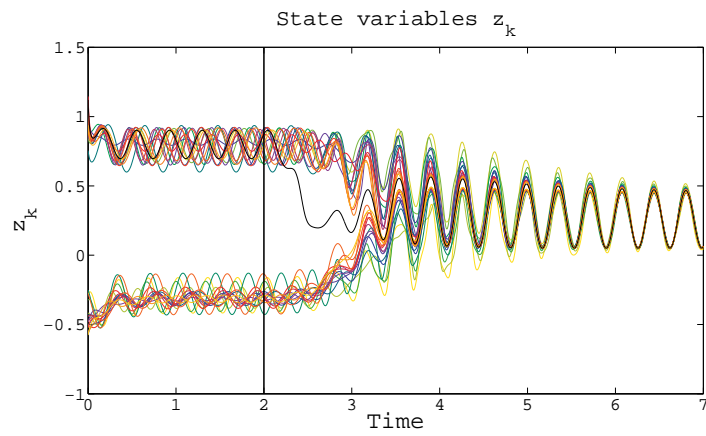
(c)

Fig. 2.6: Time evolution of the **state variables**  $x_k$  and  $z_k$  (Figures 2.6(a) & 2.6(b)) and **parametric variables**  $\omega_k$  (Figure 2.6(c)) for 30 homogeneous local dynamics with ellipsoidal attractor as in Figure 2.4, interacting through a “All-to-All” network. The FIEDLER number is 30. Coupling dynamics and parametric dynamics are switched on at  $t = 2$  (black solid line).

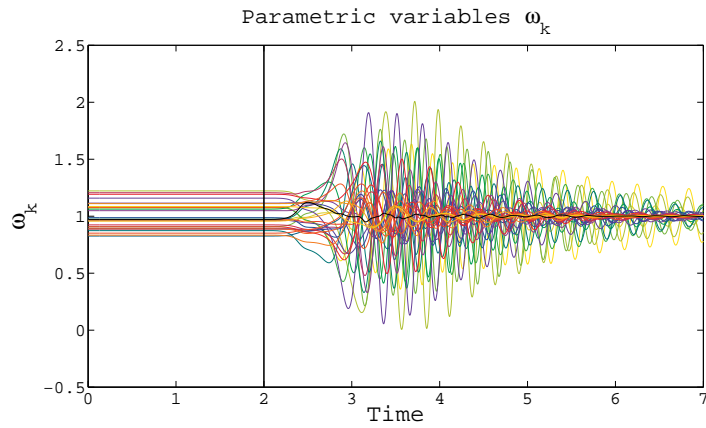




(a)



(b)



(c)

Fig. 2.7: Time evolution of the **state variables**  $x_k$  and  $z_k$  (Figures 2.7(a) & 2.7(b)) and **parametric variables**  $\omega_k$  (Figure 2.7(c)) for 30 homogeneous local dynamics with ellipsoidal attractor as in Figure 2.4, interacting through a “All-to-One” network. The FIEDLER number is 1. **Coupling dynamics and parametric dynamics are switched on at  $t = 2$**  (black solid line).

the same time scale is chosen in all examples. The FIEDLER number for each network is reported.

For  $t \in [0, 13]$ , neither the **coupling dynamics** nor the **parametric dynamics** are switched on (i.e.  $C_k \equiv P_k \equiv 0$  for all  $k$ ) - **local dynamics** are governed by their local parameters and attractors. At  $t = 13$ , only **coupling dynamics** are switched on (see black solid line) and finally at  $t = 37$ , **parametric dynamics** are switched on (see black dashed line). Note that for the “All-to-All” network, the “ordered” state reached between  $t = 13$  and  $t = 37$  (i.e. when there is no adaptive mechanism in effect -  $P_k \equiv 0$  for all  $k$ ) is a trivial dynamics (fixed point), whereas for the randomly distributed and “All-to-One” network cyclo-stationary states seem to be attained. We observe this phenomenon in numerical experiments where the time interval on which the **coupling dynamics** act has been enlarged.

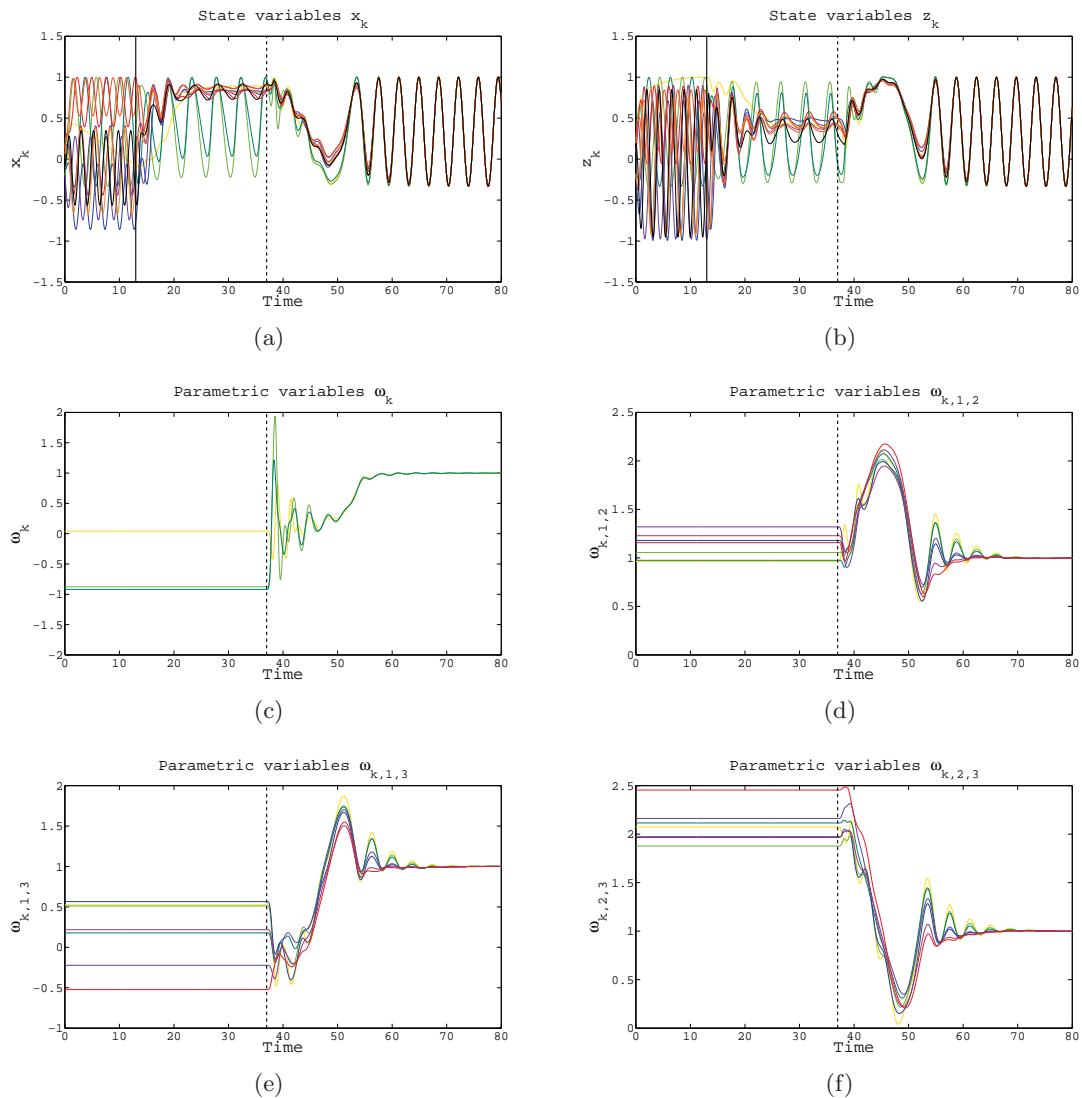


Fig. 2.8: Time evolution of the **state variables**  $x_k$  and  $z_k$  (Figures 2.8(a) & 2.8(b)) and **parametric variables**  $\omega_k$ ,  $\omega_{k,1,2}$  (Figures 2.8(c) & 2.8(d)) and  $\omega_{k,1,3}$ ,  $\omega_{k,2,3}$  (Figures 2.8(e) & 2.8(f)) for 10 heterogeneous local dynamics defined in Example (2.3), interacting through a randomly distributed network. The FIEDLER number is 1.3825. **Coupling dynamics** are switched on at  $t = 13$  (black solid line) and **parametric dynamics** at  $t = 37$  (black dashed line).

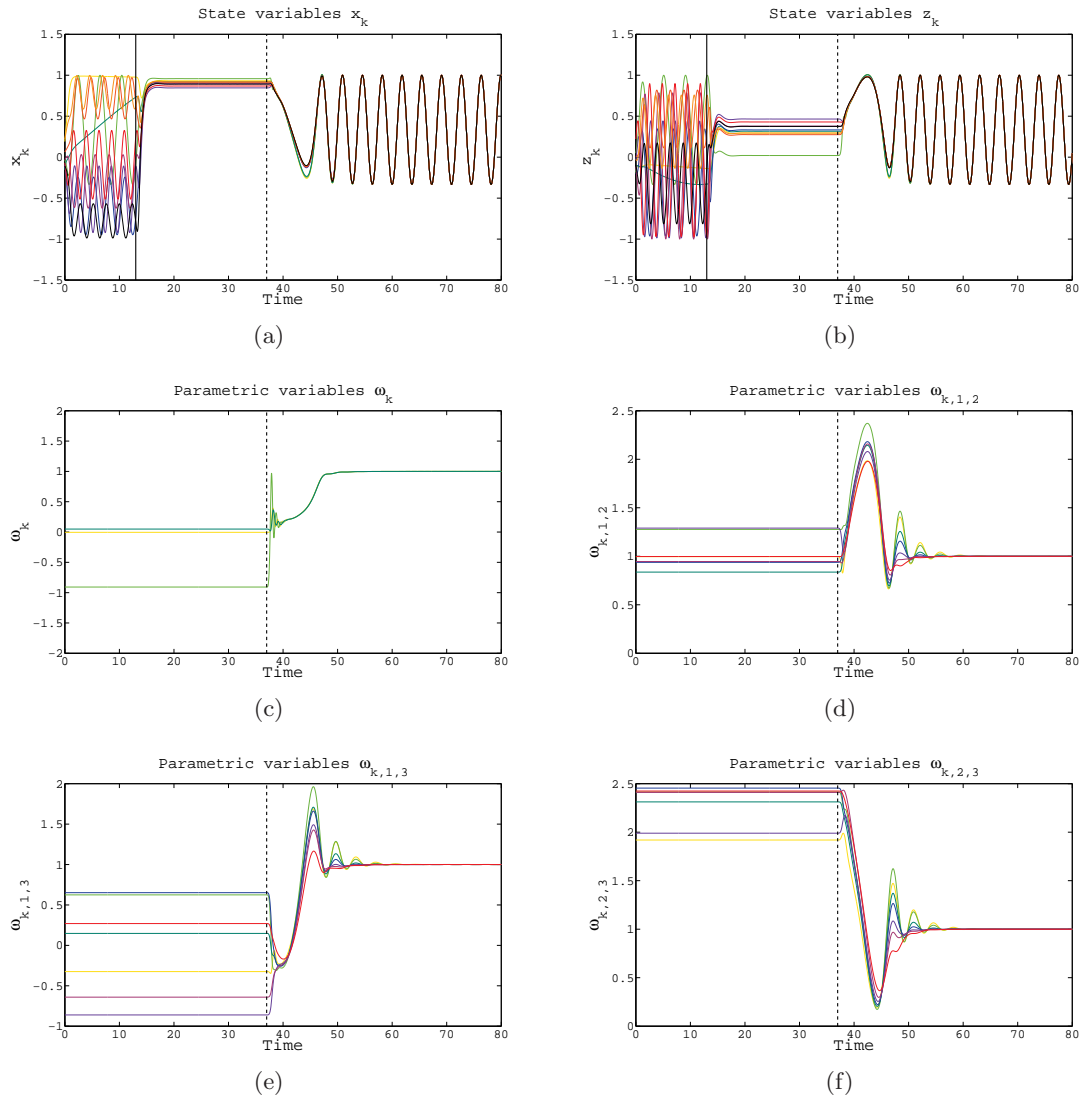


Fig. 2.9: Time evolution of the state variables  $x_k$  and  $z_k$  (Figures 2.9(a) & 2.9(b)) and parametric variables  $\omega_k$ ,  $\omega_{k,1,2}$  (Figures 2.9(c) & 2.9(d)) and  $\omega_{k,1,3}$ ,  $\omega_{k,2,3}$  (Figures 2.9(e) & 2.9(f)) for 10 heterogeneous local dynamics defined in Example (2.3), interacting through a “All-to-All” network. The FIEDLER number is 10. Coupling dynamics are switched on at  $t = 13$  (black solid line) and parametric dynamics at  $t = 37$  (black dashed line).

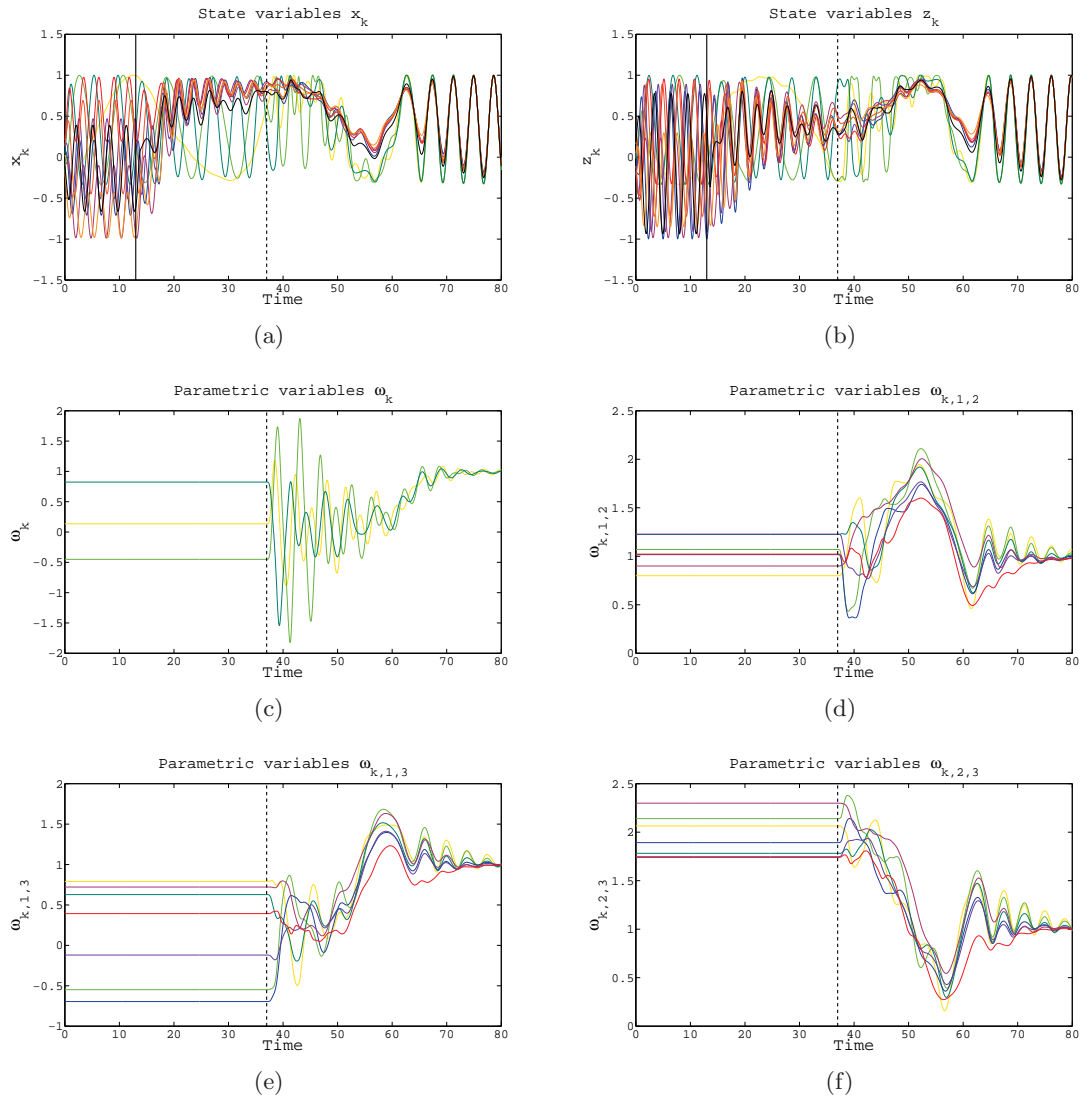


Fig. 2.10: Time evolution of the state variables  $x_k$  and  $z_k$  (Figures 2.10(a) & 2.10(b)) and parametric variables  $\omega_k$ ,  $\omega_{k,1,2}$  (Figures 2.10(c) & 2.10(d)) and  $\omega_{k,1,3}$ ,  $\omega_{k,2,3}$  (Figures 2.10(e) & 2.10(f)) for 10 heterogeneous local dynamics defined in Example (2.3), interacting through a “All-to-One” network. The FIEDLER number is 1. Coupling dynamics are switched on at  $t = 13$  (black solid line) and parametric dynamics at  $t = 37$  (black dashed line).

## Networks of Mixed Canonical-Dissipative Systems with Adapting Flow and Geometric Parameters

Tal como un péndulo

Así, el ser que ha despertado, como un péndulo viviente, ha de sostenerse en movimiento incesante, sostenido por un punto remoto, transformando el desfallecimiento en pausa, y la pausa, en lugar de más honda y obediente oscilación, revelando así su secreto de ser un diapasón del imperceptible fluir musical del interior del tiempo vivo.

María ZAMBRANO

In this chapter, the complex dynamical system is composed of one  $N$ -vertex network with constant edges. The **local dynamics** are 2-dimensional belonging to the class of mixed canonical-dissipative (MCD) systems. The **coupling dynamics** derives from the gradient of a Laplacian potential (i.e. diffusive coupling). Adaptation occurs in the **local dynamics**. Here, flow parameters as well as geometric parameters are allowed to adapt.

### 3.1 Network's Dynamical System

In this section, we detail the constituent parts that compose the global dynamics

$$\begin{aligned}
 \dot{x}_k &= \omega_k \frac{\partial H}{\partial y}(X_k, \Gamma_k) - \frac{\partial A}{\partial x}(X_k, \Gamma_k) - c_k \sum_{j=1}^N l_{k,j} x_j, \\
 \dot{y}_k &= \underbrace{-\omega_k \frac{\partial H}{\partial x}(X_k, \Gamma_k) - \frac{\partial A}{\partial y}(X_k, \Gamma_k)}_{\text{local dynamics}} - \underbrace{c_k \sum_{j=1}^N l_{k,j} y_j}_{\text{coupling dynamics}}, \\
 \dot{\omega}_k &= -s_{\omega_k} \sum_{j=1}^N l_{k,j} (x_j y_k - y_j x_k), \\
 \dot{\Gamma}_k &= \underbrace{P_k^\Gamma(X, \Gamma)}_{\text{parametric dynamics}},
 \end{aligned} \quad k = 1, \dots, N. \quad (3.1)$$

**Local Dynamics** Local systems belong to the class of MCD systems (refer to Section 3.1.1).

**Coupling Dynamics** The gradient of a Laplacian potential characterizes the interactions of the **state variables** (refer to Section 3.1.2).

**Parametric Dynamics** Adaptive mechanisms tune the values of **parametric variables** that control the circulation rate and shape of the local attractors (refer to Section 3.1.3).

#### 3.1.1 Local Dynamics: $L_k$

The **local dynamics** belong to the class Mixed Canonical-Dissipative (MCD) systems as presented in Example (1.1) and for which we recall their dynamics

$$\begin{aligned}
L_1(X_k; \Lambda_k) &:= w_k \frac{\partial H}{\partial y}(X_k; \Gamma_k) - (H(X_k; \Gamma_k) - r_k) \frac{\partial H}{\partial x}(X_k; \Gamma_k), \\
L_2(X_k; \Lambda_k) &:= \underbrace{-w_k \frac{\partial H}{\partial x}(X_k; \Gamma_k)}_{\text{canonical evolution}} - \underbrace{(H(X_k; \Gamma_k) - r_k) \frac{\partial H}{\partial y}(X_k; \Gamma_k)}_{\text{dissipative evolution}},
\end{aligned} \tag{3.2}$$

where  $X_k = (x_k, y_k)$  are the **state variables** and  $\Lambda_k = \{w_k, \Gamma_k\}$  are, for the time being, fixed and constant parameters with  $w_k$  a scalar and  $\Gamma_k = \{r_k, \mathbf{g}_{k,1}, \dots, \mathbf{g}_{k,q-2}\} \in \mathbb{R}^{q-1}$ . As we have done for the examples in Section 1.1.1, we will sometimes use the following notation for the geometric parameters:  $\Gamma_k = \{r_k, \mathbf{a}_k, \mathbf{b}_k, \mathbf{d}_k, \dots\}$ . The *dissipative evolution* is due to the gradient of the potential  $A(X; \Gamma_k) := \frac{1}{2}(H(X; \Gamma_k) - r_k)^2$ . In this chapter, we consider only a collection of **homogenous** MCD oscillators which, in accordance with Definition 1.1, have identical Hamiltonian functional but with different  $\Gamma_k$ -values. We also assume here that for each  $k$ , the set  $\mathcal{L}_{\Gamma_k} := \{X \in \mathbb{R}^2 \mid H(X; \Gamma_k) - r_k = 0\}$  is a unique closed curve in  $\mathbb{R}^2$  surrounding the origin. In Eqs. (5.2), the parameter  $w_k$  controls the angular velocity of the *canonical evolution* while the  $\Gamma_k$  determine the shape of the attractor.

### 3.1.2 Coupling Dynamics: $C_k$

Let  $L$  be a Laplacian matrix associated to a connected and undirected network with positive adjacency entries. **Local dynamics** are coupled together via the gradient of a Laplacian potential (refer to Example (1.5))  $V(X) = \frac{1}{2}(\langle x \mid Lx \rangle + \langle y \mid Ly \rangle)$  with  $x = (x_1, \dots, x_N)$  (idem for  $y$ ). Explicitly, the coupling to be considered is

$$\begin{aligned}
C_{k,1}(X) &:= -c_k \sum_{j=1}^N l_{k,j} x_j, \\
C_{k,2}(X) &:= -c_k \sum_{j=1}^N l_{k,j} y_j,
\end{aligned}$$

where  $c_k > 0$  are strictly positive, fixed and constant, *coupling strengths* and  $l_{k,j}$  are the entries of  $L$ .

### 3.1.3 Parametric Dynamics: $P_k$

In this chapter, adaptation in the local systems' parameter concerns the flow parameters  $w_k$  as well as the geometric parameters  $\Gamma_k$ . As discussed in Section 1.2.1, we let the fixed and constant  $\Lambda_k$  become time-dependent. That is

$$\begin{aligned}
\Lambda_k &= \{w_k, r_k, \mathbf{g}_{k,1}, \dots, \mathbf{g}_{k,q-2}\} \\
&= \{w_k, r_k, \mathbf{a}_k, \mathbf{b}_k, \mathbf{d}_k, \dots\} \rightsquigarrow (\omega_k(t), \rho_k(t), \alpha_k(t), \beta_k(t), \delta_k(t), \dots) \\
&= (\omega_k(t), \rho_k(t), \gamma_{k,1}(t), \dots, \gamma_{k,q-2}(t)) = \Lambda_k(t).
\end{aligned}$$

Their rate of change  $\dot{\omega}_k$  and  $\dot{\Gamma}_k$  are determined by the **parametric dynamics**  $P_k^\omega$  and  $P_k^\Gamma$ . Here, for each  $k$ ,  $P^\omega$  is a function of  $X = (X_1, \dots, X_N)$  only, where as, in general,  $P^\Gamma$  depends on  $X = (X_1, \dots, X_N)$  and on  $\Gamma = (\Gamma_1, \dots, \Gamma_N)$ . Interactions are through the same connected and undirected network with positive adjacency entries that is considered in Section 3.1.2. By introducing the **parametric dynamics**,  $\omega_k$  and  $\Gamma_k$  have acquired the status of variables of the global dynamical system and are known as **flow parametric variables** (f-PV) and **geometric parametric variables** (g-PV) respectively (refer to Section 1.2.1).

The functions  $P_k^\omega$  and  $P_k^\Gamma$  must fulfill the objectives presented in Section 1.2.4. Apart from Section 5.2.2, it is required in this chapter that the  $\Lambda_k(t)$  ultimately converge towards a common and constant set  $\Lambda_c$  (i.e.  $\lim_{t \rightarrow \infty} \Lambda_k(t) = \Lambda_c$  for  $k = 1, \dots, N$ ).

Adaptive angular velocities  $\omega_k$  (i.e. f-PV) have been discussed in Chapter 2 and so we briefly present their dynamics below. In Section 3.1.3.2, we introduce additional dynamics on the g-PV  $\Gamma_k$  that shape the attractor. Both, f-PV and g-PV, interact through the network as discussed in Section 3.1.2.

### 3.1.3.1 Dynamics of Flow Parametric Variables

Following the idea presented in Section 2.1.3.1, the parametric dynamics  $P_k^\omega$  for the f-PV  $\omega_k$  reads

$$\dot{\omega}_k = -s_{\omega_k} \sum_{j=1}^N l_{k,j} (x_j y_k - y_j x_k),$$

where  $0 < s_{\omega_k}$  are strictly positive, fixed, *susceptibility constants* and  $l_{k,j}$  are the entries of  $L$ . As already seen,

$$J_\omega(\omega_1, \dots, \omega_N) := \sum_{k=1}^N \frac{\omega_k}{s_{\omega_k}}.$$

is a constant of motion (refer to Lemma D.1, Appendix D).

### 3.1.3.2 Dynamics of Geometric Parametric Variables

We now present an explicit form of  $P_k^\Gamma$ , the parametric dynamics for g-PV. We allow  $\rho_k$  to be now parametric variable with dynamics defined as

$$\dot{\rho}_k = -s_{\rho_k} \sum_{j=1}^N l_{k,j} H(X_j, \Gamma_j), \quad (3.3)$$

where  $0 < s_{\rho_k}$  are strictly positive, fixed, *susceptibility constants*. For parametric variable  $\gamma_{k,s}$  (those that directly influence the Hamiltonian functional), we define their parametric dynamics as

$$\dot{\gamma}_{k,s} = \pm s_{\gamma_{k,s}} \sum_{j=1}^N l_{k,j} \frac{\partial H}{\partial \gamma_s}(X_j, \Gamma_j), \quad (3.4)$$

where  $0 < s_{\gamma_{k,s}}$  are strictly positive, fixed, *susceptibility constants* and where the sign  $\pm$  will be determined below.

As in Section 2.1.3.1, to unveil the adaptive process, we again consider a simple illustration involving three weakly coupled stable limit cycle oscillators connected as shown in Figure 2.1. Each oscillator has its own limit cycle  $\mathcal{L}_{\Gamma_k}$  (with  $\Gamma_k = (\rho_k, \alpha_k)$ ) which are here, for simplicity, ellipses and are given, respectively, by  $H(X, \alpha_k) - \rho_k = 0$  with  $H(X, \alpha_k) := \alpha_k x^2 + y^2$ . We now discuss separately the adaptation of  $\rho_k$  and on  $\alpha_k$ . For these two g-PV, we again, as in Section 2.1.3.1, consider a snapshot approach for the adaptive mechanisms (i.e. a discretization of the time  $\{t_n\}_{n=0}^\infty$  with  $t_0 = 0$  and  $t_{n+1} := t_n + h$  for a given small positive  $h$ ).

#### Different $\rho_k$ , common $\alpha_k = \alpha_c$

Without loss of generality, assume that  $\rho_1(0) < \rho_2(0) < \rho_3(0)$ . Each oscillator is initiated at time  $t_0 = 0$  at  $(0, \sqrt{\rho_k(0)})$  respectively (i.e. each on its respective limit cycle). Qualitatively, after a small time-lapse  $h$ , the scenario is sketched in Figure 3.1. We assume they are weakly coupled and thus neglect the effect of the **coupling dynamics**. Hence, for simplicity, we represent oscillators on their attractor. For explanatory reasons, we deliberately elongated the oscillators' trajectories in Figure 3.1. We now examine each oscillator's behavior individually at time  $t = t_0 + h$ . We refrain from explicitly writing the parameter  $\alpha_c$  since it is common to all Hamiltonians.

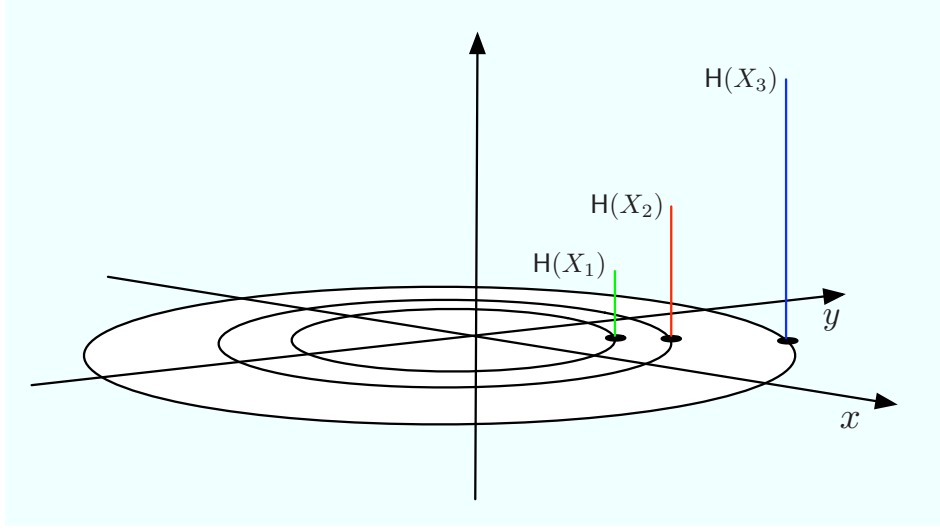


Fig. 3.1: On the  $x - y$  axis, position at time  $t_0 + h$  of three oscillators initiated, respectively, on  $(0, \sqrt{\rho_k(0)})$  at  $t_0 = 0$ . On the third axis, the Hamiltonian heights of the oscillators are represented.

#### Oscillator 1

The first oscillator has a lower Hamiltonian height than the second one, hence for adaptation, our rule implies

at time  $t = t_0 + h$  oscillator 1 must go “up” to adjust with oscillator 2

Since  $H(X_2) - H(X_1) > 0$ , we propose

$$\rho_1(t_0+h) := \rho_1(t_0) + h(H(X_2) - H(X_1)) .$$

#### Oscillator 2

For the second oscillator, adaptation implies

at time  $t = t_0 + h$  oscillator 2 must go “down” to adjust with oscillator 1  
oscillator 2 must go ‘up” to adjust with oscillator 3

Since  $H(X_1) - H(X_2) < 0$  and  $H(X_3) - H(X_2) > 0$ , we propose

$$\rho_2(t_0+h) := \rho_2(t_0) + h(H(X_1) - H(X_2) + H(X_3) - H(X_2)) .$$

#### Oscillator 3

Finally, the same reasoning implies for the third oscillator

$$\rho_3(t_0+h) := \rho_3(t_0) + h(H(X_2) - H(X_3))$$

since  $H(X_2) - H(X_3) < 0$ .

This can be done at any time step  $t_n$  and it is straightforwardly generalized to  $N$  oscillators by including the edge weights  $a_{k,j}$ . We propose

$$\rho_k(t_n+h) = \rho_k(t_n) + h \sum_{j \neq k}^N a_{k,j} (H(X_j) - H(X_k)) = \rho_k(t_n) - h \sum_{j=1}^N l_{k,j} H(X_j) .$$



Since  $l_{k,j} = -a_{k,j}$  for  $k \neq j$  and  $l_{k,k} = \sum_{j \neq k}^N a_{k,j}$  for all  $k$ . The continuous time version of this procedure can be obtained as

$$\frac{\rho_k(t_n+h) - \rho_k(t_n)}{h} = - \sum_{j=1}^N l_{k,j} \mathbf{H}(X_j)$$

and therefore if we let  $h$  tend to zero ( $h \rightarrow 0$ ), we have  $\dot{\rho}_k = - \sum_{j=1}^N l_{k,j} \mathbf{H}(X_j)$ . We therefore have, after introducing the susceptibility constants  $s_{\rho_k}$ , Eqs. (3.3). Note that, we have a constant of motion as in Eq. (2.5), that is

$$J_\rho(\rho_1, \dots, \rho_N) := \sum_{k=1}^N \frac{\rho_k}{s_{\rho_k}}. \quad (3.5)$$

Indeed, for  $\{\rho_k(t)\}_{k=1}^N$  orbits of Eqs. (3.3), we have

$$\frac{d[J(\rho_1(t), \dots, \rho_N(t))]}{dt} = \sum_{k=1}^N \frac{\dot{\rho}_k(t)}{s_{\rho_k}} = - \sum_{k=1}^N \sum_{j=1}^N l_{k,j} \mathbf{H}(X_j) = 0,$$

where the last equality follows from Lemma D.2 in Appendix D, the last equality is zero. As for the f-PV in Chapter 2, whether a consensual  $\rho_c$  is reached, its value does not depend on the topology of the network.

### Generalization

For homogeneous MCD oscillators, this adaptive mechanism can be generalized for arbitrary Hamiltonian  $\mathbf{H}(X, I_k)$  and Eq. (3.5) still remains a constant of motion.

#### Different $\alpha_k$ , common $\rho_k = \rho_c$

In  $\mathbb{R}^3$ , consider the level surface  $\mathcal{S} := \{(X, \alpha) \in \mathbb{R}^2 \times ]\underline{\alpha}, \bar{\alpha}[ \mid \mathbf{H}(X, \alpha) = \alpha x^2 + y^2 - 1 = 0\}$  for given  $\underline{\alpha}, \bar{\alpha} \in \mathbb{R}_{>0}$ . For a fixed  $\alpha$ , the level curve  $\mathcal{L}_\alpha := \{X \in \mathbb{R}^2 \mid \mathbf{H}(X; \alpha) - 1 = 0\} \subset \mathcal{S}$  is the stable MCD limit cycle. The smaller  $\alpha$ , the more the limit cycle is stretched in the  $x$ -direction as shown in Figure 3.2(a). The geometry of  $\mathcal{S}$  implies that  $\frac{\partial \mathbf{H}}{\partial \alpha}(X_1, \alpha_1) - \frac{\partial \mathbf{H}}{\partial \alpha}(X_2, \alpha_2) > 0$  if  $\alpha_1 < \alpha_2$  and  $X_1$  and  $X_2$  are aligned with  $(0, 0)$  (i.e.  $\frac{y_1}{x_1} = \frac{y_2}{x_2}$ ). We sketch the third coordinate  $\frac{\partial \mathbf{H}}{\partial \alpha}$  of the gradient  $\nabla \mathbf{H} = (\frac{\partial \mathbf{H}}{\partial x}, \frac{\partial \mathbf{H}}{\partial y}, \frac{\partial \mathbf{H}}{\partial \alpha})$  in Figure 3.2(b) to compare the sizes.

Without loss of generality, assume that  $\alpha_1(0) < \alpha_2(0) < \alpha_3(0)$ . Initiate all three oscillators at  $t_0 = 0$  with respective points  $(0, 1, \alpha_k(0))$  lying on their respective limit cycles. Qualitatively, after a small time-lapse  $h$ , the scenario is sketched in Figure 3.2(a). For simplicity, we represent the oscillators on their attractor and thus omit the coupling dynamics effect. We do, however, suppose that the coupling is strong enough for the oscillators to have a common angular velocity. For our explanation, we deliberately enlarge the representation in Figure 3.2(a). We now examine each oscillator's behavior individually at time  $t = t_0 + h$ .

#### Oscillator 1

The first oscillator has a lower level curve than the second one, hence for adaptation, our rule implies

at time  $t = t_0 + h$  oscillator 1 must "shorten" to adjust with oscillator 2

Since  $\frac{\partial \mathbf{H}}{\partial \alpha}(X_1, \alpha_1) - \frac{\partial \mathbf{H}}{\partial \alpha}(X_2, \alpha_2) > 0$ , we propose

$$\alpha_1(t_0+h) := \alpha_1(t_0) + h \left( \frac{\partial \mathbf{H}}{\partial \alpha}(X_1, \alpha_1) - \frac{\partial \mathbf{H}}{\partial \alpha}(X_2, \alpha_2) \right).$$



$$J_\alpha(\alpha_1, \dots, \alpha_N) := \sum_{k=1}^N \frac{\alpha_k}{s_{\alpha_k}} . \quad (3.6)$$

is a constant of motion for  $\{\alpha_k(t)\}_{k=1}^N$  orbits of Eqs.(3.4). Again, if a consensual and common  $\alpha_c$  is reached, its value does not depend on the network topology.

### Generalization

For homogenous MCD oscillators, let the sets of g-PV parameters  $\Gamma_k$  have the same values (i.e.  $\Gamma_k = \Gamma_j$  for all  $k, j$ ) except for the parameter  $\gamma_v$ . That is,  $\gamma_{k,v}$  not necessarily equal to  $\gamma_{j,v}$  for  $k, j$ . We refrain from explicitly writing the other g-PV parameters since they are fixed and all equal (i.e.  $\Gamma_k \setminus \gamma_{k,v} = \Gamma_j \setminus \gamma_{j,v}$  for all  $k, j$ ) and so we here write the Hamiltonian as  $H(X; \gamma_{k,v})$ . The geometry of the level surface  $\mathcal{S}_\rho := \{(X, \gamma) \in \mathbb{R}^2 \times \gamma_v, \bar{\gamma}_v \mid H(X; \gamma) - \rho = 0\}$  (for given  $\gamma_v, \bar{\gamma}_v \in \mathbb{R}$ ) will influence the dynamics on  $\gamma_{k,v}$ .

Define  $\gamma_{m,v}, \gamma_{M,v} \in [\gamma_v, \bar{\gamma}_v]$ , two values of the parameter  $\gamma_v$ , as

$$\begin{aligned} \gamma_{m,v} &:= \min\{\gamma_{j,v}(0)\}_{j=1}^N \quad \text{and} \\ \gamma_{M,v} &:= \max\{\gamma_{j,v}(0)\}_{j=1}^N . \end{aligned} \quad (3.7)$$

Let  $X_m(z) := (r_m(z) \sin(z), r_m(z) \cos(z))$  and  $X_M(z) := (r_M(z) \sin(z), r_M(z) \cos(z))$ ,  $z \in [0, 2\pi]$ , be a parametrization of the closed curve given by the respective limit cycles, that is the level curves  $\mathcal{L}_{\gamma_m} := \{X \in \mathbb{R}^2 \mid H(X; \gamma_m) = \rho\} \subset \mathcal{S}_\rho$  and  $\mathcal{L}_{\gamma_M} := \{X \in \mathbb{R}^2 \mid H(X; \gamma_M) = \rho\} \subset \mathcal{S}_\rho$  respectively. These parametrizations start at  $z = 0$  on the  $y$ -axis (i.e. 12 o'clock) and make one revolution, always staying on their respective limit cycle. As above, consider the difference between the third coordinate of the gradient of the surface level  $\mathcal{S}_\rho$ , but now being averaged on the respective closed curves, that is

$$o := \int_0^{2\pi} \frac{\partial H}{\partial \gamma_v}(X_m(z); \gamma_{m,v}) - \frac{\partial H}{\partial \gamma_v}(X_M(z); \gamma_{M,v}) dz . \quad (3.8)$$

If  $o \neq 0$ , we define  $\hat{\gamma}_{k,m} = \text{sgn}(o) s_{\gamma_{k,m}} \sum_{j=1}^N l_{k,j} \frac{\partial H}{\partial \gamma_v}(X_j, \Gamma_j)$ , where  $\text{sgn}(x)$  is the signum function<sup>1</sup>.

Note that whenever  $o = 0$ , further characterization on the level surface  $\mathcal{S}_\rho$  is requested for the sign to be determined.

## 3.2 Dynamics of the Network

In this section, we discuss homogeneous MCD for which the global dynamics reads

$$\begin{aligned} \dot{x}_k &= L_1(x_k, y_k, A_k) - c_k \sum_{j=1}^N l_{k,j} x_j , \\ \dot{y}_k &= L_2(x_k, y_k, A_k) - c_k \sum_{j=1}^N l_{k,j} y_j , \\ \dot{\omega}_k &= -s_{\omega_k} \sum_{j=1}^N l_{k,j} (x_j y_k - y_j x_k) , \\ \dot{\rho}_k &= -s_{\rho_k} \sum_{j=1}^N l_{k,j} H(X_j, \Gamma_j) , \\ \dot{\gamma}_{k,s} &= \pm s_{\gamma_{k,s}} \sum_{j=1}^N l_{k,j} \frac{\partial H}{\partial \gamma_s}(X_j, \Gamma_j) , \end{aligned} \quad \begin{aligned} k &= 1, \dots, N , \\ s &= 1, \dots, q-2 , \end{aligned} \quad (3.9)$$

<sup>1</sup> For  $x \in \mathbb{R}$ , the signum function is: -1 if  $x < 0$ , 0 if  $x = 0$  and 1 if  $x > 0$ .

where  $L_1$  and  $L_2$  are defined in Section 3.1.1 and where  $s_{\omega_k} > 0$ ,  $s_{\rho_k} > 0$  and  $s_{\gamma_{k,s}}$  are susceptibility constants (the sign of  $s_{\gamma_{k,s}}$  depends on  $o$ , as discussed at the end of Section 3.1.3.2).

Let us emphasize that Eqs. (3.9) admits  $q$  constants of motion

$$\begin{aligned} J_\omega(\omega_1, \dots, \omega_N) &= \sum_{j=1}^N \frac{\omega_j}{s_{\omega_j}}, & J_\rho(\rho_1, \dots, \rho_N) &= \sum_{j=1}^N \frac{\rho_j}{s_{\rho_j}}, \\ J_{\gamma_s}(\gamma_{1,s}, \dots, \gamma_{N,s}) &= \sum_{j=1}^N \frac{\gamma_{j,s}}{s_{\gamma_{j,s}}} & s &= 1, \dots, q-2. \end{aligned} \quad (3.10)$$

Observe that when  $s_{\omega_k} = s_{\rho_k} = s_{\gamma_{k,s}} = 0$  for all  $k$  and  $s$ , Eqs.(3.9) reduces to a network of coupled limit cycle oscillators, all with the same  $L \equiv (L_1, L_2)$  but with different  $A_k$ . As shown by numerical simulations in [26], small heterogeneity in the  $A_k$  still enables the use of the master stability function to characterize synchronized motion.

Once the susceptibility constants are none zero, the adaptive mechanisms influence the **local dynamics** with the aim to drive the global dynamical system into a consensual oscillatory state. In this asymptotic regime one has

$$\begin{aligned} \lim_{t \rightarrow \infty} \|X_k(t) - \varphi_c(t)\| &= 0 \quad \forall k \quad \text{and} \quad \varphi_c(t) \quad \text{is periodic and defined below in 3.12,} \\ \text{and, for } k = 1, \dots, N, \quad \lim_{t \rightarrow \infty} A_k(t) &= A_c \quad \text{with constant } A_c. \end{aligned} \quad (3.11)$$

Once reached, this state remains permanent (i.e. even if interactions are switched off, all **local dynamics** still oscillate with the same frequency and on the same limit cycle). We now discuss the existence of a consensual oscillatory state and the convergence towards it.

### Existence of a consensual oscillatory state

The dynamical system defined by Eqs. (3.9) admits the periodic solution

$$\varphi(t) = (\varphi_c(t), A_c, \dots, \varphi_c(t), A_c) \in \mathbb{R}^{N(2+q)} \quad \varphi(0) = (X_0, A_c, \dots, X_0, A_c) \quad (3.12)$$

where, for all  $k$ ,  $\varphi_c(t) = (\varphi_x(t), \varphi_y(t))$  solves the canonical part of the MCD with initial conditions on the attractor, i.e.  $X_0 = (x_0, y_0) \in \mathcal{L}_{\Gamma_c} = \{X \in \mathbb{R}^2 \mid H(X, \Gamma_c) - \rho_c = 0\}$  and  $A_c = (\omega_c, \Gamma_c)$  is a given constant vector (i.e. common and fixed set of parameters for all oscillators). For coherence,  $\Gamma_c$  is chosen such that the **local dynamics** are well defined MCD. This periodic solution defines, in the  $\mathbb{R}^{(2+q)N}$ , a parametrization of the set (here a curve) on which its orbits circulates on, namely

$$\mathcal{C}_{A_c} := \{(X, A) \in \mathbb{R}^{2N} \times \mathbb{R}^{qN} \mid X_1 \in \mathcal{L}_{\Gamma_c}, X_k = X_j \quad \forall k, j \quad \text{and} \quad A_k = A_c \quad \forall k\}. \quad (3.13)$$

### Convergence towards a consensual oscillatory state

As discussed in Section 1.2.1, we are interested in the following two issues: **convergence** (i.e. if the network is initiated out of a consensual oscillatory state, will it converge to such state?) and **limit values** (if yes, to which consensual oscillatory state will it converge to?). For explanatory reasons, we first discuss the limit values and then the convergence.

**Limit Values** - The aim is to analytically express the values  $A_c$  in 3.11. For given initial conditions  $(X_k(0), A_k(0))$  of Eqs. (3.9), suppose that the network converges towards a consensual oscillatory state (i.e. 3.11 holds). This implies that

$$\lim_{t \rightarrow \infty} A_k(t) = \lim_{t \rightarrow \infty} (\omega_k(t), \rho_k(t), \gamma_{k,1}(t), \dots, \gamma_{k,q-2}(t)) = (\omega_c, \rho_c, \gamma_{c,1}, \dots, \gamma_{c,q-2}) = A_c$$

for all  $k$ . We want to determine the value of  $A_c$ . Due to the existence of the constants of motion in 3.10, we have

$$J_\omega(\omega(t)) = \mathbf{C}_1 \quad \forall t, \quad J_\rho(\rho(t)) = \mathbf{C}_2 \quad \forall t, \quad J_{\gamma_s}(\gamma_s(t)) = \mathbf{C}_{2+s} \quad s = 1, \dots, q-2,$$

with  $\omega(t) = (\omega_1(t), \dots, \omega_N(t))$ ,  $\rho(t) = (\rho_1(t), \dots, \rho_N(t))$  and  $\gamma_s(t) = (\gamma_{1,s}(t), \dots, \gamma_{N,s}(t))$  ( $s = 1, \dots, q-2$ ) orbits of Eqs. (3.9). Therefore, for the initial conditions  $(X_k(0), \Lambda_k(0))$  and provided 3.11 holds, then we have

$$\begin{aligned} J_\omega(\omega(0)) &= \lim_{t \rightarrow \infty} J_\omega(\omega(t)) = J_\omega(\lim_{t \rightarrow \infty} \omega(t)) = J_\omega(\omega_c \mathbf{1}) = \omega_c \sum_{j=1}^N \frac{1}{s_{\omega_j}}, \\ J_\rho(\rho(0)) &= \lim_{t \rightarrow \infty} J_\rho(\rho(t)) = J_\rho(\lim_{t \rightarrow \infty} \rho(t)) = J_\rho(\rho_c \mathbf{1}) = \rho_c \sum_{j=1}^N \frac{1}{s_{\rho_j}}, \\ J_{\gamma_s}(\gamma_s(0)) &= \lim_{t \rightarrow \infty} J_{\gamma_s}(\gamma_s(t)) = J_{\gamma_s}(\lim_{t \rightarrow \infty} \gamma_s(t)) = J_{\gamma_s}(\gamma_{c,s} \mathbf{1}) = \gamma_{c,s} \sum_{j=1}^N \frac{1}{s_{\gamma_{j,s}}} \quad s = 1, \dots, q-2. \end{aligned}$$

Hence, the consensual values  $\Lambda_c$  of the **parametric variables** are analytically expressed as

$$\omega_c = \frac{\sum_{j=1}^N \frac{\omega_j(0)}{s_{\omega_j}}}{\sum_{j=1}^N \frac{1}{s_{\omega_j}}}, \quad \rho_c = \frac{\sum_{j=1}^N \frac{\rho_j(0)}{s_{\rho_j}}}{\sum_{j=1}^N \frac{1}{s_{\rho_j}}}, \quad \gamma_{c,s} = \frac{\sum_{j=1}^N \frac{\gamma_{j,s}(0)}{s_{\gamma_{j,s}}}}{\sum_{j=1}^N \frac{1}{s_{\gamma_{j,s}}}} \quad s = 1, \dots, q-2. \quad (3.14)$$

We emphasize that the consensual values  $\Lambda_c$  only depend on the susceptibility constants and the distribution of the initial parameters  $\Lambda_k(0)$ , but neither on the network topology (i.e. not on  $L$ ) nor on the initial conditions of the **state variables** (i.e. on  $X_k(0)$ ).

**Convergence** - The convergence towards a consensual oscillatory state is a stability problem of an orbit of Eqs. (3.9). For given initial conditions  $(X_k(0), \Lambda_k(0))$ , one has the periodic solution in (3.12) by defining  $\Lambda_c$  as in 3.14. Now that  $\Lambda_c$  is fixed, one has to see whether the set  $\mathcal{C}_{\Lambda_c}$  (c.f. 3.13) is asymptotically Poincaré stable (refer to Appendix A). To do so, one can analyze the FLOQUET exponents of the first variational equation of Eqs. (3.9) (refer to Appendix A, in Section A.1.1).

Observe that, if consensual values  $\Lambda_c$  are fixed beforehand (i.e. before the initial conditions  $\Lambda_k(0)$  are given), then, because of the constants of motion in 3.10, a necessary condition for  $\mathcal{C}_{\Lambda_c}$  to be asymptotically Poincaré stable, is that the  $\Lambda_k(0)$  satisfy the following equations

$$\begin{aligned} J_\omega(\omega_1(0), \dots, \omega_N(0)) &= \omega_c \sum_{j=1}^N \frac{1}{s_{\omega_j}}, \quad J_\rho(\rho_1(0), \dots, \rho_N(0)) = \rho_c \sum_{j=1}^N \frac{1}{s_{\rho_j}}, \\ J_{\gamma_s}(\gamma_{1,s}(0), \dots, \gamma_{N,s}(0)) &= \gamma_{c,s} \sum_{j=1}^N \frac{1}{s_{\gamma_{j,s}}} \quad s = 1, \dots, q-2. \end{aligned}$$

That is to say, initial conditions  $\Lambda_k(0)$  are on hyperplanes. These equations imply that

$$\omega_c \sum_{j=1}^N \frac{1}{s_{\omega_j}} = J_\omega(\omega_c + \epsilon_{\omega_1}(0), \dots, \omega_c + \epsilon_{\omega_N}(0)) = \sum_{j=1}^N \frac{\omega_c}{s_{\omega_j}} + \sum_{j=1}^N \frac{\epsilon_{\omega_j}(0)}{s_{\omega_j}}$$

and therefore

$$\sum_{j=1}^N \frac{\epsilon_{\omega_j}(0)}{s_{\omega_j}} = 0. \quad (3.15)$$

For the perturbations  $\epsilon_{\rho_k}(0)$  and  $\epsilon_{\gamma_{k,s}}(0)$ , the same argument leads to Eq. (3.15) with the respective susceptibility constants.

The first variational equation of Eqs. (3.9) is a  $N(q+2) \times N(q+2)$  matrix. For  $N$  large, one encounters computational problems when it is used in calculations. Through an adequate change of basis, it is reduced to  $N$  systems of dimension  $q$ . This is shown in the following lemma.



The total derivative of the  $Q_k$  functions is a  $m \times m$  bloc matrix with each bloc being of size  $N \times N$ . The  $k, j$  bloc is

$$d_k K \begin{pmatrix} l_{1,1} \frac{\partial Q_k}{\partial y_{1,j}}(Y_1) & \dots & l_{1,N} \frac{\partial Q_k}{\partial y_{N,j}}(Y_N) \\ \vdots & \ddots & \vdots \\ l_{N,1} \frac{\partial Q_k}{\partial y_{1,j}}(Y_1) & \dots & l_{N,N} \frac{\partial Q_k}{\partial y_{N,j}}(Y_N) \end{pmatrix}.$$

For each block, the partial derivatives are identical once they are all evaluated at  $\varphi(t)$ . We use the following notation:  $\frac{\partial Q_k}{\partial y_j}(\varphi_c) := \frac{\partial Q_k}{\partial y_{s,j}}(\varphi_c)$ ,  $s = 1, \dots, N$ . We therefore have a  $m \times m$  bloc matrix with  $d_k \frac{\partial Q_k}{\partial y_j}(\varphi_c) K L$  as bloc  $k, j$ .

The total derivative of the  $R_k$  functions is a  $m \times m$  bloc matrix with each bloc being of size  $N \times N$ . The  $k, j$  bloc is

$$d_k K \begin{pmatrix} \sum_{s \neq 1}^N l_{1,s} \frac{\partial R_k}{\partial y_{1,j}}(Y_s, Y_1) & \dots & l_{1,N} \frac{\partial R_k}{\partial y_{N,j}}(Y_N, Y_1) \\ \vdots & \ddots & \vdots \\ l_{N,1} \frac{\partial R_k}{\partial y_{1,j}}(Y_1, Y_N) & \dots & \sum_{s \neq N}^N l_{N,s} \frac{\partial R_k}{\partial y_{N,j}}(Y_s, Y_N) \end{pmatrix},$$

with diagonal matrix  $K$  with entries  $k_k$ . For each block, the partial derivatives off the diagonal are identical once they are all evaluated at  $\varphi(t)$ . We use the following notation:  $\frac{\partial R_k}{\partial y_j}(\varphi_c, \varphi_c) := \frac{\partial R_k}{\partial y_{s,j}}(\varphi_c, \varphi_c)$ ,  $s = 1, \dots, N$ . Since  $R_k(Y_s, Y_v) = -R_k(Y_v, Y_s)$ , then

$$\frac{\partial R_k}{\partial y_{v,j}}(Y_s, Y_v) = \partial_{y_{v,j}}[-R_k(Y_v, Y_s)] = -\frac{\partial R_k}{\partial y_{v,j}}(Y_v, Y_s)$$

Therefore, evaluated at  $\varphi(t)$ , we have  $\frac{\partial R_k}{\partial y_{v,j}}(\varphi_c, \varphi_c) = -\frac{\partial R_k}{\partial y_{v,j}}(\varphi_c, \varphi_c) = -\frac{\partial R_k}{\partial y_j}(\varphi_c, \varphi_c)$  and so, for the diagonal terms, we obtain

$$\sum_{s \neq 1}^N l_{v,s} \left( -\frac{\partial R_k}{\partial y_j}(\varphi_c, \varphi_c) \right) = \frac{\partial R_k}{\partial y_j}(\varphi_c, \varphi_c) \left( -\sum_{s \neq 1}^N l_{v,s} \right) = \frac{\partial R_k}{\partial y_j}(\varphi_c, \varphi_c) l_{v,v} \quad v = 1, \dots, N.$$

We therefore have a  $m \times m$  bloc matrix with  $d_k \frac{\partial R_k}{\partial y_j}(\varphi_c, \varphi_c) K L$  as bloc  $k, j$ . Thus the first variational equation for the solution  $\varphi(t)$  of Eqs. (3.9) is

$$\dot{\epsilon} = J(t)\epsilon \tag{3.19}$$

with  $\epsilon = (\epsilon_1, \dots, \epsilon_m)$ ,  $\epsilon_j = (\epsilon_{1,j}, \dots, \epsilon_{N,j})$ ,  $\epsilon_{k,j}$  is the perturbation on the  $j^{\text{th}}$  variable of the  $k^{\text{th}}$  local system and the  $(Nm \times Nm)$  Jacobian  $J(t)$  is (omitting the dependence on  $\varphi_c(t)$ )

$$J(t) = \begin{pmatrix} \frac{\partial F_1}{\partial y_1} Id & \dots & \frac{\partial F_1}{\partial y_m} Id \\ \vdots & \ddots & \vdots \\ \frac{\partial F_m}{\partial y_1} Id & \dots & \frac{\partial F_m}{\partial y_m} Id \end{pmatrix} + \begin{pmatrix} d_1 K L \left( \frac{\partial Q_1}{\partial y_1} + \frac{\partial R_1}{\partial y_1} \right) & \dots & d_1 K L \left( \frac{\partial Q_1}{\partial y_m} + \frac{\partial R_1}{\partial y_m} \right) \\ \vdots & \ddots & \vdots \\ d_m K L \left( \frac{\partial Q_m}{\partial y_1} + \frac{\partial R_m}{\partial y_1} \right) & \dots & d_m K L \left( \frac{\partial Q_m}{\partial y_m} + \frac{\partial R_m}{\partial y_m} \right) \end{pmatrix}.$$

Let  $K^{\frac{1}{2}}$  be the diagonal matrix with  $\sqrt{k_k}$  on its diagonal. Then

$$K^{-\frac{1}{2}} d_j K L K^{\frac{1}{2}} = d_j K^{-\frac{1}{2}} K L K^{\frac{1}{2}} = d_j K^{\frac{1}{2}} L K^{\frac{1}{2}}.$$

Since  $K^{\frac{1}{2}} L K^{\frac{1}{2}}$  is symmetric, there exists an orthonormal matrix  $O$  such that  $O^T K^{\frac{1}{2}} L K^{\frac{1}{2}} O = D(\kappa)$  where  $D(\kappa)$  is a diagonal matrix with  $\kappa = (\kappa_1, \dots, \kappa_N)$  on its diagonal, which is its spectrum. Hence,  $K^{\frac{1}{2}} O$  diagonalizes  $d_j K L$  for all  $j$ . Changing the basis of  $J$  by  $Q$ , a  $m \times m$  bloc matrix (blocs of size

$N \times N$ ) with  $K^{\frac{1}{2}}O$  on its diagonal makes  $J$  a  $m \times m$  bloc matrix with each bloc being a diagonal matrix of size  $N \times N$ . Another change in basis with  $P$  as defined in 3.18 (i.e. recollecting the local variables together) leads to

$$P^{-1}Q^{-1}\dot{\epsilon} = P^{-1}Q^{-1}J(t)QPP^{-1}Q^{-1}\epsilon \iff \dot{\epsilon}_k = J_k(t)\epsilon_k \quad k = 1, \dots, N,$$

with  $P^{-1}Q^{-1}\epsilon = \epsilon = (\epsilon_1, \dots, \epsilon_N)$ ,  $\epsilon_k \in \mathbb{R}^m$  and where  $J_k(t)$  is the  $m \times m$  matrix given by (omitting the dependence on  $\varphi_c(t)$ )

$$\tilde{J}_k(t) = \begin{pmatrix} \frac{\partial F_1}{\partial y_1} & \cdots & \frac{\partial F_1}{\partial y_m} \\ \vdots & \ddots & \vdots \\ \frac{\partial F_m}{\partial y_1} & \cdots & \frac{\partial F_m}{\partial y_m} \end{pmatrix} + \kappa_k D \begin{pmatrix} \frac{\partial G_1}{\partial y_1} + \frac{\partial R_1}{\partial y_1} & \cdots & \frac{\partial G_1}{\partial y_m} + \frac{\partial R_1}{\partial y_m} \\ \vdots & \ddots & \vdots \\ \frac{\partial G_m}{\partial y_1} + \frac{\partial R_m}{\partial y_1} & \cdots & \frac{\partial G_m}{\partial y_m} + \frac{\partial R_m}{\partial y_m} \end{pmatrix}.$$

We therefore have

$$\dot{\epsilon}_k = \left( \mathfrak{D}F_{(\varphi_c(t))} + \kappa_k D (\mathfrak{D}Q_{(\varphi_c(t))} + \mathfrak{D}R_{(\varphi_c(t), \varphi_c(t))}) \right) \epsilon_k \quad k = 1, \dots, N.$$

Since  $L$  is a Laplacian matrix associated to a symmetric adjacency matrix with positive entries and  $K^{\frac{1}{2}}LK^{\frac{1}{2}}$  is a left and right multiplication of  $L$  by an identical positive definite diagonal matrix  $K^{\frac{1}{2}}$ , then the sign of its spectrum coincides with  $L$  (refer to Lemma D.3 in Appendix D), that is  $\kappa_k > 0$  for  $k = 2, \dots, N$  and  $\kappa_1 = 0$  (i.e. one can always rearrange the columns of  $O$  such that the zero eigenvalue appears in the first element of  $K$ ).

□

Note that this presentation generalizes the formalism in [37] since here coupling strengths are node dependent and the interaction may account for inter coupled coupling functions  $R$ . We now present the stability lemma that concerns the convergence of Eqs. (3.9) towards a consensual oscillatory state. We do not yet have a complete proof and so this is a conjecture.

**Lemma 3.2.** *For Eqs. (3.9) we suppose that for each node  $k$ , the coupling strengths and each susceptibility constants are related as follow*

$$c_k = c \, k_k \quad s_{\omega_k} = s_{\omega} k_k \quad s_{\rho_k} = s_{\rho} k_k \quad \text{and} \quad s_{\gamma_{k,l}} = s_{\gamma_l} k_k \quad l = 1, \dots, q-2, \quad (3.20)$$

for given  $c, s_{\omega}, s_{\rho}, s_{\gamma_l}$  ( $l = 1, \dots, q-2$ ) and  $k_k > 0$  for  $k = 1, \dots, N$ . For a given consensual set  $\Lambda_c$ , suppose that initial conditions  $\omega_k(0), \rho_k(0), \gamma_{k,1}(0), \dots, \gamma_{k,q-2}(0)$  satisfy Eqs. (3.15). Then, if all the FLOQUET exponents for all  $N-1$  Systems in 3.17 with  $k = 2, \dots, N$  have strictly negative real parts,  $\mathcal{C}_{\Lambda_c}$  is Poincaré asymptotically stable.

We present a tentative proof.

Eqs. (3.9) are a particular case of Eqs. 3.16 where here  $Y_k = (X_k, \omega_k, \Gamma_k)$ ,  $D$  is a diagonal matrix with  $(c, c, s_{\omega}, s_{\rho}, s_{\gamma_1}, \dots, s_{\gamma_{q-2}})$  on its diagonal and  $Q$  and  $R$  are coupling functions which here read as

$$Q(Y_j) = (x_j, y_j, 0, H(X_j, \Gamma_j), \frac{\partial H}{\partial \gamma_{j,1}}(X_j, \Gamma_j), \pm \frac{\partial H}{\partial \gamma_{j,1}}(X_j, \Gamma_j), \dots, \pm \frac{\partial H}{\partial \gamma_{j,q-2}}(X_j, \Gamma_j)) \quad ,$$

$$R(Y_j, Y_k) = (0, 0, x_j y_k - y_j x_k, 0, 0, \dots, 0).$$

In this case, the Jacobian in Eqs. 3.17, denoted here  $J_k(t)$ , becomes (refer to Appendix F)



$$\begin{pmatrix} \frac{\partial \mathcal{L}_1}{\partial x} - \mathbf{C}\kappa_k & \frac{\partial \mathcal{L}_1}{\partial y} & \frac{\partial \mathcal{L}_1}{\partial \omega} & \frac{\partial \mathcal{L}_1}{\partial \rho} & \frac{\partial \mathcal{L}_1}{\partial \gamma_1} & \cdots & \frac{\partial \mathcal{L}_1}{\partial \gamma_{q-2}} \\ \frac{\partial \mathcal{L}_2}{\partial x} & \frac{\partial \mathcal{L}_2}{\partial y} - \mathbf{C}\kappa_k & \frac{\partial \mathcal{L}_2}{\partial \omega} & \frac{\partial \mathcal{L}_2}{\partial \rho} & \frac{\partial \mathcal{L}_2}{\partial \gamma_1} & \cdots & \frac{\partial \mathcal{L}_2}{\partial \gamma_{q-2}} \\ -\varphi_y(t)\mathbf{S}_\omega\kappa_k & \varphi_x(t)\mathbf{S}_\omega\kappa_k & \mathbf{0} & \mathbf{0} & \mathbf{0} & \cdots & \mathbf{0} \\ -\frac{\partial \mathbf{H}}{\partial x}\mathbf{S}_\rho\kappa_k & -\frac{\partial \mathbf{H}}{\partial y}\mathbf{S}_\rho\kappa_k & \mathbf{0} & -\frac{\partial \mathbf{H}}{\partial \rho}\mathbf{S}_\rho\kappa_k & -\frac{\partial \mathbf{H}}{\partial \gamma_1}\mathbf{S}_\rho\kappa_k & \cdots & -\frac{\partial \mathbf{H}}{\partial \gamma_{q-2}}\mathbf{S}_\rho\kappa_k \\ \frac{\partial^2 \mathbf{H}}{\partial x \partial \gamma_1}\mathbf{S}_{\gamma_1}\kappa_k & \frac{\partial^2 \mathbf{H}}{\partial y \partial \gamma_1}\mathbf{S}_{\gamma_1}\kappa_k & \mathbf{0} & \frac{\partial^2 \mathbf{H}}{\partial \rho \partial \gamma_1}\mathbf{S}_{\gamma_1}\kappa_k & \frac{\partial^2 \mathbf{H}}{\partial \gamma_1^2}\mathbf{S}_{\gamma_1}\kappa_k & \cdots & \frac{\partial^2 \mathbf{H}}{\partial \gamma_{q-2} \gamma_1}\mathbf{S}_{\gamma_1}\kappa_k \\ \vdots & \vdots & \vdots & \vdots & \vdots & \ddots & \vdots \\ \frac{\partial^2 \mathbf{H}}{\partial x \partial \gamma_{q-2}}\mathbf{S}_{\gamma_{q-2}}\kappa_k & \frac{\partial^2 \mathbf{H}}{\partial y \partial \gamma_{q-2}}\mathbf{S}_{\gamma_{q-2}}\kappa_k & \mathbf{0} & \frac{\partial^2 \mathbf{H}}{\partial \rho \partial \gamma_{q-2}}\mathbf{S}_{\gamma_{q-2}}\kappa_k & \frac{\partial^2 \mathbf{H}}{\partial \gamma_{q-2}^2}\mathbf{S}_{\gamma_{q-2}}\kappa_k & \cdots & \frac{\partial^2 \mathbf{H}}{\partial \gamma_{q-2} \gamma_1}\mathbf{S}_{\gamma_{q-2}}\kappa_k \end{pmatrix}$$

By hypothesis, for  $k = 2, \dots, N$ , all FLOQUET exponents for the above  $N - 1$  Systems have strictly negative real parts.

For  $k = 1$ , we have  $\dot{\varepsilon}_{\omega_1}(t) = \dot{\varepsilon}_{\rho_1}(t) = \dot{\varepsilon}_{\gamma_{1,s}}(t) = 0$  for all  $t$  and  $s = 1, \dots, q - 2$ , thus they are all constant functions, taking the value of their respective initial conditions. However, since the initial conditions  $\omega_k(0)$  satisfy Eqs. (3.15), then  $\varepsilon_{\omega_1}(0) = 0$  and thus  $\varepsilon_{\omega_1}(t) = 0$  for all  $t$ . This is because the first column of  $O$  is  $n_1(k_1^{-\frac{1}{2}}, \dots, k_N^{-\frac{1}{2}})^\top$  with  $n_1 = (\sum_{j=1}^N k_j^{-1})^{-\frac{1}{2}}$ . This corresponds to an eigenvector of the eigenvalue  $\kappa_1 = 0$  of the matrix  $K^{\frac{1}{2}}LK^{\frac{1}{2}}$ . In changing the basis, we have the product  $O^\top K^{-\frac{1}{2}}\varepsilon_{\omega}(t)$  of which the first coordinate is

$$\varepsilon_{\omega_1}(t) = n_1 \sum_{j=1}^N \frac{\varepsilon_{\omega_j}(t)}{k_j} = n_1 \mathbf{s}_\omega \sum_{j=1}^N \frac{\varepsilon_{\omega_j}(t)}{\mathbf{s}_{\omega_j}}$$

and at  $t = 0$ , the above is zero by Eq. (3.15). Since Eq. (3.15) holds (with the respective susceptibility constants) for the other perturbation, then the same reasoning enables us to conclude that  $\varepsilon_{\rho_1}(t) = \varepsilon_{\gamma_{1,1}}(t) = \dots = \varepsilon_{\gamma_{1,q-2}}(t) = 0$ . Therefore, for  $k = 1$ ,  $\dot{\varepsilon}_1 = \mathcal{J}_1(t)\varepsilon_1$  is reduced to

$$\begin{pmatrix} \dot{\varepsilon}_{x_1} \\ \dot{\varepsilon}_{y_1} \end{pmatrix} = \begin{pmatrix} \frac{\partial \mathcal{L}_1}{\partial x}(\varphi_1(t), \Lambda_c) & \frac{\partial \mathcal{L}_1}{\partial y}(\varphi_1(t), \Lambda_c) \\ \frac{\partial \mathcal{L}_2}{\partial x}(\varphi_1(t), \Lambda_c) & \frac{\partial \mathcal{L}_2}{\partial y}(\varphi_1(t), \Lambda_c) \end{pmatrix} \begin{pmatrix} \varepsilon_{x_1} \\ \varepsilon_{y_1} \end{pmatrix} \quad (3.21)$$

and the above equation is the variational equation for a MCD. It has one FLOQUET exponent which is zero and since

$$\int_0^T \text{tr}(\mathfrak{D}\mathcal{L}(\varphi_1(t), \Lambda_c)) dt < 0,$$

its other FLOQUET exponent is strictly negative (refer to Appendix A, in Section A.1.1). Here  $\mathfrak{D}\mathcal{L}(\varphi_1(t), \Lambda_c)$  is the  $2 \times 2$  matrix in Eq. (3.21) and by straight calculations, we have  $\text{tr}(\mathfrak{D}\mathcal{L}(\varphi_1(t), \Lambda_c)) = \omega_c \frac{\partial^2 \mathbf{H}}{\partial x \partial y}(\varphi_1(t), \Lambda_c) - \frac{\partial \mathbf{H}}{\partial x}(\varphi_1(t), \Lambda_c)^2 - \omega_c \frac{\partial^2 \mathbf{H}}{\partial y \partial x}(\varphi_1(t), \Lambda_c) - \frac{\partial \mathbf{H}}{\partial y}(\varphi_1(t), \Lambda_c)^2 = -(\frac{\partial \mathbf{H}}{\partial x}(\varphi_1(t), \Lambda_c)^2 + \frac{\partial \mathbf{H}}{\partial y}(\varphi_1(t), \Lambda_c)^2) < 0$ .

Therefore the first variational equation has one FLOQUET exponent equal to zero plus  $q$  other due to the  $q$  constants of motion. The remaining FLOQUET exponents have strictly negative real parts. We now need to apply a similar asymptotic stability theorem as in Section A.1.1, Appendix A showing that the  $q + 1$  zero exponents can be put aside when considering the asymptotic stability issue. Note that in the ‘‘classical’’ case (i.e. when theorem in Section A.1.1, Appendix A is applied), there is always one FLOQUET exponent equal to zero corresponding to tangential direction of the orbit.

### 3.2.1 Network of Ellipsoidal Hopf Oscillators

Let us here focus on Eqs.(3.9) with  $\mathbf{L}$  given by

$$\begin{aligned}\dot{x}_k &= \omega_k \beta_k y_k - (\alpha_k x_k^2 + \beta_k y_k^2 - \rho_k) \alpha_k x_k, \\ \dot{y}_k &= -\omega_k \alpha_k x_k - (\alpha_k x_k^2 + \beta_k y_k^2 - \rho_k) \beta_k y_k,\end{aligned}\quad k = 1, \dots, N.$$

The Hamiltonian is  $H(x, y, \alpha, \beta) = \alpha x^2 + \beta y^2$  and all **local dynamics** are rescaled in time with  $x(t) \mapsto x(2t)$ . There is one f-PV  $\omega_k$  and three g-PV  $\Gamma_k = (\rho_k, \gamma_{k,1}, \gamma_{k,2}) = (\rho_k, \alpha_k, \beta_k)$  (i.e.  $q = 4$ ). The sign in front of the adaptive mechanism is  $+$ , for both,  $\alpha_k$  and  $\beta_k$ . To show this, fix  $\rho$ ,  $\beta$ , define  $\alpha_m$  and  $\alpha_M$  as in 3.7. Parametrization of the respective limit cycles  $\mathcal{L}_{\alpha_m}$  and  $\mathcal{L}_{\alpha_M}$  is done with  $X_m(z) = \sqrt{\rho}(\frac{\sin(z)}{\sqrt{\alpha_m}}, \frac{\cos(z)}{\sqrt{\beta}})$  and  $X_M(z) = \sqrt{\rho}(\frac{\sin(z)}{\sqrt{\alpha_M}}, \frac{\cos(z)}{\sqrt{\beta}})$  for  $z \in [0, 2\pi]$ . Since  $\frac{\partial H}{\partial \alpha}(x, y, \alpha, \beta) = x^2$  and because  $0 < \alpha_m < \alpha_M$ , the integral in 3.8 becomes

$$\int_0^{2\pi} \rho \frac{\sin(z)^2}{\alpha_m} - \rho \frac{\sin(z)^2}{\alpha_M} dz = \rho \left( \frac{1}{\alpha_m} - \frac{1}{\alpha_M} \right) \pi > 0.$$

Along the same lines, the conclusion is also true for  $\beta_k$ . Here, the periodic solution in 3.12 becomes

$$\varphi_k(t) = (\sin(t), \cos(t)) \quad k = 1, \dots, N \quad \Lambda_c = (1, 1, 1, 1) \quad \text{and} \quad X_0 = (0, 1).$$

Therefore the curve for which we want to infer its stability (c.f. 3.13) is given by

$$\mathcal{C}_1 := \{(X, \Lambda) \in \mathbb{R}^{2N} \times \mathbb{R}^{4N} \mid X_1 \in \mathbb{S}^1, X_k = X_j \ \forall k, j \text{ and } \Lambda_k = \mathbf{1} \ \forall k\}.$$

where  $\mathbf{1}$  is a  $q$  dimensional vector of 1. To ease the presentation, we focus on the case for which  $\mathbf{s} = \mathbf{s}_\omega = \mathbf{s}_\rho = \mathbf{s}_\alpha = \mathbf{s}_\beta$ . Therefore, as we have seen, we need to study the FLOQUET exponents of the  $N - 1$  systems in 3.17. The Jacobian here reads as

$$J_k(t) = \begin{pmatrix} -2S(t)^2 - c\kappa_k & 1 - 2C(t)S(t) & C(t) & S(t) & -S(t)^3 & C(t) - C(t)^2S(t) \\ -1 - 2C(t)S(t) & -2C(t)^2 - c\kappa_k & -S(t) & C(t) & -S(t) - S(t)^2C(t) & -C(t)^3 \\ -C(t)s\kappa_k & S(t)s\kappa_k & 0 & 0 & 0 & 0 \\ -2S(t)s\kappa_k & -2C(t)s\kappa_k & 0 & 0 & -S(t)^2s\kappa_k & -C(t)^2s\kappa_k \\ 2S(t)s\kappa_k & 0 & 0 & 0 & 0 & 0 \\ 0 & 2C(t)s\kappa_k & 0 & 0 & 0 & 0 \end{pmatrix}$$

with  $C(t) = \cos(t)$  and  $S(t) = \sin(t)$  and where  $\kappa_j$  ( $j = 1, \dots, N$ ) are the eigenvalues of  $K^{\frac{1}{2}}LK^{\frac{1}{2}}$ . For couples  $(c\kappa_k, s\kappa_k) \in ]0, 2[ \times ]0, 4[$ , we numerically calculate the FLOQUET exponents of the system

$$\dot{\varepsilon}_k = J_k(t)\varepsilon_k. \quad (3.22)$$

We assign a black point to each couple with FLOQUET exponents with strictly negative real parts. The overall result is a stability diagram shown in Figure 3.3.

### 3.2.2 Miscellaneous Remark: Variation in the Adaptive mechanism

In this section, we present an alternative adaptive mechanism for the  $\rho_k$ . Here, we choose:  $\mathbf{s}_k := \mathbf{s}_{\rho_k} = \mathbf{s}_{\alpha_k} = \mathbf{s}_{\beta_k}$  and the dynamics reads as

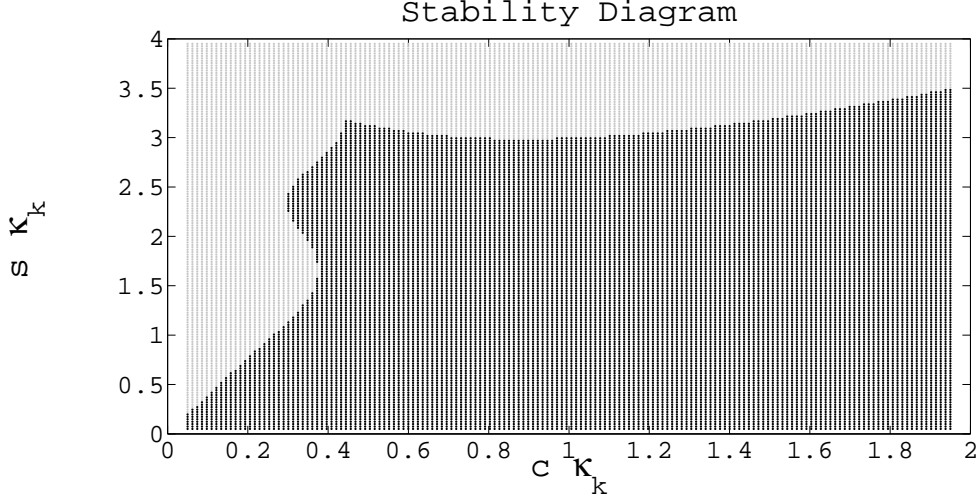


Fig. 3.3: Stability diagram showing which pair  $(c_k, s_k)$  makes the system given by Eqs. (3.22) have FLOQUET exponents with strictly negative real part (black points). The grid consists of 160 equidistant points between 0.05 and 1.95 (0.05 and 3.95) for the  $x$ -axis (for the  $y$ -axis).

$$\begin{aligned}
\dot{x}_k &= \omega_k \beta_k y_k - (\alpha_k x_k^2 + \beta_k y_k^2 - \rho_k) \alpha_k x_k - c_k \sum_{j=1}^N l_{k,j} x_j, \\
\dot{y}_k &= -\omega_k \alpha_k x_k - (\alpha_k x_k^2 + \beta_k y_k^2 - \rho_k) \beta_k y_k - c_k \sum_{j=1}^N l_{k,j} y_j, \quad k = 1, \dots, N, \\
\dot{\omega}_k &= -s_{\omega_k} \sum_{j=1}^N l_{k,j} (x_j y_k - y_j x_k), \\
\dot{\rho}_k &= -s_k \sum_{j=1}^N l_{k,j} (x_j^2 + y_j^2), \\
\dot{\alpha}_k &= s_k \sum_{j=1}^N l_{k,j} x_j^2, \\
\dot{\beta}_k &= s_k \sum_{j=1}^N l_{k,j} y_j^2,
\end{aligned} \tag{3.23}$$

It is interesting to remark that with this alternative adaptive mechanism, we are in the presence of  $N$  additional constants of motion. We know already that for all  $t \geq 0$ , we have

$$\begin{aligned}
J_\omega(\omega_1(t), \dots, \omega_N(t)) &= \sum_{j=1}^N \frac{\omega_j(t)}{s_{\omega_j}} = \sum_{j=1}^N \frac{\omega_j(0)}{s_{\omega_j}}, & J_\rho(\rho_1(t), \dots, \rho_N(t)) &= \sum_{j=1}^N \frac{\rho_j(t)}{s_j} = \sum_{j=1}^N \frac{\rho_j(0)}{s_j}, \\
J_\alpha(\alpha_1(t), \dots, \alpha_N(t)) &= \sum_{j=1}^N \frac{\alpha_j(t)}{s_j} = \sum_{j=1}^N \frac{\alpha_j(0)}{s_j}, & J_\beta(\beta_1(t), \dots, \beta_N(t)) &= \sum_{j=1}^N \frac{\beta_j(t)}{s_j} = \sum_{j=1}^N \frac{\beta_j(0)}{s_j},
\end{aligned}$$

with  $\omega_k(t)$ ,  $\rho_k(t)$ ,  $\alpha_k(t)$  and  $\beta_k(t)$  ( $k = 1, \dots, N$ ) orbits of Eqs. (3.23). We further have, for  $k = 1, \dots, N$ ,

$$J_k(\rho_k(t), \alpha_k(t), \beta_k(t)) = \rho_k(t) + \alpha_k(t) + \beta_k(t) = \rho_k(0) + \alpha_k(0) + \beta_k(0) \tag{3.24}$$

since

$$\frac{d[\mathbf{J}_k(\rho_k, \alpha_k, \beta_k)]}{dt} = \dot{\rho}_k + \dot{\alpha}_k + \dot{\beta}_k = -\mathbf{s}_k \sum_{j=1}^N l_{k,j} (x_j^2 + y_j^2) + \mathbf{s}_k \sum_{j=1}^N l_{k,j} x_j^2 + \mathbf{s}_k \sum_{j=1}^N l_{k,j} y_j^2 = 0 .$$

Let us emphasize that in this case, the adaptation is only due to the **state variables**. That is, the adaptive mechanisms depend only on  $x_k$  and  $y_k$  but not on the set of g-PV  $\rho_k, \alpha_k$  and  $\beta_k$ . Under certain conditions, the adaptive mechanism together with the coupling drive the network towards a consensual oscillatory state where, asymptotically, one has

$$\lim_{t \rightarrow \infty} \|X_k(t) - \varphi_c(t)\| = 0 \quad \forall k \quad \text{and} \quad \varphi_c(t) \quad \text{is periodic and defined bellow in 3.26,}$$

$$\text{and, for } k = 1, \dots, N, \quad \lim_{t \rightarrow \infty} (\omega_k(t), \rho_k(t), \alpha_k(t), \beta_k(t)) = \left( \frac{\bar{\omega}}{\bar{\rho}_k}, \bar{\rho}_k, \bar{\alpha} \bar{\rho}_k, \bar{\beta} \bar{\rho}_k \right) \quad (3.25)$$

with constants  $\bar{\omega}, \bar{\rho}_1, \dots, \bar{\rho}_N, \bar{\alpha}$  and  $\bar{\beta}$ .

The asymptotic consensual values for the **parametric variables** are not necessarily the same for all oscillators although the **state variables** all converge to a common periodic function.

### Existence a consensual oscillatory state

The dynamical system defined by Eqs. (3.23) admits the periodic solution

$$\varphi_c(t) = \left( \frac{\sin(\bar{\omega} \sqrt{\bar{\alpha} \bar{\beta}} t)}{\sqrt{\bar{\alpha}}}, \frac{\cos(\bar{\omega} \sqrt{\bar{\alpha} \bar{\beta}} t)}{\sqrt{\bar{\beta}}} \right), \quad \omega_k(t) = \frac{\bar{\omega}}{\bar{\rho}_k}, \quad \rho_k(t) = \bar{\rho}_k, \quad \alpha_k(t) = \bar{\alpha} \bar{\rho}_k \quad (3.26)$$

and  $\beta_k(t) = \bar{\beta} \bar{\rho}_k \quad \forall k$ ,

where  $\bar{\omega}, \bar{\rho}_1, \dots, \bar{\rho}_N, \bar{\alpha}$  and  $\bar{\beta}$  are given constants. Let us verify the solution. Since the **state variables** are all equal, the vector field for the **parametric variables** is zero (i.e. the last four equalities in Eqs. (3.23) vanish). So we have the constant solution taking the values of its initial conditions:  $(\omega_k(t), \rho_k(t), \alpha_k(t), \beta_k(t)) = (\omega_k(0), \rho_k(0), \alpha_k(0), \beta_k(0)) = \left( \frac{\bar{\omega}}{\bar{\rho}_k}, \bar{\rho}_k, \bar{\alpha} \bar{\rho}_k, \bar{\beta} \bar{\rho}_k \right)$ . Again, because the **state variables** are all equal, the **coupling dynamics** are zero. The dissipative part of the MCD also vanishes since  $\alpha_k(t)x_k(t)^2 + \beta_k(t)y_k(t)^2 - \rho_k(t) = \bar{\alpha} \bar{\rho}_k \frac{\sin(\bar{\omega} \sqrt{\bar{\alpha} \bar{\beta}} t)^2}{\bar{\alpha}} + \bar{\beta} \bar{\rho}_k \frac{\cos(\bar{\omega} \sqrt{\bar{\alpha} \bar{\beta}} t)^2}{\bar{\beta}} - \bar{\rho}_k = 0$ . Finally,  $\varphi_c(t)$  solves the canonical part since, deriving the  $x$ -coordinate with respect to  $t$ , we obtain

$$\dot{\varphi}_x(t) = \bar{\omega} \sqrt{\bar{\beta}} \cos(\bar{\omega} \sqrt{\bar{\alpha} \bar{\beta}} t) \quad \text{and} \quad \omega_k(t) \beta_k(t) y_k(t) = \frac{\bar{\omega}}{\bar{\rho}_k} \bar{\beta} \bar{\rho}_k \frac{\cos(\bar{\omega} \sqrt{\bar{\alpha} \bar{\beta}} t)}{\sqrt{\bar{\beta}}} = \bar{\omega} \sqrt{\bar{\beta}} \cos(\bar{\omega} \sqrt{\bar{\alpha} \bar{\beta}} t),$$

$$\dot{\varphi}_y(t) = -\bar{\omega} \sqrt{\bar{\alpha}} \sin(\bar{\omega} \sqrt{\bar{\alpha} \bar{\beta}} t) \quad \text{and} \quad -\omega_k(t) \alpha_k(t) x_k(t) = -\frac{\bar{\omega}}{\bar{\rho}_k} \bar{\alpha} \bar{\rho}_k \frac{\sin(\bar{\omega} \sqrt{\bar{\alpha} \bar{\beta}} t)}{\sqrt{\bar{\alpha}}} = \bar{\omega} \sqrt{\bar{\alpha}} \sin(\bar{\omega} \sqrt{\bar{\alpha} \bar{\beta}} t).$$

This concludes the verification of the solution.

### Convergence towards a consensual oscillatory state

**Convergence** - We do not attempt to analytically show that convergence towards a consensual oscillatory state may exist under certain conditions. The first problem encountered in doing so is that the Jacobian matrix is time dependent. Although it is periodic, one generally can not analytically calculate the FLOQUET exponents. Secondly, because of the heterogeneity of the consensual values  $(\bar{\omega}_k, \bar{\rho}_k, \bar{\alpha}_k, \bar{\beta}_k)$ , the Jacobian is generally not digonalizable. Therefore, we here suppose that convergence towards a consensual oscillatory state holds (i.e. 3.25 holds). Several numerical simulations confirm the convergence.

**Limit Values** - If 3.25 holds, then the values  $\bar{\omega}, \bar{\rho}_1, \dots, \bar{\rho}_N, \bar{\alpha}$  and  $\bar{\beta}$  are analytically expressed as

$$\bar{\omega} = \frac{\sum_{j=1}^N \frac{\omega_j(0)}{s_{\omega_j}}}{\sum_{j=1}^N \frac{1}{s_{\omega_j} \bar{\rho}_j}}, \quad \bar{\rho}_k = \frac{\mathbf{C}_k \sum_{j=1}^N \frac{\rho_j(0)}{s_j}}{\sum_{j=1}^N \frac{\mathbf{C}_j}{s_j}} \quad \text{for } k = 1, \dots, N, \quad \bar{\alpha} = \frac{\sum_{j=1}^N \frac{\alpha_j(0)}{s_j}}{\sum_{j=1}^N \frac{\bar{\rho}_j}{s_j}}, \quad \bar{\beta} = \frac{\sum_{j=1}^N \frac{\beta_j(0)}{s_j}}{\sum_{j=1}^N \frac{\bar{\rho}_j}{s_j}},$$

with  $\mathbf{C}_k := \rho_k(0) + \alpha_k(0) + \beta_k(0)$ . All four equalities derive from the the  $N + 4$  constants of motion of the system and by the fact that we suppose that  $\lim_{t \rightarrow \infty} (\omega_k(t), \rho_k(t), \alpha_k(t), \beta_k(t)) = (\frac{\bar{\omega}}{\bar{\rho}_k}, \bar{\rho}_k, \bar{\alpha}\bar{\rho}_k, \bar{\beta}\bar{\rho}_k)$ . From 3.24, we have

$$\mathbf{C}_k = \lim_{t \rightarrow \infty} (\rho_k(t) + \alpha_k(t) + \beta_k(t)) = \bar{\rho}_k(1 + \bar{\alpha} + \bar{\beta}) \quad \forall k,$$

so that  $\frac{\mathbf{C}_j}{\mathbf{C}_k} = \frac{\bar{\rho}_j}{\bar{\rho}_k} \Leftrightarrow \bar{\rho}_j = \bar{\rho}_k \frac{\mathbf{C}_j}{\mathbf{C}_k}$ . Therefore we obtain

$$\sum_{j=1}^N \frac{\rho_j(0)}{\mathbf{s}_j} = \lim_{t \rightarrow \infty} \sum_{j=1}^N \frac{\rho_j(t)}{\mathbf{s}_j} = \sum_{j=1}^N \frac{\bar{\rho}_k \mathbf{C}_j}{\mathbf{s}_j} = \frac{\bar{\rho}_k}{\mathbf{C}_k} \sum_{j=1}^N \frac{\mathbf{C}_j}{\mathbf{s}_j}.$$

Having  $\bar{\rho}_k$ , the other three constants can be derived

$$\begin{aligned} \sum_{j=1}^N \frac{\omega_j(0)}{\mathbf{s}_{\omega_j}} &= \lim_{t \rightarrow \infty} \sum_{j=1}^N \frac{\omega_j(t)}{\mathbf{s}_{\omega_j}} = \sum_{j=1}^N \frac{\bar{\omega}}{\bar{\rho}_j \mathbf{s}_{\omega_j}} = \bar{\omega} \sum_{j=1}^N \frac{1}{\mathbf{s}_{\omega_j} \bar{\rho}_j}, \\ \sum_{j=1}^N \frac{\alpha_j(0)}{\mathbf{s}_j} &= \lim_{t \rightarrow \infty} \sum_{j=1}^N \frac{\alpha_j(t)}{\mathbf{s}_j} = \sum_{j=1}^N \frac{\bar{\alpha} \bar{\rho}_j}{\mathbf{s}_j} = \bar{\alpha} \sum_{j=1}^N \frac{\bar{\rho}_j}{\mathbf{s}_j}, \\ \sum_{j=1}^N \frac{\beta_j(0)}{\mathbf{s}_j} &= \lim_{t \rightarrow \infty} \sum_{j=1}^N \frac{\beta_j(t)}{\mathbf{s}_j} = \sum_{j=1}^N \frac{\bar{\beta} \bar{\rho}_j}{\mathbf{s}_j} = \bar{\beta} \sum_{j=1}^N \frac{\bar{\rho}_j}{\mathbf{s}_j}. \end{aligned}$$

### 3.3 Numerical Simulations

We present numerical simulations with three different types of MCD systems. As in Section 2.3, the coordinates of  $\mathbf{1s}(a,b,N) \in \mathbb{R}^N$  are defined as  $\mathbf{1s}(a,b,N)_j := a + (j-1)\frac{b-a}{N-1}$ ,  $j = 1, \dots, N$ .

#### 3.3.1 Ellipsoidal HOPF Oscillators

For the 10 local dynamics defined in Section 3.2.1, two network topologies are considered: “All-to-All” and “All-to-One”. We choose the coupling strengths and susceptibility constants as  $(\mathbf{c}_1, \dots, \mathbf{c}_N) = \mathbf{1s}(1,1,1,10)$ ,  $(\mathbf{s}_{\omega_1}, \dots, \mathbf{s}_{\omega_N}) = \mathbf{1s}(1,0.1,1,10)$ ,  $(\mathbf{s}_{\rho_1}, \dots, \mathbf{s}_{\rho_N}) = \frac{1}{\mathbf{1s}(1,10,10)}$ ,  $(\mathbf{s}_{\alpha_1}, \dots, \mathbf{s}_{\alpha_N}) = \mathbf{1s}(1,0.1,10)^2$  and  $(\mathbf{s}_{\beta_1}, \dots, \mathbf{s}_{\beta_N}) = \mathbf{1s}(1,0.1,10)^{\frac{1}{2}}$  where  $\frac{1}{(\cdot)}$ ,  $(\cdot)^2$  and  $(\cdot)^{\frac{1}{2}}$  are taken on the coordinates. The initial conditions for **state variables**  $(x_k(0), y_k(0))$  are randomly uniformly distributed on  $] - 0.1, 0.1[$ . The initial conditions for the **parametric variables**  $(\omega_k(0), \rho_k(0), \alpha_k(0), \beta_k(0))$  are randomly (uniform distribution) drawn from  $]1.5, 2[ \times ]0.95, 1.05[ \times ]0.5, 1[ \times ]1.5, 1.75[$ .

Figure 3.4 shows the resulting dynamics for the **parametric variables**  $(\alpha_k$  and  $\beta_k)$ . From these numerical simulations, we observe that the convergence rate depends on the network topology. The larger the algebraic connectivity (e.g. “All-to-All” coupling), the faster the convergence. In Section 5.2.0.1, we analytically establish the interplay between the two.

#### 3.3.2 CASSINI Oscillators

Consider 13 MCD systems with CASSINI type Hamiltonian  $H(x, y, \alpha) = ((x - \sqrt{\alpha})^2 + y^2)((x + \sqrt{\alpha})^2 + y^2)$ . The level surface  $\mathcal{S}_1$  (c.f Figure 3.5(a)) determines a minus sign as a prefactor of the  $\alpha_k$  adaptive mechanism. To show this, fix  $\rho$  and define  $\alpha_m$  and  $\alpha_M$  as in 3.7. Parametrization of the respective limit cycles  $\mathcal{L}_{\alpha_m}$  and  $\mathcal{L}_{\alpha_M}$  are  $X_m(z) = (r_m(z) \sin(z), r_m(z) \cos(z))$  and  $X_M(z) = (r_M(z) \sin(z), r_M(z) \cos(z))$  for  $z \in [0, 2\pi]$  with

$$r_m(z) := \sqrt{\alpha_m} \sqrt{-\cos(2z) + \sqrt{\cos(2z)^2 - 1 + \frac{\rho}{\alpha_m^2}}}$$

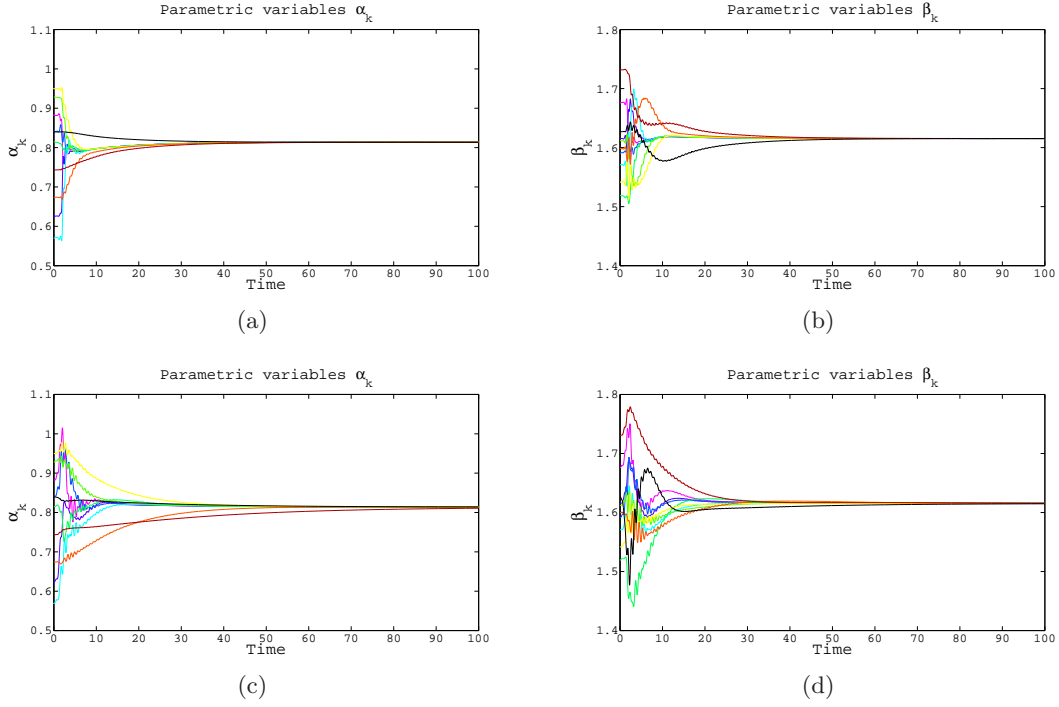


Fig. 3.4: Time evolution of the **parametric variables**  $\alpha_k$  and  $\beta_k$  (Figures 3.4(a) & 3.4(b)) for 10 ellipsoidal HOPF oscillators, interacting through a “All-to-All”. The algebraic connectivity is equal to 10. Time evolution of the **parametric variables**  $\alpha_k$  and  $\beta_k$  (Figures 3.4(c)) & 3.4(d)) for 10 ellipsoidal HOPF oscillators, interacting through a “All-to-One”. The algebraic connectivity is equal to 1.

and similarly for  $r_M(z)$  with  $\alpha_M$  instead of  $\alpha_m$ . Since  $\frac{\partial H}{\partial \alpha}(x, y, \alpha) = 2(y^2 - x^2 + \alpha)$  the integral in 3.8 becomes

$$\begin{aligned}
& 2 \int_0^{2\pi} r_m(z)^2 \cos(2z) dz - 2 \int_0^{2\pi} r_M(z)^2 \cos(2z) dz + 2 \int_0^{2\pi} \alpha_m - \alpha_M dz \\
&= 2\alpha_m \int_0^{2\pi} -\cos(2z)^2 + \cos(2z) \sqrt{\cos(2z)^2 - 1 + \frac{\rho}{\alpha_m^2}} dz \\
&\quad - 2\alpha_M \int_0^{2\pi} -\cos(2z)^2 + \cos(2z) \sqrt{\cos(2z)^2 - 1 + \frac{\rho}{\alpha_M^2}} dz + 4\pi(\alpha_m - \alpha_M) \\
&= 4\pi(\alpha_m - \alpha_M) - 2(\alpha_m - \alpha_M) \int_0^{2\pi} \cos(2z)^2 dz + 2\alpha_m \int_0^{2\pi} \cos(2z) \sqrt{-\sin(2z)^2 + \frac{\rho}{\alpha_m^2}} dz \\
&\quad - 2\alpha_M \int_0^{2\pi} \cos(2z) \sqrt{-\sin(2z)^2 + \frac{\rho}{\alpha_M^2}} dz \\
&= 4\pi(\alpha_m - \alpha_M) - 2(\alpha_m - \alpha_M)\pi = 2\pi(\alpha_m - \alpha_M) < 0,
\end{aligned}$$

as  $0 < \alpha_m < \alpha_M$ ,  $\int_0^{2\pi} \cos(2z)^2 dz = \left[ \frac{z}{2} + \frac{\sin(4z)}{8} \right]_0^{2\pi} = \pi$  and (see, for example, p. 423 in [3])

$$\begin{aligned}
\int_0^{2\pi} \cos(2z) \sqrt{-\sin(2z)^2 + \frac{\rho}{\alpha_m^2}} dz &= \frac{\sqrt{\rho}}{\alpha_m} \int_0^{2\pi} \cos(2z) \sqrt{1 - \frac{\alpha_m^2}{\rho} \sin(2z)^2} dz \\
&= \frac{\sqrt{\rho}}{\alpha_m} \left[ \frac{\sin(2z)}{4} \sqrt{1 - \frac{\alpha_m^2}{\rho} \sin(2z)^2} + \frac{\sin^{-1}\left(\frac{\alpha_m}{\sqrt{\rho}} \sin(2z)\right)}{4 \frac{\alpha_m}{\sqrt{\rho}}} \right]_0^{2\pi} = 0.
\end{aligned}$$

The same holds for the the integral involving  $\alpha_M$ .

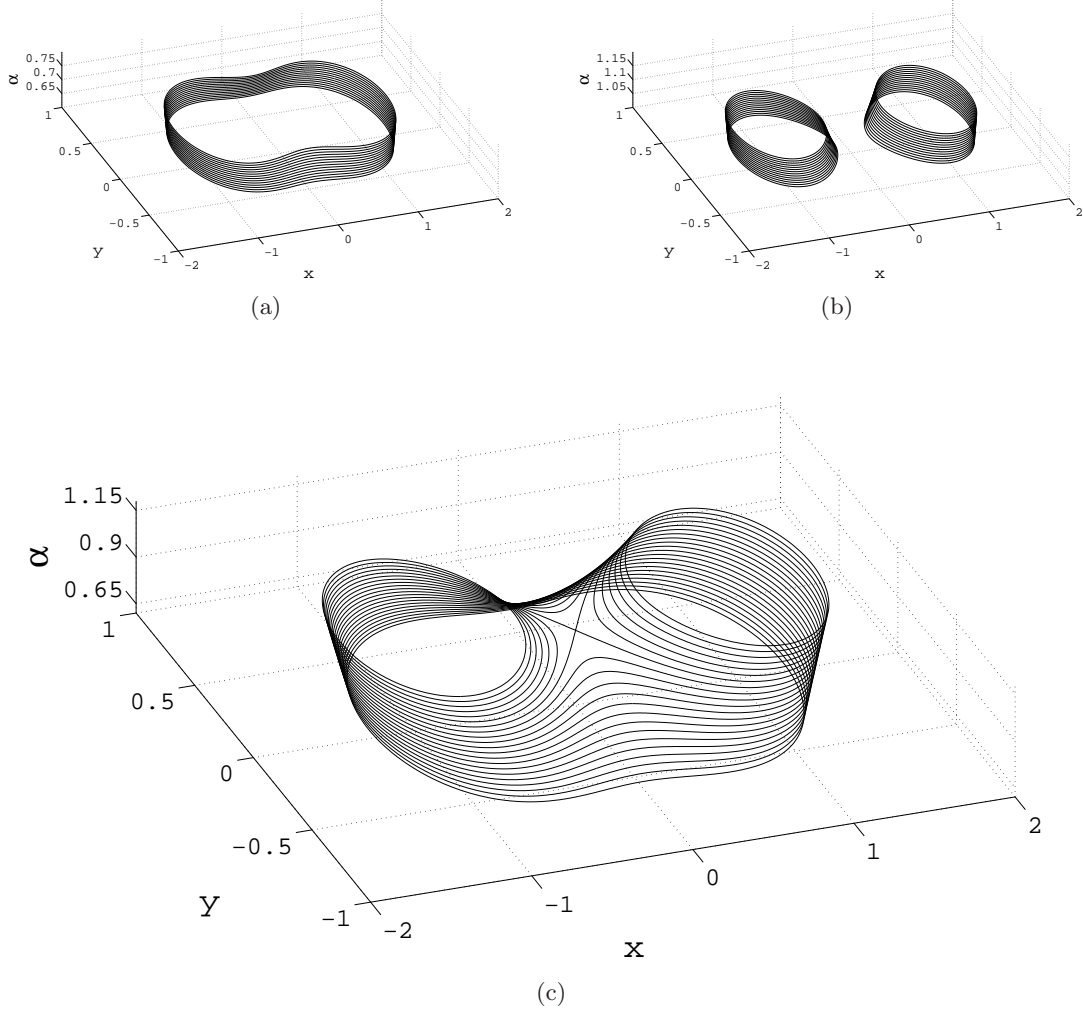


Fig. 3.5: The level surface  $\mathcal{S}_1$  with the CASSINI Hamiltonian  $H(x, y, \alpha) = ((x - \sqrt{\alpha})^2 + y^2)((x + \sqrt{\alpha})^2 + y^2)$  for  $\alpha$  ranging from 0.65 to 0.75 (Figure 3.5(a)), for  $\alpha$  ranging from 1.05 to 1.15 (Figure 3.5(b)) and for  $\alpha$  ranging from 0.65 to 1.15 (Figure 3.5(c)).

The network topology consists of a (3, All)-KC: three “Königsberg Clusters” and all edges are connected to a single vertex (c.f. Figure 3.7(c)). We choose the coupling strengths as  $c_k = 0.5$  for all  $k$  except for  $c_3 = c_7 = c_{11} = 0.05$  and  $c_{13} = 0.005$  and the susceptibility constants coincide with  $c_k$  except for  $s_{\alpha_{13}} = 0.0005$  (i.e.  $s_{\omega_k} = s_{\rho_k} = s_{\alpha_k} = c_k$  for all  $k$  and  $s_{\alpha_{13}} = 0.0005$ ). Vertices 3, 7 and 11 are those with four edges in each “Königsberg Cluster” and vertex 13 connects the clusters together. The initial conditions for **state variables**  $(x_k(0), y_k(0))$  are randomly uniformly distributed on  $]0, 0.1[^2$ . The initial conditions for the **parametric variables**  $(\omega_k(0), \rho_k(0), \alpha_k(0))$  are



randomly (uniform distribution) drawn from  $]0.98, 1.02[ \times ]0.99, 1.01[ \times ]0.65, 0.75[$ . The following coloring scheme is adopted: the green trajectories follow the MCD that are on the left “Königsberg Cluster”, in blue for those on the top cluster, in red for the right cluster and black is for the MCD on the middle vertex connecting all other vertices. The resulting dynamics is shown in Figure 3.6.

### MCD with two Attracting Sets

So far, we have always supposed that the attractor for each MCD is one closed curve. Here, we numerically investigate the case, when, for certain values of  $\rho$  and  $\alpha$ , the MCD exhibits two disjoint attracting sets. This is realized with the CASSINI type Hamiltonian when, for example,  $\rho = 1$  and  $\alpha > 1$  (and thus violating the condition for the parameters in Example 1.1). Figure 3.5(b) shows the surface level  $\mathcal{S}_1$  with the CASSINI Hamiltonian with  $1.05 \leq \alpha \leq 1.15$ . What is a simple connected surface in Figure 3.5(a), becomes a couple of closed ribbons in Figure 3.5(b). We first present numerical results when adaptation occurs only on the  $\rho_k$  (the  $\alpha_k$  being held fixed and common to all oscillators). Then we show numerical simulations when both,  $\rho_k$  and  $\alpha_k$ , are g-PV.

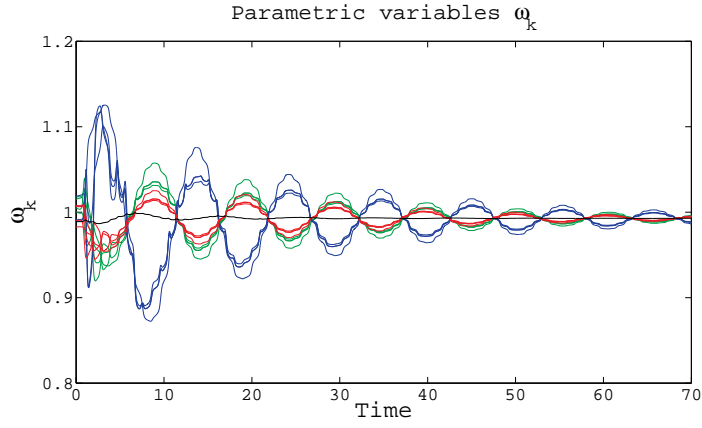
**Adapting  $\rho_k$ , fixed and common  $\alpha_k$**  - Consider five MCD systems having the same CASSINI Hamiltonian  $H(x, y; 1) = ((x - 1)^2 + y^2)((x + 1)^2 + y^2)$  (here  $\alpha$  is fixed, constant and common parameter, that is  $\alpha_k(t) = \mathbf{a} = 1$  for all  $t$ ). The network topology consists of a (1, One)-KC (one “Königsberg Cluster” connected to one vertex as in Figure 3.7(a)). We choose the coupling strengths as  $\mathbf{c}_k = 3$  for all  $k$  and the susceptibility constants as  $(\mathbf{s}_{\omega_1}, \dots, \mathbf{s}_{\omega_N}) = \mathbf{1s}(0.75, 3.5)$  and  $(\mathbf{s}_{\rho_1}, \dots, \mathbf{s}_{\rho_N}) = (1, 1, 1, 1, 0.01)$ . The initial conditions for **state variables**  $(x_k(0), y_k(0))$  are randomly uniformly distributed on  $] -0.1, 0.1]^2$ . The initial conditions for the **parametric variables**  $(\omega_k(0), \rho_k(0))$  are randomly (uniform distribution) drawn from  $]0.95, 1.05[ \times ]0.85, .95[$ , except for  $\omega_5(0) = 0.85$  and  $\rho_5(0) = 1.05$ .

Figure 3.9 shows the transient dynamics of the **state**  $(x_k)$  and **parametric variables**  $(\omega_k$  and  $\rho_k)$ . The initial  $\rho_k(0)$  for the first four oscillators (those on the “Königsberg Cluster”) are chosen such that their attractor is one of CASSINI’s ovals, while  $\rho_5(0) = 1.05$  is such that its attractor is simply connected (c.f. Figure 3.8). For  $t \in [0, 7]$ , there are no network interactions: oscillators converge towards their respective local attractor as shown in Figure 3.9(a) (two oscillators converge to the right oval, two to the left, and one on the closed curve (black trajectory)). At  $t = 7$ , **coupling** and **parametric dynamics** are switched on and, after a short transient, all oscillators are attracted by the left oval and ultimately to the single closed curve.

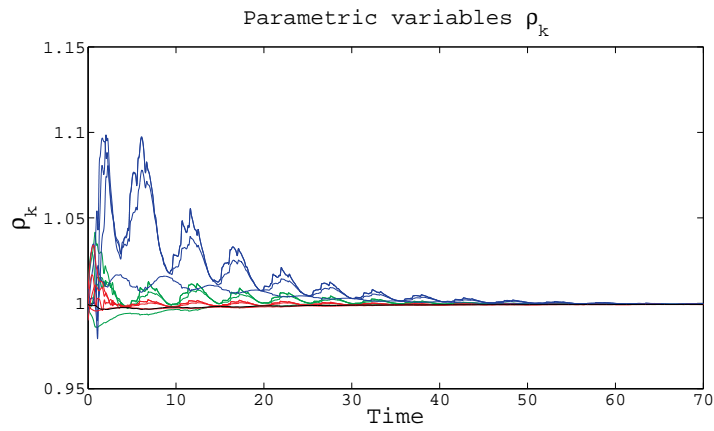
The fifth vertex has a small  $\mathbf{s}_{\rho_5}$  but a relative large  $\mathbf{s}_{\omega_5}$ . Thanks to the adaptive mechanism, it will attract the other  $\rho_k$  close to its value  $\rho_5(0) = 1.05$ , and hence all oscillators converge towards the single closed curve. Due to its *stubbornness* (i.e.  $\mathbf{s}_{\rho_5}$  is “small”),  $\rho_5(t)$  is barely perturbed by the rest of the network. However,  $\omega_k(t)$  is strongly influenced by the interactions (i.e.  $\mathbf{s}_{\omega_5}$  is “large”) - see black trajectory in Figures 3.9(b) and 3.9(c)).

**Adapting  $\rho_k$  and  $\alpha_k$**  - Consider 13 MCD systems with CASSINI’s Hamiltonian. We set the sign prefactor of the adaptive mechanism for  $\alpha_k$  as  $+$ . The network topology consists of a (3, All)-KC: three “Königsberg Clusters” and all edges are connected to a single vertex (c.f. Figure 3.7(c)). We choose the coupling strengths as  $\mathbf{c}_k = 0.5$  for all  $k$  except for  $\mathbf{c}_3 = \mathbf{c}_7 = \mathbf{c}_{11} = 0.05$  and  $\mathbf{c}_{13} = 0.005$  and the susceptibility constants are all one tenth of the *coupling strengths* (i.e.  $\mathbf{s}_{\omega_k} = \mathbf{s}_{\rho_k} = \mathbf{s}_{\alpha_k} = 0.1\mathbf{c}_k$  for all  $k$ ). The initial conditions for **state variables**  $(x_k(0), y_k(0))$  are randomly uniformly distributed on  $]0.07, 0.17[ \times ]0, 0.1[$  except for  $x_k(0)$ ,  $k \in \{3, 7, 11, 13\}$ , that are randomly uniformly distributed on  $] -0.3, -0.2[$ . This corresponds to the situation where the oscillators that are on vertices that are well connected (i.e. vertices with four edges in the “Königsberg Clusters” and the vertex connected to all other vertices) have initial conditions that are closer to the left CASSINI oval. These vertices also have relatively smaller coupling strengths and susceptibility constants. The initial conditions for the **parametric variables**  $(\omega_k(0), \rho_k(0), \alpha_k(0))$  are randomly (uniform distribution) drawn from  $]0.98, 1.02[ \times ]0.99, 1.01[ \times ]1.05, 1.15[$ . Figure 3.10 shows the transient dynamics of the 13 MCD systems with CASSINI type Hamiltonian having adaptivity on

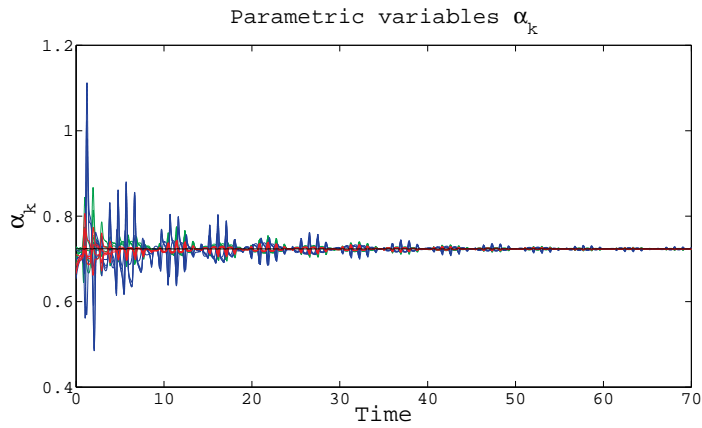




(a)



(b)



(c)

Fig. 3.6: Time evolution of the parametric variables  $\omega_k$ ,  $\rho_k$  and  $\alpha_k$  (Figures 3.6(a), 3.6(b) & 3.6(c)) for 13 CASSINI oscillators, interacting through a (3, All)-KC network. The coloring scheme is: green for MCD on the left cluster, blue for MCD on the top cluster, red for MCD on the right cluster and black for the MCD on the middle vertex.

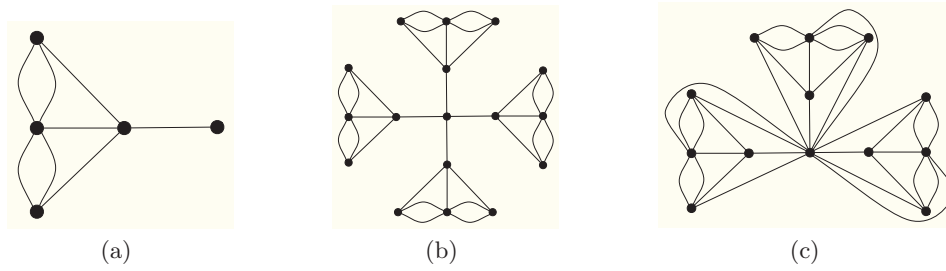


Fig. 3.7: A (1, One)-KC network topology (Figure 3.7(a)). Topology of a (4, One)-KC: four “Königsberg Clusters” connected by a single vertex (Figure 3.7(b)). One vertex connected to all vertices of all three “Königsberg Clusters”: (3, All)-KC (Figure 3.7(c)). The entries  $a_{k,j} = a_{j,k}$  of the adjacency matrices count the number of edges connecting vertex  $k$  with vertex  $j$  (i.e. two when there are two edges in the “Königsberg Clusters”).

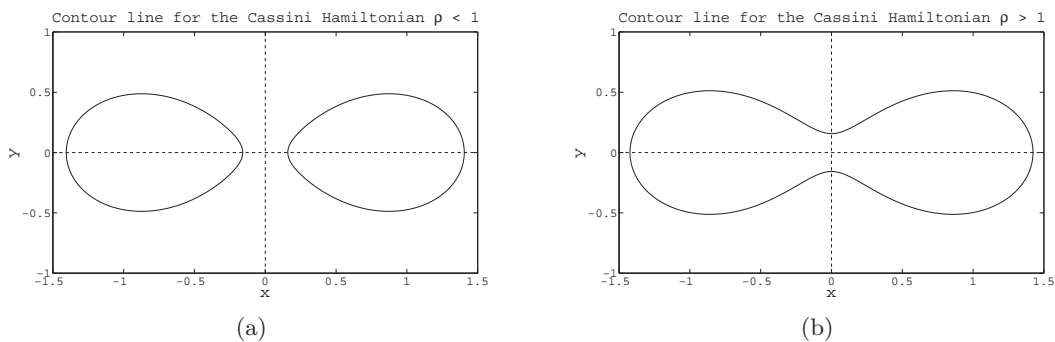


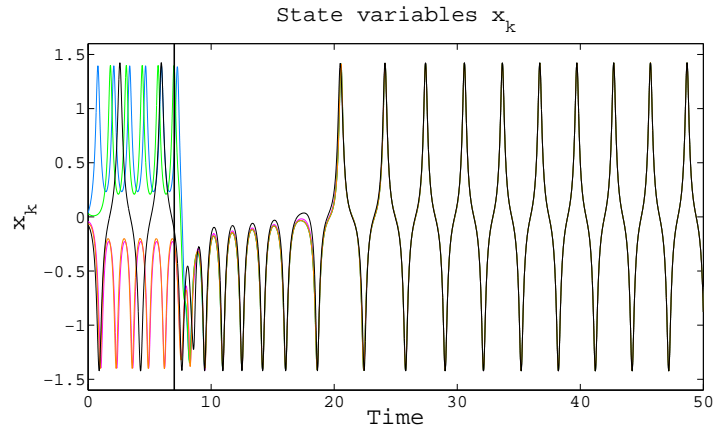
Fig. 3.8: Two contour lines for the Cassini Hamiltonian ( $H(x, y) = \rho$ ). Figure 3.8(a) shows two closed curves (here  $\rho = 0.95$ ) and Figure 3.8(b) shows one closed curve (here  $\rho = 1.05$ ).

$\rho_k$  and  $\alpha_k$  and when two attractors coexist.

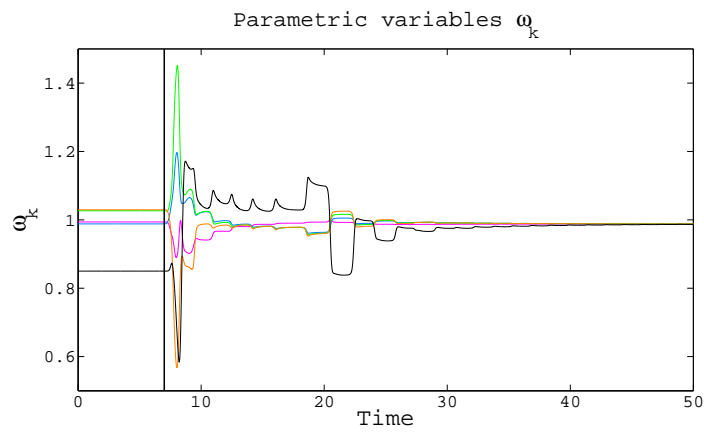
The above setting, was calculated for 100 numerical simulations. In most cases (here 87), the network converged to a consensual state as in Figure 3.10. However, in some cases (here 13), one oscillator (or several of them) located in one of the “Königsberg Clusters” was attracted to the right CASSINI oval. Out of the 13 cases where, 10 times did the network converge towards an apparently periodic state where the **parametric variables**  $\omega_k(t)$ ,  $\rho_k(t)$  and  $\alpha_k(t)$  no longer converged towards fixed and constant values but rather towards periodic functions. This is shown in Figure 3.11. In the remaining cases (i.e. 3 times), the dynamical system did not converge to an ordered state for the integration time (c.f. Figure 3.12).

For another set of 100 numerical simulations, the initial conditions for **state variables**  $x_k$  are shifted to the left (i.e. closer to the left attractor). More precisely,  $(x_k(0), y_k(0))$  are randomly uniformly distributed on  $]0, 0.1[^2$  except for  $x_k(0)$ ,  $k \in \{3, 7, 11, 13\}$ , that are randomly uniformly distributed on  $] -0.4, -0.3[$ . Here, for all the simulations, the network converged towards a consensual state as in Figure 3.10. Intuitively, the closer the initial conditions to an attractor (whether the right or the left CASSINI oval), the more probable the oscillators do converge to it.

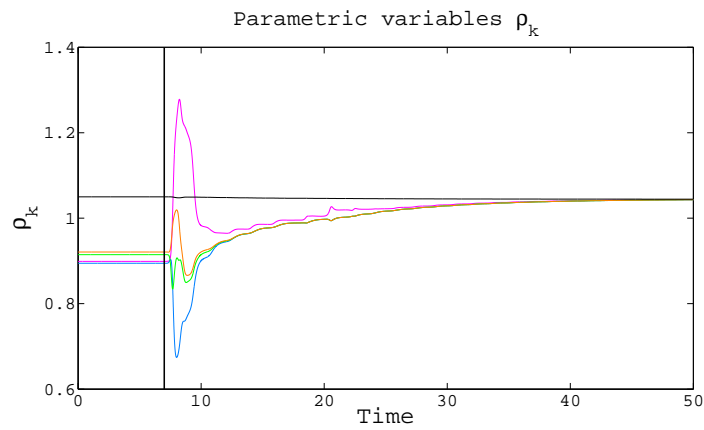
For arbitrary initial conditions, it is difficult to predict which attractor will be selected by the oscillators. To gain further insight, we proceeded to the following numerical experiment. Take two coupled MCD systems with CASSINI type Hamiltonian and choose the coupling strengths as  $c_1 = c_2 = 1$  and the susceptibility constants as  $s_{\omega_1} = s_{\omega_2} = 0.1$ . Each oscillator has  $\alpha_k$  as a single g-PV (i.e. the other **parametric variables** are constant -  $\omega_k(t) = \rho_k(t) = r = w = 1$  for all  $t$  and  $k = 1, 2$ ). Fix the initial conditions for the  $y$ -coordinate **state variables** as  $y_1(0) = y_2(0) = 0$  and



(a)

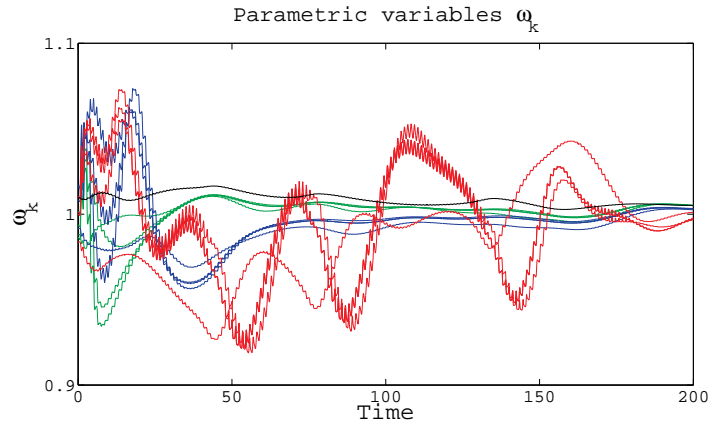


(b)

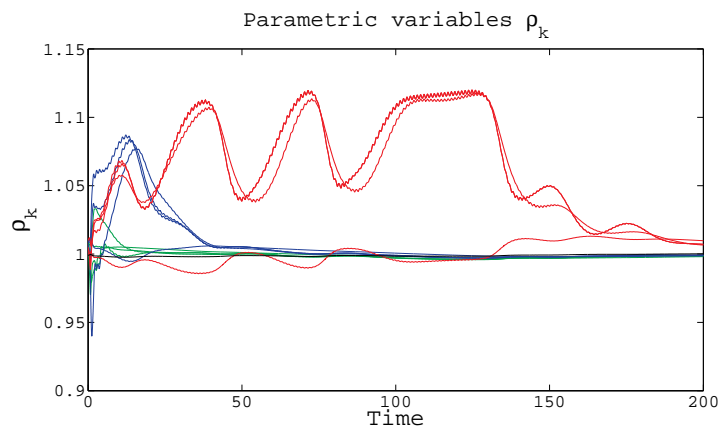


(c)

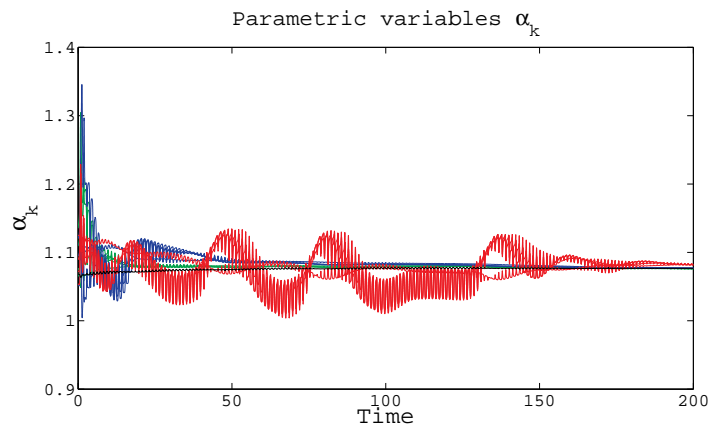
Fig. 3.9: Time evolution of the state variables  $x_k$  (Figure 3.9(a)) and the parametric variables  $\omega_k$  and  $\rho_k$  (Figures 3.9(b) & 3.9(c)) for five CASSINI oscillators, interacting through a (1, One)-KC network. Coupling and parametric dynamics are switched on at  $t = 7$  (black solid line).



(a)



(b)



(c)

Fig. 3.10: Time evolution of the parametric variables  $\omega_k$ ,  $\rho_k$  and  $\alpha_k$  (Figures 3.10(a), 3.10(b) & 3.10(c)) for 13 CASSINI oscillators, interacting through a (4, All)-KC network. The coloring scheme is: green for MCD on the left cluster, blue for MCD on the top cluster, red for MCD on the right cluster and black for the MCD on the middle vertex.

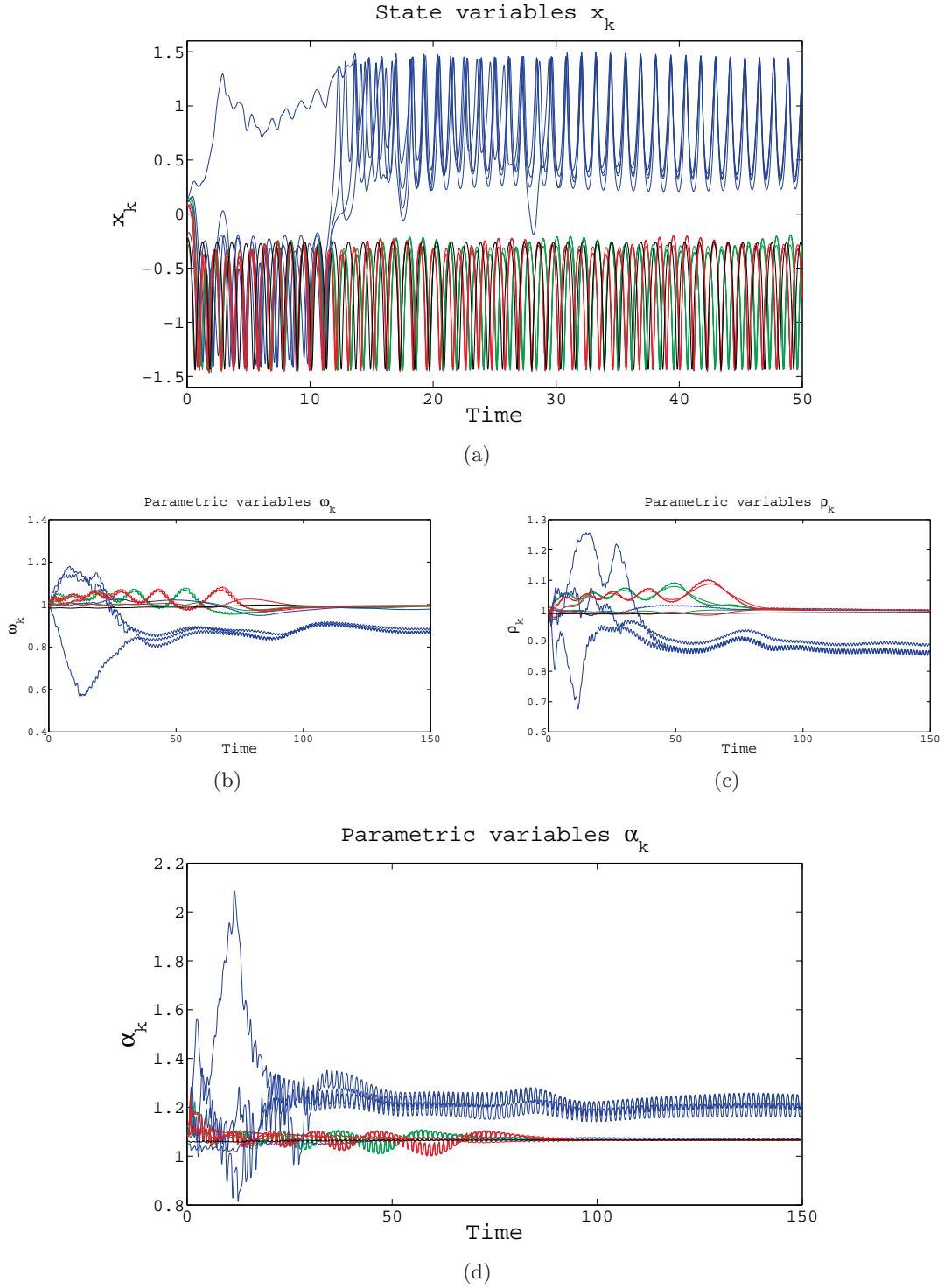


Fig. 3.11: Time evolution of the **state variables**  $x_k$  (Figure 3.11(a)) and **parametric variables**  $\omega_k$ ,  $\rho_k$  and  $\alpha_k$  (Figures 3.11(b), 3.11(c) & 3.11(d)) for 13 CASSINI oscillators, interacting through a (4, All)-KC network. The coloring scheme is: green for MCD on the left cluster, blue for MCD on the top cluster, red for MCD on the right cluster and black for the MCD on the middle vertex.

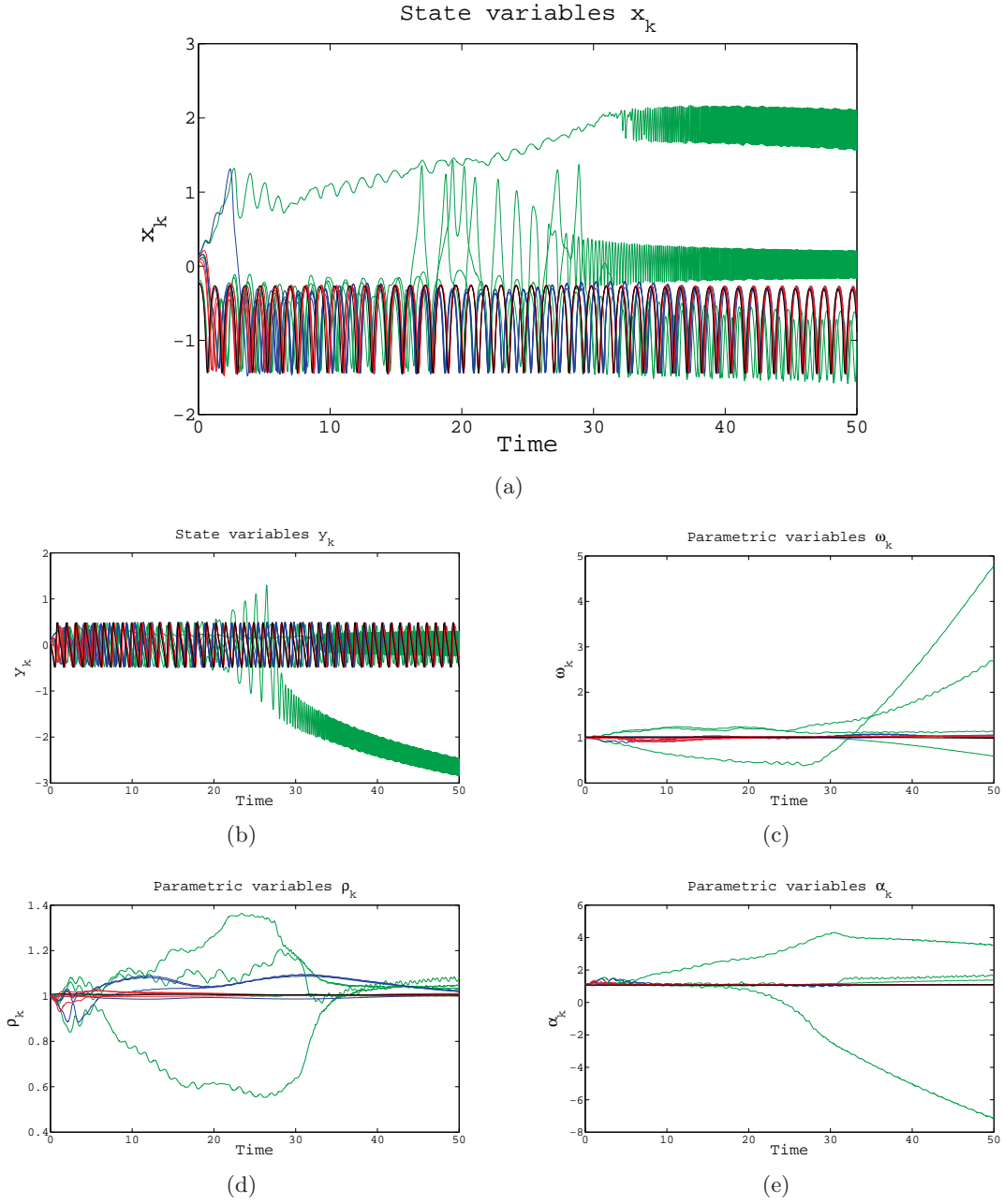


Fig. 3.12: Time evolution of the state variables  $x_k$  and  $y_k$  (Figures 3.12(a) & 3.12(b)) and parametric variables  $\omega_k$ ,  $\rho_k$  and  $\alpha_k$  (Figures 3.12(c), 3.12(d) & 3.12(e)) for 13 CASSINI oscillators, interacting through a (4, All)-KC network. The coloring scheme is: green for MCD on the left cluster, blue for MCD on the top cluster, red for MCD on the right cluster and black for the MCD on the middle vertex.

the initial conditions for the parametric variables as  $\alpha_1(0) = 1.005$  and  $\alpha_2(0) = 1.025$ . Then, in  $[-1.5, 1.5]^2$ , set up a grid where each side of the grid has 256 equidistant points in  $[-1.5, 1.5]$  (i.e.  $256 \times 256$  points). Each point in this grid is an initial condition for the state variables  $(x_1(0), x_2(0))$ . On that grid, place a black point if the two oscillators converge to the right CASSINI oval and a red point if both go to the left oval. For initial conditions where no consensual oscillatory state is reached (whether on the right or on the left attractor) place a grey point. The resulting picture of the grid is shown in Figure 3.13. Note that the grey points are very seldom. They are observed on the border of the two large black and red region.

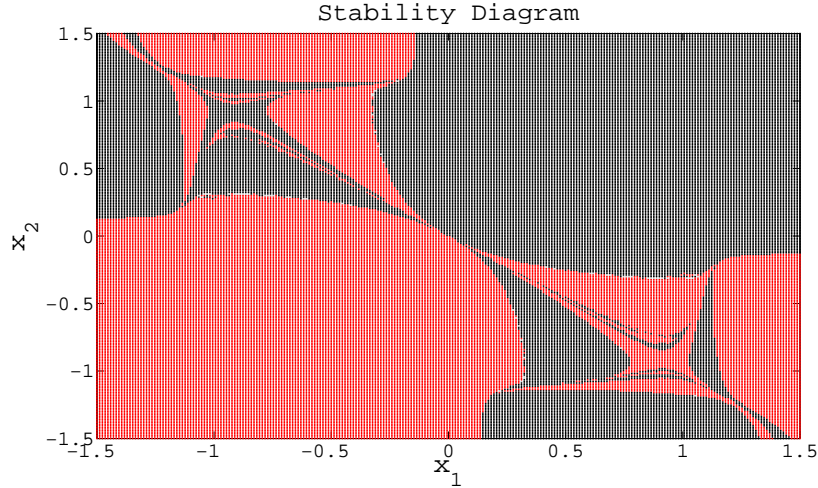


Fig. 3.13: Stability diagram showing which pair of  $x$ -coordinate initial conditions  $(x_1(0), x_2(0))$  (here  $y_1(0) = y_2(0) = 0$ ,  $\alpha_1(0) = 1.005$  and  $\alpha_2(0) = 1.025$ ) make two CASSINI oscillators converge either to a consensual oscillatory state on the right CASSINI oval (black points), to a consensual oscillatory state on the left CASSINI oval (red points) or when no consensual oscillatory state is reached (grey points). The grid consists of 256 equidistant points between  $-1.5$  and  $1.5$  for both sides.

The adaptive mechanism used in this numerical experiment is the one presented in Eqs. (3.9), namely

$$\dot{\alpha}_k = \frac{1}{10} \sum_{j=1}^N l_{k,j} \frac{\partial H}{\partial \alpha_j}(x_j, y_j, \alpha_j) = \frac{1}{10} \sum_{j=1}^N l_{k,j} 2(y_j^2 - x_j^2 + \alpha_j).$$

An identical investigation was repeated with a different adaptive mechanism. In the sum of the above adaptive mechanism, the terms  $2(y_j^2 - x_j^2)$  was used instead of  $2(y_j^2 - x_j^2 + \alpha_j)$  (i.e. the  $\alpha_j$  were taken out). It is interesting to remark that the same stability diagram is produced as in Figure 3.13 except that no grey points were observed.

### 3.3.3 MATHEWS-LAKSHMANAN Oscillators

Figure 3.15 shows the transient dynamics of 17 MCD systems with Hamiltonian given by  $H(x, y) = \log(\cosh(y)) + \frac{1}{2} \log(\alpha_k + x^2)$  and here  $\Gamma_k$  is reduced to a single parameter  $\alpha_k > 0$ . The sign in front of the adaptive mechanism for  $\alpha_k$  and  $\beta_k$  is  $+$ . To show this, we numerically calculated the value  $o$  of the integral in 3.8 with  $\alpha_m = 0.95$  and  $\alpha_M = 1.05$  and for different values of  $\rho$ , i.e. for parametrizations at different Hamiltonian levels  $\rho$ .

The network topology consists of a (4, One)-KC: four ‘‘Königsberg Clusters’’ connected by a single vertex (c.f. Figure 3.7(b)). We choose the coupling strengths as  $(c_1, \dots, c_N) = 1s(3.25, 0.8125, 17)$  and the susceptibility constants as  $(s_{\omega_1}, \dots, s_{\omega_N}) = 1s(0.25, 7.5, 17)$ ,

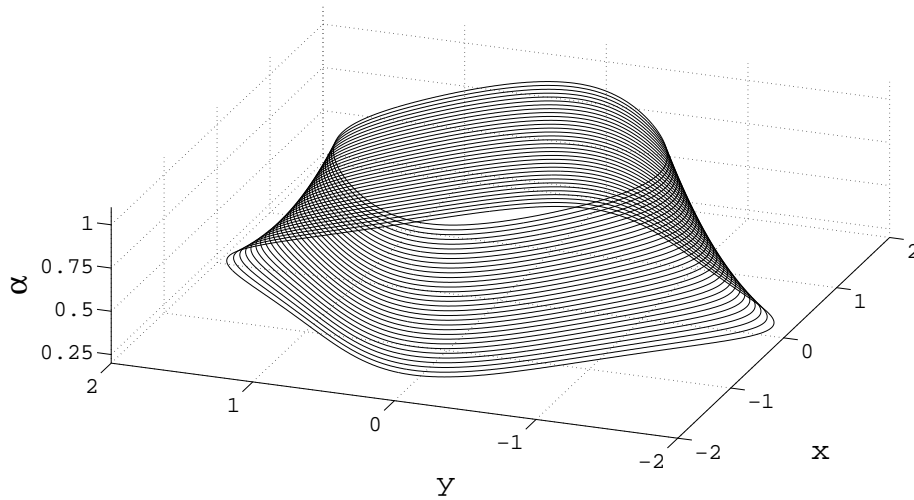


Fig. 3.14: The level surface  $\mathcal{S}_{0.55}$  with the MATHEWS-LAKSHMANAN Hamiltonian  $H(x, y, \alpha) = \log(\cosh(y)) + \frac{1}{2} \log(\alpha + x^2)$ ,  $\rho = 0.55$  and  $\alpha$  ranges from 0.25 to 1.05.

$(s_{\rho_1}, \dots, s_{\rho_N}) = \mathbf{1} + \mathbf{1s}(-1, 1, 17)^2$ ,  $(s_{\alpha_1}, \dots, s_{\alpha_N}) = \mathbf{2} - \mathbf{1s}(-1, 1, 17)^2$ . The initial conditions for **state variables**  $(x_k(0), y_k(0))$  are randomly uniformly distributed on  $] - 0.1, 0.1[^2$ . The initial conditions for the **parametric variables**  $(\omega_k(0), \rho_k(0), \alpha_k(0))$  are randomly (uniform distribution) drawn from  $]1, 3[ \times ]0.5, 0.6[ \times ]0.95, 1.05[$ . We choose the following coloring scheme: the green trajectories are for the MCD that are on the left “Königsberg Cluster”, in blue for those on the top cluster, in red for the right cluster, those in orange, for the bottom “Königsberg Cluster” and finally, black is for the MCD on the middle vertex connecting all other four clusters. The resulting dynamics is shown in Figure 3.15.



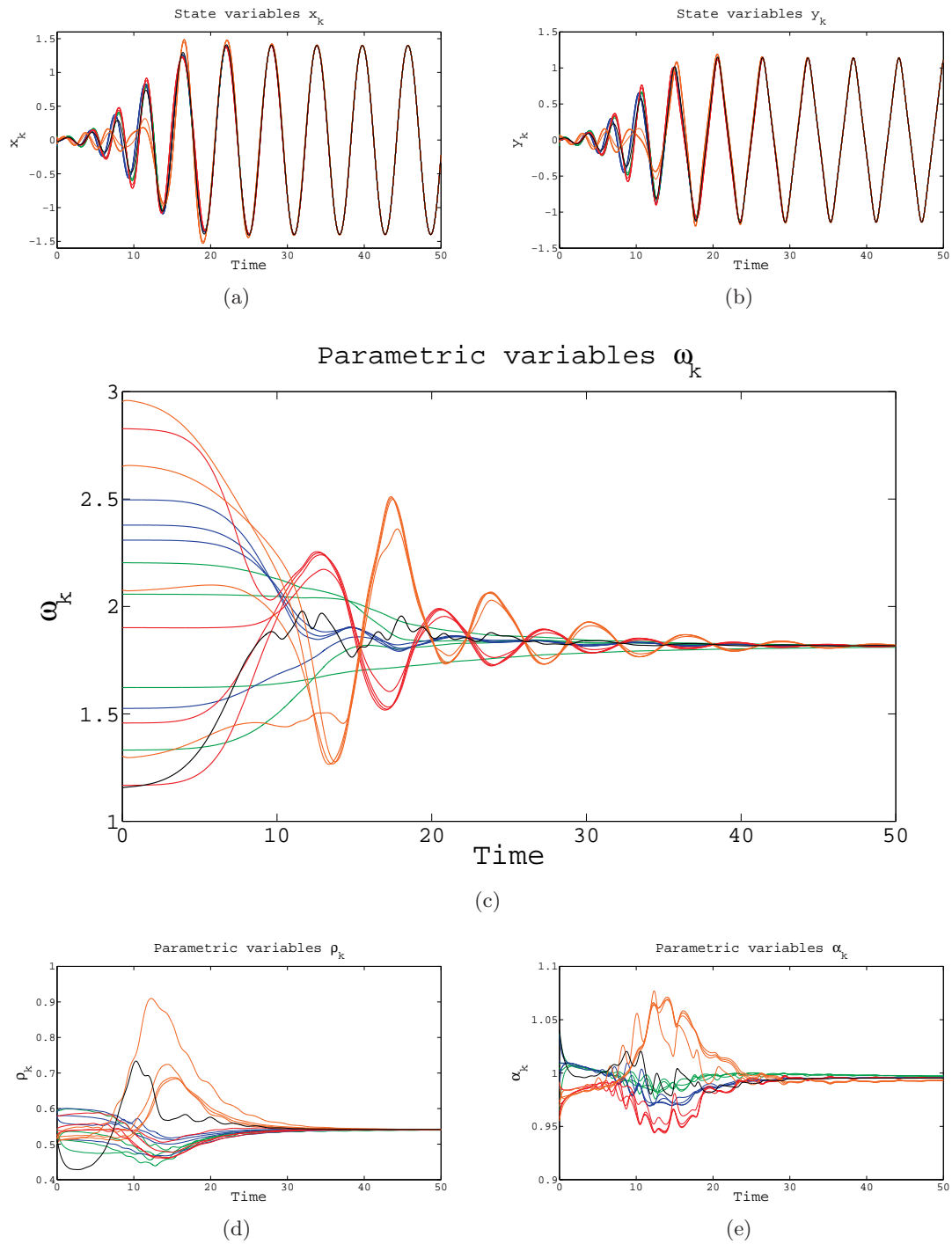


Fig. 3.15: Time evolution of the **state variables**  $x_k$  and  $y_k$  (Figures 3.15(a) & 3.15(b)) and the **parametric variables**  $\omega_k$ ,  $\rho_k$  and  $\alpha_k$  (Figures 3.15(c), 3.15(d) & 3.15(e)) for 17 MATHEWS-LAKSHMANAN oscillators, interacting through a (4, One)-KC network. The coloring scheme is: green for MCD on the left cluster, blue for MCD on the top cluster, red for MCD on the right cluster, orange for MCD on the bottom cluster and black for the MCD on the middle vertex.



# Networks of Mixed Canonical-Dissipative Systems with Adapting Coupling Weights

Et qui n'est, chaque fois, ni tout à fait la même

Ni tout à fait une autre, [...]

Paul VERLAINE

In this chapter, the complex dynamical system is composed of one  $N$ -vertex network with constant edges. The **local dynamics** are 2-dimensional belonging to the class of mixed canonical-dissipative (MCD) systems. The **coupling dynamics** is of a diffusive type (i.e. sum of Laplacian entries with coupling functions). Adaptation occurs in the **local dynamics** as well as in the **coupling dynamics**. Here, flow parameters as well as coupling weights are allowed to adapt but not the geometric parameters.

## 4.1 Network's Dynamical System

In this section, we detail the constituent parts that compose the global dynamics

$$\begin{aligned}
 \dot{x}_k &= \omega_k \frac{\partial H_k}{\partial y}(X_k; \Gamma_k) - \frac{\partial A_k}{\partial x}(X_k; \Gamma_k) - \underbrace{c_k \sum_{j=1}^N l_{k,j} \mu_j Q_{x_j}(X_j; \Gamma_j)}_{\text{coupling dynamics}} \\
 \dot{y}_k &= \underbrace{-\omega_k \frac{\partial H_k}{\partial x}(X_k; \Gamma_k) - \frac{\partial A_k}{\partial y}(X_k; \Gamma_k)}_{\text{local dynamics}} - \underbrace{c_k \sum_{j=1}^N l_{k,j} \nu_j Q_{y_j}(X_j; \Gamma_j)}_{\text{coupling dynamics}} \\
 \dot{\omega}_k &= -s_{\omega_k} \underbrace{\sum_{j=1}^N l_{k,j} \left\langle \begin{pmatrix} \mu_j R_{x_j}(X_j; \Gamma_j) \\ \nu_j R_{y_j}(X_j; \Gamma_j) \end{pmatrix} \middle| \begin{pmatrix} \mu_k R_{y_k}(X_k; \Gamma_k) \\ -\nu_k R_{x_k}(X_k; \Gamma_k) \end{pmatrix} \right\rangle}_{\text{parametric dynamics}} \quad k = 1, \dots, N. \\
 \dot{\mu}_k &= B_k^\mu(X, \mu, \nu) \\
 \dot{\nu}_k &= \underbrace{B_k^\nu(X, \mu, \nu)}_{\text{binding dynamics}}
 \end{aligned} \tag{4.1}$$

**Local Dynamics** Local systems belong to the class of MCD systems (refer to Section 4.1.1).

**Coupling Dynamics** A Laplacian matrix with **coupling functions** will characterize the **state variable interactions** (refer to Section 4.1.2).

**Binding Dynamics** The values of parameters controlling different network connections are themselves modified by **state variables interactions** (refer to Section 4.1.4).

**Parametric Dynamics** A generalized adaptive mechanism will determine the adaptivity of the **flow parametric variables** (refer to Section 4.1.3).

#### 4.1.1 Local Dynamics: $L_k$

The **local dynamics** belong to the class of mixed canonical-dissipative (MCD) systems as presented in Example (1.1) and for which we recall their dynamics

$$\begin{aligned} L_{k,1}(X_k; \Lambda_k) &:= \omega_k \frac{\partial H_k}{\partial y}(X_k; \Gamma_k) - (H_k(X_k; \Gamma_k) - r_k) \frac{\partial H_k}{\partial x}(X_k; \Gamma_k) \\ L_{k,2}(X_k; \Lambda_k) &:= \underbrace{-\omega_k \frac{\partial H_k}{\partial x}(X_k; \Gamma_k)}_{\text{canonical evolution}} - \underbrace{(H_k(X_k; \Gamma_k) - r_k) \frac{\partial H_k}{\partial y}(X_k; \Gamma_k)}_{\text{dissipative evolution}} \end{aligned} \quad k = 1, \dots, N, \quad (4.2)$$

where  $X_k = (x_k, y_k)$ ,  $\Lambda_k = \{\omega_k, \Gamma_k\}$  are, for the time being, fixed parameters where  $\omega_k$  (i.e. flow parameter) controls the angular velocity of the *canonical evolution* while the set  $\Gamma_k = \{r_k, \mathbf{g}_{k,1}, \dots, \mathbf{g}_{k,q_k-2}\} \in \mathbb{R}^{q_k-1}$  (i.e. geometric parameter) shapes the potential  $A(X; \Gamma_k) := \frac{1}{2}(H_k(X; \Gamma_k) - r_k)^2$  whose gradient is responsible for the *dissipative evolution*.

In accordance with Definition 1.1, **homogenous** MCD oscillators have the same Hamiltonian functional (i.e.  $H_k(\cdot; \Gamma_*) \equiv H_j(\cdot; \Gamma_*)$  for all  $k, j$  and  $\Gamma_*$ ) but the values of their parameters may be different. By definition, this implies that all **local dynamics** have the same number of parameters (i.e.  $|\Lambda_k| = |\Lambda_j|$  for all  $j, k$ ).

If the Hamiltonian functionals are not equal (i.e. there exists  $k, j, \Gamma_k$  and  $\Gamma_j$  such that  $H_k(\cdot; \Gamma_k) \not\equiv H_j(\cdot; \Gamma_j)$ ), **local dynamics** will be referred to as **heterogenous** MCD oscillators.

#### 4.1.2 Coupling Dynamics: $C_k$

As discussed in Section 1.1.2, here **local dynamics** are coupled together through a linear combination of coupling functions, that is

$$\begin{aligned} C_{k,1}(X; \Delta) &:= c_k \sum_{j=1}^N l_{k,j} u_j Q_{x_j}(X_j; \Gamma_j), \\ C_{k,2}(X; \Delta) &:= c_k \sum_{j=1}^N l_{k,j} v_j Q_{y_j}(X_j; \Gamma_j), \end{aligned}$$

where  $0 < c_k$  are strictly positive, fixed and constant, *coupling strengths*,  $l_{k,j}$  are the entries of  $L$ , a Laplacian matrix associated to a connected and undirected network with positive adjacency entries. For the time being  $u_k, v_k \in \Delta$  are fixed and constant **coupling weights**,  $\Gamma_k$  is the set of geometric parameters of the  $k^{th}$  Hamiltonian of the local dynamics and finally  $Q_x, Q_y$  are two **coupling functions** on  $\mathbb{R}^{2N}$  onto  $\mathbb{R}^N$ .

The coupling weights add an extra weight on the already defined weights  $a_{k,j}$  of  $A$ . These enable to break the symmetry of  $A$ . Indeed, one now may have  $a_{k,j} u_j \neq a_{j,k} u_k$  as in general  $u_j \neq u_k$ <sup>1</sup>. For identical  $u_k$ , the  $A$  symmetry is restored. This corresponds to a simple rescaling of the coupling strength  $c_k$ .

#### 4.1.3 Parametric Dynamics: $P_k$

Apart from Section 4.2.3, in this chapter, **local dynamics** will only adapt their flow parameters  $w_k$ . We generalize the **parametric dynamics** presented in Section 2.1.3.1. From now on,  $\omega_k$  are f-PV. As in Section 4.1.2, consider two **coupling functions**  $R_x, R_y$  on  $\mathbb{R}^{2N}$  onto  $\mathbb{R}^N$  with the f-PV adaptive mechanism

<sup>1</sup> The interacting factor of the  $k^{th}$  oscillator connected to the  $j^{th}$  is  $a_{k,j} u_j$  which is not necessarily equal to  $a_{j,k} u_k$ , the interacting factor of the  $j^{th}$  oscillator connected to the  $k^{th}$ , since, in general,  $u_k \neq u_j$ .

$$\dot{\omega}_k = -s_{\omega_k} \sum_{j=1}^N l_{k,j} \left( \mathbf{u}_j \mathbf{R}_{x_j}(X_j; \Gamma_j) \mathbf{v}_k \mathbf{R}_{y_k}(X_k; \Gamma_k) - \mathbf{v}_j \mathbf{R}_{y_j}(X_j; \Gamma_j) \mathbf{u}_k \mathbf{R}_{x_k}(X_k; \Gamma_k) \right),$$

where  $0 < s_{\omega_k}$  are strictly positive, fixed, *susceptibility constants* and  $l_{k,j}$  are the entries of  $L$  ( $L$  is the Laplacian matrix associated to the network considered in Section 4.1.2). Similar to Section 4.1.2,  $\mathbf{u}_k$  and  $\mathbf{v}_k$  are **coupling weights** and  $\Gamma_k$  is the set of parameters of the Hamiltonian of the  $k^{\text{th}}$  local system. As we have seen,

$$J_{\omega}(\omega_1, \dots, \omega_N) := \sum_{k=1}^N \frac{\omega_k}{s_{\omega_k}}, \quad (4.3)$$

is a constant of motion (refer to Lemma D.1, Appendix D).

We now present an explicit example of a network of heterogeneous MCD for which a consensual solution exists if the coupling functions are adequately chosen.

**Example 4.1. Network of HOPF (H) and MATHEWS-LAKSHMANAN (ML) MCD**

Consider a collection of  $N$  heterogeneous MCD composed of HOPF (H) and MATHEWS-LAKSHMANAN (ML) oscillators with respective potentials

$$\begin{aligned} \mathbf{A}_H(X; \Gamma_H) &:= \frac{1}{2}(x^2 + y^2 - r_H)^2, \\ \mathbf{A}_{ML}(X; \Gamma_{ML}) &:= \frac{1}{2}(\log(\cosh(y)) + \frac{1}{2} \log(\mathbf{a} + x^2) - r_{ML})^2, \end{aligned}$$

with  $\Gamma_H := \{r_H\}$  and  $\Gamma_{ML} := \{\mathbf{a}, r_{ML}\}$ . These parameters are chosen such that they satisfy  $r_H = \exp(2r_{ML}) - \mathbf{a}$ . For a given  $N$ -vertex network as in Section 4.1.2 with  $N$  vertices, let the first  $v$  vertices have H MCD and the  $N - v$  others have ML MCD. Define the coupling function for both, **coupling and parametric dynamics** as (we omit the parameters  $\Gamma_H$  and  $\Gamma_{ML}$ )

$$\begin{array}{ll} k = 1, \dots, v & n = v + 1, \dots, N \\ \mathbf{Q}_{x_k}(X) = \mathbf{R}_{x_k}(X) = x & \mathbf{Q}_{x_n}(X) = \mathbf{R}_{x_n}(X) = x \\ \mathbf{Q}_{y_k}(X) = \mathbf{R}_{y_k}(X) = y & \mathbf{Q}_{y_n}(X) = \mathbf{R}_{y_n}(X) = \exp(r_{ML}) \tanh(y). \end{array}$$

The network's dynamical system is, for  $k = 1, \dots, v$

$$\begin{aligned} \dot{x}_k &= \omega_k y_k - \frac{\partial \mathbf{A}_H}{\partial x}(X_k) - c_k \sum_{j=1}^N l_{k,j} x_j, \\ \dot{y}_k &= -\omega_k x_k - \frac{\partial \mathbf{A}_H}{\partial y}(X_k) - c_k S_k(y), \\ \dot{\omega}_k &= -s_{\omega_k} \left( \left( \sum_{j=1}^N l_{k,j} x_j \right) y_k - S_k(y) x_k \right), \end{aligned}$$

and for  $n = v + 1, \dots, N$

$$\begin{aligned} \dot{x}_n &= \omega_n \tanh(y_n) - \frac{\partial \mathbf{A}_{ML}}{\partial x}(X_n) - c_n \sum_{j=1}^N l_{n,j} x_j, \\ \dot{y}_n &= -\omega_n \frac{x_n}{\mathbf{a} + x_n^2} - \frac{\partial \mathbf{A}_{ML}}{\partial y}(X_n) - c_n S_n(y), \\ \dot{\omega}_n &= -s_{\omega_n} \left( \left( \sum_{j=1}^N l_{n,j} x_j \right) \exp(r_{ML}) \tanh(y_n) - S_n(y) x_n \right), \end{aligned}$$

with  $S_k(y) := \sum_{j=1}^v l_{k,j} y_j + \sum_{j=v+1}^N l_{k,j} \exp(r_{ML}) \tanh(y_j)$  and omitting the parameters  $\Gamma_H$  and  $\Gamma_{ML}$ .

Note that the system possesses the constant of motion in 4.3.

Despite of the strong heterogeneity in the local dynamics, we emphasize that the choice of the coupling functions allows the existence of a consensual oscillatory state. Indeed, we have

$$\begin{aligned}
x_k(t) &= \sqrt{r_H} \sin(\omega_H t) , \\
y_k(t) &= \sqrt{r_H} \cos(\omega_H t) , & k = 1, \dots, v , \\
\omega_k(t) &= \omega_H , \\
x_n(t) &= \sqrt{\exp(2r_{ML}) - a} \sin\left(\frac{\omega_{ML}}{\exp(r_{ML})} t\right) , \\
y_n(t) &= \tanh^{-1}\left(\frac{\sqrt{\exp(2r_{ML}) - a}}{\exp(r_{ML})} \cos\left(\frac{\omega_{ML}}{\exp(r_{ML})} t\right)\right) , & n = v + 1, \dots, N , \\
\omega_n(t) &= \omega_{ML} ,
\end{aligned}$$

where  $\omega_H := \frac{\omega_{ML}}{\exp(r_{ML})}$  and  $\omega_{ML}$  is a given constant. For given initial  $\omega_k(0)$  ( $k = 1, \dots, N$ ) and supposing the system converges to this consensual state, the consensual  $\omega_{ML}$  is analytically determined. The constant of motion implies

$$\sum_{k=1}^N \frac{\omega_k(0)}{s_{\omega_k}} = \sum_{k=1}^v \frac{\omega_k(t)}{s_{\omega_k}} + \sum_{n=v+1}^N \frac{\omega_n(t)}{s_{\omega_n}} \quad \forall t \geq 0$$

and since we suppose that  $\lim_{t \rightarrow \infty} \omega_k(t) = \omega_H$  and  $\lim_{t \rightarrow \infty} \omega_n(t) = \omega_{ML}$  and here  $\omega_H = \frac{\omega_{ML}}{\exp(r_{ML})}$ , then, asymptotically, we have

$$\begin{aligned}
\sum_{k=1}^N \frac{\omega_k(0)}{s_{\omega_k}} &= \omega_H \sum_{k=1}^v \frac{1}{s_{\omega_k}} + \omega_{ML} \sum_{n=v+1}^N \frac{1}{s_{\omega_n}} = \frac{\omega_{ML}}{\exp(r_{ML})} \sum_{k=1}^v \frac{1}{s_{\omega_k}} + \omega_{ML} \sum_{n=v+1}^N \frac{1}{s_{\omega_n}} \\
&= \omega_{ML} \left( \exp(-r_{ML}) \sum_{k=1}^v \frac{1}{s_{\omega_k}} + \sum_{n=v+1}^N \frac{1}{s_{\omega_n}} \right)
\end{aligned}$$

and so

$$\omega_{ML} = \frac{\sum_{k=1}^N \frac{\omega_k(0)}{s_{\omega_k}}}{\exp(-r_{ML}) \sum_{k=1}^v \frac{1}{s_{\omega_k}} + \sum_{n=v+1}^N \frac{1}{s_{\omega_n}}} .$$

In Example 4.1, the coupling functions  $Q_{y_n}$  and  $R_{y_n}$  for  $n = v + 1, \dots, N$  are defined with a factor  $\exp(r_{ML})$ . This factor is necessary for the existence of the consensual oscillatory state. This factor can alternatively be interpreted as a coupling weight since one can define  $u_k := 1$  for  $k = 1, \dots, v$ ,  $\nu_n := \exp(r_{ML})$  for  $n = v + 1, \dots, N$ . One may now raise the question: if the coupling weights are not exactly set for the consensual state to exist, can one introduce adaptive mechanisms on the coupling weights such that they adapt in order to drive the network to a consensual oscillatory state?

In response to the last question, we now present a network adaptation obtained by the **binding dynamics** and occurring in the **coupling dynamics**.

#### 4.1.4 Binding Dynamics: $B_k$

In this chapter, adaptation in the **coupling dynamics** concerns the coupling weights  $w_k$ . As discussed in Section 1.2.1, we let the fixed and constant  $\mu_k$  and  $\nu_k$  become time-dependent, that is

$$\{\mathbf{u}_k, \mathbf{v}_k\} \rightsquigarrow (\mu_k(t), \nu_k(t)) .$$

Their rate of change  $\dot{\mu}_k$  and  $\dot{\nu}_k$  are determined by the **binding dynamics**  $B \equiv (B^\mu, B^\nu) \equiv (B_1^\mu, \dots, B_N^\mu, B_1^\nu, \dots, B_N^\nu)$ . In general,  $B$  is a function of  $X = (X_1, \dots, X_N)$ ,  $\mu = (\mu_1, \dots, \mu_N)$  and  $\nu = (\nu_1, \dots, \nu_N)$ , responsible for the interactions of  $\mu_k$  and  $\nu_k$ . Similar to the **coupling** and

**parametric dynamics**, these interactions occur via the connected and undirected network with positive adjacency entries that is considered in Section 4.1.2. By introducing the **binding dynamics**,  $\mu_k$  and  $\nu_k$  acquire the status of variables of the global dynamical system and are known as **coupling parametric variables (c-PV)**.

The functions  $B^\mu$  and  $B^\nu$  must fulfill the objectives presented in Section 1.2.5. By doing so, time-dependent coupling weights  $(\mu_k(t), \nu_k(t))$  ultimately converge towards constants (i.e.  $\lim_{t \rightarrow \infty} (\mu_k(t), \nu_k(t)) = (\bar{\mu}_k, \bar{\nu}_k)$  for  $k = 1, \dots, N$ ). Note that coupling weights do not necessarily all converge to a common value. In general, it is preferable to have coupling weights with different values. Indeed, the network may consist of heterogeneous MCD (or homogeneous MCD with different valued parameters) or the coordinates of coupling functions may be of different types (e.g. some of the Identity type, some of the Gradient type, etc). Therefore, by adjusting the values of the coupling weights, each vertex  $k$  can adjust its output signal  $(Q_{x_k}(X; \Psi), Q_{y_k}(X; \Psi))$  in order to increase the likelihood for the emergence of some desired asymptotic behavior.

We now present different types of **binding dynamics**. We first focus on the case when the c-PV  $\mu$  and  $\nu$  have the same coordinates (i.e.  $\mu_k = \nu_k$  for all  $k$ ). Here, we exhibit three types of **binding dynamics**. We then consider the case when the c-PV  $\mu$  and  $\nu$  do not have the same coordinates (i.e.  $\mu_k \neq \nu_k$  for all  $k$ ). Here, we present one type of **binding dynamics**.

#### Same $\mu$ and $\nu$ ( $\mu_k = \nu_k$ for all $k$ )

Inspired by the **parametric dynamics** for  $\rho_k$  in Eq. (3.3), we define the type of **binding dynamics** for  $\mu_k$  as

$$\dot{\mu}_k = s_{\mu_k} \sum_{j=1}^N l_{k,j} H_j(X_j; \Gamma_j), \quad (4.4)$$

where  $0 < s_{\mu_k}$  are strictly positive, fixed, *susceptibility constants* and  $l_{k,j}$  are the entries of  $L$ . As we have seen,

$$J_\mu(\mu_1, \dots, \mu_N) := \sum_{k=1}^N \frac{\mu_k}{s_{\mu_k}}$$

is a constant of motion (refer to Lemma D.1, Appendix D). Observe that Eqs. (4.4) exhibits a similar adaptive mechanism to the **vertex-based strategy** in [12]. This second type of **binding dynamics** reads

$$\dot{\mu}_k = s_{\mu_k} \left\| \sum_{j=1}^N l_{k,j} H(X_j) \right\|,$$

with  $H$  an output function. However, for this last dynamics, we do not have the constant of motion  $J_\mu$ . In Eqs. (4.4), we note that while depending on  $X_j$ ,  $H_j$  and  $\Gamma_j$ , it does not depend on the c-PV  $\mu_j$ . Hence, another type (the third one) of **binding dynamics** is

$$\dot{\mu}_k = -s_{\mu_k} \sum_{j=1}^N l_{k,j} \mu_j^2 (x_j^2 + y_j^2). \quad (4.5)$$

leading to the existence of the constant of motion  $J_\mu$ . Note that in Eqs. (4.5) the term  $(x_j^2 + y_j^2)$  can be replaced by any other positive function. This is also the case for Eqs. (4.4) where any other positive functional can play the role of the Hamiltonian  $H_j$ .

#### Different $\mu$ and $\nu$ ( $\mu_k \neq \nu_k$ for all $k$ )

Based on Eqs. (4.5), we define the **binding dynamics** as (c-PV are given for the  $x$  and  $y$ -coordinates)

$$\dot{\mu}_k = -s_{\mu_k} \sum_{j=1}^N l_{k,j} \mu_j^2 x_j^2 \quad \text{and} \quad \dot{\nu}_k = -s_{\nu_k} \sum_{j=1}^N l_{k,j} \nu_j^2 y_j^2. \quad (4.6)$$

where  $0 < s_{\nu_k}$  are strictly positive, fixed, *susceptibility constants* and, as the other **binding dynamics**, we have the following constant of motion

$$J_{\nu}(\nu_1, \dots, \nu_N) := \sum_{k=1}^N \frac{\nu_k}{s_{\nu_k}}.$$

## 4.2 Dynamics of the Network

In this section we first consider a network of homogeneous local systems with **binding dynamics** characterized by Eq. (4.4) (i.e. c-PV independent). We then discuss the dynamics of a network of heterogeneous local **dynamics** that share an identical limit cycle with **binding dynamics** characterized by Eq. (4.5) (i.e. c-PV dependent). We show a particular case where two c-PV may be introduced (refer to Section 4.2.2). Finally, we go beyond the frame of this chapter and present a network of oscillators with all the three types of adaptation (refer to Section 4.2.3).

### 4.2.1 Homogeneous Case with c-PV independent Binding Dynamics

In this Section, we consider homogeneous MCD. We suppose that the value of the parameters in  $\Gamma_k$  are fixed and common to all Hamiltonian except for  $r_k$ , whose value is fixed but node dependent (i.e.  $\{\mathbf{g}_{k,1}, \dots, \mathbf{g}_{k,q-2}\} = \{\mathbf{g}_{j,1}, \dots, \mathbf{g}_{j,q-2}\}$  for all  $k, j$  and  $r_k$  may be different). We also suppose the Hamiltonians to be  $r$ -independent (i.e.  $\frac{\partial H}{\partial r} \equiv 0$ ). We refrain from explicitly writing the parameters  $\Gamma_k$ . For the **coupling dynamics**, the coupling functions are of the Gradient type coupling functions and Identity for the **parametric dynamics**. Here, the c-PV  $\mu$  and  $\nu$  have the same coordinates (i.e.  $\mu_k = \nu_k$  for all  $k$ ) and Eqs. (4.4) are chosen for the **binding dynamics**. The global dynamics is

$$\begin{aligned} \dot{x}_k &= \omega_k \frac{\partial H}{\partial y}(X_k) - (H(X_k) - r_k) \frac{\partial H}{\partial x}(X_k) - c_k \sum_{j=1}^N l_{k,j} \mu_j \frac{\partial H}{\partial x}(X_j) . \\ \dot{y}_k &= -\omega_k \frac{\partial H}{\partial x}(X_k) - (H(X_k) - r_k) \frac{\partial H}{\partial y}(X_k) - c_k \sum_{j=1}^N l_{k,j} \mu_j \frac{\partial H}{\partial y}(X_j) . \\ \dot{\omega}_k &= -s_{\omega_k} \sum_{j=1}^N l_{k,j} (x_j y_k - y_j x_k) . \\ \dot{\mu}_k &= s_{\mu_k} \sum_{j=1}^N l_{k,j} H(X_j) . \end{aligned} \quad k = 1, \dots, N . \quad (4.7)$$

Let us emphasize that Eqs. (4.7) has two constant of motions

$$J_{\omega}(\omega_1, \dots, \omega_N) = \sum_{j=1}^N \frac{\omega_j}{s_{\omega_j}}, \quad J_{\mu}(\mu_1, \dots, \mu_N) = \sum_{j=1}^N \frac{\mu_j}{s_{\mu_j}} . \quad (4.8)$$

When  $s_{\mu_k} = 0$  (with  $\mu_k(0) = 1$ ), then, because of the heterogeneity in the Hamiltonian heights (i.e.  $r_k$ ), it is, in general, not possible for the network to fully synchronize (i.e.  $X_j(t) = X_k(t)$  for all  $k$  and  $j$ ). However, by introducing the c-PV  $\mu_k$ , the **coupling dynamics** itself changes. This opens the possibility for the network to reach a synchronized oscillatory state. In this asymptotic regime, one has

$$\begin{aligned} \lim_{t \rightarrow \infty} \|X_k(t) - \varphi_c(t)\| &= 0 \quad \forall k \quad \text{and} \quad \varphi_c(t) \quad \text{is periodic and defined bellow in 4.10,} \\ \text{and, for } k = 1, \dots, N, \quad \lim_{t \rightarrow \infty} (\omega_k(t), \mu_k(t)) &= (\omega_c, \bar{\mu}_k) \quad \text{with constants } \omega_c \text{ and } \bar{\mu}_k \text{ (for all } k\text{).} \end{aligned} \quad (4.9)$$

It is important to note that this state, once reached, is not permanent. That is, if interactions are switched off (i.e.  $L = \mathbf{0}$ ), **local dynamics** will converge towards the attractor that is given by their own Hamiltonian height (i.e.  $\mathcal{L}_{r_k} = \{X \in \mathbb{R}^2 \mid H(X) = r_k\}$ ). On the other hand, the **parametric**



variables  $\omega_k$  remain at their asymptotic value  $\omega_c$  (if the switching off takes place after the system converged). Since the frequency of a MCD oscillator is, in general, amplitude dependent (i.e. depends on  $r_k$ ), each MCD oscillate at its own frequency modulated by the factor  $\omega_c$ . However, this is not the case for HOPF oscillators (i.e. frequency of oscillation is independent of  $r_k$ ) which will continue to oscillate with the same frequency but each local system will regain its natural amplitude. Hence, one may speak off a “semi-consensual” state since the common dynamical pattern is not fully destroyed once connections are removed<sup>2</sup>. We now discuss the existence of a synchronized oscillatory state and the convergence towards it.

### Existence of a synchronized oscillatory state

The dynamical system defined by Eqs. (4.7) admits the periodic solution

$$\varphi_c(t), \quad \omega(t) = \omega_c \quad \text{and} \quad \mu_k(t) = \bar{\mu}_k \quad \forall k, \quad (4.10)$$

where, for all  $k$ ,  $\varphi_c(t) = (\varphi_x(t), \varphi_y(t))$  is the solution of the canonical part of the MCD with  $\omega_c$  a given constant and with initial conditions on  $\mathcal{L}_{\bar{r}}$  (i.e.  $X_0 = (x_0, y_0) \in \mathcal{L}_{\bar{r}} = \{X \in \mathbb{R}^2 \mid \mathbf{H}(X) = \bar{r}\}$ ) with

$$\bar{r} := \frac{\sum_{j=1}^N \frac{r_j}{c_j}}{\sum_{j=1}^N \frac{1}{c_j}}, \quad (4.11)$$

and, finally,  $\bar{\mu} = (\bar{\mu}_1, \dots, \bar{\mu}_N)$  a constant vector satisfying the equation

$$L\mu = b, \quad (4.12)$$

where  $b = D^{-1}(r - \bar{r}\mathbf{1})$  with diagonal matrix  $D^{-1}$  with  $c_k^{-1}$  on its diagonal,  $r = (r_1, \dots, r_N)$  and  $\mathbf{1}$  is a  $N$  dimensional vector of 1. A solution to Eq. (4.12) exists since

$$\exists \mu \quad \text{such that} \quad L\mu = b \quad \iff \quad b \in \text{Im}(L) \quad \iff \quad \langle b \mid u\mathbf{1} \rangle = 0 \quad \forall u$$

and this scalar product is equivalent to defining 4.11.

Let us verify the solution. We first start with the fact that  $\varphi_k(t) = \varphi_j(t)$  for all  $k$  and  $j$  and so  $\dot{\omega}_k(t) = 0$  for all  $k$ . Secondly,  $\mathbf{H}(\varphi_k(t)) = \bar{r}$  for all  $k$  implying  $\dot{\mu}_k(t) = 0$  for all  $k$ . Hence, f-PV and c-PV have a constant evolution:

- $\omega_k(t) = \omega_k(0)$  for all  $t$  and the initial conditions are chosen to be common to all oscillators (i.e.  $\omega_k(0) := \omega_c$  for all  $k$  and there are no constraints on the actual value of  $\omega_c$ ),
- $\mu(t) = (\mu_1(t), \dots, \mu_N(t)) = \mu(0)$  for all  $t$  and the initial conditions  $\mu(0) := \bar{\mu}$  are chosen such that  $\bar{\mu}$  satisfy Eqs. (4.12).

Since  $\varphi_k(t)$  solves only the canonical part of the MCD, then the rest of the vector field in Eqs. (4.7) must be zero, that is, for all  $k$ ,

$$\begin{aligned} -(u - r_k) \frac{\partial \mathbf{H}}{\partial x}(\varphi_k(t)) - c_k \sum_{j=1}^N l_{k,j} \mu_j \frac{\partial \mathbf{H}}{\partial x}(\varphi_k(t)) &= 0, \\ -(u - r_k) \frac{\partial \mathbf{H}}{\partial y}(\varphi_k(t)) - c_k \sum_{j=1}^N l_{k,j} \mu_j \frac{\partial \mathbf{H}}{\partial y}(\varphi_k(t)) &= 0. \end{aligned}$$

For both coordinates  $x$  and  $y$ , we have, in matrix notation,  $-(\bar{r}\mathbf{1} - r) - DL\mu = \mathbf{0}$  which is Eq. (4.12) and this concludes the verification of the solution.

<sup>2</sup> Note that in this particular case (i.e. network with HOPF oscillators), a “semi-consensual” state may be reached without the **binding dynamics**.

### Convergence towards a synchronized oscillatory state

**Convergence** - Here, the complexity of the resulting linearized system precludes, as far as we are aware, to get analytical results for the convergence in 4.9.

**Limit Values** - If 4.9 holds, then the values  $\omega_c$  and  $\bar{\mu}$  are analytically expressed as

$$\omega_c = \frac{\sum_{j=1}^N \frac{\omega_j(0)}{s_{\omega_j}}}{\sum_{j=1}^N \frac{1}{s_{\omega_j}}} \quad \bar{\mu} = \begin{pmatrix} \hat{L} \\ 1/s_{\mu} \end{pmatrix}^{-1} \begin{pmatrix} \hat{b} \\ \mathbf{C} \end{pmatrix}.$$

where  $\hat{L}$  is  $L$  without its last line (i.e. an  $(N-1) \times N$  matrix),  $1/s_{\mu} = (\frac{1}{s_{\mu_1}} \dots \frac{1}{s_{\mu_N}})$ ,  $\hat{b}$  is  $b$  without its last coordinate (i.e. an  $(N-1)$  dimensional vector) and  $\mathbf{C} = \sum_{j=1}^N \frac{\mu_j(0)}{s_{\mu_j}}$ .

The first equality is a direct consequence of the constant of motion  $J_{\omega}$  in 4.8 which implies that

$$\sum_{j=1}^N \frac{\omega_j(t)}{s_{\omega_j}} = \sum_{j=1}^N \frac{\omega_j(0)}{s_{\omega_j}} \quad \forall t$$

and because  $\lim_{t \rightarrow \infty} \omega_j(t) = \omega_c$  for all  $j$ , then

$$\lim_{t \rightarrow \infty} \sum_{j=1}^N \frac{\omega_j(t)}{s_{\omega_j}} = \sum_{j=1}^N \frac{\omega_c}{s_{\omega_j}} = \sum_{j=1}^N \frac{\omega_j(0)}{s_{\omega_j}} \iff \omega_c = \frac{\sum_{j=1}^N \frac{\omega_j(0)}{s_{\omega_j}}}{\sum_{j=1}^N \frac{1}{s_{\omega_j}}}.$$

The second equality comes from the fact that  $\bar{\mu}$  solves Eq. (4.12) and due to  $J_{\mu}$  in 4.8, then  $\bar{\mu}$  must solve the overdetermined system ( $N+1$  equations,  $N$  unknowns)

$$\begin{pmatrix} L \\ 1/s_{\mu} \end{pmatrix} \mu = \begin{pmatrix} b \\ \mathbf{C} \end{pmatrix}. \quad (4.13)$$

Removing the  $N^{th}$  equation in System 4.13 (i.e. the last line of  $L$ ) leads to a system of equations with matrix

$$\begin{pmatrix} \hat{L} \\ 1/s_{\mu} \end{pmatrix}.$$

This last matrix is invertible because summing a linear combination of its rows gives

$$\sum_{k=1}^{N-1} \nu_k l_k + \nu_N 1/s_{\mu} = \mathbf{0} \implies \sum_{k=1}^{N-1} \underbrace{(\nu_k l_{k,k} + \nu_k \sum_{j \neq k} l_{k,j})}_{=0} + \nu_N \sum_{k=1}^N \frac{1}{s_{\mu_k}} = 0 \implies \nu_N = 0,$$

where  $l_j = (l_{j,1}, \dots, l_{j,N})$  is the  $j^{th}$  line of the symmetric matrix  $L$ . Since  $L$  has rank  $N-1$  (Laplacian matrix associated to a connected network) then  $\nu_1 = \dots = \nu_{N-1} = 0$ . Hence, one determines  $\bar{\mu}$ .

#### 4.2.2 Heterogenous Case with c-PV dependent Binding Dynamics

In this Section, we consider a collection of heterogeneous MCD. The parameters  $\Gamma_k$  of each Hamiltonian are fixed and constant and we will not be explicitly written. For the **coupling** and **parametric dynamics**, the coupling functions are of the Identity type. Here, again, the c-PV  $\mu$  and

$\nu$  have the same coordinates (i.e.  $\mu_k = \nu_k$  for all  $k$ ). However, here Eqs. (4.5) characterize the binding dynamics. The global dynamics is

$$\begin{aligned}
\dot{x}_k &= \omega_k \frac{\partial H_k}{\partial y}(X_k) - (H_k(X_k) - r_k) \frac{\partial H_k}{\partial x}(X_k) - c_k \sum_{j=1}^N l_{k,j} \mu_j x_j \\
\dot{y}_k &= -\omega_k \frac{\partial H_k}{\partial x}(X_k) - (H_k(X_k) - r_k) \frac{\partial H_k}{\partial y}(X_k) - c_k \sum_{j=1}^N l_{k,j} \mu_j y_j \\
\dot{\omega}_k &= -s_{\omega_k} \sum_{j=1}^N l_{k,j} (x_j y_k - y_j x_k) \\
\dot{\mu}_k &= -s_{\mu_k} \sum_{j=1}^N l_{k,j} \mu_j^2 (x_j^2 + y_j^2)
\end{aligned} \tag{4.14} \quad k = 1, \dots, N.$$

As for Eqs. (4.7), Eqs. (4.14) admits the two constant of motions written in 4.8.

Observe that when  $s_{\mu_k} = 0$  (with  $\mu_k(0) = 1$ ), the coupling dynamics is the gradient of a Laplacian potential (c.f. Example 1.5) who's action is to drive the state variables as close as possible to one another (respectively for  $x_k$  and  $y_k$ ). However, due to the heterogeneity in the Eqs. (4.14) (not only because of the different Hamiltonian heights (i.e.  $r_k$ ) but also because of the different Hamiltonian functionals (i.e.  $H_k$ )), full synchronization (i.e.  $X_j(t) = X_k(t)$  for all  $k$  and  $j$ ) will not, in general, be reached.

However, for a suitable class of MCD, a consensual oscillatory state may be reached. An illustration is given by the class of **homothetic** MCD that are now defined.

**Definition 4.1.** *A collection of heterogeneous MCD are **homothetic** if, for any  $\omega \in \mathbb{R}$ , there exists a function  $\bar{\varphi}(t)$  (depending on  $\omega$ ) and strictly positive constants  $v_1, \dots, v_N$  such that, for all  $k$ ,*

$$\begin{aligned}
\varphi_k &: \mathbb{R}_{\geq 0} \longrightarrow \mathcal{L}_{r_k} \\
t &\longmapsto v_k \bar{\varphi}(t)
\end{aligned}$$

is the solution of

$$\begin{cases} \dot{x} = \omega \frac{\partial H_k}{\partial y}(x, y) \\ \dot{y} = -\omega \frac{\partial H_k}{\partial x}(x, y) \end{cases} \quad \text{with } \varphi_k(0) = v_k (\bar{\varphi}_x(0), \bar{\varphi}_y(0)) \in \mathcal{L}_{r_k} = \{X \in \mathbb{R}^2 \mid H_k(X) - r_k = 0\}.$$

A collection of **homothetic homogeneous** MCD are similarly defined with omission of the index  $k$  of the Hamiltonians.

In other words, a collection of **homothetic** MCD (whether homogeneous or heterogeneous) are stable limit cycle oscillators with their respective attractor being related by a homothecy. Furthermore, they have, on their limit cycle, identical angular velocity (i.e. circulating on their attractor at the same angular speed). The following Lemma gives a characterization of **homothetic** MCD (whether homogeneous or not) according to the gradient of the Hamiltonians.

**Lemma 4.1.** *For a collection of homothetic (homogenous or heterogeneous) MCD we have, for all  $k, j$  and  $t$*

$$\varphi_k(t) = \frac{v_k}{v_j} \varphi_j(t) \iff \nabla H_k(\varphi_k(t)) = \frac{v_k}{v_j} \nabla H_j(\varphi_j(t)).$$

where  $\varphi_k(t)$  is defined as in Definition 4.1.

*Proof.* Since  $\varphi_k(t) = v_k \bar{\varphi}(t)$  and  $\varphi_j(t) = v_j \bar{\varphi}(t)$ , then  $\varphi_k(t) = \frac{v_k}{v_j} \varphi_j(t)$  and so

$$\varphi_k(t) = \frac{v_k}{v_j} \varphi_j(t) \iff \dot{\varphi}_k(t) = \frac{v_k}{v_j} \dot{\varphi}_j(t) \iff$$

$$\omega \begin{pmatrix} \frac{\partial H_k}{\partial y}(\varphi_k(t)) \\ -\frac{\partial H_k}{\partial x}(\varphi_k(t)) \end{pmatrix} = \frac{v_k}{v_j} \omega \begin{pmatrix} \frac{\partial H_j}{\partial y}(\varphi_j(t)) \\ -\frac{\partial H_j}{\partial x}(\varphi_j(t)) \end{pmatrix} \iff \nabla H_k(\varphi_k(t)) = \frac{v_k}{v_j} \nabla H_j(\varphi_j(t)).$$

□

Therefore, a collection of homotetic MCD have their **state variables** differing only by a constant when all **local dynamics** are on their attractor (which is identical for all oscillators up to a homothety). Thus, in this situation, for nonzero  $s_{\mu_k}$ , the adaptive mechanism tunes the value of the **parametric variables**  $\mu_k$ , modifying the coupling functions. Under certain conditions, the network can be brought to a consensual oscillatory state where the **state and parametric variables** have the following asymptotic behavior

$$\begin{aligned} \lim_{t \rightarrow \infty} \|X_k(t) - v_k \bar{\varphi}(t)\| &= 0 \quad \forall k, \quad \text{and} \quad \bar{\varphi}(t) \text{ is periodic and defined below in 4.17,} \\ \text{and, for } k = 1, \dots, N, \quad \lim_{t \rightarrow \infty} (\omega_k(t), \mu_k(t)) &= (\omega_c, \frac{\bar{\mu}}{v_k}) \quad \text{with constants } \omega_c \text{ and } \bar{\mu}. \end{aligned} \quad (4.15)$$

Once reached, this state is permanent. That is, if interactions are switched off (i.e.  $L = \mathbf{0}$ ), **local dynamics** remain on their respective local attractor given by their individual Hamiltonian height (i.e.  $\mathcal{L}_{r_k} = \{X \in \mathbb{R}^2 \mid H_k(X) = r_k\}$ ). Let us emphasize that adaptation in the coupling function makes **state variable** differ from one another by only a constant (i.e.  $\lim_{t \rightarrow \infty} X_k(t) = v_k \bar{\varphi}(t)$  for all  $k$ ). Therefore, under these circumstances, the **parametric variables**  $\omega_k$  converge towards a constant since, for all  $k$ ,

$$\begin{aligned} \lim_{t \rightarrow \infty} \left( -s_{\omega_k} \sum_{j=1}^N l_{k,j} (x_j(t) y_k(t) - y_j(t) x_k(t)) \right) \\ = -s_{\omega_k} \sum_{j=1}^N l_{k,j} (v_j \bar{\varphi}_x(t) v_k \bar{\varphi}_y(t) - v_j \bar{\varphi}_y(t) v_k \bar{\varphi}_x(t)) \\ = -s_{\omega_k} \sum_{j=1}^N l_{k,j} v_j v_k (\bar{\varphi}_x(t) \bar{\varphi}_y(t) - \bar{\varphi}_y(t) \bar{\varphi}_x(t)) = 0 \end{aligned} \quad (4.16)$$

with  $\bar{\varphi}(t) = (\bar{\varphi}_x(t), \bar{\varphi}_y(t))$ . We now discuss the existence of a consensual oscillatory state and the convergence towards it.

### Existence of a consensual oscillatory state

The dynamical system defined by Eqs. (4.14) admits the periodic solution

$$v_k \bar{\varphi}(t), \quad \omega_k(t) = \omega_c \quad \text{and} \quad \mu_k(t) = \frac{\bar{\mu}}{v_k} \quad \forall k, \quad (4.17)$$

where, for a  $\omega_c$  a given constant,  $v_k \bar{\varphi}(t)$  are defined as in Definition 4.1 (since we consider a collection of homothetic MCD) and  $\bar{\mu}$  is a given constant.

Let us verify the solution. For all  $k$ ,  $v_k \bar{\varphi}(t)$  solves the canonical part with zero dissipation (i.e. the dissipative part is zero). The **coupling dynamics** vanishes because, for any vector  $\mu = (\mu_1, \dots, \mu_N)$ , we have, for all  $t$ ,

$$D L D(v) \mu \bar{\varphi}_x(t) = \mathbf{0} \iff L D(v) \mu = \mathbf{0} \iff \mu_k = \frac{\bar{\mu}}{v_k} \quad \forall k \quad (\bar{\mu} \text{ a given constant}), \quad (4.18)$$

where  $D$  and  $D(v)$  are diagonal matrices with  $c_k$  and  $v_k$  on their diagonals respectively and  $\mathbf{0}$  is a  $N$ -dimensional zero vector. The same holds for the  $y$ -coordinate  $\bar{\varphi}_y(t)$ . From the last line in 4.16, we have that the **parametric dynamics** for the  $\omega_k$  also vanish and for  $\mu_k$ , we have (for all  $k$ )

$$\sum_{j=1}^N l_{k,j} \left( \frac{\bar{\mu}^2}{v_j^2} \right) (v_j^2 \bar{\varphi}_x(t)^2 + v_j^2 \bar{\varphi}_y(t)^2) = \bar{\mu}^2 \|\bar{\varphi}(t)\|^2 \sum_{j=1}^N l_{k,j} = 0.$$

This concludes the verification of the solution.

### Convergence towards a consensual oscillatory state

**Convergence** - Here, the complexity of the resulting linearized system precludes, as far as we are aware, to get analytical results for the convergence in 4.15.

**Limit Values** - If 4.15 holds, then the values  $\omega_c$  and  $\bar{\mu}$  are analytically expressed as

$$\omega_c = \frac{\sum_{j=1}^N \frac{\omega_j(0)}{s_{\omega_j}}}{\sum_{j=1}^N \frac{1}{s_{\omega_j}}} \quad \bar{\mu} = \frac{\sum_{j=1}^N \frac{\mu_j(0)}{s_{\mu_j}}}{\sum_{j=1}^N \frac{1}{s_{\mu_j} v_j}} .$$

The first equality is a direct consequence of the constant of motion  $J_\omega$  in 4.8 and the fact that  $\lim_{t \rightarrow \infty} \omega_k(t) = \omega_c$ . The same is true for the second equality since

$$\sum_{j=1}^N \frac{\mu_j(t)}{s_{\mu_j}} = \sum_{j=1}^N \frac{\mu_j(0)}{s_{\mu_j}} \quad \forall t .$$

In the view of  $J_\mu$  in 4.8 and since  $\lim_{t \rightarrow \infty} \mu_k(t) = \frac{\bar{\mu}}{v_k}$  for all  $k$ , we obtain

$$\lim_{t \rightarrow \infty} \left( \sum_{j=1}^N \frac{\mu_j(t)}{s_{\mu_j}} \right) = \sum_{j=1}^N \frac{\bar{\mu}}{s_{\mu_j} v_j} = \sum_{j=1}^N \frac{\mu_j(0)}{s_{\mu_j}} \quad \Longleftrightarrow \quad \bar{\mu} = \frac{\sum_{j=1}^N \frac{\mu_j(0)}{s_{\mu_j}}}{\sum_{j=1}^N \frac{1}{s_{\mu_j} v_j}} .$$

#### 4.2.2.1 Two types of c-PV

Consider Eqs. (4.14) with a collection of ellipsoidal HOPF MCD where the set  $\Gamma_k = \{\mathbf{a}_k, \mathbf{b}_k, r_k\}$  are fixed and constant parameters close to one and another (i.e.  $\|\Gamma_k - \Gamma_j\|$  is “small” for all  $k$  and  $j$ ). Let  $\nu$  be the c-PV of the  $y$  coordinate. The **binding dynamics** is given by Eqs. (4.6). Explicitly, the dynamical system is

$$\begin{aligned} \dot{x}_k &= \omega_k \mathbf{b}_k y_k - (\mathbf{a}_k x_k^2 + \mathbf{b}_k y_k^2 - r_k) \mathbf{a}_k x_k - c_k \sum_{j=1}^N l_{k,j} \mu_j x_j , \\ \dot{y}_k &= -\omega_k \mathbf{a}_k x_k - (\mathbf{a}_k x_k^2 + \mathbf{b}_k y_k^2 - r_k) \mathbf{b}_k y_k - c_k \sum_{j=1}^N l_{k,j} \nu_j y_j , \\ \dot{\omega}_k &= -s_{\omega_k} \sum_{j=1}^N l_{k,j} (\mu_j x_j \nu_k y_k - \nu_j y_j \mu_k x_k) , \\ \dot{\mu}_k &= -s_{\mu_k} \sum_{j=1}^N l_{k,j} \mu_j^2 x_j^2 , \\ \dot{\nu}_k &= -s_{\nu_k} \sum_{j=1}^N l_{k,j} \nu_j^2 y_j^2 , \end{aligned} \quad k = 1, \dots, N . \quad (4.19)$$

Not only does System 4.19 possesses the two constants of motion presented in 4.8, it additionally has a third one, namely

$$J_\nu(\nu_1, \dots, \nu_N) = \sum_{j=1}^N \frac{\nu_j}{s_{\nu_j}} , \quad (4.20)$$

When  $s_{\omega_k} = s_{\mu_k} = s_{\nu_k} = 0$ , then Eqs. (4.19) describes the dynamics of a network of homogeneous MCD with different valued parameters and where the coupling for the  $x$  and  $y$  coordinates is

realized via the same network but with different weights  $\mu_k$  and  $\nu_k$ . The aim of the adaptive mechanisms is to change the values of the f-PV  $\omega_k$  and the c-PV  $\mu_k$  and  $\nu_k$ . This allows the network to reach a consensual oscillatory state where

$$\begin{aligned} \lim_{t \rightarrow \infty} \|X_k(t) - D(\Gamma_k)\bar{\varphi}(t)\| &= 0 \quad \forall k, \quad \text{and} \quad D(\Gamma_k)\bar{\varphi}(t) \text{ is periodic and defined below in 4.22,} \\ \text{and, for } k = 1, \dots, N, \quad \lim_{t \rightarrow \infty} (\omega_k(t), \mu_k(t), \nu_k(t)) &= \left( \frac{\bar{\omega}}{\sqrt{\mathbf{a}_k \mathbf{b}_k}}, \bar{\mu} \frac{\sqrt{\mathbf{a}_k}}{\sqrt{r_k}}, \bar{\nu} \frac{\sqrt{\mathbf{b}_k}}{\sqrt{r_k}} \right) \\ &\text{with constants } \bar{\omega}, \bar{\mu} \text{ and } \bar{\nu}. \end{aligned} \tag{4.21}$$

This state is permanent - once reached, the network maintains this dynamical state and this even if interactions are switched off.

### Existence of a consensual oscillatory state

The dynamical system defined by Eqs. (4.19) admits the periodic solution

$$\begin{aligned} D(\Gamma_k)\bar{\varphi}(t) &= \left( \frac{\sqrt{r_k}}{\sqrt{\mathbf{a}_k}} \sin(\bar{\omega} t), \frac{\sqrt{r_k}}{\sqrt{\mathbf{b}_k}} \cos(\bar{\omega} t) \right), \quad \omega_k(t) = \frac{\bar{\omega}}{\sqrt{\mathbf{a}_k \mathbf{b}_k}}, \quad \mu_k(t) = \bar{\mu} \frac{\sqrt{\mathbf{a}_k}}{\sqrt{r_k}}, \\ \text{and } \nu_k(t) &= \bar{\nu} \frac{\sqrt{\mathbf{b}_k}}{\sqrt{r_k}} \quad \forall k, \end{aligned} \tag{4.22}$$

with  $D(\Gamma_k) = \sqrt{r_k} \begin{pmatrix} \frac{1}{\sqrt{\mathbf{a}_k}} & 0 \\ 0 & \frac{1}{\sqrt{\mathbf{b}_k}} \end{pmatrix}$ ,  $\bar{\varphi}(t) = (\sin(\bar{\omega} t), \cos(\bar{\omega} t))$ , and where  $\bar{\omega}$ ,  $\bar{\mu}$  and  $\bar{\nu}$  are given constants.

Let us verify the solution. The canonical part of each MCD is solved by  $D(\Gamma_k)\bar{\varphi}(t)$ . We indeed have

$$\begin{aligned} \frac{\sqrt{r_k}}{\sqrt{\mathbf{a}_k}} \dot{\varphi}_x(t) &= \frac{\sqrt{r_k}}{\sqrt{\mathbf{a}_k}} \bar{\omega} \cos(\bar{\omega} t) \quad \text{and} \quad \omega_k(t) \mathbf{b}_k y_k(t) = \frac{\bar{\omega}}{\sqrt{\mathbf{a}_k \mathbf{b}_k}} \mathbf{b}_k \frac{\sqrt{r_k}}{\sqrt{\mathbf{b}_k}} \cos(\bar{\omega} t) = \bar{\omega} \frac{\sqrt{r_k}}{\sqrt{\mathbf{a}_k}} \cos(\bar{\omega} t), \\ \frac{\sqrt{r_k}}{\sqrt{\mathbf{b}_k}} \dot{\varphi}_y(t) &= -\frac{\sqrt{r_k}}{\sqrt{\mathbf{b}_k}} \bar{\omega} \sin(\bar{\omega} t) \quad \text{and} \quad -\omega_k(t) \mathbf{a}_k x_k(t) = \frac{\bar{\omega}}{\sqrt{\mathbf{a}_k \mathbf{b}_k}} \mathbf{a}_k \frac{\sqrt{r_k}}{\sqrt{\mathbf{a}_k}} \sin(\bar{\omega} t) = \bar{\omega} \frac{\sqrt{r_k}}{\sqrt{\mathbf{b}_k}} \sin(\bar{\omega} t). \end{aligned}$$

The dissipative part of each MCD vanishes since  $\mathbf{a}_k x_k(t)^2 + \mathbf{b}_k y_k(t)^2 - r_k = \mathbf{a}_k \frac{r_k}{\mathbf{a}_k} \sin(\bar{\omega} t)^2 + \mathbf{b}_k \frac{r_k}{\mathbf{b}_k} \cos(\bar{\omega} t)^2 - r_k = 0$ . The **coupling dynamics** is zero since, for all  $k$ ,

$$\mathbf{c}_k \sum_{j=1}^N l_{k,j} \mu_j x_j = \mathbf{c}_k \sum_{j=1}^N l_{k,j} \bar{\mu} \frac{\sqrt{\mathbf{a}_j}}{\sqrt{r_j}} \frac{\sqrt{r_j}}{\sqrt{\mathbf{a}_j}} \sin(\bar{\omega} t) = \mathbf{c}_k \bar{\mu} \sin(\bar{\omega} t) \sum_{j=1}^N l_{k,j} = 0$$

and the same holds for the  $y$ -coordinate. For the **parametric variables** to be constant, we must verify that the parametric dynamics is null. This is true since, for all  $k$

$$\begin{aligned} \mu_j x_j \nu_k y_k - \nu_j y_j \mu_k x_k &= \bar{\mu} \frac{\sqrt{\mathbf{a}_j}}{\sqrt{r_j}} \frac{\sqrt{r_j}}{\sqrt{\mathbf{a}_j}} \sin(\bar{\omega} t) \bar{\nu} \frac{\sqrt{\mathbf{b}_k}}{\sqrt{r_k}} \frac{\sqrt{r_k}}{\sqrt{\mathbf{b}_k}} \cos(\bar{\omega} t) \\ &\quad - \bar{\nu} \frac{\sqrt{\mathbf{b}_j}}{\sqrt{r_j}} \frac{\sqrt{r_j}}{\sqrt{\mathbf{b}_j}} \cos(\bar{\omega} t) \bar{\mu} \frac{\sqrt{\mathbf{a}_k}}{\sqrt{r_k}} \frac{\sqrt{r_k}}{\sqrt{\mathbf{a}_k}} \sin(\bar{\omega} t) = 0 \end{aligned}$$

and so  $\dot{\omega}_k = 0$  for all  $k$ . For  $\mu_k$ , we have, for all  $k$ ,

$$\sum_{j=1}^N l_{k,j} \mu_j^2 x_j^2 = \sum_{j=1}^N l_{k,j} \bar{\mu}^2 \frac{\mathbf{a}_j}{r_j} \frac{r_j}{\mathbf{a}_j} \sin(\bar{\omega} t)^2 = \bar{\mu}^2 \sin(\bar{\omega} t)^2 \sum_{j=1}^N l_{k,j} = 0$$

and the same holds for the  $\nu$ -coordinate. This concludes the verification of the solution.

### Convergence towards a consensual oscillatory state

**Convergence** - Here, the complexity of the resulting linearized system precludes, as far as we are aware, to get analytical results for the convergence in 4.21.

**Limit Values** - If 4.21 holds, then the values  $\bar{\omega}$ ,  $\bar{\mu}$  and  $\bar{\nu}$  are analytically expressed as

$$\bar{\omega} = \frac{\sum_{j=1}^N \frac{\omega_j(0)}{s_{\omega_j}}}{\sum_{j=1}^N \frac{1}{s_{\omega_j} \sqrt{a_j b_j}}}, \quad \bar{\mu} = \frac{\sum_{j=1}^N \frac{\mu_j(0)}{s_{\mu_j}}}{\sum_{j=1}^N \frac{\sqrt{a_j}}{s_{\mu_j} \sqrt{r_j}}}, \quad \bar{\nu} = \frac{\sum_{j=1}^N \frac{\nu_j(0)}{s_{\nu_j}}}{\sum_{j=1}^N \frac{\sqrt{b_j}}{s_{\nu_j} \sqrt{r_j}}}.$$

All three equalities derive, respectively, from the constant of motions  $J_\omega$  and  $J_\mu$  in 4.8 and  $J_\nu$  in 4.20, and from the fact that  $\lim_{t \rightarrow \infty} (\omega_j(t), \mu_j(t), \nu_j(t)) = (\frac{\bar{\omega}}{\sqrt{a_j b_j}}, \bar{\mu} \frac{\sqrt{a_j}}{\sqrt{r_j}}, \bar{\nu} \frac{\sqrt{b_j}}{\sqrt{r_j}})$  for all  $j$ , that is

$$\begin{aligned} \sum_{j=1}^N \frac{\omega_j(0)}{s_{\omega_j}} &= \lim_{t \rightarrow \infty} \sum_{j=1}^N \frac{\omega_j(t)}{s_{\omega_j}} = \sum_{j=1}^N \frac{\frac{\bar{\omega}}{\sqrt{a_j b_j}}}{s_{\omega_j}} = \bar{\omega} \sum_{j=1}^N \frac{1}{s_{\omega_j} \sqrt{a_j b_j}}, \\ \sum_{j=1}^N \frac{\mu_j(0)}{s_{\mu_j}} &= \lim_{t \rightarrow \infty} \sum_{j=1}^N \frac{\mu_j(t)}{s_{\mu_j}} = \sum_{j=1}^N \frac{\bar{\mu} \frac{\sqrt{a_j}}{\sqrt{r_j}}}{s_{\mu_j}} = \bar{\mu} \sum_{j=1}^N \frac{\sqrt{a_j}}{s_{\mu_j} \sqrt{r_j}}, \\ \sum_{j=1}^N \frac{\nu_j(0)}{s_{\nu_j}} &= \lim_{t \rightarrow \infty} \sum_{j=1}^N \frac{\nu_j(t)}{s_{\nu_j}} = \sum_{j=1}^N \frac{\bar{\nu} \frac{\sqrt{b_j}}{\sqrt{r_j}}}{s_{\nu_j}} = \bar{\nu} \sum_{j=1}^N \frac{\sqrt{b_j}}{s_{\nu_j} \sqrt{r_j}}. \end{aligned}$$

#### 4.2.3 Miscellaneous Remark: Three types of adapting parameters: f-PV, g-PV and c-PV

In this chapter, we focused on adapting flow parameters and coupling weights and not on shaping the local attractor. We here make an overlap with Chapter 3 where all three types of adaptation may operate simultaneously. Consider again Eqs. (4.14) with a collection of ellipsoidal Hopf MCD but now  $\Gamma_k = \{\mathbf{b}_k, r_k\}$  (and again, we suppose that  $\|\Gamma_k - \Gamma_j\|$  is “small” for all  $k$  and  $j$ ). What was in Section 4.2.2.1 a fixed and constant parameter  $\mathbf{a}_k$  becomes here  $\alpha_k$ , a g-PV. Instead of having two c-PV as in Section 4.2.2.1, we here have an attractor shaping phenomena as discussed in Chapter 3. For the  $y$ -coordinate,  $\nu$  is the c-PV and its dynamics is given Eqs. (4.6). The dynamical system is

$$\begin{aligned} \dot{x}_k &= \omega_k \mathbf{b}_k y_k - (\alpha_k x_k^2 + \mathbf{b}_k y_k^2 - r_k) \alpha_k x_k - c_k \sum_{j=1}^N l_{k,j} x_j, \\ \dot{y}_k &= -\omega_k \alpha_k x_k - (\alpha_k x_k^2 + \mathbf{b}_k y_k^2 - r_k) \mathbf{b}_k y_k - c_k \sum_{j=1}^N l_{k,j} \nu_j y_j, \\ \dot{\omega}_k &= -s_{\omega_k} \sum_{j=1}^N l_{k,j} (x_j \nu_k y_k - \nu_j y_j x_k), \\ \dot{\alpha}_k &= s_{\alpha_k} \sum_{j=1}^N l_{k,j} x_j^2, \\ \dot{\nu}_k &= -s_{\nu_k} \sum_{j=1}^N l_{k,j} \nu_j^2 y_j^2, \end{aligned} \quad k = 1, \dots, N. \quad (4.23)$$

Eqs. (4.23) possesses the two constant of motion presented in 4.8 and a third one

$$J_\alpha(\alpha_1, \dots, \alpha_N) = \sum_{j=1}^N \frac{\alpha_j}{s_{\alpha_j}}. \quad (4.24)$$

System (4.23) is a mixture of three different types of adaptation. The first tunes the flow of the dynamical system on its attractor. The second shapes the attractor itself and the third one adjusts

weights in the interactions. All three adaptive mechanisms, under suitable conditions, drive the system into a consensual oscillatory state, asymptotically characterized by

$$\begin{aligned} \lim_{t \rightarrow \infty} \|X_k(t) - D(\Gamma_k)\bar{\varphi}(t)\| &= 0 \quad \forall k, \quad \text{and} \quad D(\Gamma_k)\bar{\varphi}(t) \text{ is periodic and defined below in 4.26,} \\ \text{and, for } k = 1, \dots, N, \quad \lim_{t \rightarrow \infty} (\omega_k(t), \alpha_k(t), \nu_k(t)) &= \left( \frac{\bar{\omega}}{\sqrt{\bar{\alpha}r_k b_k}}, \bar{\alpha}r_k, \bar{\nu} \frac{\sqrt{b_k}}{\sqrt{r_k}} \right) \\ &\text{with constants } \bar{\omega}, \bar{\alpha} \text{ and } \bar{\nu}. \end{aligned} \tag{4.25}$$

Again, as in Section 4.2.2, once this state is reached, removing the interactions does not alter the permanent characteristics of the dynamics.

### Existence of a consensual oscillatory state

The dynamical system defined by Eqs. (4.23) admits the periodic solution

$$\begin{aligned} D(\Gamma_k)\bar{\varphi}(t) &= \left( \frac{\sin(\bar{\omega}t)}{\sqrt{\bar{\alpha}}}, \frac{\sqrt{r_k}}{\sqrt{b_k}} \cos(\bar{\omega}t) \right), \quad \omega_k(t) = \frac{\bar{\omega}}{\sqrt{\bar{\alpha}r_k b_k}}, \quad \alpha_k(t) = \bar{\alpha}r_k, \\ \text{and } \nu_k(t) &= \bar{\nu} \frac{\sqrt{b_k}}{\sqrt{r_k}} \quad \forall k, \end{aligned} \tag{4.26}$$

with  $D(\Gamma_k) = \begin{pmatrix} 1 & 0 \\ 0 & \frac{\sqrt{r_k}}{\sqrt{b_k}} \end{pmatrix}$ ,  $\bar{\varphi}(t) = \left( \frac{\sin(\bar{\omega}t)}{\sqrt{\bar{\alpha}}}, \cos(\bar{\omega}t) \right)$  and where  $\bar{\omega}$ ,  $\bar{\alpha}$  and  $\bar{\nu}$  are given constants.

Let us verify the solution. The canonical part of each MCD is solved by  $D(\Gamma_k)\bar{\varphi}(t)$  because

$$\begin{aligned} \dot{\bar{\varphi}}_x(t) &= \frac{1}{\sqrt{\bar{\alpha}}} \bar{\omega} \cos(\bar{\omega}t) \quad \text{and} \quad \omega_k(t) b_k y_k(t) = \frac{\bar{\omega}}{\sqrt{\bar{\alpha}r_k b_k}} b_k \frac{\sqrt{r_k}}{\sqrt{b_k}} \cos(\bar{\omega}t) = \frac{\bar{\omega}}{\sqrt{\bar{\alpha}}} \cos(\bar{\omega}t), \\ \frac{\sqrt{r_k}}{\sqrt{b_k}} \dot{\bar{\varphi}}_y(t) &= -\frac{\sqrt{r_k}}{\sqrt{b_k}} \bar{\omega} \sin(\bar{\omega}t) \quad \text{and} \quad -\omega_k(t) \alpha_k(t) x_k(t) = -\frac{\bar{\omega}}{\sqrt{\bar{\alpha}r_k b_k}} \bar{\alpha}r_k \frac{1}{\sqrt{\bar{\alpha}}} \sin(\bar{\omega}t) = -\frac{\bar{\omega} \sqrt{r_k}}{\sqrt{b_k}} \sin(\bar{\omega}t). \end{aligned}$$

The dissipative part of each MCD vanishes since  $\alpha_k x_k(t)^2 + b_k y_k(t)^2 - r_k = \bar{\alpha}r_k \frac{1}{\bar{\alpha}} \sin(\bar{\omega}t)^2 + b_k \frac{r_k}{b_k} \cos(\bar{\omega}t)^2 - r_k = 0$ . Similarly to Section 4.2.2.1, one calculates the **coupling dynamics** and finds it is zero for both,  $x$  and  $y$ -coordinate. For the **parametric variables** to be constant, we must verify that the **parametric dynamics** is itself null. This is true and directly follows from similar arguments as those given in Section 4.2.2.1. This concludes the verification of the solution.

### Convergence towards a consensual oscillatory state

**Convergence** - Here, the complexity of the resulting linearized system precludes, as far as we are aware, to get analytical results for the convergence in 4.25.

**Limit Values** - If 4.25 holds, then the values  $\bar{\omega}$ ,  $\bar{\alpha}$  and  $\bar{\nu}$  are analytically expressed as

$$\bar{\omega} = \frac{\sum_{j=1}^N \frac{\omega_j(0)}{s_{\omega_j}}}{\sum_{j=1}^N \frac{1}{s_{\omega_j} \sqrt{\bar{\alpha}r_j b_j}}}, \quad \bar{\alpha} = \frac{\sum_{j=1}^N \frac{\alpha_j(0)}{s_{\alpha_j}}}{\sum_{j=1}^N \frac{r_j}{s_{\alpha_j}}}, \quad \bar{\nu} = \frac{\sum_{j=1}^N \frac{\nu_j(0)}{s_{\nu_j}}}{\sum_{j=1}^N \frac{\sqrt{b_j}}{s_{\nu_j} \sqrt{r_j}}}.$$

All three equalities derive, respectively, from the constant of motions  $J_\omega$  and  $J_\nu$  in 4.8 and  $J_\alpha$  in 4.24, and from the fact that  $\lim_{t \rightarrow \infty} (\omega_j(t), \alpha_j(t), \nu_j(t)) = \left( \frac{\bar{\omega}}{\sqrt{\bar{\alpha}r_j b_j}}, \bar{\alpha}r_j, \bar{\nu} \frac{\sqrt{b_j}}{\sqrt{r_j}} \right)$  for all  $j$ . Indeed, one obtains



$$\begin{aligned}
\sum_{j=1}^N \frac{\omega_j(0)}{s_{\omega_j}} &= \lim_{t \rightarrow \infty} \sum_{j=1}^N \frac{\omega_j(t)}{s_{\omega_j}} = \sum_{j=1}^N \frac{\bar{\omega}}{\sqrt{\bar{\alpha} r_j b_j} s_{\omega_j}} = \bar{\omega} \sum_{j=1}^N \frac{1}{s_{\omega_j} \sqrt{\bar{\alpha} r_j b_j}}, \\
\sum_{j=1}^N \frac{\alpha_j(0)}{s_{\alpha_j}} &= \lim_{t \rightarrow \infty} \sum_{j=1}^N \frac{\alpha_j(t)}{s_{\alpha_j}} = \sum_{j=1}^N \frac{\bar{\alpha} r_j}{s_{\alpha_j}} = \bar{\alpha} \sum_{j=1}^N \frac{r_j}{s_{\alpha_j}}, \\
\sum_{j=1}^N \frac{\nu_j(0)}{s_{\nu_j}} &= \lim_{t \rightarrow \infty} \sum_{j=1}^N \frac{\nu_j(t)}{s_{\nu_j}} = \sum_{j=1}^N \frac{\bar{\nu} \sqrt{b_j}}{\sqrt{r_j} s_{\nu_j}} = \bar{\nu} \sum_{j=1}^N \frac{\sqrt{b_j}}{s_{\nu_j} \sqrt{r_j}}.
\end{aligned}$$

### 4.3 Numerical Simulations

We present numerical simulations for

- homogeneous MCD, once with `binding dynamics` characterized by Eq. (4.4) as in Eqs. (4.7) (refer to Section 4.3.1), and once with Eq. (4.5) as in Eqs. (4.14) for homogeneous MCD (refer to Section 4.3.2),
- for ellipsoidal HOPF oscillators with two c-PV as in Eqs. (4.19) (refer to Section 4.3.3), and with all three types of adaptation as in Eqs. (4.23) (refer to Section 4.3.4),
- and finally a network of heterogeneous MCD with HOPF and MATHEWS-LAKSHMANAN oscillators as in Example (4.1) (refer to Section 4.3.5).

In all simulations, the initial conditions for `state variables`  $(x_k(0), y_k(0))$  are randomly uniformly distributed on  $] -0.1, 0.1[$  and the initial conditions for the f-PV  $\omega_k$  are randomly (uniform distribution) drawn from  $]0.9, 1.1[$ . As in Section 2.3, the coordinates of  $\mathbf{1s}(a,b,N) \in \mathbb{R}^N$  are defined as  $\mathbf{1s}(a,b,N)_j := a + (j-1) \frac{b-a}{N-1}$ ,  $j = 1, \dots, N$ .

#### 4.3.1 MATHEWS-LAKSHMANAN Oscillators

Six MATHEWS-LAKSHMANAN oscillators interacted on a Tetrahedron network topology (c.f. Figure 4.3(a)). The numbering of the vertices is: the top vertex is 1, the next two bellow are 2 and 3 and the last three on the base of the triangle are 4 to 6 (from left to right). The radii of the local MCD are fixed as  $(r_1, \dots, r_N) = \mathbf{1s}(1,1.25,6)$ . We choose the coupling strengths and susceptibility constants as  $(c_1, \dots, c_N) = (0.8, 1.3, 1, 0.6, 0.6, 1.15)$ ,  $s_{\omega_k} = 1$  and  $s_{\mu_k} = \frac{1}{2}$  for all  $k$ . The initial conditions for all c-PV  $\mu$  are fixed to one.

The resulting dynamics is shown in Figure 4.1. At  $t = 70$ , the network connections are switched off ( $L = 0$ ). One can clearly observe that the synchronized state is no longer maintained after the removal of the network. However, observe that the  $\omega_k$  have reached their asymptotic value and do remain with it, even after disconnection.

The same numerical integration is carried out but with susceptibility constants  $s_{\omega_k} = \frac{1}{2}$ . Although very similar to the previous parameter configuration, here the synchronized state is not reached. This is shown in Figure 4.2. The network connections are also switched off at  $t = 70$ .

#### 4.3.2 OHR Oscillators

On a Octahedron network (c.f. Figure 4.3(b)), 10 OHR (c.f. Example 1.1) oscillators interact. The numbering of the vertices is: the top right vertex is 1 where as the bottom left is 10. The four vertices bellow vertex one, are numbered 2 to 5 (from left to right). The remaining four vertices are vertex 6 to 9 (from left to right). The radii of the local MCD are fixed as  $r_k = 1 + \pi$  for  $k$  odd and  $r_k = 1$  for  $k$  even. We choose the coupling strengths and susceptibility constants as  $c_k = 1.5$  for  $k$  odd and  $c_k = 2$  for  $k$  even,  $s_{\omega_k} = 0.1$  for  $k$  odd and  $s_{\omega_k} = 0.25$  for  $k$  even and finally  $s_{\mu_k} = 1$  for all  $k$ . The initial conditions for all c-PV  $\mu$  are fixed to one. The transient dynamics is represented in Figure 4.4.

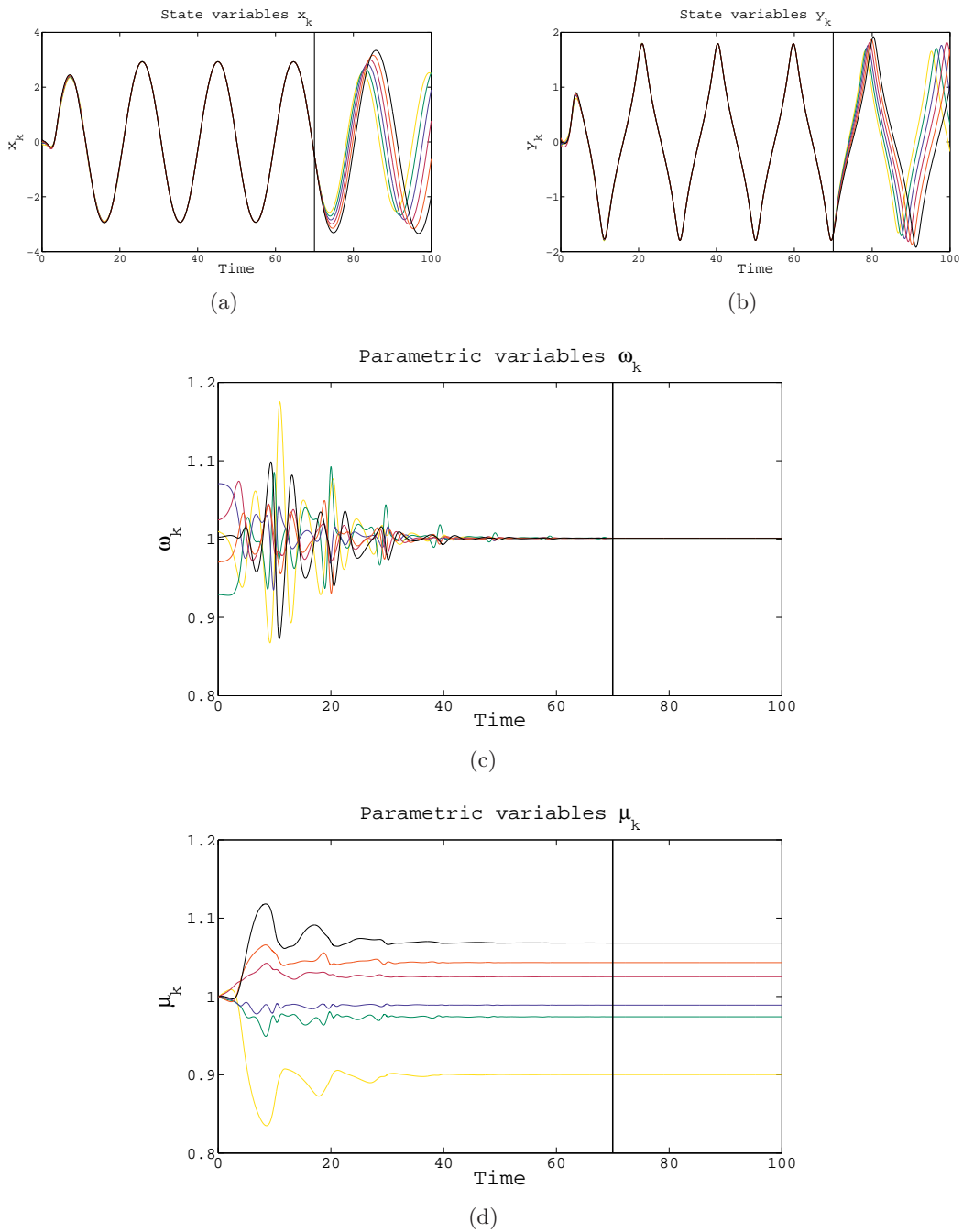


Fig. 4.1: Time evolution of the **state variables**  $x_k$  and  $y_k$  (Figures 4.1(a) & 4.1(b)), the **parametric variables**  $\omega_k$  (Figure 4.1(c)) and the **coupling parametric variables**  $\mu_k$  (Figure 4.1(d)) for six MATHEWS-LAKSHMANAN oscillators, interacting through a Tetrahedron network. The network is removed at  $t = 70$  (black solid line).

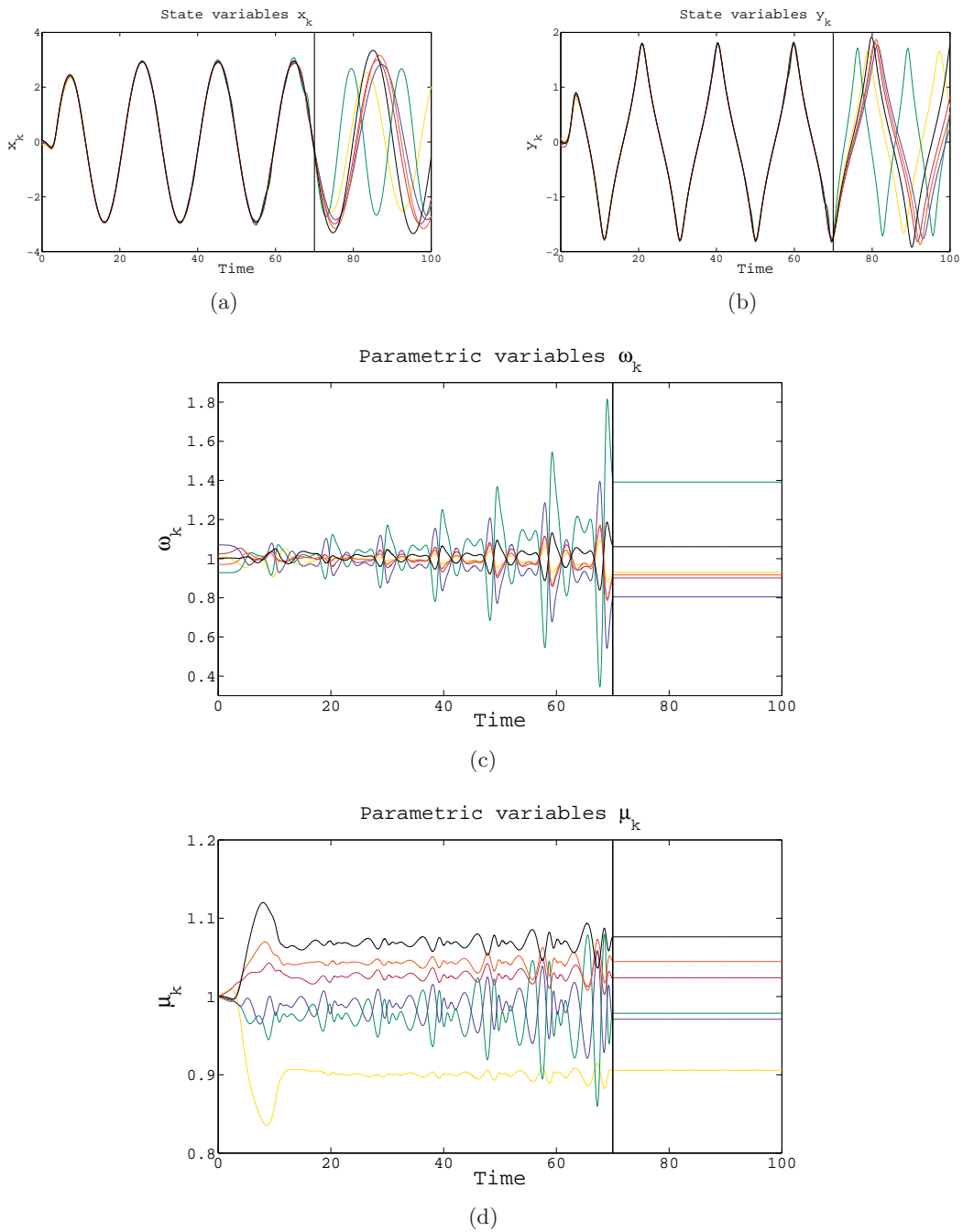


Fig. 4.2: Time evolution of the **state variables**  $x_k$  and  $y_k$  (Figures 4.2(a) & 4.2(b)), the **parametric variables**  $\omega_k$  (Figure 4.2(c)) and the **coupling parametric variables**  $\mu_k$  (Figure 4.2(d)) for six MATHEWS-LAKSHMANAN oscillators, interacting through a Tetrahedron network. The susceptibility constants  $s_{\omega_k}$  are half the values of those in Figure 4.1. The network is removed at  $t = 70$  (black solid line).

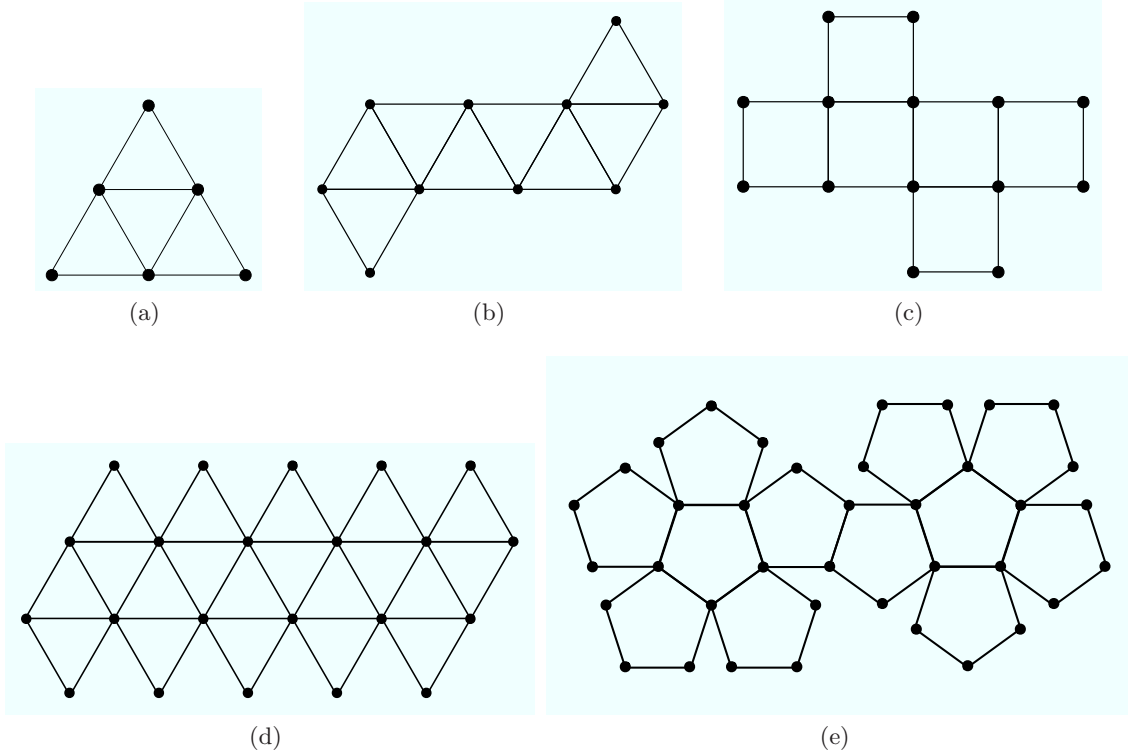


Fig. 4.3: Polyhedra network topology: a Tetrahedron network topology (Figure 4.3(a)) with algebraic connectivity equal to 1.6972, a Octahedron network topology (Figure 4.3(b)) with algebraic connectivity equal to 0.5281, a Hexahedron network topology (Figure 4.3(c)) with algebraic connectivity equal to 0.3662, a Icosahedron network topology (Figure 4.3(d)) with algebraic connectivity equal to 0.2694 and a Dodecahedron network topology (Figure 4.3(e)) with algebraic connectivity equal to 0.0573.

#### 4.3.3 Ellipsoidal HOPF Oscillators with two c-PV

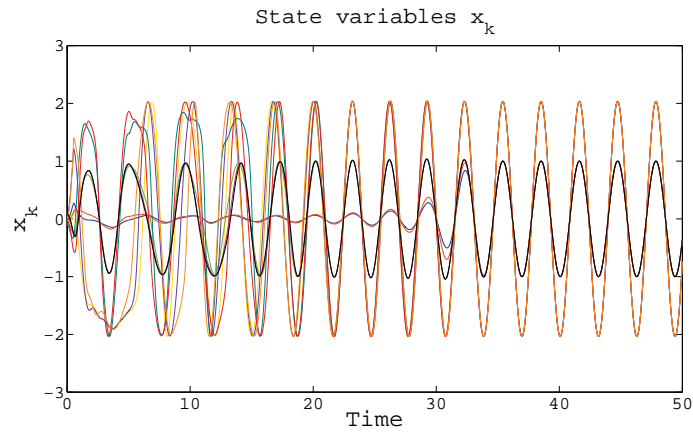
Through a 14-vertex Hexahedron network (c.f. Figure 4.3(c)), ellipsoidal HOPF oscillators interact with two c-PV in their coupling dynamics. The geometric parameters are fixed as  $(r_1, \dots, r_N) = \mathbf{1s}(1,2,14)$ ,  $(a_1, \dots, a_N) = \mathbf{1s}(0.8,1.2,14)$  and  $(b_1, \dots, b_N) = \mathbf{1s}(1.2,0.8,14)$ . We choose the coupling strengths and susceptibility constants as  $c_k = 1$  for all  $k$  and,  $(s_{\omega_1}, \dots, s_{\omega_N}) = \mathbf{1s}(0.5,1,14)$ ,  $(s_{\mu_1}, \dots, s_{\mu_N}) = \mathbf{1s}(1.4,0.7,14)$  and  $(s_{\nu_1}, \dots, s_{\nu_N}) = \mathbf{1s}(0.7,1.4,14)$ . The initial conditions for all c-PV  $\mu$  and  $\nu$  are fixed to one. The dynamics is displayed in Figure 4.5.

#### 4.3.4 Ellipsoidal HOPF Oscillators with f-PV, g-PV and c-PV

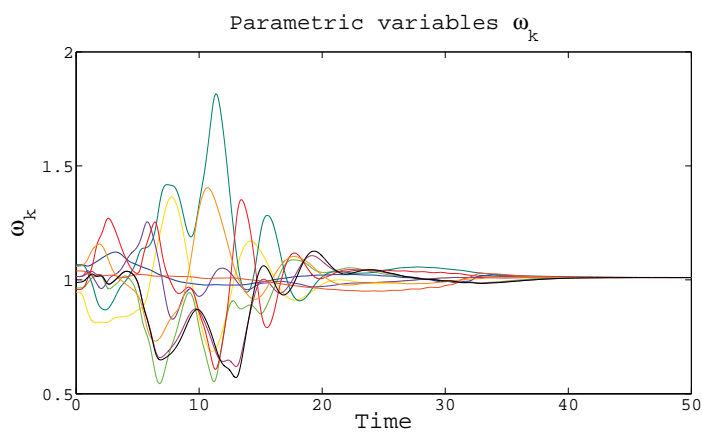
Figure 4.6 shows the three types of adaptation occurring in a Icosahedron network (c.f. Figure 4.3(d)) of 22 ellipsoidal HOPF oscillators. The geometric parameters are fixed as  $(r_1, \dots, r_N) = \mathbf{1s}(1,2,22)$  and  $(b_1, \dots, b_N) = \mathbf{1s}(1.2,0.8,22)$ . We choose the coupling strengths and susceptibility constants as  $(c_1, \dots, c_N) = \mathbf{1s}(0.65,1,22)$  and,  $(s_{\omega_1}, \dots, s_{\omega_N}) = \mathbf{1s}(0.75,0.55,22)$ ,  $(s_{\alpha_1}, \dots, s_{\alpha_N}) = \mathbf{1s}(0.2,0.3,22)$  and  $(s_{\mu_1}, \dots, s_{\mu_N}) = \mathbf{1s}(0.35,0.45,22)$ . The initial conditions for the g-PV  $\alpha_k$  are randomly (uniform distribution) drawn from  $]0.9, 1.1[$  and the initial conditions for all c-PV  $\mu$  are fixed to one.

#### 4.3.5 Heterogeneous network of HOPF and MATHEWS-LAKSHMANAN Oscillators

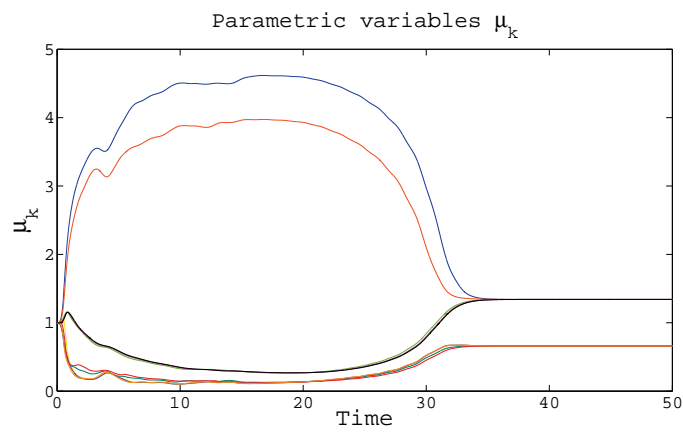
The transient dynamics of a heterogeneous network of HOPF and MATHEWS-LAKSHMANAN oscillators with flow tuning is represented in Figure 4.7. It consists of 19 HOPF and 19 MATHEWS-LAKSHMANAN oscillators interacting on a Dodecahedron network (c.f. Figure 4.3(e)). The HOPF



(a)



(b)



(c)

Fig. 4.4: Time evolution of the state variables  $x_k$  (Figure 4.4(a)), the parametric variables  $\omega_k$  (Figure 4.4(b)) and the coupling parametric variables  $\mu_k$  (Figure 4.4(c)) for 10 OHR oscillators, interacting through a Tetrahedron network.

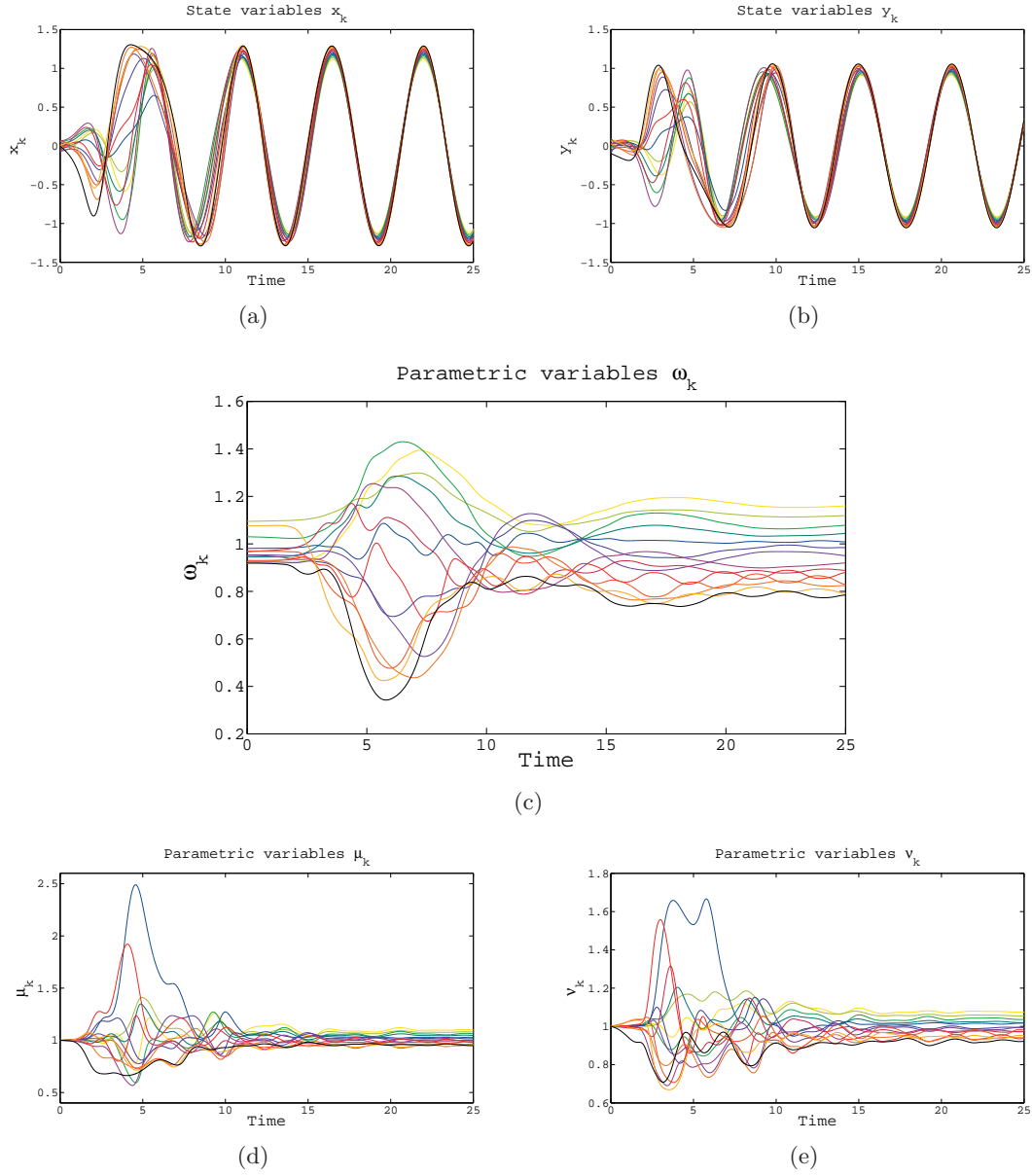


Fig. 4.5: Time evolution of the **state variables**  $x_k$  and  $y_k$  (Figure 4.5(a) & 4.5(b)), the **parametric variables**  $\omega_k$  (Figure 4.5(c)) and the **coupling parametric variables**  $\mu_k$  and  $\nu_k$  (Figures 4.5(d) & 4.5(e)) for 14 ellipsoidal HOPF oscillators, interacting through a Hexahedron network.

community are on the six left pentagons whereas the MATHEWS-LAKSHMANAN oscillators occupy the right hand side vertices. The **coupling and parametric dynamics** are defined in Example 4.1. The radii are  $r_{ML} = \frac{1}{2}$ . We choose the coupling strengths and susceptibility constants as  $c_k = 1$  and  $s_{\omega_k} = 1$  for all  $k$ .

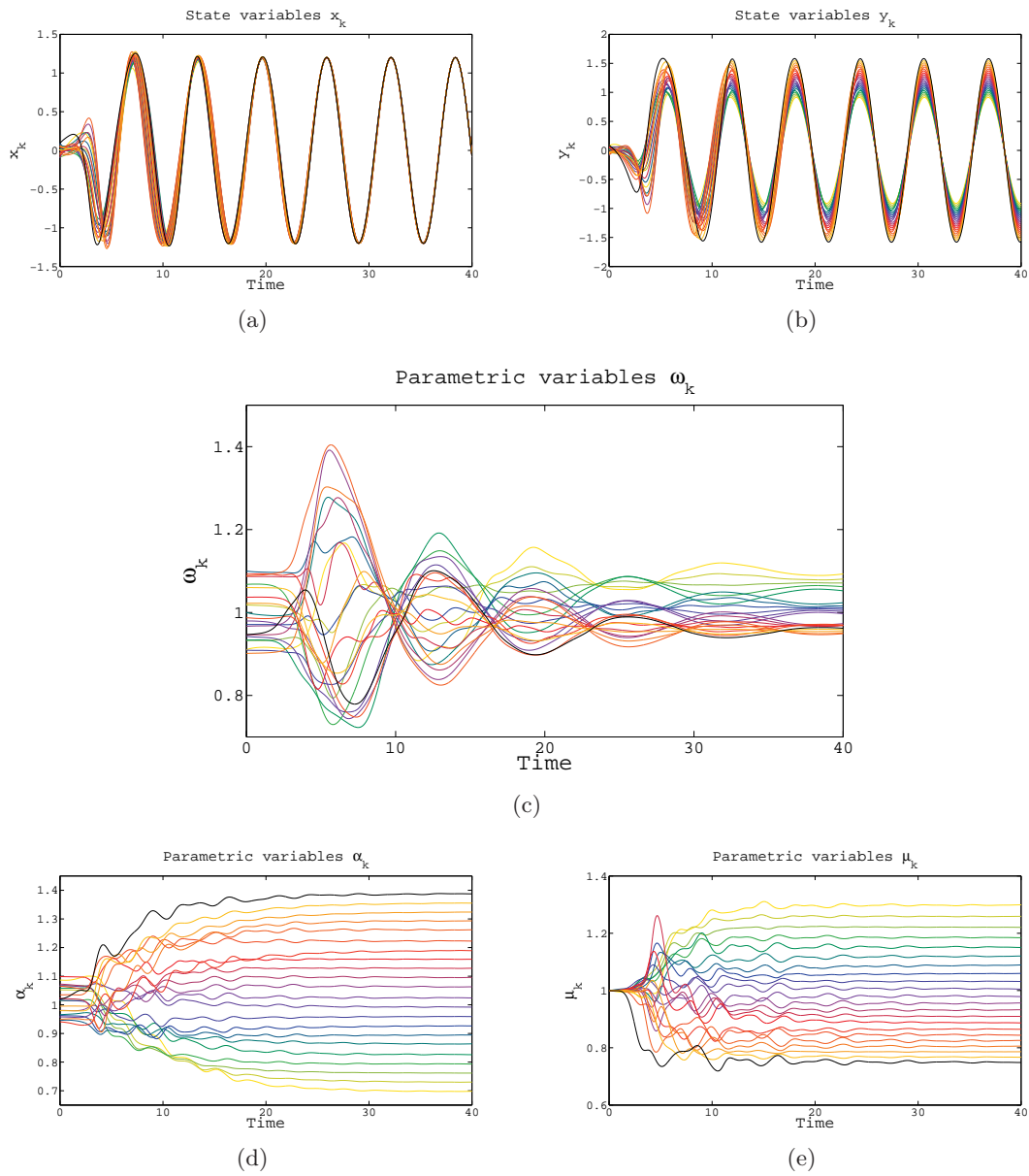
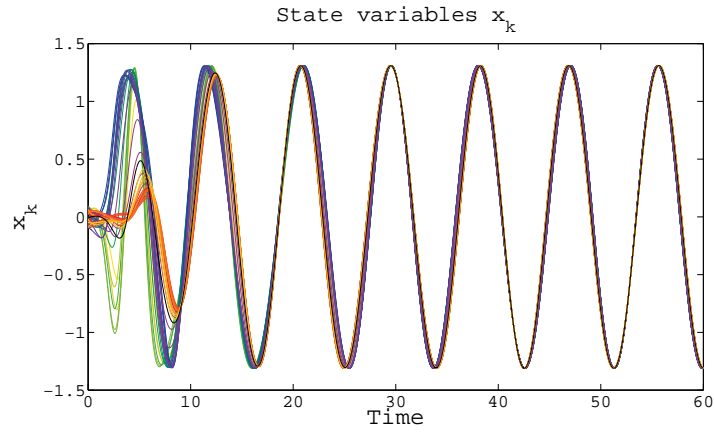
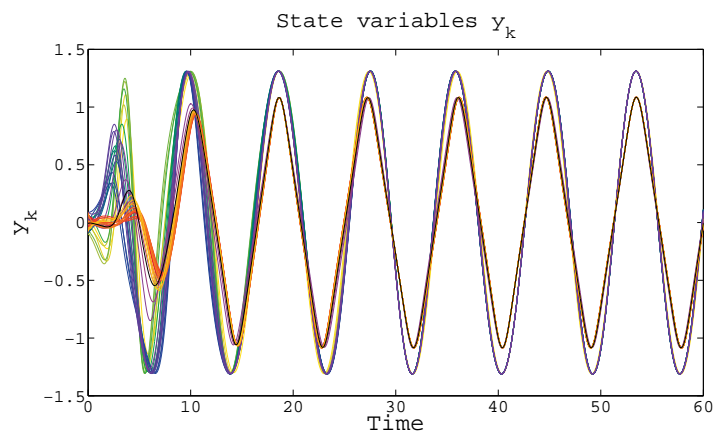


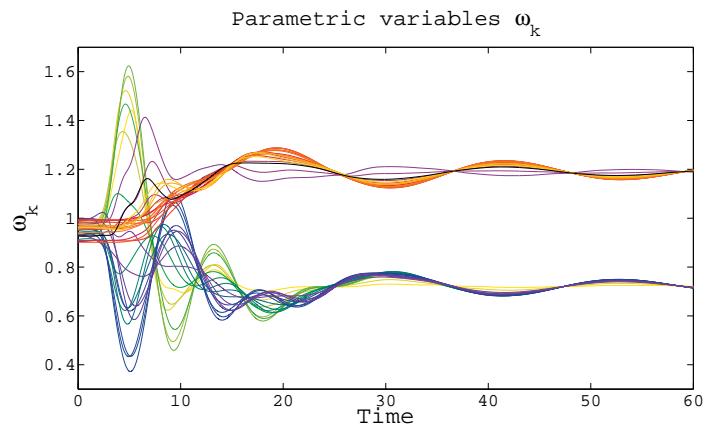
Fig. 4.6: Time evolution of the **state variables**  $x_k$  and  $y_k$  (Figures 4.6(a) & 4.6(b)), the **parametric variables**  $\omega_k$  and  $\alpha_k$  (Figures 4.6(c) & 4.6(d)) and the **coupling parametric variables**  $\mu_k$  (Figure 4.6(e)) for 22 ellipsoidal HOPF oscillators, interacting through a Icosahedron network.



(a)



(b)



(c)

Fig. 4.7: Time evolution of the **state variables**  $x_k$  and  $y_k$  (Figures 4.7(a) & 4.7(a)) and the **parametric variables**  $\omega_k$  (Figure 4.7(c)) for 19 HOPF oscillators and 19 MATHEWS-LAKSHMANAN oscillators, interacting through a Dodecahedron network.



## Time-dependent Networks of Hopf Oscillators with Adapting Frequencies and Radii

Comprenez, [...], que le mécanisme de nos âmes humaines - c'est le mécanisme de la balançoire, où le plus grand envol vers la Noblesse de l'Esprit entraîne le plus grand mouvement en retour vers la fureur de la bête.

M. AGUÉEV

In this chapter, the complex dynamical system is composed of two  $N$ -vertex networks, both with time-dependent edges. The first one affects the **state variables** while the second network couples the **parametric variables**. The **local dynamics** are 2-dimensional HOPF oscillators. The **coupling dynamics** derives from the gradient of a time-dependent Laplacian potential (i.e. time-dependent diffusive coupling). Adaptation occurs in the **local dynamics**. Here, flow parameters (i.e. frequency) as well as geometric parameters (i.e. radii) are allowed to adapt.

### 5.1 Network's Dynamical System

The constituent parts that compose the global system are

$$\begin{aligned}
 \dot{x}_k &= \omega_k y_k - (x_k^2 + y_k^2 - \rho_k) x_k - c \sum_{j=1}^N l_{k,j}^s(t) x_j \\
 \dot{y}_k &= \underbrace{-\omega_k x_k - (x_k^2 + y_k^2 - \rho_k) y_k}_{\text{local dynamics}} - \underbrace{c \sum_{j=1}^N l_{k,j}^s(t) y_j}_{\text{coupling dynamics}} \\
 \dot{\omega}_k &= -s_\omega \sum_{j=1}^N l_{k,j}^p(t) (x_j y_k - y_j x_k) \\
 \dot{\rho}_k &= \underbrace{-s_\rho \sum_{j=1}^N l_{k,j}^p(t) (x_k^2 + y_k^2)}_{\text{parametric dynamics}}
 \end{aligned} \quad k = 1, \dots, N \quad (5.1)$$

**Local Dynamics** Local systems are HOPF oscillators belonging to the class of MCD systems (refer to Section 5.1.1).

**Coupling Dynamics** The gradient of a time-dependent Laplacian potential characterizes the interactions of the **state variables** (refer to Section 5.1.2).

**Parametric Dynamics** Adaptive mechanisms are introduced through an additional time-dependent network that determines the interactions of the **parametric variables** (refer to Section 5.1.3).

#### 5.1.1 Local Dynamics: $L_k$

The **local dynamics** are chosen to be HOPF oscillators as presented in Example (1.1) (i.e. belonging to the class Mixed Canonical-Dissipative (MCD) systems) and for which we recall their dynamics

$$\begin{aligned}
L_1(X_k; \Lambda_k) &:= \quad \mathbf{w}_k y_k \quad - \quad (x_k^2 + y_k^2 - r_k) x_k \\
L_2(X_k; \Lambda_k) &:= \quad \underbrace{-\mathbf{w}_k x_k}_{\text{canonical evolution}} \quad - \quad \underbrace{(x_k^2 + y_k^2 - r_k) y_k}_{\text{dissipative evolution}}
\end{aligned} \quad k = 1, \dots, N, \quad (5.2)$$

with state variables  $X_k = (x_k, y_k)$  and, for the time being,  $\Lambda_k = \{\mathbf{w}_k, r_k\}$  fixed and constant parameters. The *dissipative evolution* drives all orbits towards the circular limit cycle defined by  $\mathcal{L}_{r_k} := \{X \in \mathbb{R}^2 \mid x^2 + y^2 - r_k = 0\}$ . The *canonical evolution* produces a  $\mathbf{w}_k$ -frequency oscillation.

### 5.1.2 Coupling Dynamics: $L_k$

Let  $L^s(t)$  be a Laplacian matrix associated to a connected and undirected time-dependent network with positive adjacency entries (refer to Appendix C), that is  $0 \leq a_{k,j}^s(t) = a_{j,k}^s(t) < b$ . The superscript  $s$  stands for the underlying network responsible for the interactions of the **state variables**  $x_k$  and  $y_k$ . The **coupling dynamics** will be defined by the gradient of the Laplacian potential (refer to Example (1.5))  $V(X) = \frac{1}{2}(\langle x \mid L^s(t)x \rangle + \langle y \mid L^s(t)y \rangle)$  with  $x = (x_1, \dots, x_N)$  (idem for  $y$ ). Explicitly, the coupling to be considered is

$$\begin{aligned}
C_{k,1}(t, X) &:= -c \sum_{j=1}^N l_{k,j}^s(t) x_j, \\
C_{k,2}(t, X) &:= -c \sum_{j=1}^N l_{k,j}^s(t) y_j,
\end{aligned}$$

where  $c > 0$  is a strictly positive, fixed and constant *coupling strength* and  $l_{k,j}^s(t)$  are the entries of  $L^s(t)$ .

### 5.1.3 Parametric Dynamics: $P_k$

From now on,  $\omega_k$  are f-PV and  $\rho_k$  are g-PV (refer to Section 1.2.1). **Parametric variables**  $\omega_k$  and  $\rho_k$  will interact through a network that differs from the one of the **state variables**. As for the network for the **state variables**, this network is connected, undirected and time-dependent with positive bounded adjacency entries (refer to Appendix C), that is  $0 \leq a_{k,j}^p(t) = a_{j,k}^p(t) < b$ . The superscript  $p$  stands for the **parametric variable** network. Its associated Laplacian matrix is denoted as  $L^p(t)$ .

Following the ideas presented in Section 2.1.3.1 and Section 3.1.3.2 respectively, the **parametric dynamics** read

$$\begin{aligned}
\dot{\omega}_k &= -s_\omega \sum_{j=1}^N l_{k,j}^p(t) (x_j y_k - y_j x_k), \\
\dot{\rho}_k &= -s_\rho \sum_{j=1}^N l_{k,j}^p(t) (x_k^2 + y_k^2),
\end{aligned}$$

where  $0 < s_\omega, s_\rho$  are, respectively, strictly positive, fixed, *susceptibility constants* and  $l_{k,j}^p(t)$  are the entries of  $L^p(t)$ . While the edges of the network are time-dependent, we still have the constants of motion that read, respectively for  $\omega_k$  and  $\rho_k$ , as

$$J_\omega(\omega_1, \dots, \omega_N) := \sum_{k=1}^N \omega_k \quad J_\rho(\rho_1, \dots, \rho_N) := \sum_{k=1}^N \rho_k. \quad (5.3)$$

This is true since both, the symmetric matrix in Lemma D.1 and the symmetric Laplacian in Lemma D.2 (refer to Appendix D) can be directly generalized to a time-dependent matrix respectively. Note that the two constants of motion no longer dependent on the susceptibility constants. This is because, for both  $\omega_k$  and  $\rho_k$ , their respective susceptibility constants are not node-dependent.

## 5.2 Dynamics of the Network

The cylindrical symmetry favors to use polar coordinates leading to (refer to Appendix G)

$$\begin{aligned}
\dot{r}_k &= -(r_k^2 - \rho_k)r_k - \mathbf{c} \sum_{j=1}^N l_{k,j}^s(t) r_j \cos(\phi_k - \phi_j) , \\
\dot{\phi}_k &= -\omega_k + \frac{\mathbf{c}}{r_k} \sum_{j=1}^N l_{k,j}^s(t) r_j \sin(\phi_k - \phi_j) , \\
\dot{\omega}_k &= -\mathfrak{s}_\omega \sum_{j=1}^N l_{k,j}^p(t) r_k r_j \sin(\phi_k - \phi_j) , \\
\dot{\rho}_k &= -\mathfrak{s}_\rho \sum_{j=1}^N l_{k,j}^p(t) r_j^2 ,
\end{aligned}
\tag{5.4}
\quad k = 1, \dots, N .$$

The **local dynamics** and the **parametric variables** evolve as a particular case of Eqs. (3.9). However, Eqs. (5.4) has two underlying networks (one network affects the **state variables** while the second network couples the **parametric variables**), both with time-dependent edges. Thus, from this point of view, it is more general than Eqs. (3.9). This generality does not prevent Eqs. (5.4) to possess two constants of motion as presented in 5.3. Note that the phase  $\phi_k$  in Eqs. (5.4) follows a KURAMOTO type dynamics as in [28] with here time-evolving frequencies, radii and network connections.

Similar to Eqs. (3.9) when the susceptibility constants  $\mathfrak{s}_\omega$  and  $\mathfrak{s}_\rho$  are zero, Eqs. (5.4) is a time-dependent network of coupled HOPF oscillators with different frequencies and amplitudes. In the case of identical frequencies and radii, synchronized orbits exists. For these orbits, the network has no influence on the local oscillators. This implies that the time evolution of the network can be arbitrary (e.g. chaotic, stochastic, etc), local systems will not be affected. As soon as one oscillator is perturbed, the network operates and whether the oscillators will converge back to a consensual state is an issue to be discussed. This has been addressed for network topologies undergoing commutative evolution (i.e.  $L^s(z)L^p(t) = L^p(t)L^s(z)$  for all  $t, z$ ) in [6].

For small mismatches in the local parameters, it is a non-trivial problem to analytically (and even numerically) determine the conditions on  $a_{k,j}^s(t)$  and  $a_{k,j}^p(t)$  for which a synchronized state exists. This especially when the edges have a nontrivial time evolution: as long as the edges keep changing in time, the synchronized state (if reached) will be continuously modified. This is due to the fact that for small mismatches in the local parameters, the synchronized state depends on the network topology.

As in the previous chapters, for non-vanishing susceptibility constants, the adaptive mechanisms tune the frequencies of the oscillators and the radii of their attractors so that, under appropriate conditions depending on the time-dependent networks, the global dynamical system is driven into a consensual oscillatory state for which one has

$$\begin{aligned}
\lim_{t \rightarrow \infty} \|(r_j(t), \phi_j(t)) - \varphi_c(t)\| &= 0 \quad \forall k \quad \text{and} \quad \varphi_c(t) \quad \text{is periodic and defined bellow in 5.6,} \\
\text{and, for } k = 1, \dots, N, \quad \lim_{t \rightarrow \infty} (\omega_k(t), \rho_k(t)) &= (\omega_c, \rho_c) \quad \text{with constant } \omega_c \text{ and } \rho_c .
\end{aligned}
\tag{5.5}$$

Once this state is reached, it is permanent (i.e. even if interactions are switched off, all **local dynamics** still oscillate with the same frequency and same amplitude). The existence of a consensual oscillatory state for non-vanishing susceptibility constants is not a difficult task, and this even with two underlying time-dependent networks. However, the convergence towards this state is not trivial. We now discuss these two issues.

### Existence of a consensual oscillatory state

The dynamical system defined by Eqs. (5.4) admits the periodic solution

$$\varphi_c(t) = (\sqrt{\rho_c}, -\omega_c t + \phi_0), \quad \omega_k(t) = \omega_c \quad \text{and} \quad \rho_k(t) = \rho_c \quad (5.6)$$

where  $\phi_0 \in [0, 2\pi[$ ,  $\omega_c$  and  $\rho_c$  are given constants. The verification is straightforward.

### Convergence towards a consensual oscillatory state

In order to discuss the convergence, we study the first variational equation for the Solution in 5.6 of Eqs. (5.4) and suppose it can be used to determine the stability of Solution in 5.6 (technical issues are discussed in [20]). For this, we need the following assumptions on the topology of the networks and on its time-dependent evolution.

#### Assumptions on the topology of the networks

We consider networks possessing the following two commutative rules

auto-commutation rule  $L^s(z)L^s(t) = L^s(t)L^s(z)$  and  $L^p(z)L^p(t) = L^p(t)L^p(z)$  for all  $t, z$ ,

hetero-commutation rule  $L^s(z)L^p(t) = L^p(t)L^s(z)$  for all  $t, z$ .

Such commutation rules hold in particular for the class of *circulant matrices*, defined as

$$\text{circ}(c_1, \dots, c_N) := \begin{pmatrix} c_1 & c_2 & \cdots & c_N \\ c_N & c_1 & \cdots & c_{N-1} \\ \vdots & \ddots & \ddots & \vdots \\ c_2 & c_3 & \cdots & c_1 \end{pmatrix}.$$

Since we are working with Laplacian matrices related to undirected networks with positive adjacency entries, we are restricted to symmetric circulant matrices with  $c_j \geq 0$  for  $j = 2, \dots, N$ , and  $c_1 = \sum_{j=2}^N c_j$ . The symmetry of the matrix implies

$$\begin{array}{ll} \text{for } N \equiv 0 \pmod{2} & \text{for } N \equiv 1 \pmod{2} \\ c_{2+j} = c_{N-j} \quad j = 0, \dots, \frac{N}{2} - 2 & c_{2+j} = c_{N-j} \quad j = 0, \dots, \frac{N+1}{2} - 2. \\ c_{\frac{N}{2}+1} \text{ no restrictions} & \end{array}$$

A basic property of circulant matrices is precisely that they are diagonalizable by the FOURRIER matrix, so we can analytically express their eigenvalues  $\zeta_j$  (c.f. [11]). For symmetric circulant matrices, we have:

for  $N \equiv 0 \pmod{2}$

$$\zeta_j = c_1 + c_{\frac{N}{2}+1} \cos(\pi(j-1)) + 2 \sum_{k=2}^{\frac{N}{2}} c_k \cos\left(\frac{2\pi}{N}(j-1)(k-1)\right) \quad j = 1, \dots, N, \quad (5.7)$$

for  $N \equiv 1 \pmod{2}$

$$\zeta_j = c_1 + 2 \sum_{k=2}^{\frac{N+1}{2}} c_k \cos\left(\frac{2\pi}{N}(j-1)(k-1)\right) \quad j = 1, \dots, N.$$

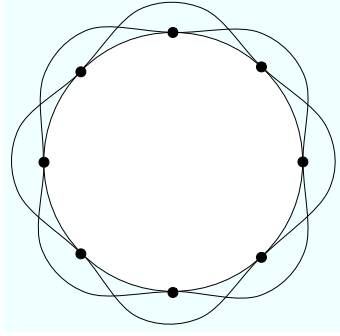
For connected and undirected networks with  $a_{k,j} \in \{0, 1\}$ , an important subclass, with a symmetric circulant matrix as their Laplacian matrix, is the  $(N, k)$  *regular lattices* defined in [36] as

**Definition 5.1.** A  $(N, k)$  *regular lattice* is a  $N$  vertex network with the following two properties

- all vertices have degree  $2k$

- the  $N$  vertices are evenly spaced on a ring in which each vertex is connected to its  $j$  nearest left and right neighbors, where  $j$  varies from 1 to  $k$ .

Every  $(N, k)$  regular lattice can be straightforwardly generalized by introducing time-dependent edges  $a_{k,j}(t)$  while preserving the commutative evolution of the Laplacian matrix. As an example, consider Figure 5.1.



$$L = \text{circ}(0, 1, 1, 0, 0, 0, 1, 1)$$

$$= \begin{pmatrix} 4 & -1 & -1 & 0 & 0 & 0 & -1 & -1 \\ -1 & 4 & -1 & -1 & 0 & 0 & 0 & -1 \\ \vdots & & & \ddots & & \vdots & & \\ -1 & -1 & 0 & 0 & 0 & -1 & -1 & 4 \end{pmatrix}$$

Fig. 5.1: A  $(8, 2)$  regular lattice with its symmetric circulant Laplacian matrix  $L$ .

### Assumptions on the time-dependent evolution

The time-dependent edges of the two networks  $a_{k,j}^s(t)$  and  $a_{k,j}^p(t)$  are sufficiently continuously differentiable functions.

Denote the eigenvalues of  $L^s(t)$  and  $L^p(t)$  by  $\zeta_k^s(t)$  and  $\zeta_k^p(t)$ . Since we here consider connected networks for all  $t$ , the matrices  $L^s(t)$  and  $L^p(t)$  have, respectively, one and only one eigenvalue that is zero for all  $t$ . Without loss of generality, we assume  $\zeta_1^s(t) = \zeta_1^p(t) = 0$  for all  $t$ . For  $k \neq 1$ , these eigenvalues are strictly positive and bounded (since coefficients of  $L^s(t)$  and  $L^p(t)$  are bounded - i.e. there exists  $b > 0$  such that  $0 < \zeta_k^s(t) < b$  and  $0 < \zeta_k^p(t) < b$  for all  $k$  and  $t$ ).

Suppose for each  $k \in \{2, \dots, N\}$ , there exists  $b_k > 0$  and  $b_k^p, b_k^\omega > 0$  such that

$$\begin{aligned} |\dot{\zeta}_k^s(t)| < b_k, \quad |\ddot{\zeta}_k^s(t)| < b_k, \quad |\dot{\zeta}_k^p(t)| < b_k \quad \text{and} \\ b_k^p &\leq 4\rho_c c s_\rho \zeta_k^s(t) \zeta_k^p(t) - b_k(2c^2 \zeta_k^s(t) + c + 2\rho_c s_\rho) \\ b_k^\omega &\leq 2\rho_c c s_\omega \zeta_k^s(t) \zeta_k^p(t) - b_k(2c^2 \zeta_k^s(t) + c + \rho_c s_\omega) \end{aligned} \quad (5.8)$$

The above conditions are satisfied if the time-dependent edges evolve slowly in time (i.e.  $b_k \ll 1$  are small) and the network is strongly connected for all time (i.e. the FIEDLER number is far from zero) with large coupling strengths and susceptibility constants. These conditions corroborate our intuition that well connected networks with slow evolving edges guarantee the convergence in 5.5.

### Linearization

Without loss of generality, we can always define the variables  $\phi_k$  and  $\omega_k$  as

$$\phi_k(t) := -\omega_c t + \phi_0 + \epsilon_{\phi_k}(t) \quad \text{and} \quad \omega_k(t) := \omega_c + \epsilon_{\omega_k}(t) \quad (5.9)$$

for  $\phi_0$  and  $\omega_c$  as in the Solution in 5.6. We then have the following system

$$\begin{aligned}
\dot{r}_k &= -(r_k^2 - \rho_k)r_k - c \sum_{j=1}^N l_{k,j}^s(t) r_j \cos(\epsilon_{\phi_k} - \epsilon_{\phi_j}), \\
\dot{\epsilon}_{\phi_k} &= -\epsilon_{\omega_k} + \frac{c}{r_k} \sum_{j=1}^N l_{k,j}^s(t) r_j \sin(\epsilon_{\phi_k} - \epsilon_{\phi_j}), \\
\dot{\epsilon}_{\omega_k} &= -s_\omega \sum_{j=1}^N l_{k,j}^p(t) r_k r_j \sin(\epsilon_{\phi_k} - \epsilon_{\phi_j}), \\
\dot{\rho}_k &= -s_\rho \sum_{j=1}^N l_{k,j}^p(t) r_j^2,
\end{aligned} \tag{5.10}$$

Eqs. (5.10) admit the fix point solution  $(r_k(t), \epsilon_{\phi_k}(t), \epsilon_{\omega_k}(t), \rho_k(t)) = (\sqrt{\rho_c}, 0, 0, \rho_c)$  for all  $k$ . From now on, we assume that  $\epsilon_{\phi_k}(0)$  and  $\epsilon_{\omega_k}(0)$  are small and we introduce other small perturbations  $\epsilon_{r_k}(0)$  and  $\epsilon_{\rho_k}(0)$  on the other two variables. On account of the constant of motions, we assume that

$$\sum_{j=1}^N \epsilon_{\omega_j}(0) = 0 \quad \text{and} \quad \sum_{j=1}^N \epsilon_{\rho_j}(0) = 0. \tag{5.11}$$

We now have to study the behavior of

$$(r_k(t), \epsilon_{\phi_k}(t), \epsilon_{\omega_k}(t), \rho_k(t)) = (\sqrt{\rho_c} + \epsilon_{r_k}(t), 0 + \epsilon_{\phi_k}(t), 0 + \epsilon_{\omega_k}(t), \rho_c + \epsilon_{\rho_k}(t)).$$

For this, we linearize the vector field given by Eqs. (5.10) around the fix point  $(\sqrt{\rho_c}, 0, 0, \rho_c)$ , and after rearranging the variables, as in 3.18 (i.e. the first  $N$  are the  $r_k$ , the second  $N$  are  $\epsilon_{\phi_k}$ , the third  $N$  are  $\epsilon_{\omega_k}$  and finally the last  $N$  are  $\rho_k$ ), we have

$$\begin{pmatrix} \dot{\epsilon}_r \\ \dot{\epsilon}_\phi \\ \dot{\epsilon}_\omega \\ \dot{\epsilon}_\rho \end{pmatrix} = \begin{pmatrix} -2\rho_c Id - cL^s(t) & \mathbf{0} & \mathbf{0} & \sqrt{\rho_c} Id \\ \mathbf{0} & -cL^s(t) & -Id & \mathbf{0} \\ \mathbf{0} & \rho_c s_\omega L^p(t) & \mathbf{0} & \mathbf{0} \\ -2\sqrt{\rho_c} s_\rho L^p(t) & \mathbf{0} & \mathbf{0} & \mathbf{0} \end{pmatrix} \begin{pmatrix} \epsilon_r \\ \epsilon_\phi \\ \epsilon_\omega \\ \epsilon_\rho \end{pmatrix}, \tag{5.12}$$

with  $\epsilon_r := (\epsilon_{r_1}, \dots, \epsilon_{r_N})$ ,  $\epsilon_\phi := (\epsilon_{\phi_1}, \dots, \epsilon_{\phi_N})$ ,  $\epsilon_\omega := (\epsilon_{\omega_1}, \dots, \epsilon_{\omega_N})$  and  $\epsilon_\rho := (\epsilon_{\rho_1}, \dots, \epsilon_{\rho_N})$  and where  $Id$  is the identity.

### Diagonalization

Since both  $L^s(t)$  and  $L^p(t)$  are symmetric for all  $t$  and because of the commutative evolution rules, there exists an orthogonal matrix  $O$  with real entries, time-independent that simultaneously diagonalizes  $L^s(t)$  and  $L^p(z)$  for all  $t$  and  $z$  (c.f. [25]). That is

$\exists O$  an orthogonal matrix (i.e.  $O^\top O = O O^\top = Id$ ) with real entries such that

$$O^\top L^s(t) O = D(\zeta^s(t)) \quad \forall t \quad \text{and} \quad O^\top L^p(z) O = D(\zeta^p(z)) \quad \forall z,$$

with diagonal matrices  $D(\zeta^s(t))$  and  $D(\zeta^p(z))$  having, respectively, on their diagonals, the spectrum  $\zeta_k^s(t)$  and  $\zeta_k^p(z)$  ( $k = 1, \dots, N$ ) of  $L^s(t)$  and  $L^p(z)$ . As  $O$  is time-independent, for a change of variable  $(\varepsilon_r, \varepsilon_\phi, \varepsilon_\omega, \varepsilon_\rho) := (O^\top \epsilon_r, O^\top \epsilon_\phi, O^\top \epsilon_\omega, O^\top \epsilon_\rho)$  we have  $(\dot{\varepsilon}_r, \dot{\varepsilon}_\phi, \dot{\varepsilon}_\omega, \dot{\varepsilon}_\rho) := (O^\top \dot{\epsilon}_r, O^\top \dot{\epsilon}_\phi, O^\top \dot{\epsilon}_\omega, O^\top \dot{\epsilon}_\rho)$ . Therefore, changing the basis of System 5.12 with a  $4 \times 4$  bloc matrix (each bloc of size  $N \times N$ ) with  $O^\top$  on its diagonal, we obtain

$$\begin{pmatrix} \dot{\varepsilon}_r \\ \dot{\varepsilon}_\phi \\ \dot{\varepsilon}_\omega \\ \dot{\varepsilon}_\rho \end{pmatrix} = \begin{pmatrix} -2\rho_c Id - cD(\zeta^s(t)) & \mathbf{0} & \mathbf{0} & \sqrt{\rho_c} Id \\ \mathbf{0} & -cD(\zeta^s(t)) & -Id & \mathbf{0} \\ \mathbf{0} & \rho_c s_\omega D(\zeta^p(t)) & \mathbf{0} & \mathbf{0} \\ -2\sqrt{\rho_c} s_\rho D(\zeta^p(t)) & \mathbf{0} & \mathbf{0} & \mathbf{0} \end{pmatrix} \begin{pmatrix} \varepsilon_r \\ \varepsilon_\phi \\ \varepsilon_\omega \\ \varepsilon_\rho \end{pmatrix},$$

which is reducible to  $2N$  2-dimensional systems of the form

$$\begin{pmatrix} \dot{\varepsilon}_{r_k} \\ \dot{\varepsilon}_{\rho_k} \end{pmatrix} = \begin{pmatrix} -2\rho_c - c\zeta_k^s(t) & \sqrt{\rho_c} \\ -2\sqrt{\rho_c}s_\rho\zeta_k^p(t) & 0 \end{pmatrix} \begin{pmatrix} \varepsilon_{r_k} \\ \varepsilon_{\rho_k} \end{pmatrix}, \quad \begin{pmatrix} \dot{\varepsilon}_{\phi_k} \\ \dot{\varepsilon}_{\omega_k} \end{pmatrix} = \begin{pmatrix} -c\zeta_k^s(t) & -1 \\ \rho_c s_\omega \zeta_k^p(t) & 0 \end{pmatrix} \begin{pmatrix} \varepsilon_{\phi_k} \\ \varepsilon_{\omega_k} \end{pmatrix}. \quad (5.13)$$

We first study the 2-dimensional systems for  $k \neq 1$ . We rewrite Eqs. (5.13) as linear second order differential equations with time-dependent coefficients

$$\begin{aligned} \ddot{\varepsilon}_{r_k} + (2\rho_c + c\zeta_k^s(t))\dot{\varepsilon}_{r_k} + (2\rho_c s_\rho \zeta_k^p(t) + c\dot{\zeta}_k^s(t))\varepsilon_{r_k} &= 0, \\ \ddot{\varepsilon}_{\phi_k} + c\zeta_k^s(t)\dot{\varepsilon}_{\phi_k} + (\rho_c s_\omega \zeta_k^p(t) + c\dot{\zeta}_k^s(t))\varepsilon_{\phi_k} &= 0. \end{aligned} \quad (5.14)$$

The general form of these equations is

$$\ddot{x} + a_1(t)\dot{x} + a_0(t)x = 0. \quad (5.15)$$

Despite the linearity of Eq. (5.15), the asymptotic stability of the zero solution (i.e  $x(t) = 0$ ) requires care due to the time-dependence of  $a_1(t)$  and  $a_0(t)$ . At this step, we invoke Theorem 1.8 from [14] which requires the following conditions on the time-dependent coefficients

$$\begin{aligned} \exists \bar{b} > 0 \text{ such that } \forall t, \quad |\dot{a}_0(t)| + |a_1(t)| &\leq \bar{b} \\ \exists \underline{b} > 0 \text{ such that } \forall t, \quad 0 < \underline{b} &\leq \dot{a}_0(t) + 2a_0(t)a_1(t) \end{aligned} \quad (5.16)$$

Let us verify the conditions in 5.16 for Eqs. (5.14). The first line of the Inequalities in 5.8 implies that

$$\begin{aligned} |2\rho_c s_\rho \dot{\zeta}_k^p(t) + c\ddot{\zeta}_k^s(t)| + |2\rho_c + c\zeta_k^s(t)| &\leq 2\rho_c s_\rho |\dot{\zeta}_k^p(t)| + c|\ddot{\zeta}_k^s(t)| + 2\rho_c + c|\zeta_k^s(t)| \\ &< 2\rho_c (s_\rho b_k + 1) + c(b_k + b) \\ |\rho_c s_\omega \dot{\zeta}_k^p(t) + c\ddot{\zeta}_k^s(t)| + |c\zeta_k^s(t)| &\leq \rho_c s_\omega |\dot{\zeta}_k^p(t)| + c|\ddot{\zeta}_k^s(t)| + c|\zeta_k^s(t)| \\ &< \rho_c s_\omega b_k + c(b_k + b). \end{aligned}$$

This verifies the first condition in 5.16. For the second condition, consider again the first line of the Inequalities in 5.8 which leads to

$$\begin{aligned} -b_k 2c^2 \zeta_k^s(t) < \dot{\zeta}_k^s(t) 2c^2 \zeta_k^s(t) &\iff -b_k < \dot{\zeta}_k^s(t) \iff -b_k 2c^2 \zeta_k^s(t) < \dot{\zeta}_k^s(t) 2c^2 \zeta_k^s(t) \\ -b_k c < \ddot{\zeta}_k^s(t) c &\iff -b_k < \ddot{\zeta}_k^s(t) \iff -b_k c < \ddot{\zeta}_k^s(t) c \\ -b_k 2\rho_c s_\rho < \dot{\zeta}_k^p(t) 2\rho_c s_\rho &\iff -b_k < \dot{\zeta}_k^p(t) \iff -b_k \rho_c s_\omega < \dot{\zeta}_k^p(t) \rho_c s_\omega. \end{aligned} \quad (5.17)$$

The left column in 5.17 together with the Inequality for  $b_k^\rho$  in 5.8 implies

$$\begin{aligned} b_k^\rho &\leq 4\rho_c c s_\rho \zeta_k^s(t) \zeta_k^p(t) - b_k (2c^2 \zeta_k^s(t) + c + 2\rho_c s_\rho) \\ &< 4\rho_c c s_\rho \zeta_k^s(t) \zeta_k^p(t) + \dot{\zeta}_k^s(t) 2c^2 \zeta_k^s(t) + \ddot{\zeta}_k^s(t) c + \dot{\zeta}_k^p(t) 2\rho_c s_\rho \\ &= 2\rho_c s_\rho \dot{\zeta}_k^p(t) + c\ddot{\zeta}_k^s(t) + 2(2\rho_c s_\rho \zeta_k^p(t) + c\dot{\zeta}_k^s(t)) (c\zeta_k^s(t)) \\ &< 2\rho_c s_\rho \dot{\zeta}_k^p(t) + c\ddot{\zeta}_k^s(t) + 2(2\rho_c s_\rho \zeta_k^p(t) + c\dot{\zeta}_k^s(t)) (c\zeta_k^s(t)) + \underbrace{2(2\rho_c s_\rho \zeta_k^p(t) + c\dot{\zeta}_k^s(t)) (2\rho_c)}_{>0} \\ &= 2\rho_c s_\rho \dot{\zeta}_k^p(t) + c\ddot{\zeta}_k^s(t) + 2(2\rho_c s_\rho \zeta_k^p(t) + c\dot{\zeta}_k^s(t)) (2\rho_c + c\zeta_k^s(t)) \end{aligned}$$

Thus the second condition in 5.16 for the top Eqs. (5.14) is verified. The right column in 5.17 together with the Inequality for  $b_k^\omega$  in 5.8 implies

$$\begin{aligned} b_k^\omega &\leq 2\rho_c c s_\omega \zeta_k^s(t) \zeta_k^p(t) - b_k (2c^2 \zeta_k^s(t) + c + \rho_c s_\omega) \\ &< 2\rho_c c s_\omega \zeta_k^s(t) \zeta_k^p(t) + \dot{\zeta}_k^s(t) 2c^2 \zeta_k^s(t) + \ddot{\zeta}_k^s(t) c + \dot{\zeta}_k^p(t) \rho_c s_\omega \\ &= \rho_c s_\omega \dot{\zeta}_k^p(t) + c\ddot{\zeta}_k^s(t) + 2(c\zeta_k^s(t)) (\rho_c s_\omega \zeta_k^p(t) + c\dot{\zeta}_k^s(t)) \end{aligned}$$

Hence the second condition in 5.16 for the bottom Eqs. (5.14) is verified. Therefore, under the assumptions for the time-dependent edges in 5.8 and the use of Theorem 1.8 from [14], we conclude

$$\lim_{t \rightarrow \infty} \varepsilon_{r_k}(t) = \lim_{t \rightarrow \infty} \varepsilon_{\phi_k}(t) = \lim_{t \rightarrow \infty} \varepsilon_{\rho_k}(t) = \lim_{t \rightarrow \infty} \varepsilon_{\omega_k}(t) = 0 \quad \forall k \neq 1. \quad (5.18)$$

For  $k = 1$ ,  $\zeta_1^s(t) = \zeta_1^p(t) = 0$  for all  $t$ . Therefore, from Eqs. (5.13) we have

$$\dot{\varepsilon}_{r_1} = -2\rho_c \varepsilon_{r_1} + \sqrt{\rho_c} \varepsilon_{\rho_1}, \quad \dot{\varepsilon}_{\rho_1} = 0 \quad \text{and} \quad \dot{\varepsilon}_{\phi_1} = -\varepsilon_{\omega_1}, \quad \dot{\varepsilon}_{\omega_1} = 0$$

and so  $\varepsilon_{\rho_1}(t) = \varepsilon_{\rho_1}(0)$  and  $\varepsilon_{\omega_1}(t) = \varepsilon_{\omega_1}(0)$  for all  $t$ . Both of these constants  $\varepsilon_{\rho_1}(0)$  and  $\varepsilon_{\omega_1}(0)$  are zero. This is because the first orthonormal base vector is  $\frac{1}{\sqrt{N}}(1, \dots, 1)$  and the first coordinates of the product  $O^\top \varepsilon_\rho$  and  $O^\top \varepsilon_\omega$  are

$$\varepsilon_{\rho_1}(0) = \frac{1}{\sqrt{N}} \sum_{j=1}^N \varepsilon_{\rho_j}(0) = 0 \quad \text{and} \quad \varepsilon_{\omega_1}(0) = \frac{1}{\sqrt{N}} \sum_{j=1}^N \varepsilon_{\omega_j}(0) = 0.$$

These two sums are due to Eqs. (5.11) (i.e. constant of motions). Therefore,  $\dot{\varepsilon}_{r_1} = -2\rho_c \varepsilon_{r_1}$  (i.e.  $\lim_{t \rightarrow \infty} \varepsilon_{r_1}(t) = 0$ ) and  $\varepsilon_{\phi_1}(t) = \varepsilon_{\phi_1}(0)$  for all  $t$ . This allows to conclude that all perturbations  $\varepsilon_{r_k}, \varepsilon_{\rho_k}$  and  $\varepsilon_{\omega_k}$  decay for all  $k$ . We now need to study how the perturbations on the phases evolve. Since  $O\varepsilon_\phi = \varepsilon_\phi$ , then  $\sum_{j=1}^N o_{k,j} \varepsilon_{\phi_j} = \varepsilon_{\phi_k}$  for all  $k$  and with  $o_{k,j}$  standing for the entries of  $O$ . With Limits in 5.18, these sums become

$$\lim_{t \rightarrow \infty} \varepsilon_{\phi_k}(t) = \lim_{t \rightarrow \infty} \sum_{j=1}^N o_{k,j} \varepsilon_{\phi_j}(t) = o_{k,1} \varepsilon_{\phi_1}(t) = \frac{1}{\sqrt{N}} \varepsilon_{\phi_1}(0) = \frac{1}{N} \sum_{j=1}^N \varepsilon_{\phi_j}(0)$$

since  $o_{k,1} = \frac{1}{\sqrt{N}}$  ( $k = 1, \dots, N$ ) are the coordinates of the first orthonormal base vector and the first coordinate of the product  $O^\top \varepsilon_\phi$  is  $\varepsilon_{\phi_1}(0) = \frac{1}{\sqrt{N}} \sum_{j=1}^N \varepsilon_{\phi_j}(0)$ . Hence all perturbations converge towards zero except those on the phase that all converge towards a constant (i.e. average phase perturbation). This corresponds to a phase shift. Therefore, the system converges towards a consensual oscillatory state.

### 5.2.0.1 Time-independent Case

Consider Eqs. 5.4 when the two underlying networks are identical and time independent. Let the coupling strengths and susceptibility constants be node dependent and related among themselves as in 3.20. Let  $\kappa_k$  be the eigenvalues of  $K^{\frac{1}{2}} L K^{\frac{1}{2}}$  where  $L$  is the associated Laplacian matrix and  $K$  is a diagonal matrix with entries  $k_k$  (c.f. Lemma 3.1). Eqs. 5.13 then becomes

$$\begin{pmatrix} \dot{\varepsilon}_{r_k} \\ \dot{\varepsilon}_{\rho_k} \end{pmatrix} = \begin{pmatrix} -2\rho_c - c\kappa_k & \sqrt{\rho_c} \\ -2\sqrt{\rho_c} s_\rho \kappa_k & 0 \end{pmatrix} \begin{pmatrix} \varepsilon_{r_k} \\ \varepsilon_{\rho_k} \end{pmatrix}, \quad \begin{pmatrix} \dot{\varepsilon}_{\phi_k} \\ \dot{\varepsilon}_{\omega_k} \end{pmatrix} = \begin{pmatrix} -c\kappa_k & -1 \\ \rho_c s_\omega \kappa_k & 0 \end{pmatrix} \begin{pmatrix} \varepsilon_{\phi_k} \\ \varepsilon_{\omega_k} \end{pmatrix}.$$

The respective eigenvalues of the above matrices are

$$\xi_{k,\pm}^\rho = \frac{-(2\rho_c + c\kappa_k) \pm \sqrt{(2\rho_c + c\kappa_k)^2 - 8\rho_c s_\rho \kappa_k}}{2}, \quad \xi_{k,\pm}^\omega = \frac{-c\kappa_k \pm \sqrt{(c\kappa_k)^2 - 4\rho_c s_\omega \kappa_k}}{2}.$$

The eigenvalues  $\xi_{k,\pm}^\rho$  and  $\xi_{k,\pm}^\omega$  determine the decay rate of the perturbations. Observe that these explicitly depend on the spectrum  $\kappa_k$  of the Laplacian matrix. Hence, the FIEDLER number, characterizing the connectivity of the network, controls the convergence rate.

It is important to remark that one can still explicitly calculate  $\xi_{k,\pm}^\rho$  and  $\xi_{k,\pm}^\omega$  for the time-dependent case (i.e. for Eqs. 5.13 - two networks with auto- and hetero-commutation and, coupling strengths and susceptibility constants not node dependent). In this case,  $\xi_{k,\pm}^\rho$  and  $\xi_{k,\pm}^\omega$  become time-dependent as well but the sign of their real parts would not change



$$\Re(\xi_{k,\pm}^\rho(t)) < 0 \quad \text{and} \quad \Re(\xi_{k,\pm}^\omega(t)) < 0 \quad \forall t, k \neq 2.$$

One emphasizes that this is however not a sufficient condition to ensure stability (i.e. for all trivial solutions in Eqs. 5.13 to be asymptotically stable). Indeed, ad hoc time-dependent coefficients of linear differential systems may destabilize the trivial solution and this even if the real part of the eigenvalues are strictly negative for all time. We now focus on *parametric resonance*, an example of such destabilization.

### 5.2.1 Parametric Resonance

When  $a_1 \equiv 0$  (i.e. no damping) and  $a_0(t) = f_0(1 + h \cos(2ft))$  in Eq. (5.15), one has the MATHIEU equation

$$\ddot{x} + f_0(1 + h \cos(2ft))x = 0. \quad (5.19)$$

with  $f_0 > 0$  and we suppose that  $h \neq 0$  is small (i.e.  $|h| \ll 1$ ). If  $f = 0$ , Eq. (5.19) reduces to a harmonic oscillator with *eigen* frequency  $\sqrt{f_0(1+h)} \simeq \sqrt{f_0}$ . It is well known (c.f. [20]) that the zero solution ( $x(t) = 0$ ) is unstable when  $\sqrt{f_0} = f$ . This instability is known as *parametric resonance* (*parametric* since it is the *eigen* frequency of the oscillator itself that is subjected to a periodic forcing).

Consider the case when the network for the **state variables** is time-independent (i.e.  $L^s(t) = L^s(0)$  for all  $t$ ) and the network for the **parametric variables** is time-periodic of period  $T$  (i.e.  $L^p(t) = L^p(t+T)$ ). In this case,  $\dot{\zeta}_k^s(t) = 0$  and  $\zeta_k^p(t) = \zeta_k^p(t+T)$ . For  $k \neq 1$ ,  $\zeta_k^p(t) > 0$  for all  $t$  and so, there exist, for each  $k$ ,  $\underline{g}_k > 0$  and  $g_k(t)$  ( $T$ -periodic) such that  $\zeta_k^p(t) = \underline{g}_k(1 + g_k(t))$ . Eqs. (5.14) are now HILL equations with dumping and read

$$\begin{aligned} \ddot{\varepsilon}_{r_k} + (2\rho_c + c\zeta_k^s)\dot{\varepsilon}_{r_k} + 2\rho_c s_\rho \underline{g}_k(1 + g_k(t))\varepsilon_{r_k} &= 0, \\ \ddot{\varepsilon}_{\phi_k} + c\zeta_k^s\dot{\varepsilon}_{\phi_k} + \rho_c s_\omega \underline{g}_k(1 + g_k(t))\varepsilon_{\phi_k} &= 0. \end{aligned} \quad (5.20)$$

When  $g_k(t) := h_k \cos(2f_k t)$  and  $h_k$  are small, Eqs. (5.20) reduce to MATHIEU equations with damping, for which parametric resonance arises whenever

$$\begin{aligned} \text{top equations} \quad 2\rho_c + c\zeta_k^s &\simeq 0 \quad (\text{i.e. negligible}) \quad \text{and} \quad \sqrt{2\rho_c s_\rho \underline{g}_k} = f_k, \\ \text{bottom equations} \quad \frac{c}{\sqrt{\rho_c}}\zeta_k^s &\simeq 0 \quad (\text{i.e. negligible}) \quad \text{and} \quad \sqrt{\rho_c s_\omega \underline{g}_k} = f_k. \end{aligned}$$

For HOPF oscillators with a relatively large consensual radius (i.e.  $\sqrt{\rho_c} \simeq 1$ ), the condition  $2\rho_c + c\zeta_k^s \simeq 0$  will not be satisfied. However, the adaptive frequency mechanism may offer the possibility of destabilizing the network dynamics via parametric resonance phenomena if

- $0 < c \ll 1$  (i.e. weakly coupled **state variables**),
- $\exists k$  such that  $0 < \zeta_k^s \ll 1$  (i.e. network for the **state variables** has a small FIEDLER number),
- $0 < s_\omega \ll 1$  (i.e. small susceptibility constants for the frequency tuning),
- ad hoc time-dependent network.

### 5.2.2 Miscellaneous Remark: Variation in the Interactions

In connection with Chapter 4, we may draw the following remarks. We first consider Eqs. (5.1) with Normalized Gradient coupling functions, for both, the **coupling** and **parametric dynamics** (c.f. 1.6). We then study a collection of homothetic Hopf oscillators in a time-dependent environment but without **binding dynamics**. In both cases, the two networks follow auto- and hetero-commutation rules.

Consider Eqs. (5.1) with Normalized Gradient coupling functions. In polar coordinates and after defining the variables  $\phi_k$  and  $\omega_k$  as in 5.9, we obtain

$$\begin{aligned}
\dot{r}_k &= -(r_k^2 - \rho_k)r_k - c \sum_{j=1}^N l_{k,j}^s(t) \cos(\epsilon_{\phi_k} - \epsilon_{\phi_j}), \\
\dot{\epsilon}_{\phi_k} &= -\epsilon_{\omega_k} + \frac{c}{r_k} \sum_{j=1}^N l_{k,j}^s(t) \sin(\epsilon_{\phi_k} - \epsilon_{\phi_j}), \\
\dot{\omega}_k &= -s_\omega \sum_{j=1}^N l_{k,j}^p(t) \sin(\epsilon_{\phi_k} - \epsilon_{\phi_j}), \\
\dot{\rho}_k &= -s_\rho \sum_{j=1}^N l_{k,j}^p(t) r_j^2,
\end{aligned} \tag{5.21}$$

Eqs. (5.21) admit the fixed point  $(\sqrt{\rho_c}, 0, 0, \rho_c)$ . Proceeding as in Section 5.2 (linearization and diagonalizing), we obtain the first variational equation for the fixed point  $(\sqrt{\rho_c}, 0, 0, \rho_c)$  of Eqs. (5.21)

$$\begin{pmatrix} \dot{\epsilon}_{r_k} \\ \dot{\epsilon}_{\rho_k} \end{pmatrix} = \begin{pmatrix} -2\rho_c & \sqrt{\rho_c} \\ -2\sqrt{\rho_c}s_\rho\zeta_k^p(t) & 0 \end{pmatrix} \begin{pmatrix} \epsilon_{r_k} \\ \epsilon_{\rho_k} \end{pmatrix}, \quad \begin{pmatrix} \dot{\epsilon}_{\phi_k} \\ \dot{\epsilon}_{\omega_k} \end{pmatrix} = \begin{pmatrix} -\frac{c}{\sqrt{\rho_c}}\zeta_k^s(t) & -1 \\ s_\omega\zeta_k^p(t) & 0 \end{pmatrix} \begin{pmatrix} \epsilon_{\phi_k} \\ \epsilon_{\omega_k} \end{pmatrix}. \tag{5.22}$$

We rewrite Eqs. (5.22) as linear second order differential equations with time-dependent coefficients

$$\begin{aligned}
\ddot{\epsilon}_{r_k} + 2\rho_c\dot{\epsilon}_{r_k} + 2\rho_cs_\rho\zeta_k^p(t)\epsilon_{r_k} &= 0, \\
\ddot{\epsilon}_{\phi_k} + \frac{c}{\sqrt{\rho_c}}\zeta_k^s(t)\dot{\epsilon}_{\phi_k} + (\rho_cs_\omega\zeta_k^p(t) + c\dot{\zeta}_k^s(t))\epsilon_{\phi_k} &= 0.
\end{aligned} \tag{5.23}$$

For  $k \neq 1$ , the asymptotic stability of the zero solution is discussed with Theorem 1.8 from [14]. Remark that with this type of coupling, there is no time-dependent coefficient in the friction term in the top line of Eqs. (5.23). For  $k = 1$ , the same arguments follow as in Section 5.2.

Consider now Eqs. (5.21) when  $s_\rho = 0$  (i.e.  $\rho_k$  become fixed parameters with values  $r_k$ ). This corresponds to a time-dependent network of coupled homothetic HOPF oscillators (c.f. 4.1) with Normalized Gradient coupling functions. The system admits the fix point  $(\sqrt{r_k}, 0, 0)$ . This offers an interesting configuration since no coupling weights are required as in Section 4.2.2 even though local system have different Hamiltonian heights. The first variational equation for the fix point  $(\sqrt{r_k}, 0, 0)$  is

$$\begin{pmatrix} \dot{\epsilon}_r \\ \dot{\epsilon}_\phi \\ \dot{\epsilon}_\omega \end{pmatrix} = \begin{pmatrix} -2D(r) & \mathbf{0} & \mathbf{0} \\ \mathbf{0} & -DD(r)^{-\frac{1}{2}}L^s(t) & -Id \\ \mathbf{0} & s_\omega L^p(t) & \mathbf{0} \end{pmatrix} \begin{pmatrix} \epsilon_r \\ \epsilon_\phi \\ \epsilon_\omega \end{pmatrix}, \tag{5.24}$$

with  $\epsilon_r := (\epsilon_{r_1}, \dots, \epsilon_{r_N})$ ,  $\epsilon_\phi := (\epsilon_{\phi_1}, \dots, \epsilon_{\phi_N})$ ,  $\epsilon_\omega := (\epsilon_{\omega_1}, \dots, \epsilon_{\omega_N})$  and diagonal matrices  $D(r)$ ,  $D$  and  $D(r)^{-\frac{1}{2}}$  with respective diagonal  $(r_1, \dots, r_N)$ ,  $(c_1, \dots, c_N)$  and  $(\frac{1}{\sqrt{r_1}}, \dots, \frac{1}{\sqrt{r_N}})$ . The upper left  $N \times N$  bloc in Eqs. (5.24) has  $N$  real negative eigenvalues, thus the radial perturbations decay exponentially.

The remaining four  $N \times N$  blocs may then be diagonalized as in Section 5.2 if the node dependent coupling strength are defined as  $c_k := cr_k$  (for some given  $c > 0$ ). Indeed, we then have  $DD(r)^{-1}L^s(t) = cD(r)D(r)^{-1}L^s(t) = cL^s(t)$ . Hence, the system is reducible to  $N$  2-dimensional systems.

For the case of time-independent networks where the two underlying networks are identical, one can relax the condition on the coupling strength. Indeed, relating the coupling strengths and the susceptible constants as

$$c_k = c \frac{k_k}{r_k} \quad \text{and} \quad s_{\omega_k} = s_\omega \frac{k_k}{r_k} \quad (k_k \text{ are given})$$

insures that the Jacobian is diagonalizable. For both cases (time-dependent and independent), the convergence issues are discussed as in Section 5.2. For more details, refer to [41].

### 5.3 Numerical Simulations

We report three types of numerical simulations. We first consider the case of two time-dependent networks. We then look at the case with constant edges which enables to appreciate the relation between convergence rate and network connectivity. Finally, we show the parametric resonance phenomena at work. As in Section 2.3, the coordinates of  $\mathbf{1s}_{(a,b,N)} \in \mathbb{R}^N$  are defined as  $\mathbf{1s}_{(a,b,N)_j} := a + (j-1)\frac{b-a}{N-1}$ ,  $j = 1, \dots, N$ . In all numerical simulations,  $\rho_k$  is not a g-PV. It is a fixed parameter with value one.

#### 5.3.1 Time-dependent

The **state** and **parametric variables** of six HOPF oscillators are coupled through time-dependent “Krupp” networks (c.f. Figure 5.2). Specifically, the adjacency matrices for the respective networks are  $A^s(t) = \text{circ}(0, 1, \cos(f_s t)^2, 0, \cos(f_s t)^2, 1)$  and  $A^p(t) = \text{circ}(0, 1, \cos(f_p t)^2, 0, \cos(f_p t)^2, 1)$ . The parameters  $f_s$  and  $f_p$  control the switching rate of the second neighbor edge of their respective network. Their values are  $f_s = 0.1$  and  $f_s = 0.15$ . The eigenvalues for the associated Laplacian matrices are

$$\begin{aligned} \zeta_1^\bullet(t) &= 0, & \zeta_4^\bullet(t) &= -4, & \zeta_k^\bullet(t) &= -1 - 3 \cos(f_\bullet t)^2 \quad k = 2, 6, \\ \zeta_k^\bullet(t) &= -3 - 3 \cos(f_\bullet t)^2 \quad k = 3, 5. \end{aligned}$$

The bullet  $\bullet$  stands for **s** and **p** respectively. The coupling strength is once chosen as  $c = \frac{1}{2}$  (c.f. Figure 5.3(a)) and once  $c = 2$  (c.f. Figure 5.3(b)). The susceptibility constant is  $s_\omega = 2$ . The initial conditions for **state variables** are  $x_k(0) = 1$  and  $y_k(0) = 0$  for all  $k$  and for the **parametric variables**  $(\omega_1(0), \dots, \omega_N(0)) = \mathbf{1s}_{(1,1.1,6)}$ . The time evolution for the  $\omega_k$  is shown in Figure 5.3.

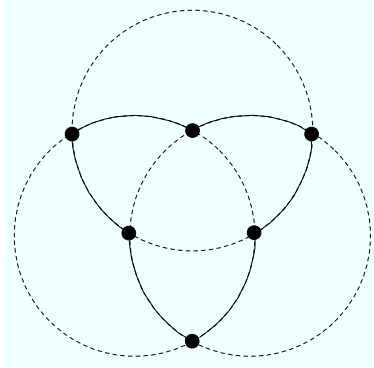
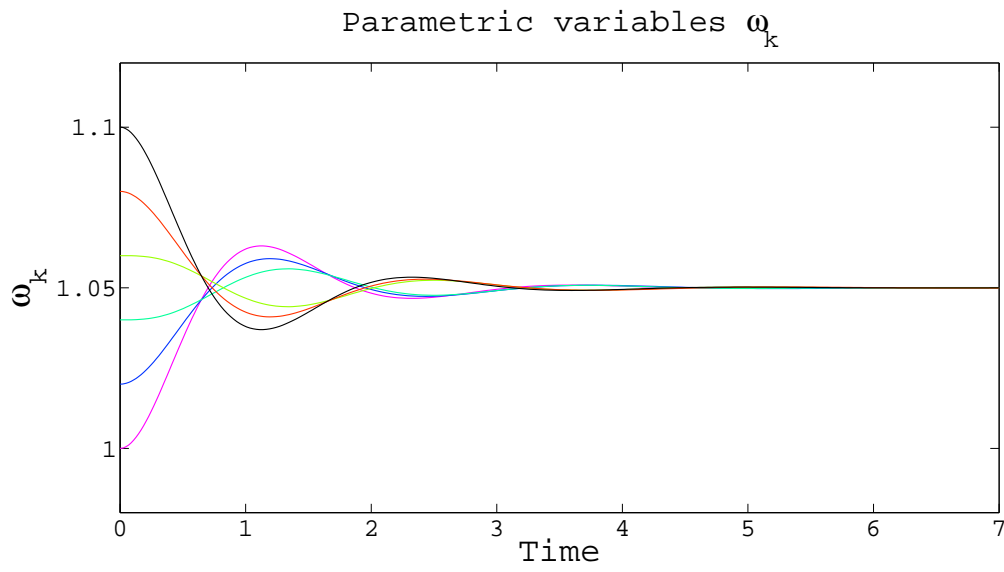


Fig. 5.2: A “Krupp” ((6,2) regular lattice) time-dependent network topology. The dashed lines represent time-dependent edges.

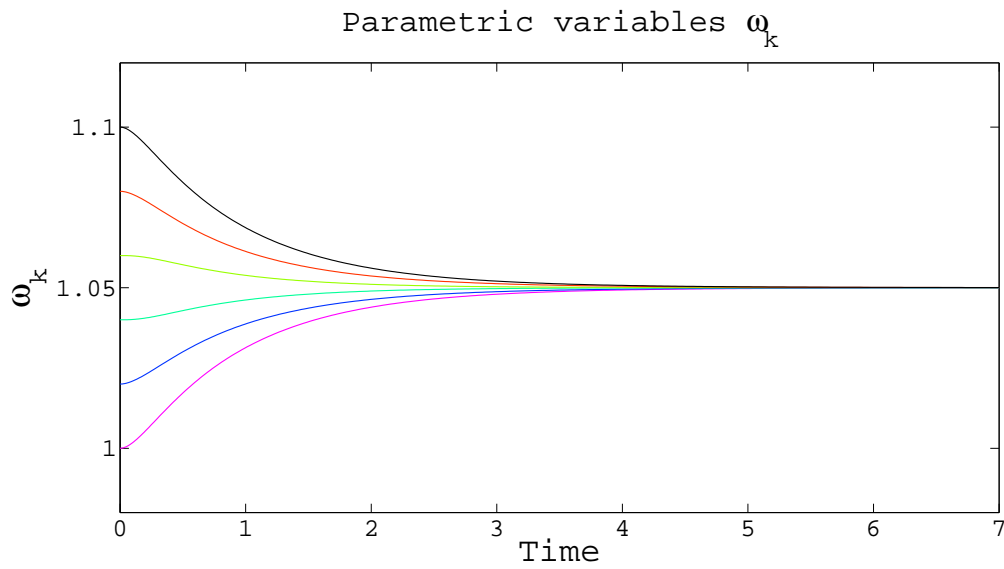
The same simulation is carried out (with identical parameter values and initial conditions) but now the network for the **state variables** has adjacency matrix  $A^s(t) = \text{circ}(0, 1, \cos(f_s t)^2, 1, \cos(f_s t)^2, 1)$  (i.e. “All-to-All” with time-dependent second neighbor edge) where as the network for the **parametric variables** is  $A^p(t) = \text{circ}(0, 1, \cos(f_p t)^2, 0, \cos(f_p t)^2, 1)$  as above. The eigenvalues for the associated Laplacian matrices are, respectively,

$$\begin{aligned} \zeta_1^s(t) &= 0, & \zeta_4^s(t) &= -6, & \zeta_1^p(t) &= 0 & \zeta_4^p(t) &= -6, \\ \zeta_k^s(t) &= -3 - 3 \cos(f_s t)^2 \quad k = 2, 3, 5, 6, & \text{and} & & \zeta_k^p(t) &= -1 - 3 \cos(f_p t)^2 \quad k = 2, 6, \\ & & & & \zeta_k^p(t) &= -3 - 3 \cos(f_p t)^2 \quad k = 3, 5 \end{aligned}$$

The resulting dynamics is found in Figure 5.4.

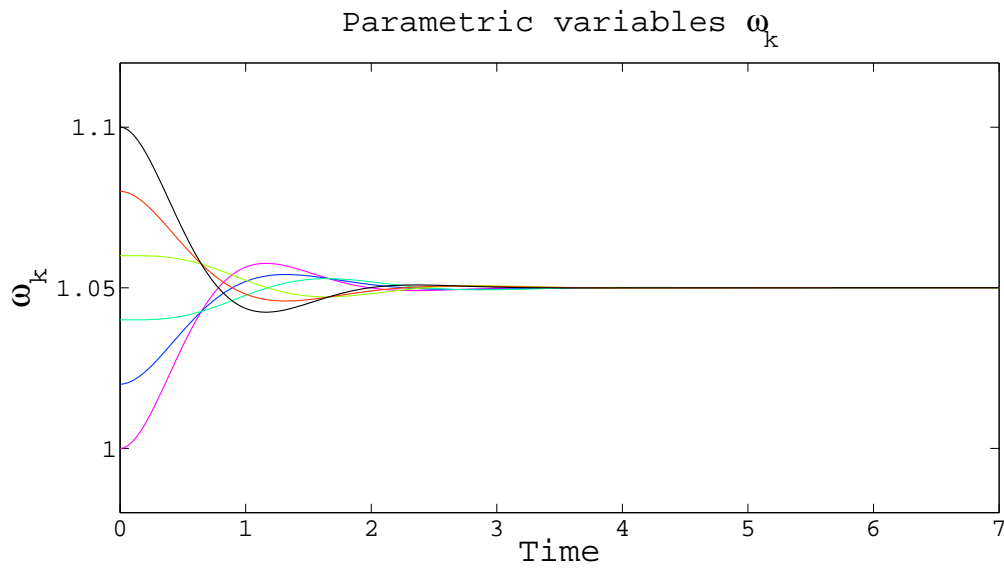


(a)

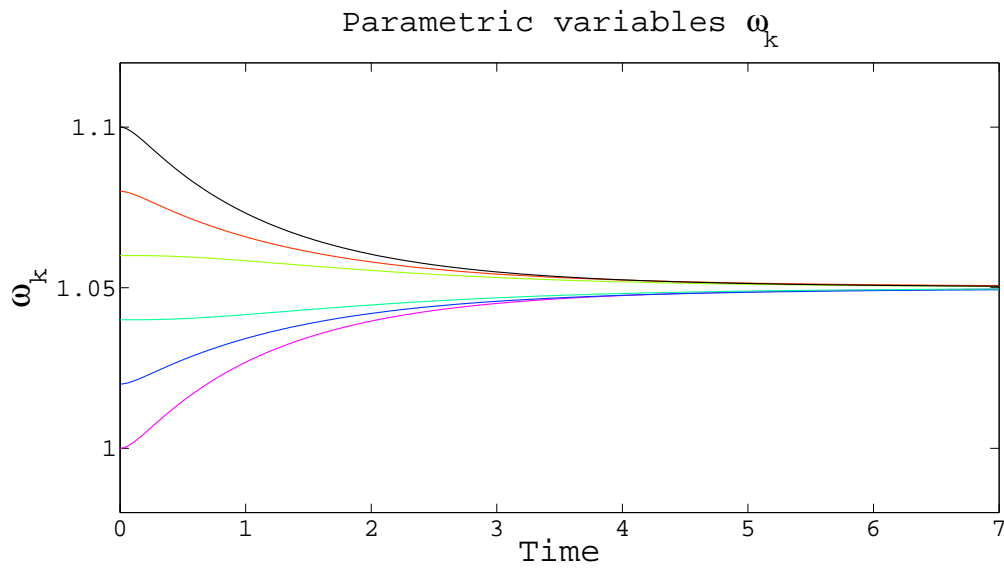


(b)

Fig. 5.3: Time evolution of the parametric variables  $\omega_k$  for six HOPF oscillators, interacting through a “Krupp” network with  $f_p = 0.15$  and susceptibility constant  $s_\omega = 2$ . The network for the state variables is a “Krupp” network with  $f_s = 0.1$ . The coupling strength is  $c = \frac{1}{2}$  in Figure 5.3(a) and  $c = 2$  in Figure 5.3(b).



(a)



(b)

Fig. 5.4: Time evolution of the parametric variables  $\omega_k$  for six HOPF oscillators, interacting through a “Krupp” network with  $f_p = 0.15$  and susceptibility constant  $s_\omega = 2$ . The network for the state variables is a “All-to-All” network with  $f_s = 0.1$ . The coupling strength is  $c = \frac{1}{2}$  in Figure 5.4(a) and  $c = 2$  in Figure 5.4(b).

Remark that the  $\omega_k$  in Figure 5.4(b) converge towards the consensual value  $\omega_c = 1.05$  slower than in all other three Figures. However, the set up in Figure 5.4(b) would at first sight suggest that the rate of convergence should be the fastest. Indeed, compare to the configuration in Figure 5.3, it has a better connected network for its **state variables**. In comparison with Figure 5.4(a), its coupling strength is four times larger. We therefore point out that we here cannot simply rely on connectivity properties of the networks to characterize convergence rates.

### 5.3.2 Time-independent

In Figure 5.6 we report numerical simulations performed with five HOPF oscillators. Here, **state** and **parametric variables** are coupled through the same time-independent network. Three different network topologies are considered: “All-to-All”, “All-to-One” and “Crystal” (c.f. Figure 5.5). For the “All-to-One” network, vertex 1 is connected to all the others. For the “Crystal” network, the numbering of the vertices is: vertex 1 to 4 are on the four corners of the square, starting from the top left corner and vertex 5 is in the middle of the square. The coupling strengths are chosen as  $c_k = 0.5$  for all  $k$  and the susceptibility constants as  $s_{\omega_1} = 4$ ,  $s_{\omega_2} = 2$ ,  $s_{\omega_3} = 5$ ,  $s_{\omega_4} = 20$ ,  $s_{\omega_5} = \frac{4}{3}$ . The initial conditions for **state variables** are  $x_k(0) = 1$  and  $y_k(0) = 0$  for all  $k$  and for the **parametric variables**  $\omega_1(0) = 9$ ,  $\omega_2(0) = 5.35$ ,  $\omega_3(0) = 6.5$ ,  $\omega_4(0) = 5$ ,  $\omega_5(0) = 7.7$ . The adaptive mechanism can be observed in Figure 5.6. All three figures have the same time scale, so we can fully appreciate the fact that the larger algebraic connectivity, the faster the convergence. Thus here the convergence rate explicitly depends on the topology of the network.

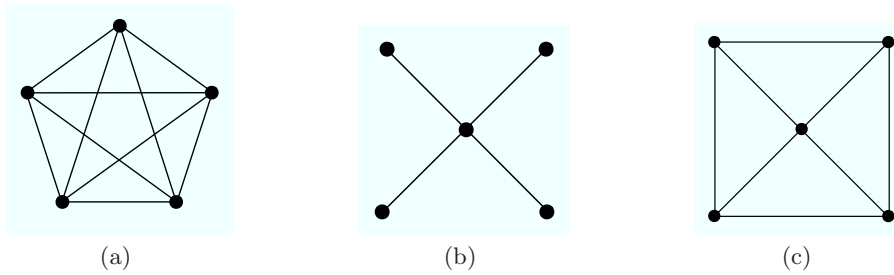


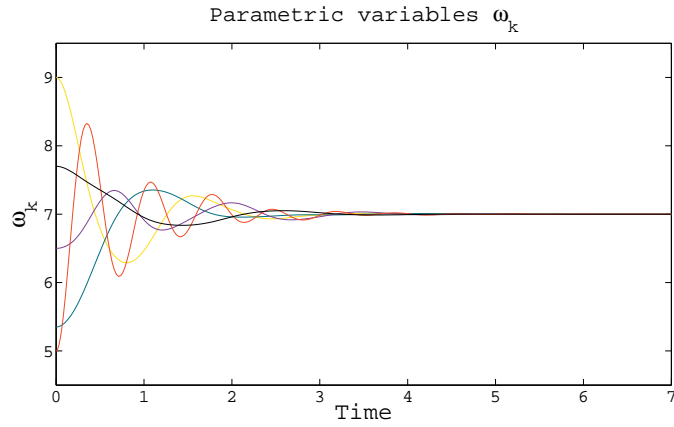
Fig. 5.5: A “All-to-All” network topology (Figure 5.5(a)) with algebraic connectivity equal to 5, a “All-to-One” network topology (Figure 5.5(b)) with algebraic connectivity equal to 1 and a “Crystal” network topology (Figure 5.5(c)) with algebraic connectivity equal to 3.

### 5.3.3 Parametric Resonance

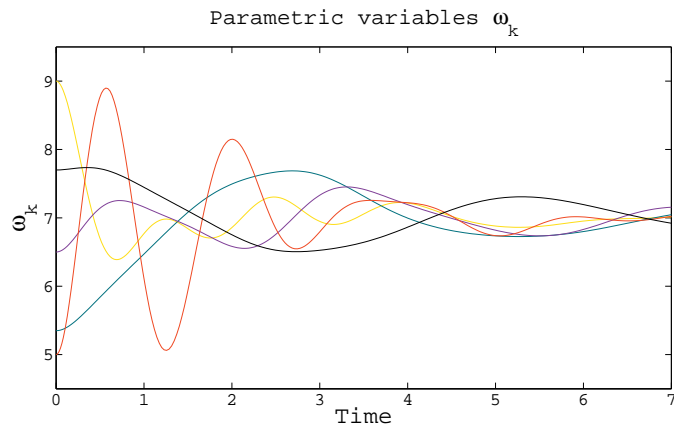
We here numerically exhibit the parametric resonance phenomena produced by the adaptive mechanism on the  $\omega_k$ . For this, six HOPF oscillators have their **state variables** coupled with a constant (6, 1) regular lattice (i.e. “First Neighbor” topology with adjacency matrix  $A^s = \text{circ}(0, 1, 0, 0, 0, 1)$ ). The **parametric variables** are coupled through a time-dependent “Krupp” network (i.e. adjacency matrix  $A^p(t) = \text{circ}(0, 1, \cos(f_p t)^2, 0, \cos(f_p t)^2, 1)$ ). The coupling strength is chosen as  $c = 0.01$  and the susceptibility constant as  $s_\omega = \frac{2}{9}$ . The initial conditions for **state variables** are again  $x_k(0) = 1$  and  $y_k(0) = 0$  for all  $k$  and for the **parametric variables**  $(\omega_1(0), \dots, \omega_N(0)) = \text{ls}(1, 1.1, 6)$ , as above. For  $k = 2, 6$ , the bottom Eqs. (5.20) become

$$\ddot{\varepsilon}_{\phi_k} + \underbrace{0.01 \dot{\varepsilon}_{\phi_k}}_{\text{negligible}} + \underbrace{\frac{5}{9}}_{f_0} \left(1 + \frac{3}{5} \cos(2f_p t)\right) \varepsilon_{\phi_k} = 0.$$

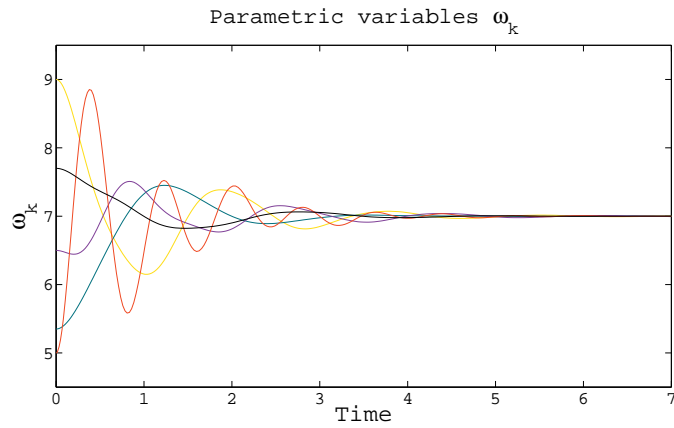
As the theory suggests, parametric resonance occurs when  $f_p = \sqrt{f_0} = \frac{\sqrt{5}}{3} = 0.7454\dots$ . Indeed, the effect of the parametric pumping on the  $\omega_k$  is numerically observable as shown in Figure 5.7. For  $k = 3, 5$ , the bottom Eqs. (5.20) become



(a)



(b)



(c)

Fig. 5.6: Time evolution of the parametric variables  $\omega_k$  for five HOPF oscillators, interacting through a “All-to-All” network (Figure 5.6(a)), through a “All-to-One” network (Figure 5.6(b)) and through a “Crystal” network (Figure 5.6(c)). The algebraic connectivities are equal to 5, 1 and 3 respectively.

$$\ddot{\varepsilon}_{\phi_k} + \underbrace{0.03\dot{\varepsilon}_{\phi_k}}_{\text{negligible}} + \underbrace{1}_{f_0} \left(1 + \frac{1}{3} \cos(2f_p t)\right) \varepsilon_{\phi_k} = 0.$$

Therefore, another switching frequency exists for parametric resonance to occur:  $f_p = \sqrt{f_0} = 1$ . The destabilization (i.e. amplification) is reported in Figure 5.8.

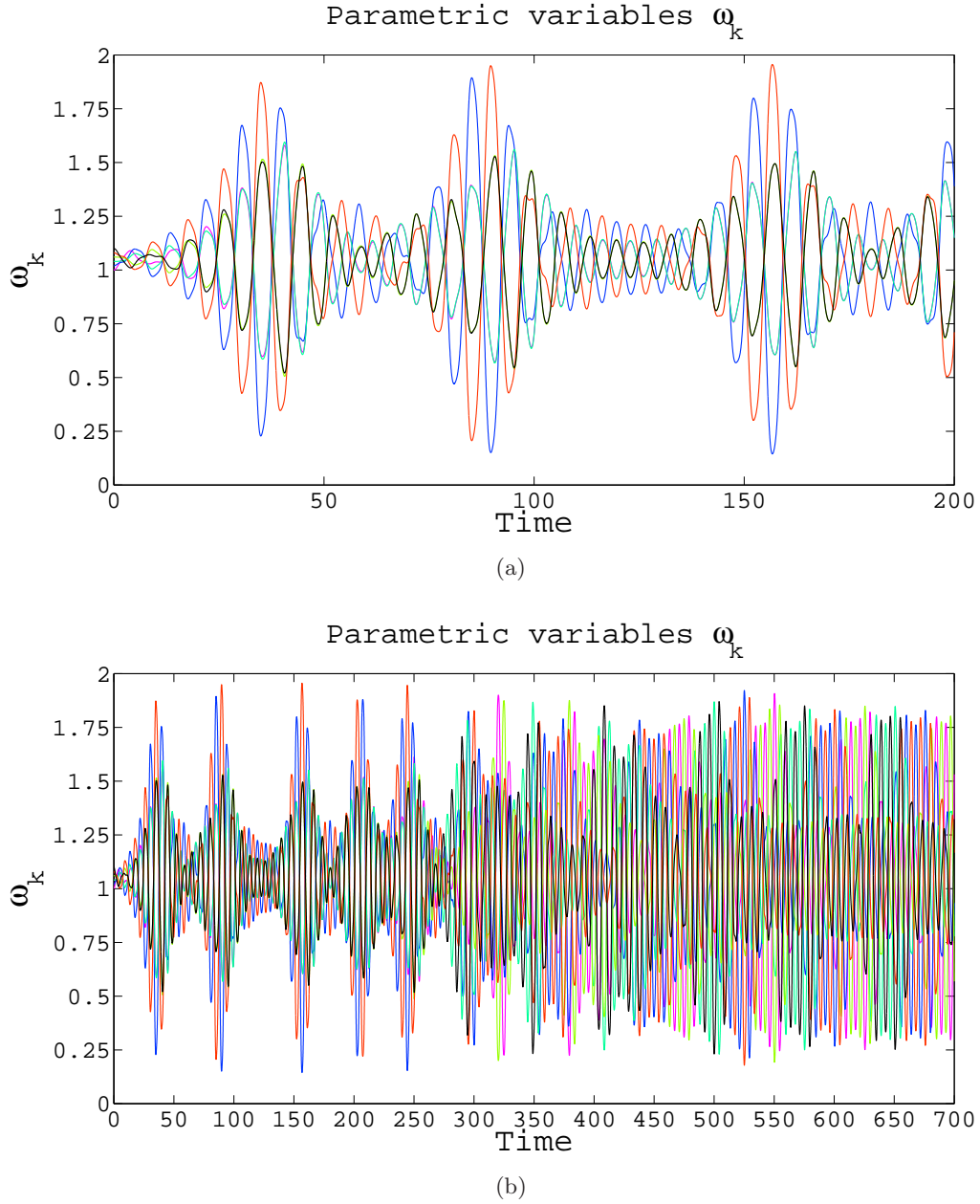
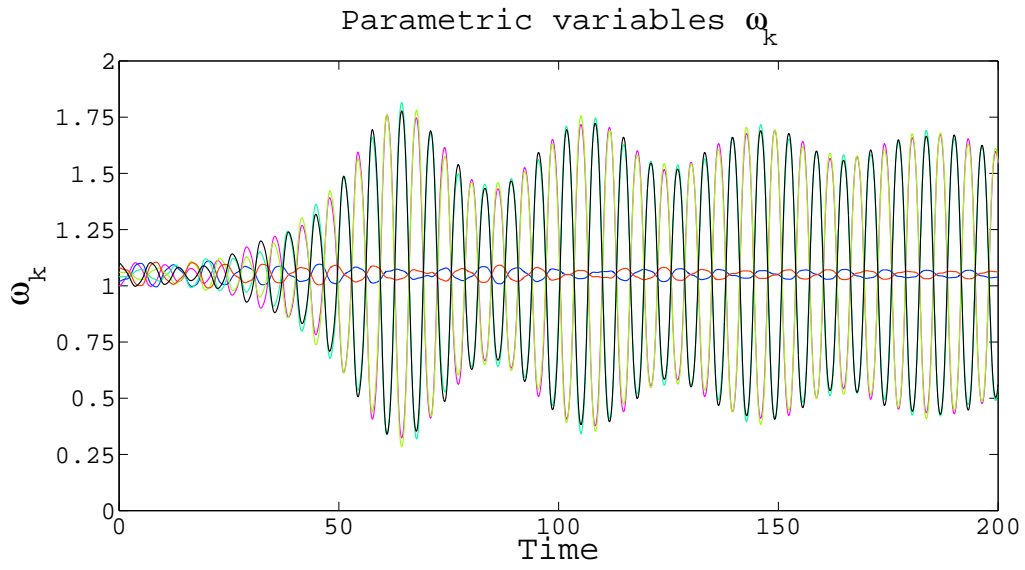
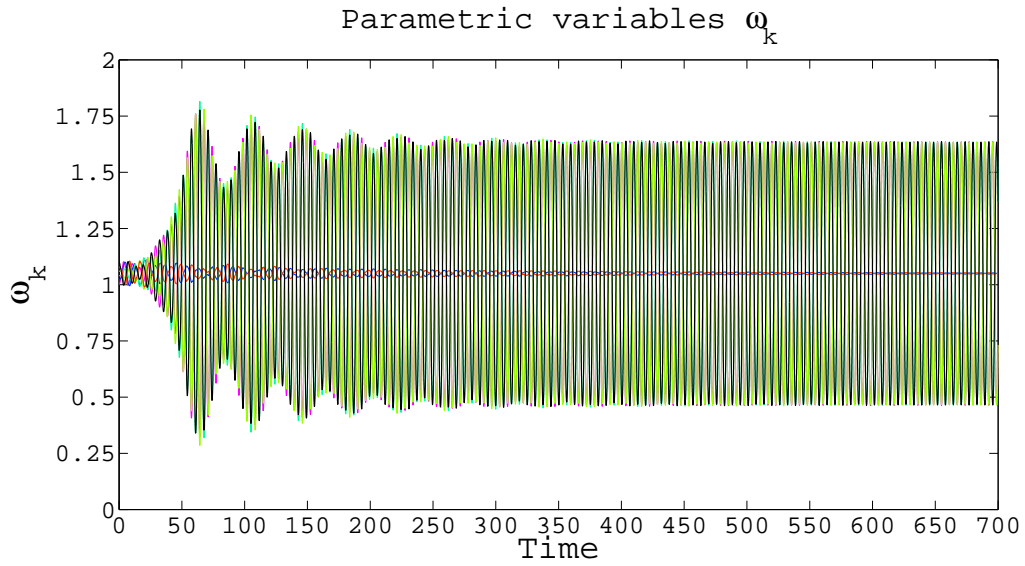


Fig. 5.7: Time evolution of the parametric variables  $\omega_k$  for six HOPF oscillators, interacting through a “Krupp” network with  $f_p = 0.75$  and susceptibility constant  $s_\omega = \frac{2}{9}$ . The network for the state variables is a constant “(6,1) regular lattice” network with coupling strength  $c = 0.01$ . The numerical integration is for the interval  $[0, 200]$  in Figure 5.7(a) and for the interval  $[0, 700]$  in Figure 5.7(b).





(a)



(b)

Fig. 5.8: Time evolution of the parametric variables  $\omega_k$  for six HOPF oscillators, interacting through a “Krupp” network with  $f_p = 1$  and susceptibility constant  $s_\omega = \frac{2}{9}$ . The network for the state variables is a constant “(6,1) regular lattice” network with coupling strength  $c = 0.01$ . The numerical integration is for the interval  $[0, 200]$  in Figure 5.8(a) and for the interval  $[0, 700]$  in Figure 5.8(b).



---

## Numerical Investigations and Perspectives

Si chaque seconde de notre vie doit se répéter un nombre infini de fois, nous sommes cloués à l'éternité comme Jésus-Christ à la croix. Cette idée est atroce.

Milan KUNDERA

### 6.1 Numerical Investigations for Networks of none O-G systems with Adapting Parameters

In this section we want to show numerically that adaptation on parameters of a dynamical system is not only restricted to O-G systems. We will consider the adaptive mechanism discussed in Section 2.1.3.1.

#### 6.1.1 Adaptive “Frequency” in Nonharmonic Oscillators

Let the local dynamics be VAN DER POL (defined as Eq. (2) in [48]), respectively, FITZHUGH-NAGUMO<sup>1</sup> oscillators. They are coupled via the gradient of a Laplacian potential. Each oscillator is equipped with a parametric variable  $\omega_k$ . It multiplies the whole vector field of each local oscillator and thus controls the angular velocity of it on its limit cycle. Here, each  $\omega_k$  plays the role of a flow parameter - a parameter that multiplies the “orthogonal” part (i.e. D) of the O-G systems. A parametric dynamics as discussed in Section 2.1.3.1 is introduced on the  $\omega_k$  parameters. Its aim is to drive all  $\omega_k$  towards a common  $\omega_c$ , hence making all oscillators having a common angular velocity on their respective limit cycles.

For the network of VAN DER POL oscillators, the dynamical system reads

$$\begin{aligned}
 \dot{x}_k &= \omega_k y_k && - \sum_{j=1}^N l_{k,j} x_k \\
 \dot{y}_k &= \underbrace{\omega_k (a(1 - x_k^2)y_k - x_k)}_{\text{local dynamics}} && - \underbrace{\sum_{j=1}^N l_{k,j} y_k}_{\text{coupling dynamics}} \\
 \dot{\omega}_k &= - \underbrace{\sum_{j=1}^N l_{k,j} (x_j y_k - y_j x_k)}_{\text{parametric dynamics}}
 \end{aligned} \tag{6.1}$$

where  $l_{k,j}$  are the entries of the Laplacian matrix  $L$  associated to the network and  $a$  is a positive parameter.

For the network of FITZHUGH-NAGUMO oscillators, the dynamical system reads

---

<sup>1</sup> The FITZHUGH-NAGUMO oscillator is here a BONHOEFFER-VAN DER POL defined as Eqs. (1) and (2) in [18].

$$\begin{aligned}
\dot{x}_k &= \omega_k \left( a(y_k + x_k - \frac{x_k^3}{3}) \right) & - & \sum_{j=1}^N l_{k,j} x_k \\
\dot{y}_k &= \underbrace{\omega_k \left( \frac{-1}{a} (x_k + y_k) \right)}_{\text{local dynamics}} & - & \underbrace{\sum_{j=1}^N l_{k,j} y_k}_{\text{coupling dynamics}} \\
\dot{\omega}_k &= - \underbrace{\sum_{j=1}^N l_{k,j} (x_j y_k - y_j x_k)}_{\text{parametric dynamics}}
\end{aligned} \tag{6.2}$$

where  $l_{k,j}$  are the entries of the Laplacian matrix  $L$  and  $a$  is a positive parameter.

We numerically investigate the dynamics given by Eqs. (6.1) and Eqs. (6.2). For both systems,  $N = 3$  and the network is a ‘‘All-to-One’’ as in Figure 2.1. For all simulations, the initial conditions for the **state variable** are  $x_1(0) = y_1(0) = -1$ ,  $x_2(0) = 0$ ,  $y_2(0) = 1$  and  $x_3(0) = 1$ ,  $y_3(0) = -1$ . The initial conditions for the **parametric dynamics** are  $\omega_1(0) := 1$ ,  $\omega_2(0) := 1.5$  and  $\omega_3(0) := 2$ .

For the network of VAN DER POL oscillators, we choose  $a = 1$  and for the FITZHUGH-NAGUMO oscillators, the parameter is  $a = 3$ . In Figure 6.1 and 6.2, we show the resulting dynamics for the coupled VAN DER POL and FITZHUGH-NAGUMO oscillators respectively.

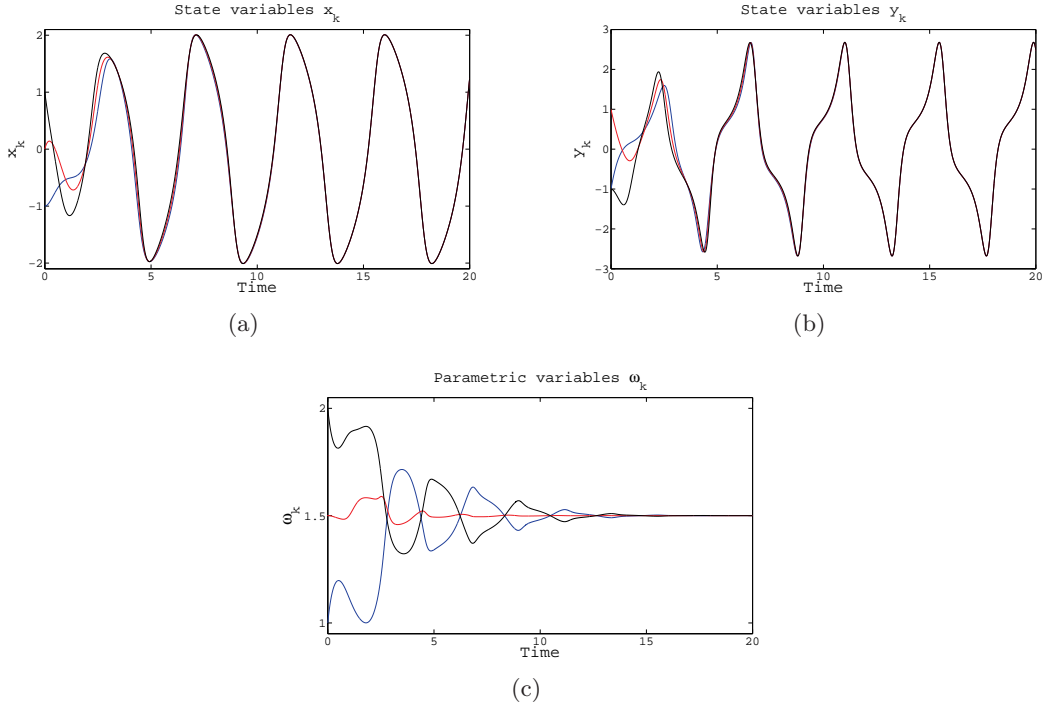


Fig. 6.1: Time evolution of the **state variables**  $x_k$  and  $y_k$  (Figures 6.1(a) & 6.1(b)) and the **parametric variables**  $\omega_k$  (Figure 6.1(c)) for three VAN DER POL oscillators, interacting through a ‘‘All-to-One’’ network.

In both case, oscillators fully synchronize and  $\omega_k$  converge to a common value  $\omega_c = 1.5$ . However,  $\omega_k$ -adaptation for a network of VAN DER POL oscillators does not seem to be as robust as for MCD systems. Indeed, Figure 6.3 shows that if the coupling is too ‘‘weak’’, the  $\omega_k(t)$  do not converge to

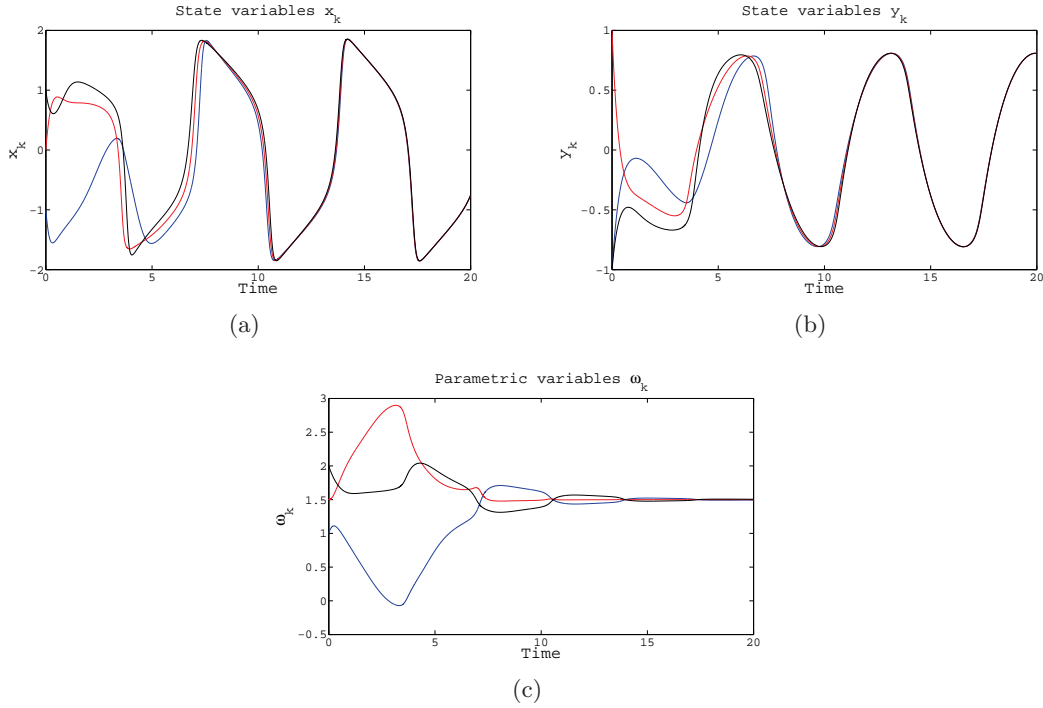


Fig. 6.2: Time evolution of the **state variables**  $x_k$  and  $y_k$  (Figures 6.2(a) & 6.2(b)) and the **parametric variables**  $\omega_k$  (Figure 6.2(c)) for three FITZHUGH-NAGUMO oscillators, interacting through a “All-to-One” network.

a fixed and constant value  $\omega_c$  but rather to periodic functions. This was never observed for MCD systems with only flow parameter adaptation. Here, all parameter values and initial conditions are the same as in Figure 6.1 except for the values of the edges that are lowered by a factor two (i.e. using the Laplacian matrix  $\frac{1}{2}L$ ). Hence, the consensual  $\omega_c$  is reached only for a certain range of connectivity and/or coupling strength.

Finally, let us remark that in the literature, one finds the VAN DER POL oscillator written as

$$\begin{aligned} \dot{x} &= y, \\ \dot{y} &= a(1 - x^2)y - bx, \end{aligned}$$

where  $a$  and  $b$  are parameters (in the above  $b = 1$ ) - they play a similar role as geometric parameters in O-G systems. **Parametric dynamics** as above can be introduced on these parameters and several numerical simulations showed that consensual parameters are reached. It must be noted, that in this case, the geometry (i.e. shape) of the limit cycle is modified, whereas in Figure 6.1, only the angular velocity is changed.

### 6.1.2 The Bouasse Sarda Regulator

In his 1943 book [40], Y. ROCARD, who at that time was an eminent specialist in nonlinear vibrations, mentions the curious two degree of freedom mechanism BOUASSE *and* SARDA’s “*tournebroche*”. The system consists of a shaft or a rotating spit with a crank of radius  $a$  on one side and a drum of radius  $r$  fastened to it on the other side. A cable winds around the drum and at its end, suspends a mass  $m_1$ , dropping under its own weight. A spring with stiffness  $k$  is attached to the crank and a mass  $m_2$  suspends from the spring. The system, which is sketched in Figure 6.4, can ideally be described by the coupled set of second order differential equations

$$\begin{aligned} (I + m_1 r^2) \ddot{\theta} + f_1 \dot{\theta} &= mgr + k(x - a \sin(\theta))a \cos(\theta), \\ m_2 \ddot{x} + f_2 \dot{x} + kx &= ka \sin(\theta) + m_2 g, \end{aligned} \tag{6.3}$$

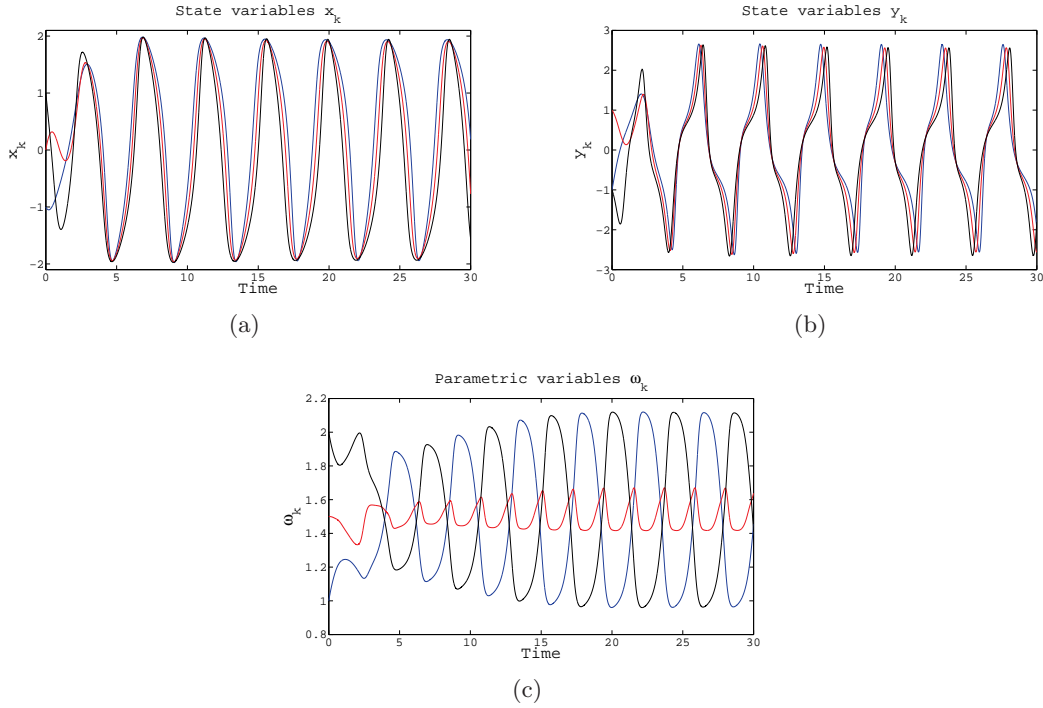


Fig. 6.3: Time evolution of the **state variables**  $x_k$  and  $y_k$  (Figures 6.3(a) & 6.3(b)) and the **parametric variables**  $\omega_k$  (Figure 6.3(c)) for three VAN DER POL oscillators, interacting through a “All-to-One” network.

where  $x$  and  $\theta$  are the two degrees of freedom of the system,  $I$  is the inertial moment of the drum,  $r$  the radius of the drum,  $a$  is the radius of the crank,  $m_1$  and  $m_2$  are the two suspending masses,  $k$  is the coefficient of stiffness of the spring,  $f_1$  and  $f_2$  are two viscous friction coefficients and  $g$  the gravitation acceleration.

We observe that the top Eq.(6.4) is essentially a nonlinear forced damped pendulum while the bottom Eq.(6.4) is a linear forced oscillator with damping. For large  $I + mr^2$ , one can consider that the angle  $\theta$  is not affected by the oscillating mass  $m_2$  and so, it evolves uniformly in time (i.e.  $\theta(t) = \omega t$ ). This implies that we have, in this limit, a single degree of freedom system, namely the bottom Eq. (6.4) tends to a forced damped harmonic oscillator. For the natural system, an intrinsic non-linearity affects dynamics given by Eqs. (6.4). This offers all the potentiality for exhibiting chaotic orbits and the existence of strange attractors, both behaviors where unknown at the time (i.e. in 1943) Y. ROCARD wrote his book.

A period-doubling cascade leading to chaotic behavior is numerically observed. For this, we fix all parameters in Eqs. (6.4) as  $I = 9.24 \times 10^{-5}$  [kg][m]<sup>2</sup>,  $r = 0.1$  [m],  $m_1 = m_2 = 0.5$  [kg],  $k = 50$ ,  $f_1 = 0.03$ ,  $f_2 = 0$  and  $g = 9.8$  [m]/[s]<sup>2</sup>. We then investigate the effect of different values of  $a$  on the dynamical system. For all numerical experiments, the initial conditions for the **state variables** are  $x(0) = \theta(0) = y(0) = z(0) = 0$  with  $y = \dot{x}$  and  $z = \dot{\theta}$ . The numerical integration is over the time interval  $[0, 110]$  and in Figure 6.5 we show the last 10 time units. One can clearly observe that increasing the crank’s radius  $a$ , makes the system bifurcate from a period one oscillating regime to a period two oscillating regime, and so on. By increasing sufficiently enough  $a$ , the system’s orbits become chaotic. This is shown in Figure 6.6.

We now consider a network where each vertex is endowed with a BOUASSE SARDA regulator. From now on, the crank’s radius is a **parametric variable** (i.e.  $a \rightsquigarrow \alpha(t)$ ) with **parametric dynamics** as discussed in Section 2.1.3.1. The dynamical system reads

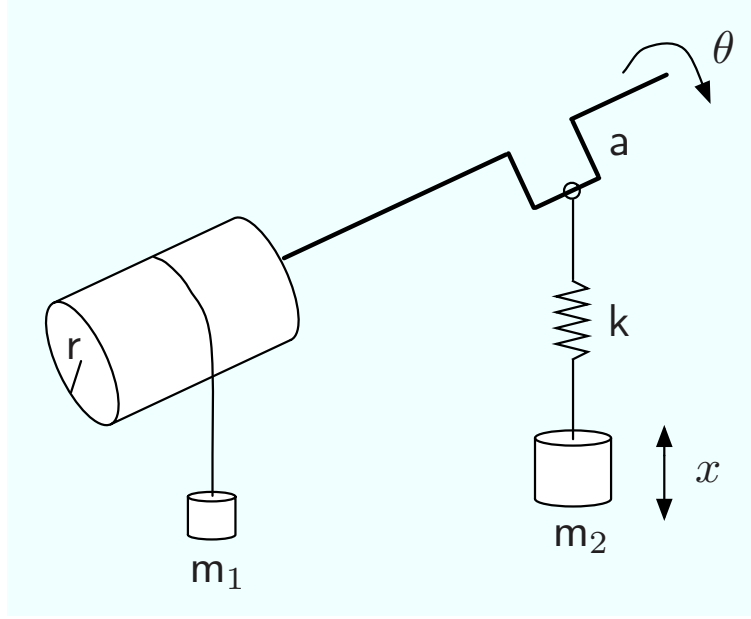


Fig. 6.4: Sketch of the BOUASSE and SARDA's "tounebroche".

$$\begin{aligned}
 \dot{x}_k &= y_k & - & c_k \sum_{j=1}^N l_{k,j} x_j, \\
 \dot{\theta}_k &= z_k & - & c_k \sum_{j=1}^N l_{k,j} \theta_j, \\
 \dot{y}_k &= \frac{m_2 g - k(x_k - \alpha_k \sin(\theta_k)) - f_2 y_k}{m_2} & - & c_k \sum_{j=1}^N l_{k,j} y_j, \\
 \dot{z}_k &= \underbrace{\frac{m_1 g r + k(x_k - \alpha_k \sin(\theta_k)) \alpha_k \cos(\theta_k) - f_1 z_k}{I + m_1 r^2}}_{\text{local dynamics}} & - & \underbrace{c_k \sum_{j=1}^N l_{k,j} z_j}_{\text{coupling dynamics}}, \\
 \dot{\alpha}_k &= \underbrace{s_k \sum_{j=1}^N l_{k,j} (x_j y_k - y_j x_k)}_{\text{parametric dynamics}}, & & 
 \end{aligned} \quad k = 1, \dots, N. \quad (6.4)$$

We numerically investigate the dynamics given by Eqs. (6.4). The network is a "All-to-One" as in Figure 2.1 (i.e.  $N = 3$ ). For all simulations, the initial conditions for the **state variable**  $(x_k(0), \theta_k(0), y_k(0), z_k(0))$  are randomly uniformly distributed on  $] -0.1, 0.1]^3$  for all three local systems.

We perform three numerical investigations, all three with the same coupling strengths  $c_k = 2$  ( $k = 1, 2, 3$ ) and with **parametric variables**  $\alpha_k(0)$  randomly (uniform distribution) drawn from  $]0.05, 0.06[$  for  $k = 1, 2, 3$  and from  $]0.092, 0.097[$  for  $k = 2$ . For such  $\alpha_k(0)$  distribution and if the three local systems are decoupled (i.e.  $L = \mathbf{0}$ ), then, because of the observed period doubling cascade (c.f. Figure 6.5), the BOUASSE SARDA regulator systems on vertex 1 and 3 are periodic (with 1-period) where as the system on vertex 2 has a chaotic behavior. Once the connections are switched on and by adequately choosing the susceptibility constants, one can influence the value of  $\alpha_c$  and hence the resulting asymptotic dynamics.

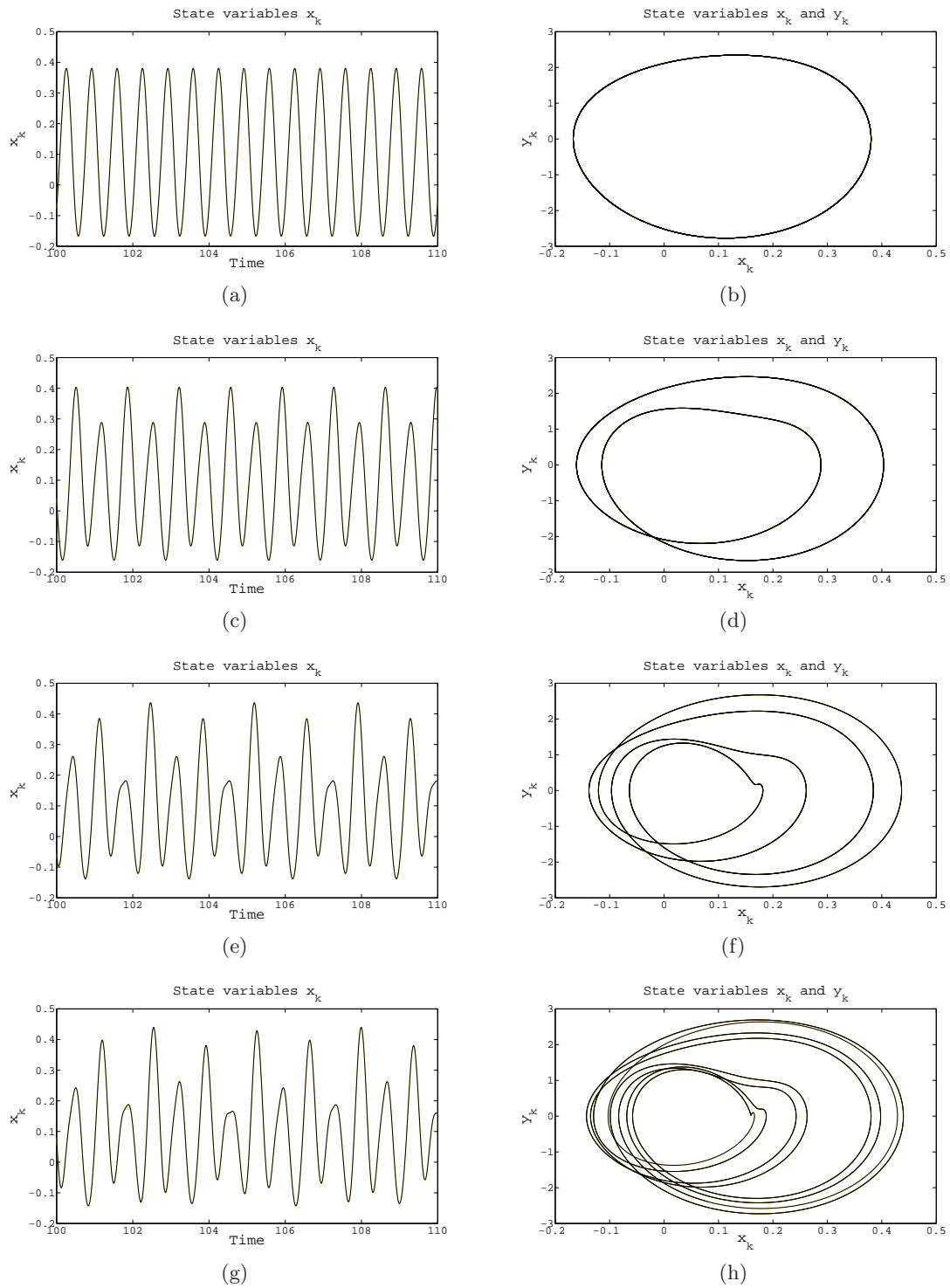
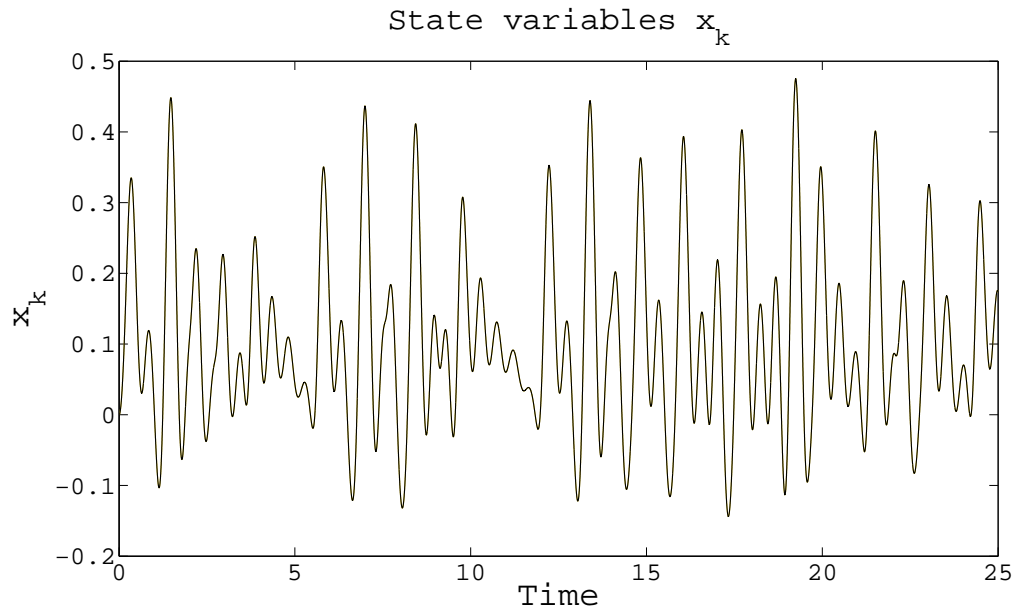
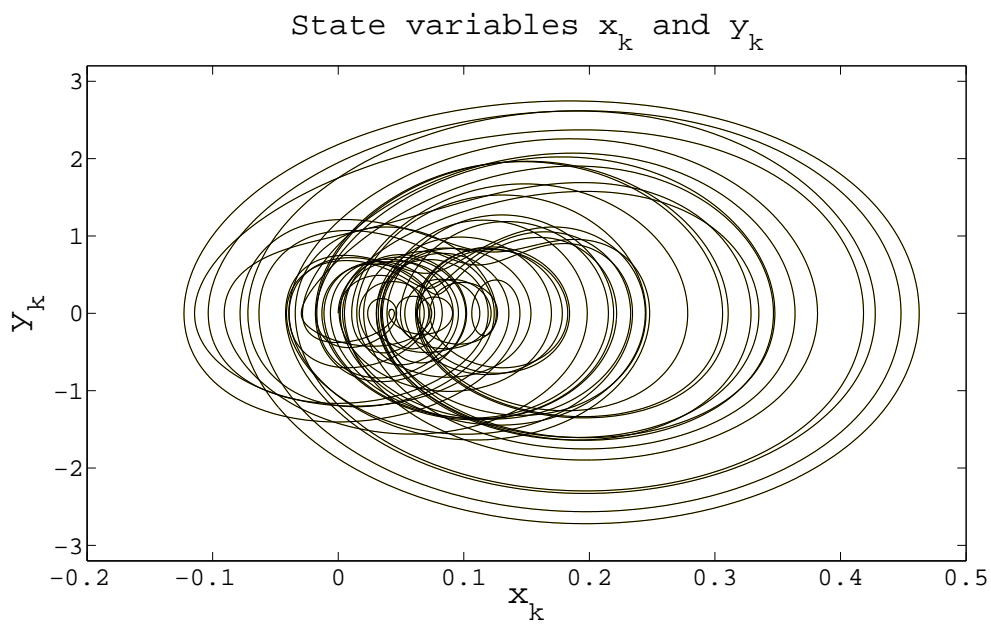


Fig. 6.5: Time evolution of the state variables  $x_k$  and state space representation of  $x_k$  and  $y_k$  for a BOUASSE SARDA regulator with parameter value  $a = 0.06$  (Figures 6.5(a) & 6.5(b)),  $a = 0.07$  (Figures 6.5(c) & 6.5(d)),  $a = 0.08$  (Figures 6.5(e) & 6.5(f)),  $a = 0.081$  (Figures 6.5(g) & 6.5(g)). Numerical integration here displayed is over the time interval [100, 110].





(a)



(b)

Fig. 6.6: Time evolution of the state variables  $x_k$  and state space representation of  $x_k$  and  $y_k$  for a BOUASSE SARDA regulator with parameter value  $a = 0.099$  (Figures 6.6(a) & 6.6(b)).

In Figure 6.7, we choose the susceptibility constants as  $(s_1, s_2, s_3) = (0.03, 0.2, 0.03)$ . The connections are switched on at  $t = 20$ . Here,  $s_1$  and  $s_3$  are relatively small and thus strongly influence the value  $\alpha_c$ . We see that the chaotic dynamics of vertex 2 rapidly converges towards a 1-period regime once connections are switched on.

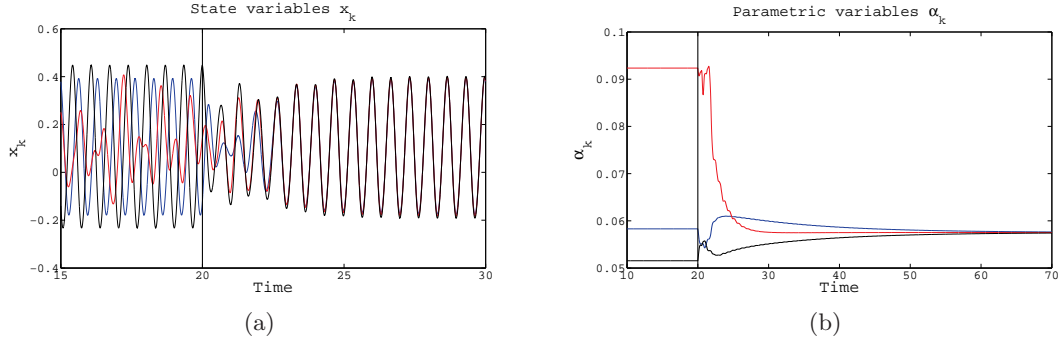


Fig. 6.7: Time evolution of the **state variables**  $x_k$  (Figure 6.7(a)) and the **parametric variables**  $\alpha_k$  (Figure 6.7(b)) for three BOUASSE SARDA regulators, interacting through a “All-to-One” network. Coupling and parametric dynamics are switched on at  $t = 20$  (black solid line).

In Figure 6.8, we choose the susceptibility constants as  $(s_1, s_2, s_3) = (0.0375, 0.01125, 0.0375)$ . The connections are switched on at  $t = 20$ . Here, the resulting value  $\alpha_c$  implies that the asymptotic dynamical behavior of the network is a 4-period regime. This is indeed observed, however the transient dynamics is worth of interest. After connections are switched on, the network converges to a 2-period regime (c.f. Figure 6.8(a)). This is clearly represented in Figure 6.8(b) which displays the  $x_k$  and  $y_k$  orbits over the time interval  $[50, 60]$ . During this time interval, the **parametric variables**  $\alpha_1$  and  $\alpha_3$  are close together while  $\alpha_2$  is still relatively far apart. In the time interval  $[80, 90]$ , the system bifurcates to a 4-period regime (c.f. Figure 6.8(d)), when all three  $\alpha_k$  are close to a common value. The 4-period regime is clearly observed in Figure 6.8(e) which displays the  $x_k$  and  $y_k$  orbits over the time interval  $[110, 120]$ .

In Figure 6.9, we choose the susceptibility constants as  $(s_1, s_2, s_3) = (0.1, 0.005, 0.1)$ . The connections are switched on at  $t = 20$ . Here,  $s_2$  is small and hence the BOUASSE SARDA regulator on vertex 2 drives its two neighbors towards a chaotic regime. Note the the network seems to fully converge in the time interval  $[0, 85]$  (c.f. Figures 6.9(a) & 6.9(c)). However, shortly after  $t = 85$ , one observes a sudden burst. Hence, a longer time interval for numerical integration is needed to be convinced of the convergence (c.f. Figures 6.9(b) & 6.9(d)).

These sudden bursts (intermittencies) appearing after the network seems to have converged are observed in other cases. As an example, we perform the following numerical experiment exhibiting this particularity. We choose the coupling strengths and the susceptibility constants as  $c_k = 3$  and  $s_k = 0.7$  for  $k = 1, 2, 3$ . The **parametric variables**  $\alpha_k$  are randomly uniformly distributed on  $]0.01, 0.03[^3$  for all three local systems. It is important to remark that here, we did introduce a minus sign as a prefactor in front of the **parametric dynamics**. The resulting dynamics is shown in Figure 6.10. We clearly observe that the  $\alpha_k$  apparently converge to a common value (c.f. Figure 6.10(c)). However, on the time interval  $[25, 35]$ , they strongly diverge (c.f. Figure 6.10(d)).

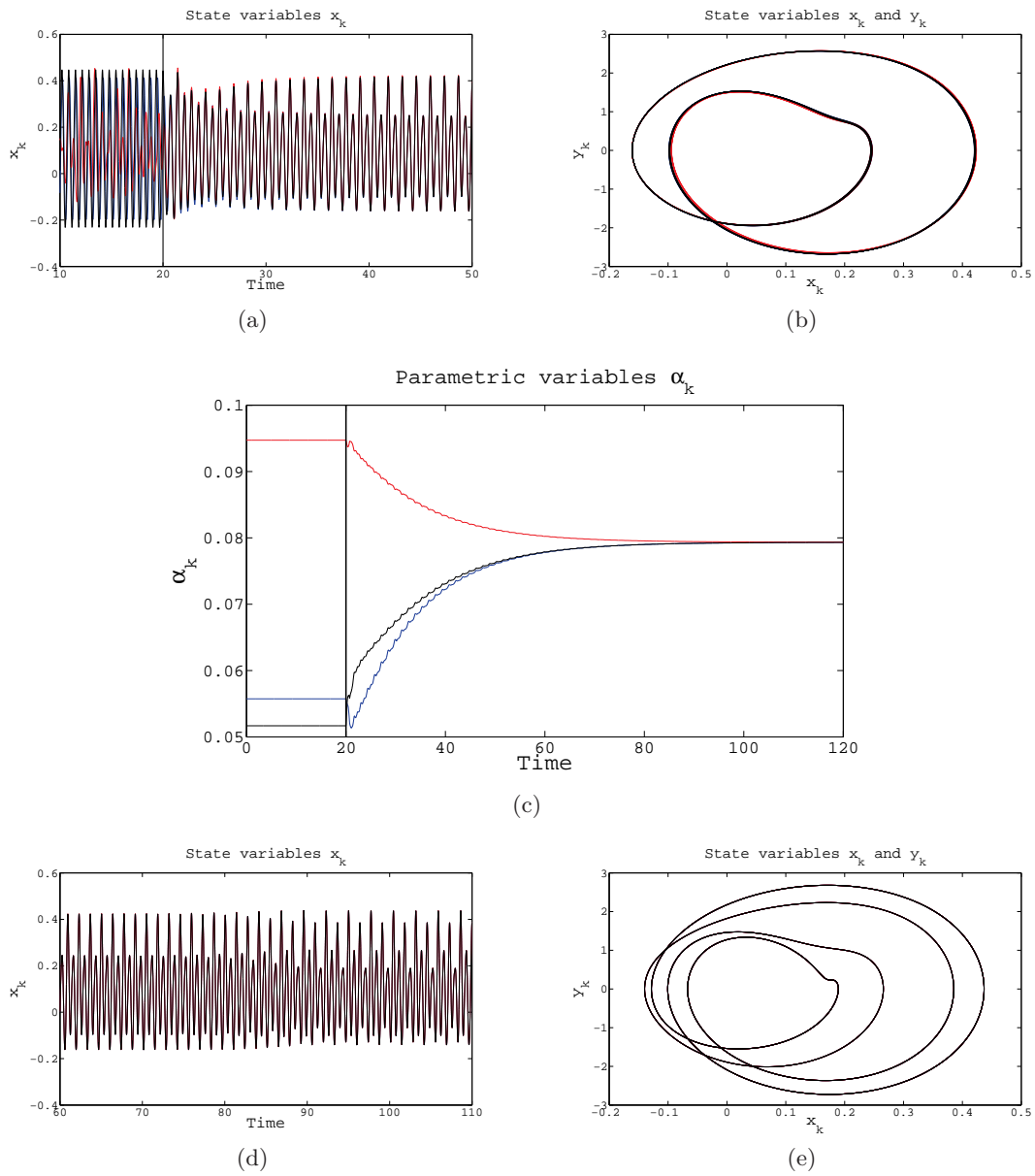
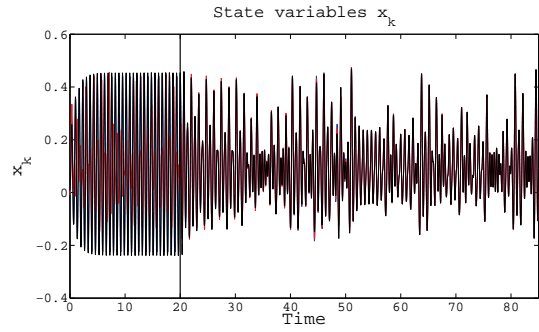
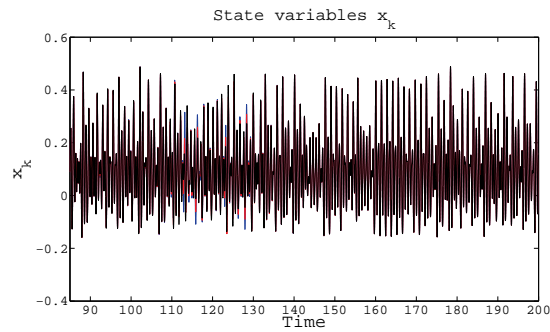


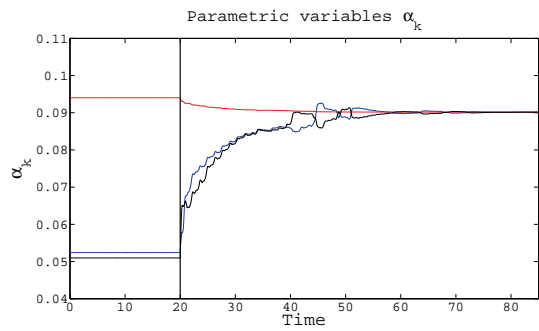
Fig. 6.8: Time evolution of the **state variables**  $x_k$  (Figures 6.8(a) for time interval  $[0, 50]$  & 6.8(d) for time interval  $[60, 110]$ ), the **parametric variables**  $\alpha_k$  (Figure 6.8(c)) and state space representation of  $x_k$  and  $y_k$  (Figures 6.8(b) for time interval  $[50, 60]$  & 6.8(e) for time interval  $[110, 120]$ ) for three BOUASSE SARDA regulators, interacting through a “All-to-One” network. **Coupling and parametric dynamics are switched on at  $t = 20$**  (black solid line).



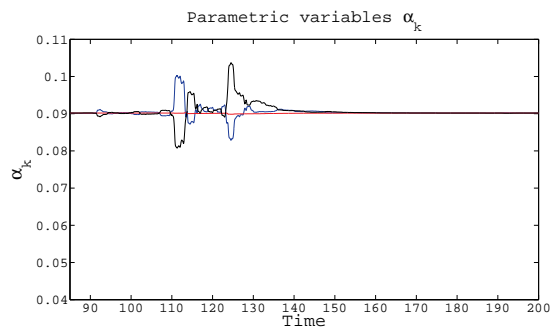
(a)



(b)



(c)



(d)

Fig. 6.9: Time evolution of the **state variables**  $x_k$  (Figures 6.9(a) for time interval  $[0, 85]$  & 6.9(b) for time interval  $[85, 200]$ ) and **parametric variables**  $\alpha_k$  (Figures 6.9(c) for time interval  $[0, 85]$  & 6.9(d) for time interval  $[85, 200]$ ) for three BOUASSE SARDA regulators, interacting through a “All-to-One” network. Coupling and parametric dynamics are switched on at  $t = 20$  (black solid line).

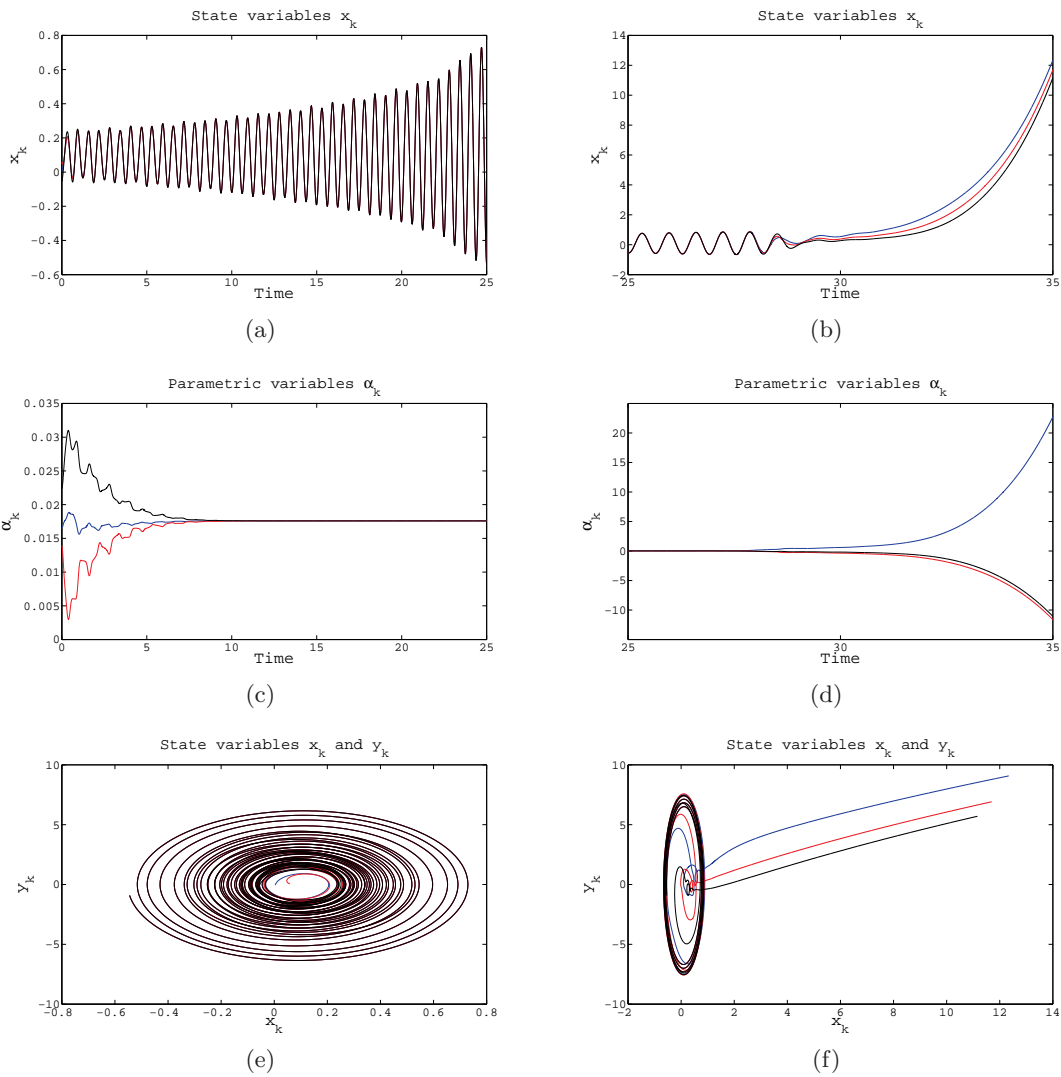


Fig. 6.10: Time evolution of the **state variables**  $x_k$  (Figures 6.10(a) for time interval  $[0, 25]$  & 6.10(b) for time interval  $[25, 35]$ ), the **parametric variables**  $\alpha_k$  (Figures 6.10(c) for time interval  $[0, 25]$  & 6.10(d) for time interval  $[25, 35]$ ) and state space representation of  $x_k$  and  $y_k$  (Figures 6.10(e) for time interval  $[0, 25]$  & 6.10(f) for time interval  $[25, 35]$ ) for three BOUASSE SARDA regulators, interacting through a “All-to-One” network.

## 6.2 Perspectives

In this section we present a list of ongoing work and new ideas for further research activities.

### Determining the prefactor for the Attractor-Shaping Mechanisms

The Integral in 3.8 is a criterion to determine the prefactor  $\pm$  for the adaptive mechanisms. However, we have not yet found a satisfactory physical interpretation of this quantity. We would like to develop another criterion that is easier to apply and with a physical and/or a more geometric interpretation.

#### Semi-plasticity

All along this thesis, the susceptibility constants were always kept fixed and constant. Local systems reluctant to modify their parameters have small susceptibility constants while those searching for change have large ones. This is a simplified vision of what is observed in nature where the willingness to change is dependent on the environment. We should therefore let susceptibility constants be environment-dependent, that is

$$s_k \rightsquigarrow S_k(X).$$

As an example (among the numerous possibilities) one may investigate the effect of the now environment-dependent susceptibility constants defined as

$$S_k(X) = \begin{cases} s_k & \text{if } \sum_{j=1}^N l_{k,j} \|X_j\| < \mathbf{q}_k \\ 0 & \text{if not} \end{cases}.$$

For a network of limit cycle oscillators, one may investigate

$$S_k(X) = \begin{cases} s_k & \text{if } \left| \sum_{j=1}^N l_{k,j} \tan^{-1}\left(\frac{y_j}{x_j}\right) \right| < \mathbf{q}_k \\ 0 & \text{if not} \end{cases}. \quad (6.5)$$

In both cases, the value of  $\mathbf{q}_k$  determines how reluctant a local agent is to modify its own features.

To study the effect of  $\mathbf{q}_k$ , we perform three numerical experiments. Consider an ‘‘All-to-One’’ network (as in Figure 2.1) of three HOPF oscillators having environment-dependent susceptibility constants as in Eq. (6.5) with  $s_k = 1$  ( $k = 1, 2, 3$ ). The coupling strengths are  $c_k = 1$  ( $k = 1, 2, 3$ ). The initial conditions for the **state variable** are  $x_k(0) = 1$  and  $y_k(0) = 0$  for  $k = 1, 2, 3$ , and for the **parametric dynamics**,  $\omega_1(0) := 2$ ,  $\omega_2(0) := 0.5$  and  $\omega_3(0) := 3$ .

For the first numerical experiment, we fix  $\mathbf{q}_k = 1$  ( $k = 1, 2, 3$ ) and switch off the network connections at  $t = 13$ . For the second and third simulations, we take  $\mathbf{q}_k = 0.5$  and  $\mathbf{q}_k = 0.25$  ( $k = 1, 2, 3$ ) respectively and switch off the network connections at  $t = 35$ . Figure 6.11 displays the three numerical experiments. Observe that in Figure 6.11(b), all three oscillators adapt their own frequency, although for some time intervals, the oscillators are too reluctant to tune their angular velocities (i.e. too out of phase with one another). On the other hand, for reluctant local agents (here, the third numerical experiment -  $\mathbf{q}_k = 0.25$ ), there is no adaptation and hence each oscillator returns to its *eigen* frequency after removing the network connections (c.f. Figure 6.11(e)). Finally, in Figure 6.11(d), oscillator 1 modifies the value of the parameter controlling its frequency while the other two oscillators were too reluctant to do so. No consensual state is reached.

Remark that there is no longer a constant of motion for networks with environment-dependent susceptibility constants. Hence, even if a consensual state is reached (as, for example, in Figure 6.11(b)), the consensual value  $\omega_c$  is not known a priori.

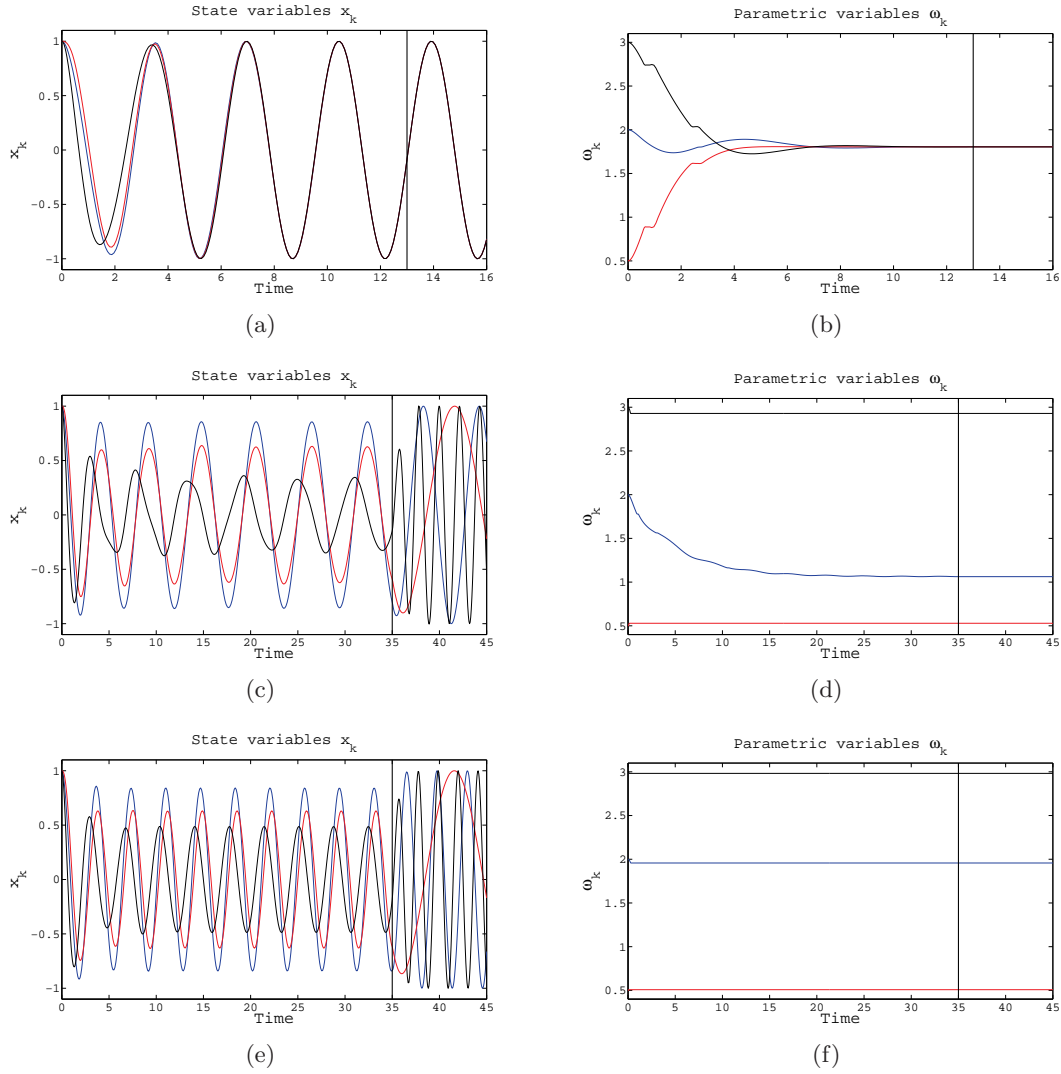


Fig. 6.11: Time evolution of the **state variables**  $x_k$  and the **parametric variables**  $\omega_k$  for three HOPF oscillators, interacting through a “All-to-One” network with parameter value  $q_k = 1$  for  $k = 1, 2, 3$  (Figures 6.11(a) & 6.11(b)),  $q_k = 0.5$  for  $k = 1, 2, 3$  (Figures 6.11(c) & 6.11(d)),  $q_k = 0.25$  for  $k = 1, 2, 3$  (Figures 6.11(e) & 6.11(f)).

### Other Coupling Potentials

We have always considered coupling potentials which vanish on the diagonal (i.e.  $X_k = X_j$  for all  $k, j$ ). Hence, the aim of these potentials is to force the network to fully synchronize. However, in many applications, one is interested in spreading out the coupled agents on the attractor while still maintaining a specified pattern. One may think of the alignment of agents along a specific curve. We should thus construct potential that fulfill these needs.

As an example, consider two HOPF oscillators that circulate on the same geographical circle with the same angular velocity but with a phase shift of  $\theta_0$ . In this case, a candidate for a coupling potential could be

$$V(X_1, X_2) = (x_1^2 - 2x_1x_2 \cos(\theta_0) + x_2^2 - \sin(\theta_0)^2)^2 + (y_1^2 - 2y_1y_2 \cos(\theta_0) + y_2^2 - \sin(\theta_0)^2)^2 .$$

### **Determining the network connectivity**

As a perspective for further research, the analytical tractability of our dynamics seems to be perfectly suitable to address the question “Can you hear the connectivity of the network?” this directly inspired by M. KAC’s famous original question “Can you hear the shape of the drum?”. In the network context, this issue could indeed find an answer by inferring the transient response obtained after perturbation of a consensual state.



---

## Towards Potential Applications

All animals are equal, but some animals are more equal than others.

George ORWELL

Apart from their pure mathematical interest, dynamical systems composed of local units interacting via several time-dependent networks are commonly encountered in modeling a wide range of natural applications. Some of the examples that tend to come to mind first are the numerous interdependent biological processes in a living organism, the myriad exchanges in entangled financial and economical systems, the complex behavior of social networks, or simply the internet and its enormous interchange of information.

Beyond the most obvious, one field to which the theoretical framework and results developed and obtained throughout this thesis can readily be applied is robot formation modeling. Robot formation modeling is a research field which tackles the problem of controlling the dynamics of a collection of interacting individual mobile robots. In general terms, controlling in this context stands for bringing the robot community to converge towards a specific static or time-dependent geometrical pattern or curve in space. Once this given formation is attained, it must be maintained as long as necessary. Furthermore, the team of robots may need to navigate along a desired path while maintaining the formation or change it in order to avoid obstacles in the environment.

Applications for the collective evolution of such teams of robots are presently receiving strong attention. Concretely, platoons of robots may be used to travel over areas of high risks of floods or natural fires for close observation and the gathering of data - or for the exploration of new environments such as caves or ocean floors. More concretely, patrolling around minefields or cordoning the perimeter of accidents or environmental catastrophes are typical examples of robot formation along a predefined curve. Note that in the case of new-territory exploration, obstacle avoidance and formation changing are particularly important.

### Free from steady communications by reaching a consensus

Consider a team of  $N$  planar robots who, initially, are randomly set in an open set of  $\mathbb{R}^2$ . Let  $X_k = (x_k, y_k)$  denote the position of the  $k^{th}$  agent. Each robot is informed of where he must go and how he must circulate once it has reached the desired location. In terms of our modeling, each robot is equipped with the gradient  $\nabla A$  (i.e. informing the robot to go to  $\mathcal{L}$ ) and the vector  $D$  (i.e. describing how to circulate on  $\mathcal{L}$ ). Furthermore, each agent is additively coupled by  $\frac{\partial V}{\partial X_k}$ , the gradient of a positive semi-definite potential  $V \geq 0$ . This potential determines how the robot community must be distributed on  $\mathcal{L}$  and we suppose it assimilates all the necessary interactions for collision avoidance. As a result of local potentials and mutual interactions, all robots are driven, without collisions, towards the specified region and arranged as needed.

Such type of robots' dynamics is very explicitly considered in [27]. In close relation with the above setting, [27] studies the following dynamical system

$$\dot{X}_k = -R(X)\nabla A(X_k) + Q(X)D(X_k)$$

with  $X = (X_1, \dots, X_N)$ , A and D form an O-G system<sup>1</sup> and where the positive scalar functions R and Q modulate the gradient and orthogonal parts of the local systems in order to avoid collisions. Since these two functions are to be seen as **coupling dynamics**, the system is of a multiplicative coupling nature.

In [27], robots are assumed to be programmed with identical behavior (i.e. homogeneous local dynamics with identical valued parameters). However, because of the omnipresence of noise in nature, it is realistic to presume that all robot receives the same local potential A but with different valued parameters. The same holds for D. For small mismatches in the local parameters, the overall effect of the dynamics is not considerably modified: robots do converge without collisions towards a nearby curve of  $\mathcal{L}$ . However, the mismatches impose that local systems must constantly communicate with their neighbors if the dynamical pattern is to be maintained. Not only do robots have different information regarding the geometric configuration (i.e. different geometric parameters) to which they should converge but also their speeds are different (i.e. different flow parameters) - a steady flow of information is mandatory to regulate all individual speeds.

This can be considered as a drawback since robot pattern formation should emerge with as little communication and human supervision as possible (as stated in [27]). Therefore, a potential solution would be to rely on adaptive mechanisms that enable the robots to do with a minimum of central coupling (i.e. be less dependent on communications).

A similar problematic occurs when a team of robots is required to follow a desired trajectory while maintaining a specific formation. Assume that all robots receive slightly corrupted information concerning the direction to be followed by the team. The global system will hopefully perform better by finding a consensual trajectory rather than by constantly updating their positions to produce the collective motion.

### Controlling the consensus

We argued that introducing adaptive mechanisms on perturbed local parameters may be beneficial for a community of robots aiming to attain and maintain a specific formation, or to change directions and to move along a specified path. Indeed, by sharing a consensual valued set of parameters, robots are less dependent of each other. The question that arises is: how can we control the consensual valued set of parameters?

Recall that for a system with one flow parameter, as for example Eqs. (2.12), the consensual parameter is

$$\omega_c := \frac{\sum_{k=1}^N \frac{\omega_k(0)}{s_k}}{\sum_{k=1}^N \frac{1}{s_k}} .$$

We see that  $\omega_c$  depends on the initial local valued parameters (i.e.  $\omega_k(0)$ ) and the susceptibility constants (i.e.  $s_k$ ). Hence, if the  $\omega_k(0)$  are randomly drawn, then  $\omega_c$  is also a random variable. Therefore, the team of robots will converge towards a randomly determined attractor and/or navigate in a random direction. Although the variance of  $\omega_k(0)$  are supposed to be small (and hence  $\omega_c$  barely fluctuates), in certain applications there are no tolerance to noise - and there is the reason for questioning the controllability of the consensual set of parameters.

Since  $\omega_c$  depends on  $s_k$ , then local system with small valued susceptibility constants (i.e. “stubborn” agent) have more influence on the resulting consensual value. This also holds in the case when there are more than one adapting parameter. This is because, through out this thesis, consensual values for the local parameters are all weighted averages (i.e. a direct consequence of the constants of motion constructed all along this thesis). Therefore, local system with small valued susceptibility

---

<sup>1</sup> The authors call the positive semi-definite function A the *shape navigation function*.

constants (i.e. “stubborn” agent) have more influence on the resulting consensual values. Numerically, this is observed in Figure 3.9 where the susceptibility constant for the Hamiltonian height is close to zero. This local system “pulls” the other Hamiltonian heights towards its initial value (c.f. Figure 6.9). An another numerical example is found in Figure 6.9 where one local system strongly influences the crank’s radius value of its neighbors and hence drives the network towards a chaotic regime.

Let us analytically study the effect of a “very stubborn” local system on the global dynamics. For this, consider Eqs. (2.12) in the extreme case where one susceptibility constant is zero. Without lost of generality, suppose  $\mathbf{s}_1 = 0$ . Then,  $\omega_1$  is no longer a **parametric variable**: it has now regained its original status of fixed and constant parameter (i.e. for a given constant  $\mathbf{w}_1$ ,  $\omega_1(t) = \mathbf{w}_1$  for all  $t$ ). Eqs. (2.12) still admit a consensual state since one can always define  $\omega_k := \mathbf{w}_1$  for  $k = 2, \dots, N$ . In this case, we suspect that all  $\omega_k$  for  $k = 2, \dots, N$  will converge towards  $\mathbf{w}_1$ . In words, the “very stubborn” local system drives the whole network towards his own dynamical behavior as it is shown by the following lemma. For this, we define

$$\mathcal{C}_{\mathbf{w}_1} := \{(X, \Omega) \in \mathbb{R}^{Np} \times \mathbb{R}^{N-1} \mid X \in \mathcal{M} \text{ and } \Omega = \mathbf{w}_1 \mathbf{1}\}$$

where  $\mathbf{1}$  is a  $N - 1$  dimensional vector of 1.

**Lemma 7.1.** *Consider the same hypothesis as in Proposition 2.2. Furthermore suppose that in Eqs. (2.12),  $\mathbf{s}_1 = 0$  and so that  $\omega_1(t) = \mathbf{w}_1$  is a constant parameter.*

*Then there exists a set  $\mathcal{U} \supset \mathcal{C}_{\mathbf{w}_1}$  such that all orbits solving System (2.12) with initial conditions in  $\mathcal{U}$  converge towards  $\mathcal{C}_{\mathbf{w}_1}$ .*

*Proof.* The convergence towards  $\mathcal{C}_{\mathbf{w}_1}$  follows from Ляпунов’s second method with Ляпунов function:

$$\mathbb{J}_{\mathbf{w}_1}(X, \Omega) := \mathbb{J}(X) + \frac{1}{2} \sum_{k=2}^N \frac{(\omega_k - \mathbf{w}_1)^2}{\mathbf{s}_k} \geq 0,$$

where  $\mathbb{J}(X)$  is defined in Proposition 2.1. By construction, we have that  $\mathcal{C}_{\mathbf{w}_1} = \{(X, \Omega) \in \mathbb{R}^{Np} \times \mathbb{R}^{N-1} \mid \mathbb{J}(X, \Omega) = 0\}$ . Computing the time derivative

$$\begin{aligned} \langle \nabla \mathbb{J}_{\omega_c}(X, \Omega) \mid (\dot{X}, \dot{\Omega}) \rangle &= \sum_{k=1}^N \left\langle \frac{1}{\mathbf{c}_k} \nabla A_k(X_k) + \frac{\partial \mathbb{V}}{\partial X_k}(X) \mid \dot{X}_k \right\rangle + \sum_{k=2}^N \frac{(\omega_k - \mathbf{w}_1)}{\mathbf{s}_k} \dot{\omega}_k \\ &= \sum_{k=2}^N \left\langle \frac{1}{\mathbf{c}_k} \nabla A_k(X_k) + \frac{\partial \mathbb{V}}{\partial X_k}(X) \mid \omega_k \mathbf{K}(X_k) - \nabla A_k(X_k) - \mathbf{c}_k \frac{\partial \mathbb{V}}{\partial X_k}(X) \right\rangle \\ &\quad + \left\langle \frac{1}{\mathbf{c}_1} \nabla A_1(X_1) + \frac{\partial \mathbb{V}}{\partial X_1}(X) \mid \mathbf{w}_1 \mathbf{K}(X_1) - \nabla A_1(X_1) - \mathbf{c}_1 \frac{\partial \mathbb{V}}{\partial X_1}(X) \right\rangle \\ &\quad - \sum_{k=2}^N \omega_k \left\langle \frac{\partial \mathbb{V}}{\partial X_k}(X) \mid \mathbf{K}(X_k) \right\rangle + \mathbf{w}_1 \sum_{k=2}^N \left\langle \frac{\partial \mathbb{V}}{\partial X_k}(X) \mid \mathbf{K}(X_k) \right\rangle \\ &= \sum_{k=2}^N \left\langle \frac{\partial \mathbb{V}}{\partial X_k}(X) \mid \omega_k \mathbf{K}(X_k) \right\rangle - \sum_{k=2}^N \mathbf{c}_k \left\| \frac{1}{\mathbf{c}_k} \nabla A_k(X_k) + \frac{\partial \mathbb{V}}{\partial X_k}(X) \right\|^2 \\ &\quad + \left\langle \frac{\partial \mathbb{V}}{\partial X_1}(X) \mid \mathbf{w}_1 \mathbf{K}(X_1) \right\rangle - \mathbf{c}_1 \left\| \frac{1}{\mathbf{c}_1} \nabla A_1(X_1) + \frac{\partial \mathbb{V}}{\partial X_1}(X) \right\|^2 \\ &\quad - \sum_{k=2}^N \omega_k \left\langle \frac{\partial \mathbb{V}}{\partial X_k}(X) \mid \mathbf{K}(X_k) \right\rangle + \mathbf{w}_1 \sum_{k=2}^N \left\langle \frac{\partial \mathbb{V}}{\partial X_k}(X) \mid \mathbf{K}(X_k) \right\rangle \\ &= \underbrace{- \sum_{k=1}^N \mathbf{c}_k \left\| \frac{1}{\mathbf{c}_k} \nabla A_k(X_k) + \frac{\partial \mathbb{V}}{\partial X_k}(X) \right\|^2}_{\leq 0} + \underbrace{\mathbf{w}_1 \sum_{k=1}^N \left\langle \frac{\partial \mathbb{V}}{\partial X_k}(X) \mid \mathbf{K}(X_k) \right\rangle}_{=0}. \end{aligned}$$

Let  $\mathcal{U}_{\mathbf{w}_1}$  be a neighborhood of  $\mathbf{w}_1 \mathbf{1}$  included in the hyperplane

$$\{\Omega \in \mathbb{R}^{N-1} \mid \sum_{k=2}^N \frac{\omega_k}{s_k} = w_1 \sum_{k=2}^N \frac{1}{s_k}\}.$$

Therefore, by taking the open set  $\mathcal{U} \supset \mathcal{M}$  whose existence we have proven in Proposition 2.1, strict negativity of  $\langle \nabla \mathcal{J}_{w_1}(X, \Omega) \mid (\dot{X}, \dot{\Omega}) \rangle < 0$  holds for all  $(X, \Omega) \in \mathcal{U} \times \mathcal{U}_{\omega_c} \setminus \mathcal{C}_{w_1}$ . Hence, the compact set  $\mathcal{C}_{w_1}$  is asymptotically stable (refer to Appendix A).

□

From Lemma 7.1, we see that we can control the collective behavior of the network while keeping the agents' local rule. This is known as “soft control” (c.f. [23]). The basic idea is to introduce a “shill” in the network. A shill is an agent that is perceived by the whole community as an ordinary agent, but its characteristic can be externally controlled. Similar to an ordinary agent, a shill has - in general - limited power (i.e. it is not usually connected to all local systems). It interacts according to the same rules as any other local system. However, its local behavior may be controlled externally and thus the collective dynamics may be influenced - or softly controlled - from the outside.

An actual realization is given in [16], where a “robotfish” is introduced into a tank with other living fishes of the same species. The “robotfish” is controlled by the experimenter and thus different types of interactions (e.g. leading the collection of fishes into a certain region) can be thoroughly studied. In our case, we may introduce a shill robot (controllable robot) into a swarm of autonomous interacting robots. This way, one would be able to softly control the consensual state emerging from self organizing entities.

---

## Conclusions

We introduced our work by stipulating four questions. It is now time to formulate the answers that result from our research.

- 1) What are the necessary conditions for convergence towards a *consensual state*?

The answer is to be circumstanced depending on which parameter adaptation we are considering.

For flow parameters, there are, roughly speaking, no particular conditions for convergence towards a consensual state. For these parameter adaptations, we are able to construct Ляпунов functions - an elegant and robust method to prove convergence of a nonlinear dynamical system towards a particular state. The precise conditions depend on the open set  $\mathcal{U}$  from Corollary 2.1. Under our general hypothesis, this set (whether large or small) always exists for all values of coupling strengths, susceptibility constants and network topologies. Thus, these systems are very robust - initial conditions far away from the consensual state can be considered.

For geometric parameters, the discussion is more difficult and we must restrict ourselves to linear analysis. Accordingly, we assume from the start that initial conditions are in the vicinity of the consensual state. Here, the conditions for convergence do depend on the value of the coupling strengths, susceptibility constants and network topologies. Furthermore, we rely on FLOQUET analysis which offers limited analytic possibilities. Hence, we must numerically calculate the exponents, and for this screen a large number of values for the coupling strengths and susceptibility constants in order to determine the conditions for convergence.

Let us mention that for MCD, adaptation of the Hamiltonian heights, as in Example 1.3, is particularly robust. Although limited to linear analysis (and thus only considering small perturbations), we have seen in the case of a constant network of HOPF oscillators with adapting frequencies and radii that the convergence towards a consensual state does not depend on the values of coupling strengths, susceptibility constants and network topologies.

We have not yet being able to analytically investigate the convergence of systems simultaneously adapting their local parameters and their coupling weights. However, numerical evidence based on numerous simulations, showed that these systems are not as robust as those only involving flow parameter adaptation.

- 2) How can  $(\bar{A}_k, \bar{\Delta})$  be calculated?

The answer to this question lies in a nut shell: the existence of constants of motion. Throughout this thesis, all adaptive mechanisms that are introduced into the complex dynamical system have a constant of motion. These constants of motion enable us to analytically determine the consensual values, and this for all systems we consider (except for the System in 4.7 where further conditions as well as the constant of motion are needed in order to calculate the asymptotic values). It is important to mention that while it is always possible to analytically determine the consensual values (thanks to the constant of motion), it was much more demanding (and still an open question for certain cases) to prove convergence towards these consensual values.

- 3) How does  $(\bar{A}_k, \bar{\Delta})$  depend on the connectivity of the network?

Apart from the System in 4.7, which possesses a synchronized state, all other systems presented in this thesis admit a consensual state for which the consensual values do not depend on the topology of the network.

- 4) How does the network influence the convergence rate towards the *consensual state*?

For a constant network of HOPF oscillators with adapting frequencies and radii we can explicitly appreciate the interplay between network connectivity and convergence rate. Numerical simulations show that it is, however, not so when the network is time-dependent. Unfortunately, Ляпунов functions can not be used to infer any results on the convergence rate, and further analysis of the magnitude of the FLOQUET exponents is required to conclude the relationship between convergence rate and network connectivity. However, our numerical simulations do corroborate this assertion.

More generally speaking, our work enables us to draw the following conclusions:

- Chapter 2 shows that flow parameters (i.e. those that do not control the geometry of the attractor) have a high propensity to adapt. Indeed, an orbit on a manifold corresponds to a system evolving with constant energy (no energy is given nor taken from its surroundings). Changing the course of the orbit while it is still evolving on the manifold means that the system modifies its dynamical behavior, but that its total energy is conserved. Intuitively, one would argue that it is less demanding to “slid” and/or to elongate (or reduce) the vector field along the manifold than it is to change the shape of the manifold itself. As an image, one may think of a Mexican hat with a small ball circulating at the bottom of its rim: it is fairly easy to change the angular velocity of the ball, while it is much more difficult to change the shape of the hat.
- The geometry of the attractor itself (i.e. the shape of the hat) is far more resilient to external manipulations. As we have seen (c.f. Chapter 3), to modify the value of a parameter that is part of a functional is much more demanding stability-wise than it is to modify a parameter that multiplies the functional. The network connectivity indeed affects the consensual dynamics (i.e. not for all network topologies do small perturbations around a consensual state decay). Nevertheless, our present contribution explicitly exhibits that attractor-shaping can be implemented in a robust manner.
- After investigating adaptation in the individual units, we show that it is possible to simultaneously adapt local systems as well as their interactions (c.f. Chapter 4). This is indeed possible for several cases: either for systems converging towards a synchronized or a consensual oscillatory state, or for systems with frequency tuning, attractor shaping and coupling weight adjustment.
- Our study shows how two different time-dependent networks (one for coupling the local systems and one for the adaptive mechanisms) either stabilize or destabilize coupled limit cycle oscillators (c.f. Chapter 5). While an analytical approach is complex for arbitrary networks, it is feasible for circulant time-oscillating networks. The resulting linear stability problem coincides with a swing motion with parametric pumping. For ad-hoc driving frequencies, parametric resonance phenomena occur and thus, in our case, precludes the possibility of the establishment of a consensual state.
- From our numerical investigations (c.f. Chapter 6) it is clear that the implementation of our adaptive mechanisms are not restricted to O-G systems. Indeed, limit cycles or more general local dynamics may possess parameters for which our explicit adaptive mechanisms dynamically change their values.
- Last but not least, let us mention that the nature of the interactions together with the network connectivity could alternatively be studied in the context of optimal control theory, provided a set of relevant objective functions are defined (c.f. Chapter 1).

Finally, and at a more conceptual level, let us state that complex networks of interacting local systems with self-adapting parameters lie at the cross-roads of two well-studied topics: synchronization and adaptation. The synchronization capability of local systems poses an old and fundamental

problem with direct relevance for chronology and positioning applications. Already discussed in the seventeenth century by C. HUYGHENS, it is remarkable that more than three centuries later this general problem continues to nourish a multidisciplinary and sophisticated research activity. More recently, growing attention is being paid to dynamic learning and adaptive issues arising in networks of interacting dynamical systems.

Synchronization produces common dynamical evolutions for as long as interactions exist - without interactions, individual characteristics are restored. Adaptation modifies local features in order for the individual units to be more cohesive with their environment. Synchronization and adaptation can be viewed as complementary mechanisms. Indeed, while synchronization expresses an “**elastic capability**” enabling dynamical systems to produce **ephemeral common dynamical patterns**, adaptive systems exhibit a “**plastic capability**” enabling the formation of **permanent common dynamical patterns**. The word associations *elastic-ephemeral* versus **plastic-permanent** emphasize that classical synchronization patterns are produced thanks to the steady action of mutual interactions - remove the interactions and all local evolutions return to their original *eigen* dynamics (i.e. “*chasser le naturel et il reveint au galop*”)<sup>2</sup>. Conversely, adaptive dynamics permanently alter the local dynamics: even after interactions are removed, local evolutions never return to their original *eigen* dynamics.

---

<sup>2</sup> “drive out natural and personal behavior and it will be back in full gallop”





---

## Appendices

### A Asymptotic Stability of a Compact Set

For  $t \in \mathbb{R}_{\geq 0}$ , let  $\Psi_t(x)$  be the flow of a dynamical system given by the ordinary differential equation  $\dot{y} = F(y)$  (i.e.  $\Psi_t(x) = y(t)$  such that  $\dot{y}(t) = F(y(t))$  and  $\Psi_0(x) = y(0) = x$ ). Here,  $F$  is a function into  $\mathbb{R}^p$  and it is sufficiently continuously differentiable in  $y$ .

For a non-empty set  $\mathcal{M} \subset \mathbb{R}^p$  and  $x \in \mathbb{R}^p$ , define the distance between  $\mathcal{M}$  and  $x$  by  $N(\mathcal{M}, x) := \inf\{\|x - z\| \mid z \in \mathcal{M}\}$  ( $\|\cdot\|$  the euclidean norm). We now define the stability of a set  $\mathcal{M}$  for the flow  $\Psi_t$ .

**Definition.** A set  $\mathcal{M}$  is asymptotically stable if it is stable and it is an attractor, that is

- **stable** - if every neighborhood  $\mathcal{U}$  of  $\mathcal{M}$  contains a set  $\mathcal{V}$  which is a neighborhood of  $\mathcal{M}$  and  $\mathcal{V}$  is positively invariant (i.e.  $\Psi_t(x) \in \mathcal{V} \ \forall x \in \mathcal{V}, \forall t \geq 0$ )
- **attractor** - if the set  $\mathcal{A}_{\mathcal{M}} := \{x \in \mathbb{R}^p \mid \lim_{t \rightarrow \infty} N(\mathcal{M}, \Psi_t(x)) = 0\}$  is a neighborhood of  $\mathcal{M}$  .

The well-known asymptotic stability result that is applied is (see Chapter VIII, Theorem 1.6 in [4])

**Theorem.** Let  $\mathcal{M} \subset \mathbb{R}^p$  be a non-empty compact set. If there exists a continuously differentiable real-valued function  $\Pi(x)$  defined on a neighborhood  $\mathcal{U}$  of  $\mathcal{M}$  such that

- $\Pi(x) = 0$  if  $x \in \mathcal{M}$  and  $\Pi(x) > 0$  if  $x \notin \mathcal{M}$
- $\langle \nabla \Pi(x) | F(x) \rangle < 0$  for  $x \notin \mathcal{M}$ ,

then  $\mathcal{M}$  is asymptotically stable.

#### A.1 Principal of Linearized Stability

Let  $\dot{z} = \mathfrak{D}F(\varphi(t), t)z$  be the first variational equation for the solution  $\varphi(t)$  (with  $\varphi(0) = \varphi_0$ ) of the ordinary differential equation  $\dot{y} = F(y, t)$ , where  $F$  is a function on  $\mathbb{R}^p \times \mathbb{R}_{\geq 0}$  onto  $\mathbb{R}^p$  and it is sufficiently continuously differentiable in  $y$  and  $t$ .

##### A.1.1 Periodic Solutions - Floquet Theory

We here consider autonomous vector fields (i.e.  $F$  is explicitly independent of  $t$ ) that admits periodic solutions of period  $T$ , that is,  $\varphi(t)$  solves  $\dot{y} = F(y)$  with  $\varphi(0) = \varphi_0$  and  $\varphi(t+T) = \varphi(t)$  for all  $t$ . Let  $R(t)$  be the principal fundamental matrix of the first variational equation  $\dot{z} = \mathfrak{D}F(\varphi(t))z$  for the periodic solution  $\varphi(t)$  of  $\dot{y} = F(y)$ , that is, all columns of  $R(t)$  solve the variational equation with  $R(0) = Id$ . The monodromy matrix is  $R(T)$ . We now define the Floquet exponents of the variational equation  $\dot{z} = \mathfrak{D}F(\varphi(t))z$ .

**Definition.** Let the eigenvalues of  $R(T)$  be  $\chi_1, \dots, \chi_p$ . They are called the characteristic multipliers for  $\dot{z} = \mathfrak{D}F(\varphi(t))z$ . The Floquet exponents  $\mu_1, \dots, \mu_p$  are defined by

$$\chi_1 = \exp(\mu_1 T), \dots, \chi_p = \exp(\mu_p T) .$$

Remarks

- In general, the **Floquet exponents** are not unique since  $\exp(z) = \exp(w) \Leftrightarrow z = w + 2\pi ik$ , with  $k \in \mathbb{Z}$  and  $z, w \in \mathbb{C}$ . However, this is not a major concern since, as we shall see below, we are interested in the real part of the **Floquet exponents** (i.e. for  $z, w \in \mathbb{C}$  such that  $\exp(z) = \exp(w)$ , then  $\Re(z) = \Re(w)$ ).
- One of the **characteristic multipliers** is always one, implying that one of the **Floquet exponents** is always zero. This is true because of the following arguments. Let  $\varphi(t)$  be a periodic solution (of period  $T$ ) of  $\dot{y} = F(y)$ . Therefore  $\dot{\varphi}(t) = F(\varphi(t))$  and differentiating this expression in time gives  $\ddot{\varphi}(t) = \mathfrak{D}F(\varphi(t))\dot{\varphi}(t)$  and hence  $\dot{\varphi}(t)$  solves  $\dot{z} = \mathfrak{D}F(\varphi(t))z$ . Note that the hypothesis that  $F$  is autonomous plays an important role at this step. Thus, since  $\dot{\varphi}(t)$  solves  $\dot{z} = \mathfrak{D}F(\varphi(t))z$ , there exists  $v \in \mathbb{R}^n$  such that  $\dot{\varphi}(t) = R(t)v$  where  $R(t)$  is the principal fundamental matrix. Evaluating this expression at  $t = 0$  and  $t = T$  gives

$$\dot{\varphi}(0) = R(0)v = Idv = v \quad \text{and} \quad \dot{\varphi}(T) = R(T)v .$$

On the other hand, since  $\varphi(t) = \varphi(t+T)$ , then  $\dot{\varphi}(t) = \dot{\varphi}(t+T)$  and so  $\dot{\varphi}(0) = \dot{\varphi}(T)$ . Therefore,  $R(T)v = v$  and hence one is an eigenvalue of  $R(T)$ .

We now define a notion of stability for periodic solutions.

**Definition.** Let  $\varphi(t)$  be a periodic solution of  $\dot{y} = F(y)$  (i.e.  $\varphi(t+T) = \varphi(t)$  for all  $t$  and  $\varphi(0) = \varphi_0$ ). Denote by  $\mathcal{C}$  the curve on which  $\varphi(t)$  evolves when  $t$  varies. Then,

- $\mathcal{C}$  is **Poincaré stable** - if  $\vartheta(t)$  (with  $\vartheta(0) = \vartheta_0$ ) is a solution of  $\dot{y} = F(y)$  such that, for all  $\epsilon > 0$  and any  $t_1$ , there is a  $\delta_\epsilon > 0$  such that  $N(\mathcal{C}, \vartheta(t_1)) < \delta_\epsilon$  implies that  $N(\mathcal{C}, \vartheta(t)) < \epsilon$  for all  $t \geq t_1$ .
- $\mathcal{C}$  **asymptotically Poincaré stable** - if  $\mathcal{C}$  is Poincaré stable and  $\lim_{t \rightarrow \infty} N(\mathcal{C}, \varphi(t)) = 0$

The well-known asymptotic stability result that is applied is (see Chapter 4, Theorem 4.8 in [20] and for a proof, Chapter 13, Theorem 2.2 in [10])

**Theorem.** Let  $\varphi(t)$  be a periodic solution of  $\dot{y} = F(y)$  (i.e.  $\varphi(t+T) = \varphi(t)$  for all  $t$  and  $\varphi(0) = \varphi_0$ ). Suppose that the first variational equation  $\dot{z} = \mathfrak{D}F(\varphi(t))z$  has Floquet exponents  $0, \mu_2, \dots, \mu_p$ , where  $\Re(\mu_j) < 0$  for all  $j = 2, \dots, p$ . Then the set  $\mathcal{C}$ , which is the curve on which  $\varphi(t)$  evolves when  $t$  varies, is asymptotically Poincaré stable.

The condition that  $\Re(\mu_j) < 0$  for all  $j = 2, \dots, p$  is equivalent to  $|\chi_j| < 1$  for all  $j = 2, \dots, p$ . To show this, let  $\chi = x + iy$  be a **characteristic multiplier** and  $\mu = u + iv$  a **Floquet exponent** (i.e.  $\chi = \exp(\mu T)$ ). Then

$$x + iy = \exp(uT + ivT) = \exp(uT) \exp(ivT) = \exp(uT)(\cos(vT) + i \sin(vT))$$

and hence  $\sqrt{x^2 + y^2} = \exp(uT) \Leftrightarrow \ln(\sqrt{x^2 + y^2}) = uT$ . Therefore  $\Re(\mu) = u < 0 \Leftrightarrow \sqrt{x^2 + y^2} = |\chi| < 1$  (since  $T \geq 0$ ).

**Two dimensional case ( $p = 2$ )**

When  $\mathcal{C}$  is a close curve in  $\mathbb{R}^2$ , then the condition for  $\mathcal{C}$  to be **asymptotically Poincaré stable** is given by

$$\int_0^T \text{tr}(\mathfrak{D}F(\varphi(t))) dt < 0 .$$

To show this, let  $\chi_1$  and  $\chi_2$  be the two **characteristic multipliers** with  $\chi_1 = 1$  (because there is always one **characteristic multiplier** that is equal to one (i.e.  $F$  is autonomous)). By definition,  $\chi_1$  and  $\chi_2$  are the roots of

$$0 = \zeta^2 - \text{tr}(R(T))\zeta + \det(R(T)) = \det(R(T) - \zeta Id) ,$$

and therefore, the product of the roots gives  $\det(R(T)) = \chi_1\chi_2 = \chi_2$ . By the Theorem bellow, we have

$$\chi_2 = \det(R(T)) = \exp\left(\int_0^T \operatorname{tr}(\mathfrak{D}F(\varphi(t))) dt\right) < 1,$$

since the argument in the exp is, by hypothesis, strictly negative.

**Theorem (LIOUVILLE).** *Let  $A(t)$  be continuous on an interval and let  $Q(t)$  be a fundamental matrix of  $\dot{z} = A(t)z$ . Then,*

$$\det(Q(t)) = \det(Q(0)) \exp\left(\int_0^t \operatorname{tr}(A(s)) ds\right)$$

$$\text{with } \operatorname{tr}(A(t)) = \sum_{j=1}^p a_{j,j}(t).$$

## B Analytic Solutions for some MCD Oscillators

### The MATHEWS-LAKSHMANAN Oscillator

Consider the Hamiltonian  $H(x, y; \mathbf{a}) = \log(\cosh(y)) + \frac{1}{2} \log(\mathbf{a} + x^2)$  that defines the following dynamical system

$$\begin{aligned} \dot{x} &= \omega \frac{\partial H}{\partial y}(x, y) = \omega \tanh(y), \\ \dot{y} &= -\omega \frac{\partial H}{\partial x}(x, y) = -\omega \frac{x}{\mathbf{a} + x^2}, \end{aligned}$$

with  $\mathbf{a} > 0$  and  $\omega \neq 0$ . Let  $\omega\sqrt{\mathbf{b}}s := x$  and  $\sqrt{\mathbf{b}}z := \tanh(y)$  for  $\mathbf{b} > 0$ , then<sup>3</sup>

$$\begin{aligned} \dot{s} &= z \\ \dot{z} &= -\frac{(\alpha - fz^2)s}{1 + fs^2} \iff (1 + fs^2)\ddot{s} + (\alpha - fs^2)s = 0, \end{aligned}$$

with  $f := \mathbf{b}\frac{\omega^2}{\mathbf{a}}$  and  $\alpha := \frac{\omega^2}{\mathbf{a}}$  and where the right-hand side of the equivalence is the MATHEWS-LAKSHMANAN oscillator as presented in [30]. Since

$$\frac{\dot{z}}{z} = \frac{\frac{dz}{dt}}{\frac{ds}{dt}} = -\frac{(\alpha - fz^2)s}{(1 + fs^2)z},$$

then, by separating the variables, we have

$$-\int \frac{2zf}{(\alpha - fz^2)} dz = \int \frac{2sf}{1 + fs^2} ds \implies \ln(\alpha - fz^2) = \ln(1 + fs^2) + \ln(k^2). \quad (\text{B.1})$$

For consistency, we have that  $k \in ]\frac{-\omega}{\sqrt{\mathbf{a}}}, \frac{\omega}{\sqrt{\mathbf{a}}}[ \setminus \{0\}$ . This is because Eq.(B.1) is equivalent to  $\frac{\frac{\omega^2 - \mathbf{b}\frac{\omega^2}{\mathbf{a}}z^2}{1 + \mathbf{b}\frac{\omega^2}{\mathbf{a}}s^2}}{k^2} = k^2$  and since  $\sqrt{\mathbf{b}}z \in ]-1, 1[$ , then  $\mathbf{b}z^2 \in [0, 1[$  and therefore

$$1 > \frac{1 - \mathbf{b}z^2}{1 + \mathbf{b}\frac{\omega^2}{\mathbf{a}}s^2} = \frac{\mathbf{a}k^2}{\omega^2} > 0 \iff \frac{\omega^2}{\mathbf{a}} > k^2 > 0$$

if we suppose that  $s$  and  $z$  are not zero simultaneously. Since Eq.(B.1) is equivalent to  $\alpha - fz^2 = (1 + fs^2)k^2$ , then

$$\frac{\frac{\omega^2}{\mathbf{a}} - \mathbf{b}\frac{\omega^2}{\mathbf{a}}z^2}{1 + \mathbf{b}\frac{\omega^2}{\mathbf{a}}s^2} = k^2 \iff \frac{1 - \mathbf{b}z^2}{1 + \mathbf{b}\frac{\omega^2}{\mathbf{a}}s^2} = \frac{\mathbf{a}}{\omega^2}k^2 \implies \alpha - fz^2 = (1 + fs^2)k^2 \implies \frac{ds}{dt} = k\sqrt{c^2 - s^2}$$

<sup>3</sup> Remember that  $1 - \tanh(y)^2 = \cosh(y)^{-2}$  and  $\frac{d \tanh}{ds}(s) = \frac{1}{\cosh(s)^2}$ .

with  $c := \sqrt{\frac{\alpha - k^2}{k^2 f}}$  ( $c$  is a strictly positive real number since  $\frac{\omega^2}{a} - k^2 > 0$ ). Again, by separating the variables, we have

$$\int \frac{ds}{\sqrt{c^2 - s^2}} = \int k dt \implies \sin^{-1}\left(\frac{s}{c}\right) = (kt + \phi).$$

Then  $s(t) = c \sin(kt + \phi)$  and  $z(t) = \dot{s}(t) = ck \cos(kt + \phi)$  and so

$$x(t) = \omega \sqrt{b} \sqrt{\frac{\omega^2}{a} - k^2} \sin(kt + \phi) = \frac{\sqrt{\omega^2 - ak^2}}{k} \sin(kt + \phi)$$

and  $y(t) = \tanh^{-1}\left(\frac{\sqrt{\omega^2 - ak^2}}{\omega} \cos(kt + \phi)\right)$ .

Verification: for  $x(t)$  we have

$$\dot{x}(t) = \sqrt{\omega^2 - ak^2} \cos(kt + \phi) = \omega \tanh(y(t))$$

and because  $\tanh(y(t)) = \frac{\sqrt{\omega^2 - ak^2}}{\omega} \cos(kt + \phi)$  then, for  $y(t)$ ,

$$\begin{aligned} \dot{y}(t) &= -k \frac{\sqrt{\omega^2 - ak^2}}{\omega} \sin(kt + \phi) \cosh(y(t))^2 = \frac{k^2}{\omega^2} \left( \frac{-\omega \sqrt{\omega^2 - ak^2}}{k} \sin(kt + \phi) \right) \cosh(y(t))^2 \\ &= \frac{-\omega x(t)}{\frac{\omega^2}{k^2} \left( 1 - \frac{\omega^2 - ak^2}{\omega^2} \cos^2(kt + \phi) \right)} = \frac{-\omega x(t)}{\frac{\omega^2}{k^2} \left( 1 - \frac{\omega^2 - ak^2}{\omega^2} + \frac{\omega^2 - ak^2}{\omega^2} \sin^2(kt + \phi) \right)} \\ &= -\omega \frac{x(t)}{a + x(t)^2}. \end{aligned}$$

Since  $(x(0), y(0))$  belongs to the limit cycle determined by  $H(x, y) = r$ , then

$$H(x(0), y(0)) = r \implies \cosh(y(0))^2 (a + x(0)^2) = \exp(2r),$$

which is equal to

$$\begin{aligned} a + \frac{\omega^2 - ak^2}{k^2} \sin^2(\phi) &= \exp(2r) \left( 1 - \frac{\omega^2 - ak^2}{\omega^2} \cos^2(\phi) \right), \\ a + \left( \frac{\omega^2}{k^2} - a \right) \sin^2(\phi) &= a \exp(2r) \frac{k^2}{\omega^2} + \exp(2r) \left( 1 - a \frac{k^2}{\omega^2} \right) \sin^2(\phi). \end{aligned}$$

Matching the coefficients leads to:  $a = a \exp(2r) \frac{k^2}{\omega^2} \Leftrightarrow \frac{\omega^2}{k^2} = \exp(2r)$  and  $\frac{\omega^2}{k^2} - a = \exp(2r) \left( 1 - a \frac{k^2}{\omega^2} \right) \Leftrightarrow \left( 1 - a \frac{k^2}{\omega^2} \right) = \exp(2r) \frac{k^2}{\omega^2} \left( 1 - a \frac{k^2}{\omega^2} \right) \Leftrightarrow \frac{\omega^2}{k^2} = \exp(2r)$ . Therefore,  $k = \frac{\omega}{\exp(r)}$ .

### The $\Gamma$ лаз Oscillator

Consider the Hamiltonian  $H(x, y; a, b) = \frac{x^2}{a(x^2 + y^2) + 1 - a} + \frac{y^2}{b(x^2 + y^2) + 1 - b}$  that defines the following dynamical system

$$\begin{aligned} \dot{x} &= \omega \frac{\partial H}{\partial y}(x, y) = \omega \left( \frac{2y(bx^2 + 1 - b)}{g_b^2} - \frac{2axy^2}{g_a^2} \right), \\ \dot{y} &= -\omega \frac{\partial H}{\partial x}(x, y) = -\omega \left( \frac{2x(ay^2 + 1 - a)}{g_a^2} - \frac{2bxy^2}{g_b^2} \right), \end{aligned}$$

with  $a, b \in ]0, 1[$ ,  $a \neq b$  and  $g_a = a(x^2 + y^2) + 1 - a$  and  $g_b = b(x^2 + y^2) + 1 - b$ . In polar coordinates, the system is<sup>4</sup>

$$\begin{aligned} \dot{r} &= 2\omega r \cos(\phi) \sin(\phi) \left( \frac{1}{b(r^2 - 1) + 1} - \frac{1}{a(r^2 - 1) + 1} \right), \\ \dot{\phi} &= -2\omega \left( \frac{(1 - a) \cos(\phi)^2}{(a(r^2 - 1) + 1)^2} + \frac{(1 - b) \sin(\phi)^2}{(b(r^2 - 1) + 1)^2} \right). \end{aligned}$$

<sup>4</sup> For  $x = r \cos(\phi)$  and  $y = r \sin(\phi)$ , then  $r\dot{r} = x\dot{x} + y\dot{y}$  and  $-\dot{\phi}r^2 = y\dot{x} - x\dot{y}$ .

It is immediate that  $r(t) = 1$  is a solution for the radius. The differential equation for the phase reduces to  $\dot{\phi} = -2\omega((1-a)\cos(\phi)^2 + (1-b)\sin(\phi)^2)$ . By separating the variables, we have

$$\int \frac{d\phi}{p^2 \cos(\phi)^2 + q^2 \sin(\phi)^2} = \int -2\omega dt \implies \frac{\tan^{-1}\left(\frac{q \tan(\phi)}{p}\right)}{pq} = -2\omega t + \frac{\theta_0}{pq},$$

with  $p^2 = 1 - a$  and  $q^2 = 1 - b$ . Then  $\phi(t) = \tan^{-1}\left(\frac{\sqrt{1-a}}{\sqrt{1-b}} \tan(-2\sqrt{1-a}\sqrt{1-b}\omega t + \theta_0)\right)$ .

Verification: For  $r(t)$  it is obvious and for  $\phi(t)$  we have, noting  $\eta(t) := -2pq\omega t + \theta_0$  and remembering that  $\tan^{-1}(x)' = \frac{1}{1+x^2}$  and  $\tan(x)' = \frac{1}{\cos(x)^2}$

$$\begin{aligned} \dot{\phi}(t) &= \frac{1}{1 + \left(\frac{p}{q}\right)^2 \tan(\eta(t))^2} \frac{p}{q} \frac{1}{\cos(\eta(t))^2} (-2pq\omega) = -2\omega \left( \frac{p^2 \frac{1}{\cos(\eta(t))^2}}{1 + \left(\frac{p}{q}\right)^2 \tan(\eta(t))^2} \right) \\ &= -2\omega \left( \frac{p^2(1 + \tan(\eta(t))^2)}{1 + \left(\frac{p}{q}\right)^2 \tan(\eta(t))^2} \right) = -2\omega \left( \frac{p^2}{1 + \left(\frac{p}{q}\right)^2 \tan(\eta(t))^2} + \frac{q^2 \left(\frac{p}{q}\right)^2 \tan(\eta(t))^2}{1 + \left(\frac{p}{q}\right)^2 \tan(\eta(t))^2} \right) \end{aligned}$$

since  $\cos(\tan^{-1}(x)) = \frac{1}{\sqrt{1+x^2}}$  and  $\sin(\tan^{-1}(x)) = \frac{x}{\sqrt{1+x^2}}$ , and so

$$\begin{aligned} \dot{\phi}(t) &= -2\omega \left( p^2 \cos(\tan^{-1}\left(\frac{p}{q} \tan(\eta(t))\right)) + q^2 \sin(\tan^{-1}\left(\frac{p}{q} \tan(\eta(t))\right)) \right) \\ &= -2\omega \left( (1-a)\cos(\phi(t))^2 + (1-b)\sin(\phi(t))^2 \right). \end{aligned}$$

## C Networks and Laplacian Matrices

A **network** is here a collection of  $N$  vertices (here labeled with indices  $1, 2, \dots, k, \dots, j, \dots, N$ ) and edges. The edges determine which vertices are connected to one and another. Each edge connecting vertex  $k$  to vertex  $j$  is given a weight (a positive or negative real number). The sum of all the weights between vertices  $k$  and  $j$  is noted as  $a_{k,j} \in \mathbb{R}$ . The  $a_{k,j}$  form the entries of the adjacency matrix  $A$  of the given network. A **network**

is **connected** if there is a path from any vertex  $k$  to any other  $j - \forall k, j \exists$  a none zero sequence

$$\{a_{k,j_1}, a_{j_1,j_2}, \dots, a_{j_m,j}\},$$

is **undirected** if  $a_{k,j} = a_{j,k}$  for all  $j, k - A = A^\top$ ,

with **positive adjacency entries** has an adjacency matrix  $A$  with positive entries  $- a_{k,j} \geq 0 \forall k, j$ ,

is **time-dependent** if its adjacency matrix is time-dependent  $- a_{k,j} : \mathbb{R}_{\geq 0} \rightarrow \mathbb{R}$  are time-dependent functions for all  $k, j$  where  $a_{k,j}(t)$  corresponds to the cumulative weights of all edges directly connecting vertex  $k$  to vertex  $j$  at time  $t$ .

A **connected and/or undirected time-dependent network with positive adjacency entries** is a network that is **connected and/or undirected with positive adjacency entries** for all  $t \in \mathbb{R}_{\geq 0}$ .

We now define the **Laplacian matrix** associated to the adjacency matrix  $A$  of the given network.

Denote by  $D(A)$  the diagonal matrix with entries  $d_{k,k} := \sum_{j=1}^N a_{k,j}$ . Then the  $N \times N$  Laplacian

matrix associated to the network is given by  $L := D(A) - A$ . A Laplacian matrix  $L$  has always a  $\zeta = 0$  as eigenvalue with  $\mathbf{1} = (1, \dots, 1) \in \mathbb{R}^N$  as an eigenvector. We have the following properties.

### Undirected Network with Positive Spectrum

For a undirected network ( $A = A^\top$ ) the Laplacian matrix is symmetric and therefore all its eigenvalues lie on  $\mathbb{R}$ . If we further suppose that  $L$  has a positive spectrum ( $\text{Spec} \subset \mathbb{R}_{\geq 0}$ ), we can define the following positive semi-definite bilinear form:  $\langle x | Lx \rangle \geq 0 \forall x \in \mathbb{R}^N$ .

### Undirected Network with Positive Adjacency Entries

For an undirected network ( $A = A^\top$ ) with positive adjacency entries ( $a_{k,j} \geq 0 \forall k, j$ ), the associated Laplacian matrix has a positive spectrum ( $\text{Spec} \subset \mathbb{R}_{\geq 0}$ ) since all eigenvalues are real ( $L$  is symmetric) and by Гершгорин's theorem (which we recall below), they are all positive.

**Theorem (Гершгорин (1931)).** *Let  $L$  be a  $N \times N$  matrix (with elements in  $\mathbb{R}$  or  $\mathbb{C}$ ). If  $\zeta$  is an eigenvalue of  $L$ , then there exist  $k$  such that*

$$|\zeta - l_{k,k}| \leq \sum_{j \neq k}^N |l_{k,j}|,$$

that is, all eigenvalues of  $L$  are in the union of the discs

$$\mathcal{D}_k := \left\{ \zeta \mid |\zeta - l_{k,k}| \leq \sum_{j \neq k}^N |l_{k,j}| \right\}.$$

### Connected Network with Positive Adjacency Entries

For a network with positive adjacency entries, all eigenvalues of  $L$  lie on the right hand side of the complex plane  $\mathbb{C}$ . If, furthermore, the network is connected, then  $L$ 's kernel is of dimension one. This is shown in the following lemma where the statement and proof are for time-dependent networks.

**Lemma.** *Let  $L(t)$  be the Laplacian matrix of a time-dependent network with positive adjacency entries. We have:*

$$\text{The network is connected } \forall t \implies \text{Dim}(\ker(L(t))) = 1 \forall t$$

*If, furthermore, the network is undirected, then we have the other direction of the implication.*

*Proof.* [ $\implies$ ] The definition of  $L(t)$  implies that  $L(t)\mathbf{1} = 0$  for all  $t$ , therefore  $\text{Dim}(\ker(L(t))) \geq 1$  for all  $t$ . Suppose that there exists  $t_0$  such that  $\text{Dim}(\ker(L(t_0))) \geq 2$ . This implies the existence of a vector  $x(t_0) := (x_1(t_0), \dots, x_N(t_0)) \in \mathbb{R}^N$  such that

- $Lx(t_0) = 0$
- $\exists j, k$  such that  $x_j(t_0) \neq x_k(t_0)$
- $\mathbf{1}$  and  $x(t_0)$  are linearly independent.

Let  $x^*(t_0) := \max_{j=1, \dots, N} \{x_j(t_0)\}$  and define  $z := x(t_0) - x^*(t_0)\mathbf{1}$ . By definition,  $z_j \leq 0$  for all  $j$ , there exist  $k$  such that  $z_k = 0$  and  $L(t_0)z = 0$ . Let  $I_0 := \{j_1, \dots, j_k\}$  such that  $z_s = 0$  for  $s \in I_0$  and  $I_+ := \{j_{k+1}, \dots, j_N\}$  such that  $z_s < 0$  for  $s \in I_+$ . We have for all  $k$

$$\begin{aligned} \sum_{j=1}^N l_{k,j}(t_0)z_j &= \left( \underbrace{\left( \sum_{j=1}^N a_{k,j}(t_0) \right) - a_{k,k}(t_0)}_{l_{k,k}(t_0)} \right) z_k - \sum_{j \neq k}^N a_{k,j}(t_0)z_j \\ &= z_k \sum_{j=1}^N a_{k,j}(t_0) - \sum_{j=1}^N a_{k,j}(t_0)z_j = 0 \end{aligned}$$

For  $k \in I_0$ ,  $z_k = 0$  and so

$$- \sum_{j=1}^N a_{k,j}(t_0)z_j = \sum_{j \in I_+}^N a_{k,j}(t_0)(-z_j) = 0$$

Since  $a_{k,j}(t_0) \geq 0$  for all  $j, k$  and  $-z_j > 0$  for  $j \in I_+$ , then  $a_{k,j}(t_0) = 0$  for  $k \in I_0$  and  $j \in I_+$  and this implies that  $\mathcal{N}$  is not connected at  $t = t_0$  since there is no path from any vertex indexed by  $k$  in  $I_0$  to any vertex indexed by  $j$  in  $I_+$ . This is in contradiction with the hypothesis.

[ $\Leftarrow$ ] Suppose that there exist  $t_0$  such that the network is not connected, which means that there exists two sets of indices  $I$  and  $I_*$  such that  $a_{k,j}(t_0) = 0$  for all  $k \in I$  and all  $j \in I_*$ . Since the network is undirected, this is also true for  $a_{j,k}$  (i.e.  $a_{j,k}(t_0) = 0$  for all  $j \in I_*$  and all  $k \in I$ ). Define a vector  $x := (x_1, \dots, x_N) \in \mathbb{R}^N$  such that  $x_s = x$  for  $s \in I$  and  $x_s = x_*$  for  $s \in I_*$  with  $x \neq x_*$ . The product  $L(t_0)x$  gives, for all  $k$ ,

$$x_k \sum_{j=1}^N a_{k,j}(t_0) - \sum_{j=1}^N a_{k,j}(t_0)x_j,$$

and for  $k \in I$

$$x \sum_{j \in I} a_{k,j}(t_0) - \sum_{j \in I} a_{k,j}(t_0)x = 0$$

since  $a_{k,j}(t_0) = 0$  for all  $j \in I_*$  with  $k \in I$ . For  $k \in I_*$ ,

$$x_* \sum_{j=1}^N \underbrace{a_{k,j}(t_0)}_{a_{j,k}} - \sum_{j=1}^N \underbrace{a_{k,j}(t_0)}_{a_{j,k}} x_j = x_* \sum_{j \in I_*} a_{j,k}(t_0) - \sum_{j \in I_*} a_{j,k}(t_0)x_* = 0.$$

We then conclude that  $L(t_0)x = 0$ , which is in contradiction with the fact that  $\text{Dim}(\ker(L(t))) = 1$ . This concludes the proof.  $\square$

### Connected and Undirected Network with Positive Adjacency Entries

For a undirected network ( $A = A^\top$ ) the Laplacian matrix is symmetric, therefore, by the Spectral Theorem,  $L$  is diagonalizable. A matrix is diagonalizable over  $\mathbb{R}$  if, and only if, its characteristic polynomial has real roots and the algebraic multiplicity (i.e. the multiplicity of the corresponding root of the characteristic polynomial) of each eigenvalue is equal to the geometric multiplicity (i.e. the dimension of the associated eigenspace). By definition of  $L$ , its kernel  $\ker(L)$  is an eigenspace. For a undirected network with positive adjacency entries, the dimension of this eigenspace is one if and only if the network is connected. Hence, since  $L$  is diagonalizable, the algebraic multiplicity of the eigenvalue zero is equal to the geometric multiplicity of the eigenspace  $\ker(L)$ . Therefore, for a connected, undirected network with positive adjacency entries, the eigenvalues  $\{\zeta_j\}_{j=1}^N$  of  $L$  are all real positive numbers except for one (say  $j = 1$ ) which is zero ( $\zeta_1 = 0$ ).

### Connectivity and Eigenvalues of Laplacian Matrices

For a connected, undirected network with positive adjacency entries, all eigenvalues of the associated Laplacian matrix are strictly positive except for one. The second smallest eigenvalue  $\zeta_2$  is known as the algebraic connectivity or FIEDLER number. Its magnitude is linked with the “connectivity” of the network and the rate at which it diffuses information. This eigenvalue can be use as a measure of “synchronizability” (c.f. [7]) and “network speed” (c.f. [36]). It plays an important role in many synchronization, consensus and self-organization of swarms problems.

The algebraic connectivity  $\zeta_2$ , as its name suggests, is linked to various notions of network “connectivity”. Among the many results in the literature, we recall two of them. In both cases, we suppose that the networks are unweighted and simple (i.e. it has no self-loops or multi-edges, therefore the adjacency matrix is made up of 0 or 1 with 0 on its diagonal).

Edge-connectivity Let  $\tau$  denote the edge-connectivity of a given  $N$ -vertex network (i.e. The edge connectivity of a nontrivial<sup>5</sup> network  $\mathcal{N}$ , denoted by  $\tau$  is the minimum number of edges

<sup>5</sup> A trivial network has one vertex and no edges.

whose removal from  $\mathcal{N}$  results on a non-connected network (definition taken in [22])). Then

$$2\tau(1 - \cos(\frac{\pi}{N})) \leq \zeta_2 \leq \tau ,$$

where  $\zeta_2$  is the algebraic connectivity of the Laplacian matrix associated to  $\mathcal{N}$ .

Non-decreasing  $\zeta_2$  Consider two networks  $\check{\mathcal{N}}$  and  $\mathcal{N}$  that have the same set of vertices. Suppose that  $\mathcal{N}$  has all edges of  $\check{\mathcal{N}}$  (i.e. intuitively expressed:  $\check{\mathcal{N}}$  is a “spanning subnetwork” of  $\mathcal{N}$ ). Then

$$\check{\zeta}_2 \leq \zeta_2 ,$$

where  $\check{\zeta}_2$  and  $\zeta_2$  are, respectively, the algebraic connectivity's of the Laplacian matrices associated to  $\check{\mathcal{N}}$  and  $\mathcal{N}$ . In other words, the algebraic connectivity, seen as a function of networks with identical set of vertices, is non-decreasing.

A proof of these results are in [17]. Note that the non-decreasing property of  $\zeta_2$  can be generalized to weighted networks with non-negative weights (c.f. [32]). Which means, that the more a networks has of edges or the greater the weights of the edges are, the greater is FIEDLER number.

In this thesis, we use the following terminology: FIEDLER number is used in the case of weighted network whereas the term algebraic connectivity, implies that the network is unweighted and simple.

### Verification for the Laplacian Potential

The fact that  $V(X) = \sum_{s=1}^p \mathbf{a}_s \langle x_s | Lx_s \rangle \geq 0$  is straightforward since  $L$  is the Laplacian matrix associated to a connected, undirected network with positive adjacency entries, hence, for each  $s$ ,  $\langle x_s | Lx_s \rangle$  is a positive semi-definite bilinear form. We must now verify Eqs. (1.4), namely  $X_k = X_j \forall k, j \iff \sum_{s=1}^p \mathbf{a}_s \langle x_s | Lx_s \rangle = 0$ .

[ $\implies$ ] The hypothesis  $X_k = (x_{k,1}, \dots, x_{k,p}) = (x_{j,1}, \dots, x_{j,p}) = X_j$  for all  $k, j \in \{1, \dots, N\}$  is equivalent to  $x_{k,s} = x_{j,s}$  for all  $k, j$  and for any fixed  $s$  ( $s = 1, \dots, p$ ), which is again equivalent to  $x_s = (x_{1,s}, \dots, x_{N,s}) = \theta_s \mathbf{1}$  for a certain real number  $\theta_s$  ( $s = 1, \dots, p$ ). The vector  $\mathbf{1}$  is an eigenvector with eigenvalue 0 of the Laplacian matrix  $L$  so that  $L\theta_s \mathbf{1} = \mathbf{0}$  and hence  $\langle \theta_s \mathbf{1} | L\theta_s \mathbf{1} \rangle = 0$  for all  $s$ .

[ $\impliedby$ ] By definition we have  $\{X \in \mathbb{R}^{pN} \mid \sum_{s=1}^p \mathbf{a}_s \langle x_s | Lx_s \rangle = 0\} = \{X \in \mathbb{R}^{pN} \mid \langle x_s | Lx_s \rangle = 0 \forall s\}$  since all the terms in the sum are positive. This set is equal to  $\{X \in \mathbb{R}^{pN} \mid Lx_s = \mathbf{0} \forall s\}$  because

[ $\subseteq$ ] Let  $X \in \mathbb{R}^{pN}$  such that  $\langle x_s | Lx_s \rangle = 0 \forall s$  ( $x_s \in \mathbb{R}^N$ ). Since  $L$  is symmetric then, by the Spectral Theorem, there exists an orthogonal basis  $\{v_j\}_{j=1}^N$  of eigenvectors of  $L$ . In this basis,

$x_s = \sum_{j=1}^N \theta_{s,j} v_j$  and so the product becomes

$$0 = \langle x_s | Lx_s \rangle = \left\langle \sum_{j=1}^N \theta_{s,j} v_j \mid \sum_{j=1}^N \theta_{s,j} \underbrace{Lv_j}_{=\zeta_j v_j} \right\rangle = \sum_{j,k=1}^N \langle \theta_{s,j} v_j \mid \zeta_k \theta_{s,k} v_k \rangle .$$

Since  $\langle v_j | v_k \rangle = 0$  for all  $j, k$  and  $j \neq k$ , we have  $0 = \langle x_s | Lx_s \rangle = \sum_{j=1}^N \theta_{s,j}^2 \zeta_j \|v_j\|^2 = \sum_{j \in I_0} \theta_{s,j}^2 \zeta_j \|v_j\|^2 + \sum_{j \in I_+} \theta_{s,j}^2 \zeta_j \|v_j\|^2$ , where  $I_0$  and  $I_+$  are the index sets such that  $\zeta_j = 0$  for  $j \in I_0$  and  $\zeta_j > 0$  for  $j \in I_+$  respectively (since  $L$  is positive semi-definite bilinear). Therefore,  $\sum_{j \in I_+} \theta_{s,j}^2 \zeta_j \|v_j\|^2 = 0$  and hence  $\theta_{s,j} = 0$  for  $j \in I_+$ . This implies that  $Lx_s = \mathbf{0}$  since



$$Lx_s = L \sum_{j=1}^N \theta_{s,j} v_j = \sum_{j=1}^N \theta_{s,j} L v_j = \sum_{j=1}^N \theta_{s,j} \zeta_j v_j = \sum_{j \in I_0} \theta_{s,j} \underbrace{\zeta_j}_{=0} v_j + \sum_{j \in I_+} \underbrace{\theta_{s,j}}_{=0} \zeta_j v_j$$

and so  $Lx_s = \mathbf{0}$ .

[ $\supseteq$ ] It is obvious.

Since the network is connected, the dimension of  $L$ 's kernel is one and so  $\ker(L) = \{x \in \mathbb{R}^N \mid \exists \theta \in \mathbb{R} \text{ such that } x = \theta \mathbf{1}\}$ . Therefore  $\{X \in \mathbb{R}^{pN} \mid \sum_{s=1}^p \mathbf{a}_s \langle x_s \mid Lx_s \rangle = 0\} = \{X \in \mathbb{R}^{pN} \mid Lx_s = \mathbf{0} \forall s\} = \{X \in \mathbb{R}^{pN} \mid \exists \theta_s \in \mathbb{R} \text{ such that } x_s = \theta_s \mathbf{1} \forall s\}$  and  $x_s = (x_{1,s}, \dots, x_{N,s}) = \theta_s \mathbf{1}$  ( $s = 1, \dots, p$ ) is equivalent to  $X_k = (x_{k,1}, \dots, x_{k,p}) = (x_{j,1}, \dots, x_{j,p}) = X_j$  for all  $k, j \in \{1, \dots, N\}$ .

## D Symmetric and Anti-Symmetric Matrices

**Lemma D.1.** Let  $L$  denote a  $N \times N$  symmetric matrix and  $x, y \in \mathbb{R}^N$ . Then

$$\sum_{k=1}^N \sum_{j=1}^N l_{k,j} (x_j y_k - y_j x_k) = 0.$$

*Proof.* By direct calculation, we obtain

$$\begin{aligned} \sum_{k=1}^N \sum_{j=1}^N l_{k,j} (x_j y_k - y_j x_k) &= \sum_{k=1}^N \left( \left( \sum_{j=1}^N l_{k,j} x_j \right) y_k - \left( \sum_{j=1}^N l_{k,j} y_j \right) x_k \right) = \langle Lx \mid y \rangle - \langle Ly \mid x \rangle \\ &\stackrel{\substack{L \text{ is symmetric}}}{=} \langle Lx \mid y \rangle - \langle y \mid Lx \rangle = 0. \end{aligned}$$

□

**Lemma D.2.** Let  $L$  denote a  $N \times N$  symmetric Laplacian matrix (i.e. the underlying network is undirected) and  $x \in \mathbb{R}^N$ . Then

$$\sum_{k=1}^N \sum_{j=1}^N l_{k,j} x_j = 0.$$

*Proof.* By direct calculation, we have

$$\sum_{k=1}^N \sum_{j=1}^N l_{k,j} x_j = \langle \mathbf{1} \mid Lx \rangle \stackrel{\substack{L \text{ is symmetric}}}{=} \langle L\mathbf{1} \mid x \rangle = 0$$

where  $\mathbf{1}$  is a  $N$  dimensional vector of 1 and  $\mathbf{1}$  is an eigenvector of  $L$  with eigenvalue zero.

□

**Lemma D.3.** Let  $L$  denote a  $N \times N$  positive semi-definite symmetric matrix and  $K$  a  $N \times N$  positive definite diagonal matrix with entries  $k_j > 0$  for all  $j$ . Then

$$\begin{aligned} &KLK \text{ is positive semi-definite (i.e. } \text{Spec}(KLK) \subset \mathbb{R}_{\geq 0} \text{) and} \\ &|\{x \in \text{Spec}(L) \mid x = 0\}| = |\{x \in \text{Spec}(KLK) \mid x = 0\}|. \end{aligned}$$

*Proof.* Let  $X \in \mathbb{R}^N$ . By direct calculation, we have

$$\langle X \mid KLKX \rangle = \sum_{k=1}^N x_k \left( \sum_{j=1}^N k_k l_{k,j} k_j x_j \right) = \sum_{k=1}^N x_k k_k \left( \sum_{j=1}^N l_{k,j} k_j x_j \right) = \langle Y \mid LY \rangle \geq 0 \forall Y \in \mathbb{R}^N,$$

where  $Y = KX$  and by hypothesis  $L$  is positive semi-definite. Therefore  $KLK$  is positive semi-definite. If  $L$  is positive definite, the  $KLK$  is also positive definite and therefore neither  $L$  nor  $KLK$  has a zero eigenvalue (i.e.  $\text{Spec}(L) \subset \mathbb{R}_{>0}$  and  $\text{Spec}(KLK) \subset \mathbb{R}_{>0}$  and so  $|\{x \in \text{Spec}(L) \mid x = 0\}| = |\{x \in \text{Spec}(KLK) \mid x = 0\}| = 0$ ). If  $L$  is not positive definite, then there exists  $n$  ( $1 \geq n \geq N$ ) such that  $\text{Dim}(\ker(L)) = n$ . Since  $L$  is symmetric, then, by the spectral theorem in  $\mathbb{R}$ , there exists an orthonormal basis  $\{O_k\}_{k=1}^N$  of eigenvectors of  $L$ . Without loss of generality, suppose that the first  $n$  basis vectors  $O_1, \dots, O_n$  are a basis of  $\ker(L)$ . Then  $K^{-\frac{1}{2}}O_1, \dots, K^{-\frac{1}{2}}O_n$  are a basis of  $\ker(KLK)$  and hence  $\text{Dim}(\ker(KLK)) = n$ . Since  $LKL$  is symmetric, it is diagonalizable and so, for each of its eigenvalues, the algebraic multiplicity is equal to the geometric multiplicity. Therefore the number of times the zero eigenvalues appears is  $n$  and hence  $|\{x \in \text{Spec}(L) \mid x = 0\}| = |\{x \in \text{Spec}(KLK) \mid x = 0\}|$ .

□

**Lemma D.4.** *Let  $T$  denote a  $p \times p$  anti-symmetric matrix and  $x, y \in \mathbb{R}^p$ . Then*

$$\sum_{\substack{s,l=1 \\ s < l}}^p t_{l,s} (y_l x_s - y_s x_l) = \langle y \mid Tx \rangle$$

and therefore  $\langle x \mid Tx \rangle = 0$ .

*Proof.* Developing the left hand side

$$\begin{aligned} \sum_{\substack{s,l=1 \\ s < l}}^p t_{l,s} (y_l x_s - y_s x_l) &= \sum_{\substack{s,l=1 \\ s < l}}^p t_{l,s} y_l x_s + \sum_{\substack{s,l=1 \\ s < l}}^p \underbrace{-t_{l,s}}_{t_{s,l}} y_s x_l \\ &= \sum_{l=1}^{p-1} y_l \left( \sum_{s=l+1}^p t_{l,s} x_s \right) + \sum_{s=2}^p y_s \left( \sum_{l=1}^{s-1} t_{s,l} x_l \right) \\ &= \langle y \mid T^{\triangleleft} x \rangle + \langle y \mid T^{\triangleright} x \rangle, \end{aligned}$$

where  $T^{\triangleleft}$  and  $T^{\triangleright}$  are respectively upper and lower triangular matrices with the entries of  $T$  implying that  $T^{\triangleleft} + T^{\triangleright} = T$ , which concludes the proof.

□

## E Equality between kernels

We have to see that for all  $X^* \in \mathcal{M}$  (c.f. (2.7)),  $\ker(\mathfrak{D}^2 \mathbb{J}(X^*)) = \ker(\mathfrak{D} \mathbb{M}(X^*))$  with

$$\mathbb{J}(X) := \mathbb{K}(X) + \mathbb{V}(X)$$

and where we define  $\mathbb{K}(X) := \sum_{k=1}^N \frac{1}{c_k} \mathbb{A}_k(X_k)$  with  $\mathbb{A}_k(X_k) := \frac{1}{2} \sum_{j \in I_k} \mathbb{G}_j(X_k)^2$ . According to our definition of  $\mathcal{M}$ , any  $X^* \in \mathcal{M}$  has the following property:  $X_1 \in \mathcal{L}$  (and therefore in any  $\mathcal{L}_k$ ) and  $X_k = X_c$  for all  $k$ .

Let  $X^* \in \mathcal{M}$ , then  $\mathfrak{D}^2 \mathbb{J}(X^*)$  is positive semi-definite (since  $X^*$  is a minimum of  $\mathbb{J}(X)$ ) and symmetric. Therefore  $\ker(\mathfrak{D}^2 \mathbb{J}(X^*)) := \{X \in \mathbb{R}^{pN} \mid \langle X \mid \mathfrak{D}^2 \mathbb{J}(X^*) X \rangle = 0\}$  and  $\langle X \mid \mathfrak{D}^2 \mathbb{J}(X^*) X \rangle = \langle X \mid \mathfrak{D}^2 \mathbb{K}(X^*) X \rangle + \langle X \mid \mathfrak{D}^2 \mathbb{V}(X^*) X \rangle$ , with both terms being positive semi-definite (since  $X^*$  is a minimum for both terms). Hence

$$X \in \ker(\mathfrak{D}^2 \mathbb{J}(X^*)) \iff \langle X \mid \mathfrak{D}^2 \mathbb{K}(X^*) X \rangle = 0 \quad \text{and} \quad \langle X \mid \mathfrak{D}^2 \mathbb{V}(X^*) X \rangle = 0$$

where  $\mathfrak{D}^2 \mathbb{K}(X)$  is a  $N \times N$  bloc matrix with blocs of dimension  $p \times p$  (i.e.  $pN \times pN$  square matrix). The  $k^{\text{th}}$  diagonal bloc is the  $p \times p$  symmetric matrix  $\frac{1}{c_k} \mathfrak{D}^2 \mathbb{A}_k(X_k)$  and reads as

$$\frac{1}{c_k} \sum_{j \in I_k} \left( \frac{\partial G_j}{\partial x_{k,s}}(X_k) \frac{\partial G_j}{\partial x_{k,r}}(X_k) + G_j(X_k) \frac{\partial^2 G_j}{\partial x_{k,s} \partial x_{r,k}}(X_k) \right) \quad r, s = 1, \dots, p,$$

while all other entries are 0. Evaluating  $\mathfrak{D}^2 K(X)$  at  $X^* \in \mathcal{M}$  gives  $\frac{1}{c_k} \sum_{j \in I_k} \left( \frac{\partial G_j}{\partial x_{k,s}}(X_k^*) \frac{\partial G_j}{\partial x_{k,r}}(X_k^*) \right)$ .

We drop the  $k$  index in the sum since it is no longer relevant (i.e.  $X_k^* = X_c^*$  for all  $k$ ) and use the notation  $\frac{\partial G_j}{\partial x_s^*} := \frac{\partial G_j}{\partial x_{k,s}}(X_c^*)$ , so that the entries of the  $p \times p$  symmetric matrix  $\mathfrak{D}^2 A_k(X_c^*)$  are  $\sum_{j \in I_k} \frac{\partial G_j}{\partial x_r^*} \frac{\partial G_j}{\partial x_s^*}$ . Since  $\mathfrak{D}^2 A_k(X_c^*)$  is positive semi-definite (since  $X_c^*$  is a minimum) for all  $k$ , we have

$$\langle X | \mathfrak{D}^2 K(X^*) X \rangle = 0 \iff \langle X_k | \frac{1}{c_k} \mathfrak{D}^2 A_k(X_c^*) X_k \rangle = 0 \quad \text{for all } k.$$

As we obtain

$$\begin{aligned} \langle X_k | \frac{1}{c_k} \mathfrak{D}^2 A_k(X_c^*) X_k \rangle &= \frac{1}{c_k} \sum_{l \in I_k} \left( \sum_{r=1}^p \sum_{s=1}^p \frac{\partial G_l}{\partial x_r^*} \frac{\partial G_l}{\partial x_s^*} x_{k,s} x_{k,r} \right) \\ &= \frac{1}{c_k} \sum_{l \in I_k} \left( \sum_{j=1}^p \left( \frac{\partial G_l}{\partial x_j^*} x_{k,j} \right)^2 + 2 \sum_{\substack{r,j=1 \\ r < j}}^p \frac{\partial G_l}{\partial x_r^*} x_{k,r} \frac{\partial G_l}{\partial x_j^*} x_{k,j} \right) \\ &= \frac{1}{c_k} \sum_{l \in I_k} \left( \sum_{j=1}^p \frac{\partial G_l}{\partial x_j^*} x_{k,j} \right)^2, \end{aligned}$$

then

$$\langle X | \mathfrak{D}^2 K(X^*) X \rangle = 0 \iff \langle \nabla G_l(X_c^*) | X_k \rangle = 0 \quad l \in I_k \quad \forall k \iff X_k \in \ker(\mathfrak{D}G(X^*)) \quad \forall k.$$

By hypothesis of Proposition 2.1 we have that  $\langle X | \mathfrak{D}^2 V(X^*) X \rangle = 0 \iff X_k = X_c$  for all  $k$ , and so

$$X \in \ker(\mathfrak{D}^2 \Pi(X^*)) \iff X_k = X_c \quad \forall k \quad \text{and} \quad X_c \in \ker(\mathfrak{D}G(X^*)) \iff X \in \ker(\mathfrak{D}M(X^*)).$$

## F Linearization and Diagonalization of Eqs. (3.9)

We proceed as in Lemma 3.1.

### Linearization

The Jacobian  $J(t)$  of System 3.9 evaluated at periodic solution in (3.12) is

$$\begin{pmatrix} \frac{\partial L_1}{\partial x} Id - C L & \frac{\partial L_1}{\partial y} Id & \frac{\partial L_1}{\partial \omega} Id & \frac{\partial L_1}{\partial \rho} Id & \frac{\partial L_1}{\partial \gamma_1} Id & \dots & \frac{\partial L_1}{\partial \gamma_{q-2}} Id \\ \frac{\partial L_2}{\partial x} Id & \frac{\partial L_2}{\partial y} Id - C L & \frac{\partial L_2}{\partial \omega} Id & \frac{\partial L_2}{\partial \rho} Id & \frac{\partial L_2}{\partial \gamma_1} Id & \dots & \frac{\partial L_2}{\partial \gamma_{q-2}} Id \\ -\varphi_y(t) S_\omega L & \varphi_x(t) S_\omega L & \mathbf{0} & \mathbf{0} & \mathbf{0} & \dots & \mathbf{0} \\ -\frac{\partial H}{\partial x} S_\rho L & -\frac{\partial H}{\partial y} S_\rho L & \mathbf{0} & -\frac{\partial H}{\partial \rho} S_\rho L & -\frac{\partial H}{\partial \gamma_1} S_\rho L & \dots & -\frac{\partial H}{\partial \gamma_{q-2}} S_\rho L \\ \frac{\partial^2 H}{\partial x \partial \gamma_1} S_{\gamma_1} L & \frac{\partial^2 H}{\partial y \partial \gamma_1} S_{\gamma_1} L & \mathbf{0} & \frac{\partial^2 H}{\partial \rho \partial \gamma_1} S_{\gamma_1} L & \frac{\partial^2 H}{\partial \gamma_1^2} S_{\gamma_1} L & \dots & \frac{\partial^2 H}{\partial \gamma_{q-2} \gamma_1} S_{\gamma_1} L \\ \vdots & \vdots & \vdots & \vdots & \vdots & \ddots & \vdots \\ \frac{\partial^2 H}{\partial x \partial \gamma_{q-2}} S_{\gamma_{q-2}} L & \frac{\partial^2 H}{\partial y \partial \gamma_{q-2}} S_{\gamma_{q-2}} L & \mathbf{0} & \frac{\partial^2 H}{\partial \rho \partial \gamma_{q-2}} S_{\gamma_{q-2}} L & \frac{\partial^2 H}{\partial \gamma_{q-2}^2} S_{\gamma_{q-2}} L & \dots & \frac{\partial^2 H}{\partial \gamma_{q-2} \gamma_1} S_{\gamma_{q-2}} L \end{pmatrix}$$

where all the partial derivative functions are evaluated at  $\varphi(t)$  (c.f. (3.12)),  $Id$  is the  $N$ -dimensional identity matrix and  $C, S_\omega, S_\rho, S_{\gamma_1}, \dots, S_{\gamma_{q-2}}$  are diagonal matrices with their respective coupling

strengths and susceptibility constants on the diagonal. Note that we did not made use of the assumption in 3.20 (i.e. coupling strengths and all susceptibility constants are independent). Thus the first variational equation of Eqs. (3.9) is

$$\dot{\epsilon} = J(t)\epsilon \quad (\text{F.1})$$

with  $\epsilon = (\epsilon_x, \epsilon_y, \epsilon_\omega, \epsilon_\rho, \epsilon_{\gamma_1}, \dots, \epsilon_{\gamma_{q-2}})$ ,  $\epsilon_x = (\epsilon_{x_1}, \dots, \epsilon_{x_N})$ ,  $\epsilon_y = (\epsilon_{y_1}, \dots, \epsilon_{y_N})$ ,  $\epsilon_\omega = (\epsilon_{\omega_1}, \dots, \epsilon_{\omega_N})$ ,  $\epsilon_\rho = (\epsilon_{\rho_1}, \dots, \epsilon_{\rho_N})$ ,  $\epsilon_{\gamma_s} = (\epsilon_{\gamma_{1,s}}, \dots, \epsilon_{\gamma_{N,s}})$  for  $s = 1, \dots, q-2$  and  $J(t)$  periodic with the same period as the periodic solution in (3.12).

### Diagonalization

With the assumption in 3.20, we can simultaneously diagonalize all the  $CL$ ,  $S_\omega L$ ,  $S_\rho L$ ,  $S_{\gamma_1} L$ ,  $\dots$ ,  $S_{\gamma_{q-2}} L$  matrices. Let  $K^{\frac{1}{2}}$  be the diagonal matrix with  $\sqrt{\kappa_1}, \dots, \sqrt{\kappa_N}$  on its diagonal. Then

$$K^{-\frac{1}{2}}CLK^{\frac{1}{2}} = cK^{-\frac{1}{2}}K L K^{\frac{1}{2}} = cK^{\frac{1}{2}}L K^{\frac{1}{2}}$$

and since  $K^{\frac{1}{2}}L K^{\frac{1}{2}}$  is symmetric, then there exists an orthonormal matrix  $O$  such that  $O^\top K^{\frac{1}{2}}L K^{\frac{1}{2}}O = D(\kappa)$ , where  $D(\kappa)$  is a diagonal matrix with its spectrum  $\kappa = (\kappa_1, \dots, \kappa_N)$  on its diagonal. Hence,  $K^{\frac{1}{2}}O$  diagonalizes  $CL$  and the same is true for all  $S_\omega L$ ,  $S_\rho L$ ,  $S_{\gamma_1} L$ ,  $\dots$ ,  $S_{\gamma_{q-2}} L$  matrices. They all share the same spectrum  $\kappa = (\kappa_1, \dots, \kappa_N)$  that is multiplied, respectively, by their coupling strength and susceptibility constants  $c$ ,  $s_\omega$ ,  $s_\rho$ ,  $s_{\gamma_1}$ ,  $\dots$ ,  $s_{\gamma_{q-2}}$ .

Changing the basis of the variational Equation F.1 by  $Q$ , a  $(2+q) \times (2+q)$ -bloc matrix (blocs of size  $N \times N$ ) with  $K^{\frac{1}{2}}O$  on its diagonal makes  $J(t)$  a  $(2+q) \times (2+q)$ -bloc matrix with each bloc being a  $N \times N$  diagonal matrix. Another change of basis with  $P$  as defined in 3.18 (i.e. recollecting the local variables together) leads to

$$P^{-1}Q^{-1}\dot{\epsilon} = P^{-1}Q^{-1}J(t)QPP^{-1}Q^{-1}\epsilon \iff \dot{\epsilon}_k = J_k(t)\epsilon_k \quad k = 1, \dots, N,$$

with  $P^{-1}Q^{-1}\epsilon = \varepsilon = (\varepsilon_1, \dots, \varepsilon_N)$ ,  $\varepsilon_k = (\varepsilon_{x_k}, \varepsilon_{y_k}, \varepsilon_{\omega_k}, \varepsilon_{\rho_k}, \varepsilon_{\gamma_{k,1}}, \dots, \varepsilon_{\gamma_{k,q-2}})$ , and where  $J_k(t)$  is the  $(2+q) \times (2+q)$  matrix given by

$$\begin{pmatrix} \frac{\partial L_1}{\partial x} - c\kappa_k & \frac{\partial L_1}{\partial y} & \frac{\partial L_1}{\partial \omega} & \frac{\partial L_1}{\partial \rho} & \frac{\partial L_1}{\partial \gamma_1} & \dots & \frac{\partial L_1}{\partial \gamma_{q-2}} \\ \frac{\partial L_2}{\partial x} & \frac{\partial L_2}{\partial y} - c\kappa_k & \frac{\partial L_2}{\partial \omega} & \frac{\partial L_2}{\partial \rho} & \frac{\partial L_2}{\partial \gamma_1} & \dots & \frac{\partial L_2}{\partial \gamma_{q-2}} \\ -\varphi_y(t)s_\omega \kappa_k & \varphi_x(t)s_\omega \kappa_k & \mathbf{0} & \mathbf{0} & \mathbf{0} & \dots & \mathbf{0} \\ -\frac{\partial H}{\partial x} s_\rho \kappa_k & -\frac{\partial H}{\partial y} s_\rho \kappa_k & \mathbf{0} & -\frac{\partial H}{\partial \rho} s_\rho \kappa_k & -\frac{\partial H}{\partial \gamma_1} s_\rho \kappa_k & \dots & -\frac{\partial H}{\partial \gamma_{q-2}} s_\rho \kappa_k \\ \frac{\partial^2 H}{\partial x \partial \gamma_1} s_{\gamma_1} \kappa_k & \frac{\partial^2 H}{\partial y \partial \gamma_1} s_{\gamma_1} \kappa_k & \mathbf{0} & \frac{\partial^2 H}{\partial \rho \partial \gamma_1} s_{\gamma_1} \kappa_k & \frac{\partial^2 H}{\partial \gamma_1^2} s_{\gamma_1} \kappa_k & \dots & \frac{\partial^2 H}{\partial \gamma_{q-2} \partial \gamma_1} s_{\gamma_1} \kappa_k \\ \vdots & \vdots & \vdots & \vdots & \vdots & \ddots & \vdots \\ \frac{\partial^2 H}{\partial x \partial \gamma_{q-2}} s_{\gamma_{q-2}} \kappa_k & \frac{\partial^2 H}{\partial y \partial \gamma_{q-2}} s_{\gamma_{q-2}} \kappa_k & \mathbf{0} & \frac{\partial^2 H}{\partial \rho \partial \gamma_{q-2}} s_{\gamma_{q-2}} \kappa_k & \frac{\partial^2 H}{\partial \gamma_{q-2}^2} s_{\gamma_{q-2}} \kappa_k & \dots & \frac{\partial^2 H}{\partial \gamma_{q-2} \partial \gamma_1} s_{\gamma_{q-2}} \kappa_k \end{pmatrix}$$

where all the partial derivative functions are evaluated at the periodic solution  $\varphi(t)$  (c.f. (3.12)). Therefore, there are  $N$  systems, each of size  $(2+q) \times (2+q)$  and only differing in the values  $c\kappa_k$ ,  $s_\omega \kappa_k$ ,  $s_\rho \kappa_k$ ,  $s_{\gamma_1} \kappa_k$ ,  $\dots$ ,  $s_{\gamma_{q-2}} \kappa_k$ .

## G Hopf Oscillators in Polar Coordinates

Consider the Hopf oscillator coupled to some given functions  $C_1$  and  $C_2$

$$\dot{x} = \omega y - (x^2 + y^2 - r)x + C_1, \quad (\text{G.1a})$$

$$\dot{y} = -\omega x - (x^2 + y^2 - r)y + C_2. \quad (\text{G.1b})$$

Expressing variables  $x(t)$  and  $y(t)$  in polar coordinates and differentiating them with respect to time gives

$$\begin{aligned} x(t) &= r(t) \cos(\phi(t)) \xrightarrow{\frac{d}{dt}} \dot{x}(t) = \dot{r}(t) \cos(\phi(t)) - r(t) \sin(\phi(t)) \dot{\phi}(t) , \\ y(t) &= r(t) \sin(\phi(t)) \xrightarrow{\frac{d}{dt}} \dot{y}(t) = \dot{r}(t) \sin(\phi(t)) + r(t) \cos(\phi(t)) \dot{\phi}(t) . \end{aligned}$$

From now on, we omit the time argument. Multiplying Eq.(G.1a) by  $x$  and Eq.(G.1b) by  $y$  and adding them gives

$$\dot{x}x + \dot{y}y = -(x^2 + y^2 - r)(x^2 + y^2) + xC_1 + yC_2 ,$$

and

$$\begin{aligned} \dot{x}x + \dot{y}y &= (\dot{r} \cos(\phi) - r \sin(\phi) \dot{\phi})(r \cos(\phi)) + (\dot{r} \sin(\phi) + r \cos(\phi) \dot{\phi})(r \sin(\phi)) \\ &= r\dot{r} \cos(\phi)^2 - r^2 \sin(\phi) \cos(\phi) \dot{\phi} + r\dot{r} \sin(\phi)^2 + r^2 \cos(\phi) \sin(\phi) \dot{\phi} = \dot{r}r . \end{aligned}$$

Since  $r^2 = x^2 + y^2$ , then, in polar coordinates, we have

$$\dot{r} = -(r^2 - r)r + \frac{1}{r}(r \cos(\phi)C_1 + r \sin(\phi)C_2) = -(r^2 - r)r + (\cos(\phi)C_1 + \sin(\phi)C_2) .$$

Multiplying Eq.(G.1a) by  $y$  and Eq.(G.1b) by  $x$  and subtracting ‘‘Eq. (G.1a)  $\times y$ ’’ with ‘‘Eq.(G.1b)  $\times x$ ’’ gives

$$\dot{x}y - \dot{y}x = \omega(x^2 + y^2) + yC_1 - xC_2 ,$$

and

$$\begin{aligned} \dot{x}y - \dot{y}x &= (\dot{r} \cos(\phi) - r \sin(\phi) \dot{\phi})(r \sin(\phi)) - (\dot{r} \sin(\phi) + r \cos(\phi) \dot{\phi})(r \cos(\phi)) \\ &= r\dot{r} \cos(\phi) \sin(\phi) - r^2 \sin(\phi)^2 \dot{\phi} - r\dot{r} \sin(\phi) \cos(\phi) - r^2 \cos(\phi)^2 \dot{\phi} = -\dot{\phi}r^2 . \end{aligned}$$

Then, in polar coordinates, we have

$$\dot{\phi} = -\omega - \frac{1}{r}(\sin \phi C_1 - \cos(\phi)C_2) .$$

Therefore the system in polar coordinates is

$$\begin{aligned} \dot{r} &= -(r^2 - r)r + (\cos(\phi)C_1 + \sin(\phi)C_2) , \\ \dot{\phi} &= -\omega - \frac{1}{r}(\sin(\phi)C_1 - \cos(\phi)C_2) . \end{aligned}$$

In the context of a network of coupled Hopf oscillators (for example, when  $C_1 = -c_k \sum_{j=1}^N l_{k,j} x_j$  and  $C_2 = -c_k \sum_{j=1}^N l_{k,j} y_j$ ) with an adaptive mechanism on  $\omega_k$ , we then have, in polar coordinates,

$$\dot{r}_k = -(r_k^2 - r)r_k - c_k \left( \cos(\phi_k) \sum_{j=1}^N l_{k,j} r_j \cos(\phi_j) + \sin(\phi_k) \sum_{j=1}^N l_{k,j} r_j \sin(\phi_j) \right) , \quad (\text{G.2a})$$

$$\dot{\phi}_k = -\omega_k + \frac{c_k}{r_k} \left( \sin(\phi_k) \sum_{j=1}^N l_{k,j} r_j \cos(\phi_j) - \cos(\phi_k) \sum_{j=1}^N l_{k,j} r_j \sin(\phi_j) \right) , \quad (\text{G.2b})$$

$$\dot{\omega}_k = -s_k \left( r_k \sin(\phi_k) \sum_{j=1}^N l_{k,j} r_j \cos(\phi_j) - r_k \cos(\phi_k) \sum_{j=1}^N l_{k,j} r_j \sin(\phi_j) \right) , \quad (\text{G.2c})$$

for  $k = 1, \dots, N$ . The last two terms in Eqs. (G.2a) become

$$\cos(\phi_k) \sum_{j=1}^N l_{k,j} r_j \cos(\phi_j) + \sin(\phi_k) \sum_{j=1}^N l_{k,j} r_j \sin(\phi_j)$$

$$= \sum_{j=1}^N l_{k,j} r_j \left( \underbrace{\cos(\phi_j) \cos(\phi_k)}_{\frac{1}{2} \cos(\phi_j + \phi_k) + \frac{1}{2} \cos(\phi_j - \phi_k)} + \underbrace{\sin(\phi_j) \sin(\phi_k)}_{\frac{1}{2} \cos(\phi_j - \phi_k) - \frac{1}{2} \cos(\phi_j + \phi_k)} \right) = \sum_{j=1}^N l_{k,j} r_j \underbrace{\cos(\phi_j - \phi_k)}_{\cos(\phi_k - \phi_j)} .$$

The last two terms in Eqs. (G.2b) become

$$\begin{aligned} & \sin(\phi_k) \sum_{j=1}^N l_{k,j} r_j \cos(\phi_j) - \cos(\phi_k) \sum_{j=1}^N l_{k,j} r_j \sin(\phi_j) \\ &= \sum_{j=1}^N l_{k,j} r_j \left( \underbrace{\cos(\phi_j) \sin(\phi_k)}_{\frac{1}{2} \sin(\phi_k + \phi_j) + \frac{1}{2} \sin(\phi_k - \phi_j)} - \underbrace{\sin(\phi_j) \cos(\phi_k)}_{\frac{1}{2} \sin(\phi_j + \phi_k) + \frac{1}{2} \sin(\phi_j - \phi_k)} \right) = \sum_{j=1}^N l_{k,j} r_j \sin(\phi_k - \phi_j) . \end{aligned}$$

The last Eqs. (G.2c) become

$$\begin{aligned} & r_k \sin(\phi_k) \sum_{j=1}^N l_{k,j} r_j \cos(\phi_j) - r_k \cos(\phi_k) \sum_{j=1}^N l_{k,j} r_j \sin(\phi_j) \\ &= \sum_{j=1}^N l_{k,j} r_j r_k \left( \underbrace{\cos(\phi_j) \sin(\phi_k)}_{\frac{1}{2} \sin(\phi_k + \phi_j) + \frac{1}{2} \sin(\phi_k - \phi_j)} - \underbrace{\sin(\phi_j) \cos(\phi_k)}_{\frac{1}{2} \sin(\phi_j + \phi_k) + \frac{1}{2} \sin(\phi_j - \phi_k)} \right) = \sum_{j \neq k}^N l_{k,j} r_j r_k \sin(\phi_k - \phi_j) . \end{aligned}$$

Therefore the system is

$$\begin{aligned} \dot{r}_k &= -(r_k^2 - r) r_k - c_k \sum_{j=1}^N l_{k,j} r_j \cos(\phi_k - \phi_j) , \\ \dot{\phi}_k &= -\omega_k + \frac{c_k}{r_k} \sum_{j=1}^N l_{k,j} r_j \sin(\phi_k - \phi_j) , \\ \dot{\omega}_k &= -s_k \sum_{j=1}^N l_{k,j} r_j r_k \sin(\phi_k - \phi_j) . \end{aligned}$$

---

## References

1. ACEBRÓN, J., SPIGLER, R. Adaptive frequency model for phase-frequency synchronization in large populations of globally coupled nonlinear oscillators. *Physical Review Letters*, 81 (1998), 2229–2232.
2. ALMENDRAL, J., LEYVA, I., SENDIÑA-NADAL, I., BOCCALETTI, S. Interacting oscillators in complex networks: Synchronization and the emergence of scale-free topologies. *International Journal of Bifurcation and Chaos*, 20 (2010), 753–763.
3. BEYER, W. H. *CRC Handbook of Mathematical Sciences*. CRC Press (West Palm Beach), 1978.
4. BHATIA, N. P., SZEGÖ, G. P. *Stability Theory of Dynamical Systems*. Springer (Berlin Heidelberg New York), 1970.
5. BLEKHMANN, I. I. *Synchronization in science and technology*. ASME Press (New York), 1988.
6. BOCCALETTI, S., HWANG, D.-U., CHAVEZ, M., AMANN, A., KURTHS, J., PECORA, L. M. Synchronization in dynamical networks: Evolution along commutative graphs. *Physical Review E*, 74 (2006), 016102.
7. BOCCALETTI, S., LATORA, V., MORENO, Y., CHAVEZ, M., HWANG, D.-U. Complex networks: Structure and dynamics. *Physics Reports*, 424 (2006), 175–308.
8. BUCK, J., BUCK, E. Mechanism of Rhythmic Synchronous Flashing of Fireflies. *Science*, 159 (1968), 1319–1327.
9. CHAVEZ, M., HWANG, D.-U., AMANN, A., HENTSCHEL, H., BOCCALETTI, S. Synchronization is enhanced in weighted complex networks. *Physical Review Letters*, 94 (2005), 218701.
10. CODDINGTON, E. A., LEVINSON, N. *Theory of Ordinary Differential Equations*. Krieger Publishing Company (Malabar), 1984.
11. DAVIS, P. J. *Circulant Matrices*. Wiley (New York), 1979.
12. DE LELLIS, P., DI BERNARDO, M., GAROFALO, F. Synchronization of complex networks through local adaptive coupling. *Chaos*, 18 (2008), 037110.
13. DE LELLIS, P., DI BERNARDO, M., GOROCHOWSKI, T. E., RUSSO, G. Synchronization and control of complex networks via contraction, adaptation and evolution. *IEEE Circuits and Systems Magazine*, 10 (2010), 64–82.
14. DUC, L. H., ILCHMANN, A., SIEGMUND, S., TARABA, P. On stability of linear time-varying second-order differential equations. *Quarterly of Applied Mathematics*, 64 (2006), 137–151.
15. ERMENTROUT, B. An adaptive model for synchrony in the firefly pteroptyx malaccae. *Journal of Mathematical Biology*, 29 (1991), 571–585.
16. FARIA, J. J., DYER, J. R., CLÉMENT, R. O., COUZIN, I. D., HOLT, N., WARD, A. J. W., WATERS, D., KRAUSE, J. A novel method for investigating the collective behaviour of fish: introducing ‘Robofish’. *Behavioral Ecology and Sociobiology*, 64 (2010), 1211–1218.
17. FIEDLER, M. Algebraic connectivity of graphs. *Czechoslovak Mathematical Journal*, 23 (1973), 298–305.
18. FITZHUGH, R. Impulses and physiological states in theoretical models of nerve membrane. *Biophysical Journal*, 1 (1961), 445–466.
19. FRANK, T. D. Active systems with nambu dynamics: with applications to rod welding for haptic length perception and self-propagating systems on two-spheres. *The European Physical Journal B*, 74 (2010), 195–203.
20. GRIMSHAW, R. *Nonlinear Ordinary Differential Equations*. Blackwell Scientific Publications (Oxford), 1990.
21. GROS, C. *Complex and Adaptive Dynamical Systems*. Springer (Berlin Heidelberg), 2008.
22. GROSS, J. L., YELLEN, J. *Handbook of Graph Theory*. CRC Press (Boca Raton), 2004.
23. HAN, J., LI, M., GUO, L. Soft control on collective behavior of a group of autonomous agents by a skill agent. *Journal of Systems Science and Complexity*, 19 (2006), 54–62.
24. HONGLER, M.-O., RYTER, D. Hard mode stationary states generated by fluctuations. *Zeitschrift für Physik B*, 31 (1978), 333–337.
25. HORN, R., JOHNSON, C. *Matrix Analysis*. Cambridge University Press (Cambridge), 1985.
26. HRAMOV, A. E., KHRAMOVA, A. E., KORONOVSKII, A. A., BOCCALETTI, S. Synchronization in networks of slightly nonidentical elements. *International Journal of Bifurcation and Chaos*, 3 (2008), 845–850.

27. HSIEH, M.-Y. A., LOIZOU, S., KUMAR, V. Stabilization of Multiple Robots on Stable Orbits via Local Sensing. In Proceedings of *IEEE International Conference on Robotics and Automation*, 2007.
28. KURAMOTO, Y. Cooperative Dynamics of Oscillator Community. *Progress of Theoretical Physics*, 79 (1984), 223–240.
29. LIU, H., CHEN, J., LU, J., CAO, M. Generalized synchronization in complex dynamical networks via adaptive couplings. *Physica A*, 389 (2010), 1759–1770.
30. MATHEWS, P., LAKSHMANAN, M. On a unique nonlinear oscillator. *The Quarterly of Applied Mathematics*, 32 (1974), 215–218.
31. MCGRAW, P. N., MENZINGER, M. Clustering and the synchronization of oscillator networks. *Physical Review E*, 72 (2005), 015101.
32. MOHAR, B. The Laplacian Spectrum of Graphs. In *Graph Theory, Combinatorics, and Applications*, Y. ALAVI, G. CHARTRAND, O. OELLERMANN, A. SCHWENK (Eds.). Wiley (New York), 1991, 871–898.
33. MORENO, Y., PACHECO, A. Synchronization of Kuramoto oscillators in scale-free networks. *Europhysics Letters*, 68 (2004), 603–609.
34. MOTTER, A., ZHOU, C., KURTHS, J. Enhancing complex-network synchronization. *Europhysics Letters*, 69 (2005), 334–340.
35. NAMBU, Y. Generalized hamiltonian dynamics. *Physical Review D*, 7 (1973), 2405–2412.
36. OLFATI-SABER, R. Algebraic Connectivity Ratio of Ramanujan Graphs. In Proceedings of *Proceedings of the 2007 American Control Conference*, 2007.
37. PECORA, L. M., CARROLL, T. L. Master stability functions for synchronized coupled systems. *Physical Review Letters*, 80 (1998), 2109–2112.
38. PIKOVSKY, A., ROSENBLUM, M., KURTHS, J. *Synchronization*. Cambridge University Press (Cambridge), 2001.
39. RIGHETTI, L., BUCHLI, J., IJSPEERT, A. Dynamic Hebbian Learning in Adaptive Frequency Oscillators. *Physica D*, 216 (2006), 269–281.
40. ROCARD, Y. *Dynamique générale des vibrations*. Masson et C<sup>ie</sup> (Paris), 1943.
41. RODRIGUEZ, J., HONGLER, M.-O. Networks of Limit Cycle Oscillators with Parametric Learning Capability. In *Recent Advances in Nonlinear Dynamics and Synchronization: Theory and Applications*, K. KYAMAKYA, W. A. HALANG, H. UNGER, J. C. CHEDJOU, N. F. RULKOV, Z. LI (Eds.). Springer (Berlin Heidelberg), 2009, 17–48.
42. RODRIGUEZ, J., HONGLER, M.-O. Networks of Mixed Canonical-Dissipative Systems and Dynamic Hebbian Learning. *International Journal of Computational Intelligence Systems*, 2 (2009), 140–146.
43. RODRIGUEZ, J., HONGLER, M.-O. Parametric Resonance in Time-Dependent Networks of Hopf Oscillators. In Proceedings of *ECCS'10 - European Conference on Complex Systems*, 2010.
44. RODRIGUEZ, J., HONGLER, M.-O. Networks of Self-Adaptive Dynamical Systems. *IMA Journal of Applied Mathematics* (Under Revision).
45. RODRIGUEZ, J., HONGLER, M.-O., BLANCHARD, P. Self-Adaptive Attractor-Shaping for Oscillators Networks. In Proceedings of *The Joint INDS'11 & ISTET'11 - Third International Workshop on non-linear Dynamics and Synchronization and Sixteenth International Symposium on Theoretical Electrical Engineering*, 2011.
46. SCHWEITZER, F. *Brownian Agents and Active Particles*. Springer (Berlin Heidelberg New York), 2003.
47. SCHWEITZER, F., EBELING, W., TILCH, B. Statistical mechanics of canonical-dissipative systems and applications to swarm dynamics. *Physical Review E*, 64 (2001), 021110.
48. STUMPERS, F. Balth. van der Pol's Work on Nonlinear Circuits. *IRE Transactions on Circuit Theory*, 7 (1960), 366–367.
49. TANAKA, H.-A., LICHTENBERG, A. J., OISHI, S. Self-synchronization of coupled oscillators with hysteretic responses. *Physica D*, 100 (1997), 279–300.
50. TAYLOR, D., OTT, E., RESTREPO, J. G. Spontaneous synchronization of coupled oscillator systems with frequency adaptation. *Physical Review E*, 81 (2010), 046214.



---

# Curriculum Vitae

Julio RODRIGUEZ

Contact: julio.rodriguez@a3.epfl.ch

## Education

- 2001 - 2004      Licence en Mathématiques, Université de Genève
- 2004 - 2007      Maîtrise universitaire en Mathématiques, Université de Genève. Master thesis: *A new portfolio optimization based on entropy*, supervised by Professor M. GANDER (Section de mathématiques) and Professor M. GILLI (Département d'économétrie)

## Recent Professional Experience

- 2007 - 2011      Assistant at the Laboratoire de Production Microtechnique, Ecole polytechnique fédérale de Lausanne. Supervised and guided students's semester projects.
- 2006 - 2007      Assistant at the Section de mathématiques, Université de Genève.

## Publications

### Articles and Book chapters

RODRIGUEZ, J., HONGLER, M.-O. Networks of Mixed Canonical-Dissipative Systems and Dynamic Hebbian Learning. *International Journal of Computational Intelligence Systems*, 2 (2009), 140-146.

RODRIGUEZ, J., HONGLER, M.-O. Networks of Limit Cycle Oscillators with Parametric Learning Capability. In *Recent Advances in Nonlinear Dynamics and Synchronization: Theory and Applications*, K. KYAMAKYA, W. A. HALANG, H. UNGER, J. C. CHEDJOU, N. F. RULKOV, Z. LI (Eds.). Springer (Berlin Heidelberg), 2009, 17-48.

RODRIGUEZ, J., HONGLER, M.-O. Networks of Self-Adaptive Dynamical Systems. *IMA Journal of Applied Mathematics* (Under Revision).

### International Conference and Workshop Proceedings

RODRIGUEZ, J., HONGLER, M.-O. Networks of Mixed Canonic-Dissipative Systems and Dynamic Hebbian Learning. In *Proceedings of INDS'08 - First International Workshop on Nonlinear Dynamics and Synchronization*, 2008.

HONGLER, M.-O., FILLIGER, R., BLANCHARD, Ph., RODRIGUEZ, J. Noise Induced Temporal Patterns in Populations of Globally Coupled Oscillators. In *Proceedings of INDS'09 - Second International Workshop on Nonlinear Dynamics and Synchronization*, 2009.

RODRIGUEZ, J., HONGLER, M.-O. Parametric Resonance in Time-Dependent Networks of Hopf Oscillators. In Proceedings of *ECCS'10 - European Conference on Complex Systems*, 2010. Received a "Special Mention - paper with remarkable overall quality".

J. RODRIGUEZ, M.-O. HONGLER and Ph. BLANCHARD. Self-Adaptive Attractor-Shaping for Oscillators Networks. In Proceedings of *The Joint INDS'11 & ISTET'11 - Third International Workshop on nonlinear Dynamics and Synchronization and Sixteenth International Symposium on Theoretical Electrical Engineering*, 2011.

## Selected Talks

14.05.2008 Networks of Mixed Canonic-Dissipative Systems and Dynamic Hebbian Learning. *Séminaire d'analyse numérique*, Section de mathématiques, Université de Genève, Genève, Suisse.

18-19.07.2008 Networks of Mixed Canonic-Dissipative Systems and Dynamic Hebbian Learning. *INDS'08 - First International Workshop on Nonlinear Dynamics and Synchronization*, Alpen-Adria-Universität Klagenfurt, Klagenfurt, Österreich.

24.10.2008 Network of Limit Cycle Oscillators with Parametric Learning Capability. *Seminar Analysis und Numerik*, Mathematisches Institut, Universität Basel, Basel, Schweiz.

25-29.05.2009 Networks of Mixed Canonical-Dissipative Systems with Plastic Dynamics. *Stochastics and Real World Models 2009*, Universität Bielefeld, Bielefeld, Deutschland.

10.06.2009 Networks of Limit Cycle Oscillators with Plastic Dynamics. *Rencontre franco-suisse sur le bruit et les non linéarités*, Laboratoire de Psychologie et NeuroCognition, Université Pierre-Mendès France, Grenoble, France.

20-21.07.2009 Noise Induced Temporal Patterns in Populations of Globally Coupled Oscillators. *INDS'09 - Second International Workshop on Nonlinear Dynamics and Synchronization*, Alpen-Adria-Universität Klagenfurt, Klagenfurt, Österreich.

26-31.07.2009 Globally Coupled Phase Oscillators with Super-diffusive Noise. *Madeira Math Encounters XXXVII*, Centro de Ciências Matemáticas, Universidad da Madeira, Funchal, Madeira, Portugal.

14-18.02.2010 Frequency Adaptation in Networks of Coupled Limit Cycle Oscillators. *SOCONT - Stochastic Optimal Control*, Quinta Bela São Tiago Hotel, Funchal, Madeira, Portugal.

03-07.05.2010 Networks of Limit Cycle Oscillators with Parametric Dynamics. *Chinese-German Meeting on Stochastic Analysis and Related Fields*. Academy of Mathematics and Systems Science, Chinese Academy of Science, Beijing, People's Republic of China.

12.05.2010 Parametric Resonance in Networks of Adaptive Frequency Oscillators. *Sfb 555 - Complex Nonlinear Processes*, Institut für Physik, Humboldt-Universität, Berlin, Deutschland.

05-09.07.2010 Networks of Adaptive Frequency Oscillators and Parametric Resonance. *Nonlinear Dynamics on Networks*. Національна академія наук України, Київ, Україна.

13-17.09.2010 Parametric Resonance in Time-Dependent Networks of Phase Oscillators. *ECCS'10 - European Conference on Complex Systems*. ISCTE - Instituto Universitário de Lisboa (Instituto Superior de Ciências do Trabalho e da Empresa), Lisboa, Portugal.

18-22.07.2011 Globally Coupled Phase Oscillators driven by Ballistic Noise Source. *Stochastics and Real World Models 2011*, Universität Bielefeld, Bielefeld, Deutschland.

25-27.07.2011 Self-Adaptive Attractor-Shaping for Oscillators Networks. *INDS'11 & ISTET'11*  
- *Third International Workshop on nonlinear Dynamics and Synchronization and Sixteenth  
International Symposium on Theoretical Electrical Engineering*, Alpen-Adria-Universität Klagenfurt, Klagenfurt, Österreich.

### **Research Visits and Exchange Stays**

12.01-11.12.2009 Continuation of my thesis with Professor Ph. BLANCHARD at the Fakultät für Physik, Universität Bielefeld, Bielefeld, Deutschland.

15.07-15.08.2010 Collaboration with the Beijing-Bielefeld Internationales Graduiertenkolleg (IGK) - Stochastics and Real World - team at the Academy of Mathematics and Systems Science, Chinese Academy of Science, Beijing, People's Republic of China.